

Increased complexity in interstellar chemistry: Detection and chemical modeling of ethyl formate and *n*-propyl cyanide in Sgr B2(N) [★]

A. Belloche¹, R. T. Garrod^{2,1}, H. S. P. Müller^{3,1}, K. M. Menten¹, C. Comito¹, and P. Schilke¹

¹ Max-Planck Institut für Radioastronomie, Auf dem Hügel 69, 53121 Bonn, Germany
e-mail: [belloche;kmenten;ccomito;schilke]@mpi-fr-bonn.mpg.de

² Department of Astronomy, Cornell University, 106 Space Sciences Building, Ithaca, NY 14853, USA
e-mail: rgarrod@astro.cornell.edu

³ I. Physikalisches Institut, Universität zu Köln, Zùlpicher Str. 77, 50937 Köln, Germany
e-mail: hspm@ph1.uni-koeln.de

Received 19 December 2008; accepted 17 February 2009

ABSTRACT

Context. In recent years, organic molecules of increasing complexity have been found toward the prolific Galactic center source Sagittarius B2.

Aims. We wish to explore the degree of complexity that the interstellar chemistry can reach in star-forming regions.

Methods. We carried out a complete line survey of the hot cores Sgr B2(N) and (M) with the IRAM 30 m telescope in the 3 mm range, plus partial surveys at 2 and 1.3 mm. We analyzed this spectral survey in the local thermodynamical equilibrium approximation. We modeled the emission of all known molecules simultaneously, which allows us to search for less abundant, more complex molecules. We compared the derived column densities with the predictions of a coupled gas-phase and grain-surface chemical code.

Results. We report the first detection in space of ethyl formate (C₂H₅OCHO) and *n*-propyl cyanide (C₃H₇CN) toward Sgr B2(N). The detection of *n*-propyl cyanide is based on refined spectroscopic parameters derived from combined analyses of available laboratory spectroscopic data. For each molecule, we identified spectral features at the predicted frequencies having intensities compatible with a unique rotation temperature. For an assumed source size of 3'', our modeling yields a column density of 5.4×10^{16} cm⁻², a temperature of 100 K, and a linewidth of 7 km s⁻¹ for ethyl formate. *n*-Propyl cyanide is detected with two velocity components having column densities of 1.5×10^{16} cm⁻² and 6.6×10^{15} cm⁻², respectively, for a source size of 3'', a temperature of 150 K, and a linewidth of 7 km s⁻¹. The abundances of ethyl formate and *n*-propyl cyanide relative to H₂ are estimated to be 3.6×10^{-9} and 1.0×10^{-9} , respectively. We derived column density ratios of 0.8 / 15 / 1 for the related species *t*-HCOOH / CH₃OCHO / C₂H₅OCHO and 108 / 80 / 1 for CH₃CN / C₂H₅CN / C₃H₇CN. Our chemical modeling reproduces these ratios reasonably well. It suggests that the sequential, piecewise construction of ethyl and *n*-propyl cyanide from their constituent functional groups on the grain surfaces is their most likely formation route. Ethyl formate is primarily formed on the grains by adding CH₃ to functional-group radicals derived from methyl formate, although ethanol may also be a precursor.

Conclusions. The detection in Sgr B2(N) of the next stage of complexity in two classes of complex molecule, esters and alkyl cyanides, suggests that greater complexity in other classes of molecule may be present in the interstellar medium.

Key words. astrobiology – astrochemistry – line: identification – stars: formation – ISM: individual objects: Sagittarius B2 – ISM: molecules

1. Introduction

More than 150 molecules have been discovered in the interstellar medium or in circumstellar envelopes over the past four decades (see, e.g., Müller et al. 2005¹). Among them, “complex” organic molecules with up to 13 atoms have been found, showing that the interstellar chemistry in some regions is efficient enough to achieve a relatively high degree of chemical complexity². In addition, much larger molecules have been found in meteorites discovered on Earth, including more than 80 distinct amino acids. The non-terrestrial isotopic ratios of these amino

acids, as well as their racemic distributions³, suggest that they, or at least their direct precursors, have an interstellar origin (see, e.g., Ehrenfreund et al. 2001; Bernstein et al. 2002; Elsila et al. 2007, and references therein). Interstellar chemistry is therefore very likely capable of producing more complex organic molecules than those discovered in the interstellar medium so far. However, the degree of complexity that may be reached is still an open question; the partition functions of larger molecules are large, making it much more difficult to detect such species, even if they are present in reasonably large quantities.

Grain-surface chemistry is frequently invoked as the formation mechanism of many complex species, particularly following recent determinations of some key gas-phase reaction rates. Gas-

[★] Based on observations carried out with the IRAM 30 m telescope. IRAM is supported by INSU/CNRS (France), MPG (Germany) and IGN (Spain).

¹ Visit the Cologne Database for Molecular Spectroscopy (CDMS) at <http://www.cdms.de> for an updated list.

² These molecules are “complex” for astronomers, not for biologists!

³ A racemic distribution means equal amounts of left- and right-handed enantiomers. Enantiomers are stereoisomers that are mirror images of each other and non-superposable.

phase production of methyl formate, a molecule ubiquitous in hot-core spectra, appears prohibitively slow (Horn et al. 2004), pointing to an efficient alternative. Additionally, the dissociative recombination of large organic molecular ions with electrons, which is typically the final step in the gas-phase synthesis of complex molecules, appears strongly to favor the fragmentation of complex structure (Geppert et al. 2006).

In the case of hot cores, the granular ice mantles built up during prior phases of evolution present a rich source of simple saturated molecules from which more complex species may form, as has long been realized (Millar et al. 1991). However, while the efficiency of complex molecule formation in the gas phase is limited (not exclusively) by the need to stabilize the energized complex, often resulting in fragmentation, adhesion to a grain surface allows an adduct to quickly thermalize. Thus, molecular radicals derived from the ice mantles may combine *in situ* on the grain surfaces to build up complex structures efficiently, if dust temperatures are sufficient for the reactants to meet by thermal diffusion. The hot-core models of Garrod & Herbst (2006) and Garrod et al. (2008) have demonstrated the plausibility of such mechanisms in reproducing observed abundances of many complex organic species.

The detection of new complex molecules places valuable constraints on the chemical models. In the context of the model employed, e.g., by Garrod et al. (2008), obtaining abundances of structurally-related molecules allows one to isolate the chemical behavior of the functional groups from which they are constructed, and to relate these back to more fundamental model parameters such as photodissociation rates, binding energies, and initial ice composition. Such an approach then allows further observational predictions to be made.

One of the current best sources to search for new molecules in the interstellar medium is the hot dense core Sagittarius B2(N) – hereafter Sgr B2(N) for short. This source, dubbed the “Large Molecule Heimat” by Snyder et al. (1994), is extraordinary for its rich molecular content: most complex organic molecules such as, e.g., acetic acid (CH_3COOH , Mehringer et al. 1997), glycolaldehyde ($\text{CH}_2(\text{OH})\text{CHO}$, Hollis et al. 2000), acetamide (CH_3CONH_2 , Hollis et al. 2006), and aminoacetonitrile ($\text{NH}_2\text{CH}_2\text{CN}$, Belloche et al. 2008a,b), were first discovered in Sgr B2(N). This hot core is located in the very massive and extremely active region of high-mass star formation Sagittarius B2, at a projected distance of ~ 100 pc from the Galactic center, whose distance is 8.0 ± 0.5 kpc from the Sun (Reid 1993). A second major and somewhat more evolved center of star formation activity, Sgr B2(M), is situated in its vicinity (~ 2 pc). A more detailed introduction on these two sources and their environment can be found in, e.g., Belloche et al. (2008a).

Here, we report the detection of warm compact emission from ethyl formate ($\text{C}_2\text{H}_5\text{OCHO}$) and *n*-propyl cyanide ($\text{C}_3\text{H}_7\text{CN}$) in Sgr B2(N) with the IRAM 30 m telescope. Section 2 summarizes the observational details. The detections of ethyl formate and *n*-propyl cyanide are presented in Sects. 3 and 4, respectively. Implications in terms of interstellar chemistry are discussed in Sect. 5 based on a coupled gas-phase and grain-surface chemical code. Our conclusions are summarized in Sect. 6.

2. Observations and data analysis

2.1. Observations

We observed the two hot core regions Sgr B2(N) and Sgr B2(M) in January 2004, September 2004, and January 2005 with the

IRAM 30 m telescope on Pico Veleta, Spain. We carried out a complete spectral survey toward both sources in the 3 mm atmospheric window between 80 and 116 GHz. A complete survey was performed in parallel in the 1.3 mm window between 201.8 and 204.6 GHz and between 205.0 and 217.7 GHz. Additional selected spectra were also obtained in the 2 mm window and between 219 and 268 GHz. The coordinates of the observed positions are $\alpha_{\text{J2000}}=17^{\text{h}}47^{\text{m}}20^{\text{s}}.0$, $\delta_{\text{J2000}}=-28^{\circ}22'19.0''$ for Sgr B2(N) with a systemic velocity $V_{\text{lsr}} = 64 \text{ km s}^{-1}$ and $\alpha_{\text{J2000}}=17^{\text{h}}47^{\text{m}}20^{\text{s}}.4$, $\delta_{\text{J2000}}=-28^{\circ}23'07.0''$ for Sgr B2(M) with $V_{\text{lsr}} = 62 \text{ km s}^{-1}$. More details about the observational setup and the data reduction can be found in Belloche et al. (2008a). An rms noise level of 15–20 mK on the T_{mb}^* scale was achieved below 100 GHz, 20–30 mK between 100 and 114.5 GHz, about 50 mK between 114.5 and 116 GHz, and 25–60 mK in the 2 mm window. At 1.3 mm, the confusion limit was reached for most of the spectra obtained toward Sgr B2(N).

2.2. Modeling of the spectral survey

The overall goal of our survey was to characterize the molecular content of Sgr B2(N) and (M). It also allows searches for new species once lines emitted by known molecules have been identified, including vibrationally and torsionally excited states, as well as less abundant isotopologues containing, e.g., ^{13}C , ^{18}O , ^{17}O , ^{34}S , ^{33}S , or ^{15}N . We detected about 3700 and 950 lines above 3σ over the whole 3 mm band toward Sgr B2(N) and (M), respectively. These numbers correspond to an average line density of about 100 and 25 features per GHz. Given this high line density, the assignment of a line to a given molecule can be trusted only if all lines emitted by this molecule in our frequency coverage are detected with the right intensity predicted by a model (see below) and no predicted line is missing in the observed spectrum.

We used the XCLASS software (see Comito et al. 2005) to model the emission of all known molecules in the local thermodynamical equilibrium approximation (LTE for short). Each molecule is modeled separately and assumed to be emitted by a uniform region. For each molecule, the free parameters are: source size, temperature, column density, velocity linewidth, velocity offset with respect to the systemic velocity of the source, and a flag indicating if its transitions are in emission or in absorption. For some of the molecules, it was necessary to include several velocity components to reproduce the observed spectra. The velocity components in emission are supposed to be non-interacting, i.e. the intensities add up linearly. This approximation is valid for two distinct, non-overlapping sources smaller than the beam of the telescope, but it is *a priori* less good for, e.g., a source that consists of a hot, compact region surrounded by a cold, extended envelope or two overlapping sources of spectrally overlapping optically thick emission. More details about the entire analysis are given in Belloche et al. (2008a) and the detailed results of this modeling will be published in a forthcoming article describing the complete survey (Belloche et al., in prep.). So far, we have identified 49 different molecules, 60 rare isotopologues, and lines arising from within 42 vibrationally or torsionally excited states apart from the ground state in Sgr B2(N). This represents about 60% of the lines detected above the 3σ level. In Sgr B2(M), the corresponding numbers are 42, 53, 23, and 50%, respectively.

3. Identification of ethyl formate

3.1. Ethyl formate frequencies

Ethyl formate, C_2H_5OCHO , is also known as formic acid ethyl ester, or, according to the International Union of Pure and Applied Chemistry (IUPAC), as ethyl methanoate. Its rotational spectrum was studied in the microwave (Riveros & Bright Wilson 1967) and in the millimeter wave regions up to 241 GHz (Demaison et al. 1984). The molecule occurs in two conformers. The heavy atoms C-C-O-C=O form a planar zigzag chain in the lowest *anti*-conformer which occasionally is also called the *trans*-conformer. The two conformers are depicted schematically in Medvedev et al. (2009). The terminal methyl group is rotated by $\sim 95^\circ$ to the left or to the right in the *gauche*-conformer. Because of these two options, the *gauche*-conformer would be twice as abundant as the *anti*-conformer if the energy difference between the two were zero. However, the *gauche*-conformer is 0.78 ± 0.25 kJ mol $^{-1}$ or 65 ± 21 cm $^{-1}$ or 94 ± 30 K higher in energy (Riveros & Bright Wilson 1967). Therefore, the abundance of the *gauche*-conformer is less than twice that of the *anti*-conformer, in particular at lower temperatures. Since the energy difference has been estimated at room temperature only from relative intensities in the ground state spectra and since excited vibrational states have not been taken into consideration the error in the energy difference may well be larger.

Anti-ethyl formate is a strongly prolate molecule ($A \gg B \approx C$) with electric dipole moments for *a*- and *b*-type transitions, μ_a and μ_b , of 1.85 and 0.70 D, respectively. The *gauche*-conformer is more asymmetric, *A* is smaller by approximately one third and *B* and *C* are larger by about one third. The dipole moment components are $\mu_a = 1.45$, $\mu_b = 1.05$, and $\mu_c = 0.25$ D (Riveros & Bright Wilson 1967). Internal rotation of the terminal methyl group can be neglected. Tunneling between the two *gauche*-conformers has not been observed (Riveros & Bright Wilson 1967).

In the early stages of the current study we received additional ethyl formate data from E. Herbst (Medvedev et al. 2009) based on spectra taken at the Ohio State University (OSU) and covering the frequency range 106 – 378 GHz. The predictions used for the current analysis are based on this data set. An entry for ethyl formate will be available in the catalog section of the Cologne Database for Molecular Spectroscopy (CDMS⁴, see Müller et al. 2001, 2005). The partition function of ethyl formate is 5.690×10^4 and 1.518×10^4 at 150 and 75 K, respectively. In the course of the analysis, the two conformers have been treated separately on occasion to evaluate if the abundance of either conformer is lower than would be expected under LTE conditions.

3.2. Detection of ethyl formate in Sgr B2(N)

For us to claim a reliable detection of a new molecule, it is essential that many lines of this molecule be detected in our spectral survey *and* that all the other expected lines, as predicted by our LTE model, either be blended with lines of other species or be below our detection limit (see Belloche et al. 2008a). Therefore, in the following, we inspect all transitions of ethyl formate in our frequency range. We list in Tables 1 and 2 (*online material*) only the transitions that our LTE modeling predicts to be stronger than 20 mK in the main-beam brightness temperature scale. 711 transitions of the *anti*-conformer and 478 transitions of the *gauche*-conformer are above this threshold that is conser-

vative since it is below 1.5 times the rms noise level of the *best* part of our survey (and even below the rms noise level of *most* parts of our survey). To save some space, when two transitions have a frequency difference smaller than 0.1 MHz that cannot be resolved, we list only the first one. We number the transitions in Col. 1 and give their quantum numbers in Col. 2. The frequencies, the frequency uncertainties, the energies of the lower levels in temperature units, and the $S\mu^2$ values are listed in Col. 3, 4, 5, and 6, respectively. Since the spectra are in most cases close to the line confusion limit and it is difficult to measure the noise level, we give in Col. 7 the rms sensitivity computed from the system temperature and the integration time: $\sigma = \frac{F_{\text{eff}}}{B_{\text{eff}}} \times \frac{2T_{\text{sys}}}{\sqrt{\delta f t}}$, with F_{eff} and B_{eff} the forward and beam efficiencies, T_{sys} the system temperature, δf the spectral resolution, and t the total integration time (on-source plus off-source).

We list in Col. 8 of Tables 1 and 2 comments about the blends affecting the transitions of the *anti*- and *gauche*-conformers of ethyl formate. As can be seen in these tables, most of the ethyl formate lines covered by our survey of Sgr B2(N) are heavily blended with lines of other molecules and therefore cannot be identified in this source based on our single-dish data. Only 46 of the 711 transitions of the *anti*-conformer are relatively free of contamination from other molecules, known or still unidentified according to our modeling. They are marked “Detected” or “Group detected” in Col. 8 of Table 1, and are listed with more information in Table 3. We stress that all transitions of sufficient strength predicted in the frequency range of our spectral survey are either detected or blended, i.e. no predicted transition is missing in the observed spectrum. The 46 detected transitions correspond to 24 observed features that are shown in Fig. 1 (*online material*) and labeled in Col. 8 of Table 3. For reference, we show the spectrum observed toward Sgr B2(M) in these figures also. We identified the ethyl formate lines and the blends affecting them with the LTE model of this molecule and the LTE model including all molecules (see Sect. 2.2). The parameters of our best-fit LTE model of ethyl formate are listed in Table 4, and the model is overlaid in red on the spectrum observed toward Sgr B2(N) in Fig. 1. The best-fit LTE model including all molecules is shown in green in the same figures.

For the frequency range corresponding to each detected ethyl formate feature, we list in Table 3 the integrated intensities of the observed spectrum (Col. 10), of the best-fit model of ethyl formate (Col. 11), and of the best-fit model including all molecules (Col. 12). In these columns, the dash symbol indicates transitions belonging to the same feature. Columns 1 to 7 of Table 3 are the same as in Table 1. The 1σ uncertainty given for the integrated intensity in Col. 10 was computed using the estimated noise level of Col. 7.

The measurements of the *anti*-conformer of ethyl formate are plotted in the form of a population diagram in Fig. 2a, which plots upper level column density divided by statistical weight, N_u/g_u , versus the upper level energy in Kelvins (see Goldsmith & Langer 1999). The data are shown in black and our best-fit model of ethyl formate in red. Out of 12 features encompassing several transitions, one contains transitions with different energy levels and was ignored in the population diagram (feature 17). We used equation A5 of Snyder et al. (2005) to compute the ordinate values:

$$\ln\left(\frac{N_u}{g_u}\right) = \ln\left(\frac{1.67W_T \times 10^{14}}{S\mu^2B\nu}\right) = -\frac{E_u}{T_{\text{rot}}} + \ln\left(\frac{N_T}{Z}\right), \quad (1)$$

where W_T is the integrated intensity in K km s $^{-1}$ in main-beam brightness temperature scale, $S\mu^2$ the line strength times the

⁴ <http://www.cdms.de>

Table 3. Transitions of the *anti*-conformer of ethyl formate detected toward Sgr B2(N) with the IRAM 30 m telescope.

N^a	Transition	Frequency (MHz)	Unc. ^b (kHz)	E_l^c (K)	$S\mu^2$ (D ²)	σ^d (mK)	F^e	τ^f	I_{obs}^g (K km s ⁻¹)	I_{mod}^g (K km s ⁻¹)	I_{all}^g (K km s ⁻¹)	Comments
(1)	(2)	(3)	(4)	(5)	(6)	(7)	(8)	(9)	(10)	(11)	(12)	(13)
1	15 _{2,14} – 14 _{2,13}	81779.567	4	30	51	13	1	0.05	0.52(06)	0.32	0.44	blend with U-line
16	15 _{6,10} – 14 _{6,9}	82351.854	4	54	43	19	2	0.07	1.02(08)	0.44	0.55	partial blend with C ₂ H ₅ CN, $v_{13}=1/v_{21}=1$ and U-line
17	15 _{6,9} – 14 _{6,8}	82351.858	4	54	43	19	2	–	–	–	–	–
26	15 _{2,13} – 14 _{2,12}	84081.357	4	31	51	19	3	0.05	0.53(08)	0.35	0.42	partial blend with CH ₃ CH ₃ CO, $v_l=1$
28	16 _{0,16} – 15 _{0,15}	85065.106	4	31	55	22	4	0.06	0.73(10)	0.39	0.57	partial blend with <i>c</i> -C ₂ H ₄ O
44	16 _{8,8} – 15 _{8,7}	87810.372	4	78	41	17	5	0.05	1.28(07)	0.40	1.22	partial blend with CH ₂ (OH)CHO and C ₂ H ₅ CN
45	16 _{8,9} – 15 _{8,8}	87810.372	4	78	41	17	5	–	–	–	–	–
46	16 _{7,9} – 15 _{7,8}	87826.665	4	67	44	17	6	0.06	0.99(07)	0.48	0.86	partial blend with HNCO, $v_5=1$
47	16 _{7,10} – 15 _{7,9}	87826.665	4	67	44	17	6	–	–	–	–	–
53	16 _{3,14} – 15 _{3,13}	87993.944	4	38	53	19	7	0.05	1.01(08)	0.39	0.64	partial blend with CH ₃ CH ₃ CO and U-line
54	16 _{4,12} – 15 _{4,11}	88001.562	4	43	51	19	8	0.05	0.66(08)	0.35	0.62	blend with C ₂ H ₅ CN, $v_{13}=1/v_{21}=1$
73	17 _{10,7} – 16 _{10,6}	93284.077	4	108	38	22	9	0.04	0.07(09)	0.33	0.35	uncertain baseline
74	17 _{10,8} – 16 _{10,7}	93284.077	4	108	38	22	9	–	–	–	–	–
75	17 _{9,8} – 16 _{9,7}	93292.297	4	94	42	22	10	0.05	0.56(09)	0.42	0.50	uncertain baseline
76	17 _{9,9} – 16 _{9,8}	93292.297	4	94	42	22	10	–	–	–	–	–
77	17 _{8,9} – 16 _{8,8}	93304.955	4	82	45	22	11	0.06	0.96(09)	0.51	0.67	partial blend with U-line
78	17 _{8,10} – 16 _{8,9}	93304.955	4	82	45	22	11	–	–	–	–	–
79	17 _{7,11} – 16 _{7,10}	93324.728	4	71	48	22	12	0.07	1.32(09)	0.60	0.74	partial blend with U-lines
80	17 _{7,10} – 16 _{7,9}	93324.728	4	71	48	22	12	–	–	–	–	–
81	17 _{6,12} – 16 _{6,11}	93356.821	4	62	51	22	13	0.08	1.68(10)	0.70	1.24	blend with CH ₃ CH ₃ CO and U-line?
82	17 _{6,11} – 16 _{6,10}	93356.838	4	62	51	22	13	–	–	–	–	–
83	17 _{5,13} – 16 _{5,12}	93412.160	4	54	53	22	14	0.08	1.12(10)	0.79	0.85	partial blend with U-line?
84	17 _{5,12} – 16 _{5,11}	93413.168	4	54	53	22	14	–	–	–	–	–
86	17 _{4,14} – 16 _{4,13}	93504.972	4	47	55	24	15	0.05	1.47(10)	0.44	0.87	blend with CH ₃ ¹⁸ OH
87	17 _{4,13} – 16 _{4,12}	93539.303	4	47	55	24	16	0.05	0.84(10)	0.44	0.45	no blend
94	18 _{15,3} – 17 _{15,2}	98760.931	5	202	19	18	17	0.04	0.87(09)	0.68	0.78	blend with U-line
95	18 _{15,4} – 17 _{15,3}	98760.931	5	202	19	18	17	–	–	–	–	–
96	18 _{14,4} – 17 _{14,3}	98761.079	5	181	24	18	17	–	–	–	–	–
97	18 _{14,5} – 17 _{14,4}	98761.079	5	181	24	18	17	–	–	–	–	–
98	18 _{16,2} – 17 _{16,1}	98761.555	5	224	13	18	17	–	–	–	–	–
99	18 _{16,3} – 17 _{16,2}	98761.555	5	224	13	18	17	–	–	–	–	–
100	18 _{13,5} – 17 _{13,4}	98762.218	5	162	30	18	17	–	–	–	–	–
101	18 _{13,6} – 17 _{13,5}	98762.218	5	162	30	18	17	–	–	–	–	–
102	18 _{17,1} – 17 _{17,0}	98762.790	5	248	7	18	17	–	–	–	–	–
103	18 _{17,2} – 17 _{17,1}	98762.790	5	248	7	18	17	–	–	–	–	–
104	18 _{12,6} – 17 _{12,5}	98764.650	5	144	34	18	17	–	–	–	–	–
105	18 _{12,7} – 17 _{12,6}	98764.650	5	144	34	18	17	–	–	–	–	–
118	18 _{5,14} – 17 _{5,13}	98928.453	4	58	57	18	18	0.07	2.37(09)	0.96	2.23	blend with C ₂ H ₅ CN, $v_{13}=1/v_{21}=1$
119	18 _{5,13} – 17 _{5,12}	98930.153	4	58	57	18	18	–	–	–	–	–
160	20 _{1,20} – 19 _{1,19}	105234.713	5	49	68	28	19	0.07	1.66(11)	0.76	1.27	blend with C ₂ H ₅ OH and CH ₃ OCHO
161	19 _{1,18} – 18 _{1,17}	105272.047	5	47	65	28	20	0.07	2.07(11)	0.73	0.81	blend with U-lines
162	19 _{3,16} – 18 _{3,15}	105447.141	5	52	64	37	21	0.06	1.07(15)	0.69	1.07	no blend
165	20 _{2,19} – 19 _{2,18}	108552.378	100	53	68	20	22	0.07	2.05(08)	0.79	1.24	partial blend with C ₂ H ₅ CN, $v_{15}=1$ and U-lines
233	21 _{6,16} – 20 _{6,15}	115395.797	5	81	66	60	23	0.11	2.94(23)	1.37	1.37	partial blend with U-line
234	21 _{6,15} – 20 _{6,14}	115395.986	5	81	66	60	23	–	–	–	–	–
238	22 _{1,22} – 21 _{1,21}	115595.764	5	59	75	79	24	0.08	-0.05(30)	0.99	2.22	blend with CH ₃ CH ₃ CO, $v_l=1$, uncertain baseline

Notes: ^a Numbering of the observed transitions associated with a modeled line stronger than 20 mK (see Table 1). ^b Frequency uncertainty. ^c Lower energy level in temperature units (E_l/k_B). ^d Calculated rms noise level in T_{mb} scale. ^e Numbering of the observed features. ^f Peak opacity of the modeled feature. ^g Integrated intensity in T_{mb} scale for the observed spectrum (Col. 10), the ethyl formate model (Col. 11), and the model including all molecules (Col. 12). The uncertainty in Col. 10 is given in parentheses in units of the last digit.

dipole moment squared in D², B the beam filling factor, ν the frequency in GHz, T_{rot} the rotation temperature in K, N_T the molecular column density in cm⁻², and Z the partition function. This equation assumes optically thin emission. To estimate by how much line opacities affect this diagram, we applied the opacity correction factor $C_\tau = \frac{\tau}{1-e^{-\tau}}$ (see Goldsmith & Langer 1999; Snyder et al. 2005) to the modeled intensities, using the opaci-

ties from our radiative transfer calculations (Col. 9 of Table 3); the result is shown in green in Fig. 2a. The population diagram derived from the modeled spectrum is slightly shifted upwards but its shape, in particular its slope (the inverse of which *approximately* determines the rotation temperature), is not significantly changed, since $\ln C_\tau$ does not vary much (from 0.019 to 0.053). The populations derived from the *observed* spectrum in the opti-

Table 4. Parameters of our best-fit LTE model of ethyl formate.

Size ^a ($''$)	T_{rot}^b (K)	N^c (cm^{-2})	ΔV^d (km s^{-1})	V_{off}^e (km s^{-1})
(1)	(2)	(3)	(4)	(5)
3.0	100	5.40×10^{16}	7.0	0.0

Notes: ^a Source diameter (*FWHM*). ^b Temperature. ^c Column density. ^d Linewidth (*FWHM*). ^e Velocity offset with respect to the systemic velocity of Sgr B2(N) $V_{\text{lsr}} = 64 \text{ km s}^{-1}$.

cally thin approximation are therefore not significantly affected by the optical depth of the ethyl formate transitions⁵. The scatter of the black crosses in Fig. 2a is therefore dominated by the blends with other molecules and uncertainties in the baseline removal (indicated by the downwards and upwards blue arrows, respectively).

The population diagram derived from the modeled spectrum in Fig. 2a is systematically below the measurements. Since most of the detected features of the *anti*-conformer of ethyl formate are partially blended with lines from other molecules (see Col. 13 of Table 3), we can use our model including all identified molecules (shown in green in Fig. 1) to remove the expected contribution from the contaminating molecules. Instead of computing N_u/g_u with the integrated intensities I_{obs} listed in Col. 10 of Table 3, we can use the value $I_{\text{obs}} - (I_{\text{all}} - I_{\text{mod}})$ derived from Col. 10, 11, and 12. The corrected population diagram is shown in Fig. 2b. The predicted (red) and measured (black) points are much closer to each other. A close inspection of Fig. 1 shows however that the wings of most detected features of ethyl formate are still contaminated by U-lines, which explains why the measured points are still above the predicted ones in the population diagram (our fitting method with XCLASS is mainly focused on the peak intensity, not on the integrated intensity). The only exception is feature 9 for which the level of the baseline was obviously overestimated (see panel 7 of Fig. 1).

Given the remaining uncertainties due to the contamination from U-lines, it is difficult to derive the temperature with high accuracy. However, feature 17, which can unfortunately not be shown in the population diagram since it is a blend of several transitions with different energy levels (from 149 to 253 K), is significantly detected in panel 13 of Fig. 1. This is a strong indication that the temperature cannot be much lower than 100 K. Overall, we estimate the resulting uncertainty on the derived column density to be on the order of 25%. Finally, since all detected transitions are optically thin and the region emitting in ethyl formate is most likely compact given its high temperature, column density and source size are degenerate. We fixed the source size to $3''$. This is approximately the size of the region emitting in the chemically related molecule methyl formate (CH_3OCHO) that we measured with the IRAM Plateau de Bure interferometer (see Table 5 of Belloche et al. 2008b).

From this analysis, we conclude that our best-fit model for the *anti*-conformer of ethyl formate is fully consistent with our 30 m data of Sgr B2(N). This detection of ethyl formate is, to our knowledge, the first one in space⁶.

⁵ Note that our modeled spectrum is anyway calculated with the full LTE radiative transfer that takes into account the optical depth effects (see Sect. 2.2).

⁶ Jones et al. (2007) tentatively identified three lines detected with the Australia Telescope Compact Array at ~ 86.2738 , ~ 86.9784 , and ~ 86.9787 GHz as two transitions of the *anti*-conformer of ethyl formate, the second one with two velocity components. However, our model predicts a peak temperature of the ethyl formate transition at

No feature of the *gauche*-conformer of ethyl formate is clearly detected in our spectral survey of Sgr B2(N). Only one feature at 213.6 GHz is possibly detected, but the baseline in this frequency range is very uncertain and the feature is blended with a transition of H^{13}CCCN (see Table 2). If we consider this feature as a detection, then it implies a column density a factor 2 smaller than for the *anti*-conformer. This may suggest that the distribution of ethyl formate molecules in the two conformers is not in thermodynamical equilibrium. However, we first have to evaluate the uncertainty on the ratio of the *anti*- and *gauche*-conformer populations coming from the uncertainty on the energy difference between the two conformers ($\Delta E = 65 \pm 21 \text{ cm}^{-1}$, see Sect. 3.1). With $\Delta E = 0$, the ratio would be 1/2. For the preferred energy difference of 65 cm^{-1} , we have a ratio of about 0.56/0.44 at 100 K. If we assume an energy difference of 86 cm^{-1} this ratio would change to 0.62/0.38, i.e. a variation of $\sim 30\%$. This is not enough to compensate for the factor 2 mentioned above, but can have a significant contribution. In addition, a model of the emission spectrum of the *gauche*-conformer with the same parameters as for the *anti*-conformer is not excluded because of the large uncertainty on the baseline at 213.6 GHz. Therefore, given the large densities characterizing the hot core in Sgr B2(N) (see, e.g., Belloche et al. 2008a,b), it seems unlikely that the population in the *gauche*-conformer is subthermal compared to the *anti*-conformer.

3.3. Upper limit in Sgr B2(M)

We do not detect ethyl formate in our spectral survey toward Sgr B2(M). Using the same source size, linewidth, and temperature as for Sgr B2(N) (see Table 4), we find $\sim 3\sigma$ column density upper limits of $2.0 \times 10^{16} \text{ cm}^{-2}$ and $4.0 \times 10^{16} \text{ cm}^{-2}$ in the LTE approximation for the *anti*- and *gauche*-conformers, respectively. The column density of ethyl formate is thus at least a factor ~ 3 lower toward Sgr B2(M) than toward Sgr B2(N). This is not surprising since, e.g., Nummelin et al. (2000) found that hot-core-type molecules are more abundant in Sgr B2(N) by factors 3–8 as compared to Sgr B2(M).

3.4. Comparison to related species

We easily detect the already known molecules formic acid in the *trans* form (*t*-HCOOH or *t*-HOCHO), methyl formate (CH_3OCHO), ethanol ($\text{C}_2\text{H}_5\text{OH}$), and dimethyl ether (CH_3OCH_3) in our survey toward Sgr B2(N) (see also, e.g.,

86.977087 GHz on the order of 2 mK whereas the two lines detected with the 30 m telescope close to this frequency have peak temperatures of 0.38 and 0.65 K, respectively! We identified these two lines with two velocity components of a transition of the vibrationally excited $v_{13}=1/v_{21}=1$ state of ethyl cyanide, and our modeled spectrum matches the observed lines very well. The tentative identification of Jones et al. (2007) at this frequency is therefore not confirmed. On the other hand, the line detected at ~ 86.2738 GHz in our survey is still unidentified. The frequency of the $45_{5,41}-44_{6,38}$ transition of ethyl formate mentioned by Jones et al. (2007) comes from the JPL catalog (Pickett et al. 1998, see <http://spec.jpl.nasa.gov/>). Our catalog contains a significantly different frequency for this transition (86256.5339 ± 0.0114 MHz instead of 86273.7945 ± 0.2103 MHz), and our model anyway predicts a very low peak temperature on the order of 0.3 mK for this transition. Our catalog contains two other overlapping transitions closer to 86.2738 GHz ($35_{10,26}-36_{9,27}$ and $35_{10,25}-36_{9,28}$ at 86.2703101 and 86.2703225 GHz, respectively). However, our model predicts a very low peak temperature of 0.6 mK for these transitions as well. Therefore, this tentative identification of Jones et al. (2007) is not confirmed either.

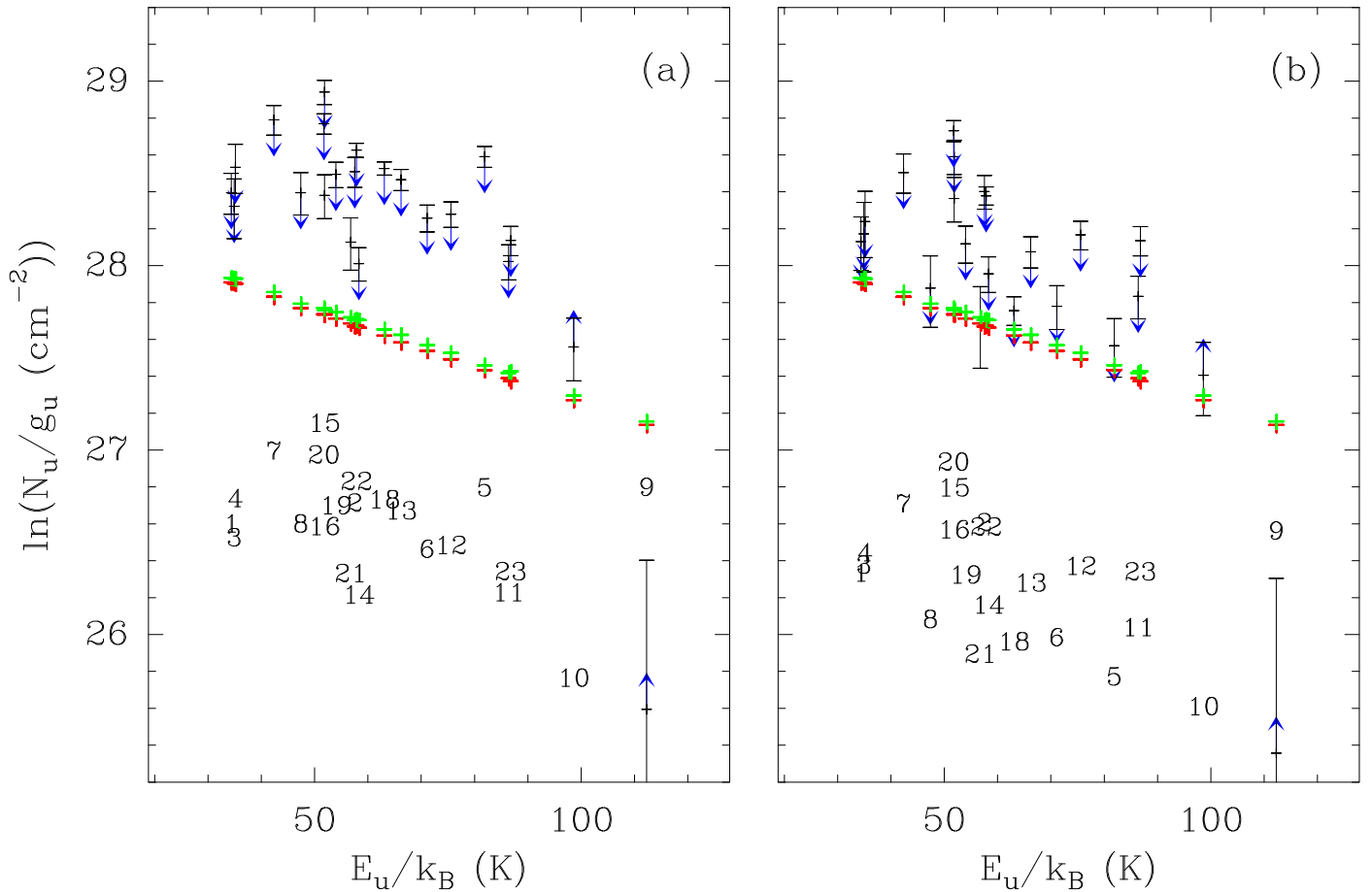


Fig. 2. a) Population diagram of the *anti*-conformer of ethyl formate in Sgr B2(N). The red points were computed in the optically thin approximation using the integrated intensities of our best-fit *model* of ethyl formate, while the green points were corrected for the opacity. The black points were computed in the optically thin approximation using the integrated intensities of the spectrum *observed* with the IRAM 30 m telescope. The error bars are 1σ uncertainties on N_u/g_u . Blue arrows pointing downwards mark the transitions blended with transitions from other molecules, while blue arrows pointing upwards indicate that the baseline removed in the observed spectrum is uncertain. The arrow length is arbitrary. The feature labels are shown in black shifted by -1.8 along the Y-axis for clarity, except for feature 9 for which it is shifted by $+1.2$. The measurement corresponding to feature 24 (at $E_u/k_B = 65$ K) is not shown since the integrated intensity measured toward Sgr B2(N) is negative, most likely because the level of the baseline was overestimated. Feature 17 is a blend of several transitions with different energy levels and was therefore also omitted. **b)** Same as **a)** but with the expected contribution from the contaminating molecules removed from the integrated intensities of the observed spectrum.

Nummelin et al. 2000; Liu et al. 2001). The parameters of our current best fit models of these molecules are listed in Table 5. All species have two velocity components that correspond to the two hot cores embedded in Sgr B2(N) (see, e.g., Belloche et al. 2008a for a discussion about these two sources). Ethyl formate may have a second velocity component too, but our survey is not sensitive enough to detect it with a significant signal-to-noise ratio. Using the same parameters as for the first velocity component but a velocity shift of 10 km s^{-1} , we estimate a 3σ upper limit of $\sim 2.4 \times 10^{16} \text{ cm}^{-2}$ for the column density of a second velocity component of ethyl formate.

The lines of formic acid are optically thin in our model, so the size of the emitting region cannot be measured with our single-dish data. It was here fixed to $5''$, assuming that a more extended region would have a lower temperature. Nummelin et al. (2000) derived a temperature of 74^{+8}_{-30} K and a beam-averaged column density of $\sim 4.2^{+2.0}_{-1.0} \times 10^{14} \text{ cm}^{-2}$ in the LTE approximation with the SEST telescope ($HPBW \sim 23''$ at 1.3 mm). They used a linewidth of 13 km s^{-1} ($FWHM$), which more or less cor-

responds to the combination of the two velocity components we identified. Their column density translates into a column density of $\sim 9.3^{+4.4}_{-2.1} \times 10^{15} \text{ cm}^{-2}$ for a source size of $5''$, i.e. about a factor 2 smaller than the sum of the column densities of both velocity components in Table 5. At least two reasons may explain this discrepancy. First of all, as we noticed in our own partial survey at 1.3 mm, the level of the baseline in this wavelength range is very uncertain for Sgr B2(N) because of the line confusion and it may easily be overestimated. Second, at these high frequencies in Sgr B2(N), the dust is partially optically thick and should partially absorb the line emission⁷. We estimate that the combina-

⁷ Lis et al. (1993) measured a peak flux of $20 \text{ Jy}/4.5'' \times 3.7''$ -beam at 227 GHz toward Sgr B2(N), i.e. 28 K in temperature unit. For a temperature of ~ 100 K, this yields a dust optical depth of ~ 0.34 . On larger scales ($\sim 10''$), Gordon et al. (1993) estimated that the dust opacity toward Sgr B2(N) reaches a value of 1 at $850 \mu\text{m}$, which implies an opacity of ~ 0.43 – 0.53 at 1.3 mm. As a result, if not taken into account, these significant opacities imply an underestimate of the line intensities by a factor ~ 1.4 – 1.7 .

Table 5. Parameters of our best-fit LTE models of formic acid, methyl formate, ethanol, and dimethyl ether.

Molecule ^a	Size ^b ($''$)	T_{rot} ^c (K)	N ^d (cm^{-2})	ΔV ^e (km s^{-1})	V_{off} ^f (km s^{-1})
(1)	(2)	(3)	(4)	(5)	(6)
<i>t</i> -HCOOH	5.0 5.0	70 70	1.50×10^{16} 7.50×10^{15}	8.0 8.0	-1.0 9.0
CH ₃ OCHO	4.0 4.0	80 80	4.50×10^{17} 1.50×10^{17}	7.2 7.2	0.0 10.0
C ₂ H ₅ OH	3.0 3.0	100 100	8.40×10^{17} 3.00×10^{17}	8.0 7.0	0.0 10.0
CH ₃ OCH ₃	2.5 2.5	130 130	2.30×10^{18} 1.10×10^{18}	6.0 6.0	0.0 10.0

Notes: ^a We used the CDMS entry for *t*-HCOOH (version 1), and the JPL entries for CH₃OCHO (ver. 1), C₂H₅OH (ver. 4), and CH₃OCH₃ (ver. 1). See references to the laboratory data therein. ^b Source diameter (*FWHM*). ^c Temperature. ^d Column density. ^e Linewidth (*FWHM*). ^f Velocity offset with respect to the systemic velocity of Sgr B2(N) $V_{\text{lsr}} = 64 \text{ km s}^{-1}$.

tion of these two effects can lead to underestimating the true line intensities by about a factor 2 or 3. In addition, assuming a temperature of 200 K, Liu et al. (2001) measured a beam-averaged column density of $1.1 \pm 0.3 \times 10^{16} \text{ cm}^{-2}$ with the BIMA interferometer at 86–90 GHz (*HPBW* $\sim 14'' \times 4''$). This translates into a column density of $\sim 6.3 \pm 1.5 \times 10^{15} \text{ cm}^{-2}$ for a source size of $5''$ and a temperature of 70 K. The interferometric detection of Liu et al. (2001) is somewhat uncertain but suggests that about half of the 30 m flux may be emitted by an extended region filtered out by the interferometer. The formic acid column density of the compact sources listed in Table 5 may therefore be overestimated by up to a factor 2.

The lines of methyl formate have opacities of up to about 1 in our model of the 3 mm spectrum, which puts only weak constraints on the source size that we fixed to $4''$. Assuming a temperature of 200 K, Nummelin et al. (2000) derived a beam-averaged column density of $\sim 5.6_{-0.1}^{+0.3} \times 10^{15} \text{ cm}^{-2}$ with the SEST telescope for the *a*-type lines and, assuming a temperature of 500 K, $\sim 4.0_{-0.4}^{+0.3} \times 10^{16} \text{ cm}^{-2}$ for the *b*-type lines. For a temperature of 80 K and a source size of $4''$, the column density of the *a*-type lines translates into a column density of $\sim 1.2 \times 10^{17} \text{ cm}^{-2}$, which is about a factor 5 smaller than the one we derived here for the sum of the two velocity components. Again, the uncertainty on the level of the baseline and the partial dust absorption at 1.3 mm may explain part of this discrepancy. In addition, we note that our model at 3 mm reproduces quite well both the *a*- and *b*-type lines with the same temperature and column density (see Appendix A, *online material*), while Nummelin et al. (2000) found an order of magnitude difference between the column densities of the two types. We believe that this discrepancy results from the fact that they did not properly take into account the line blending, which is large in Sgr B2(N) and should affect the (weak) *b*-type lines the most, and that they underestimated the line opacities of the (strong) *a*-type lines that our model predicts to be on the order of 1–3 in the 1.3 mm range. Using the BIMA interferometer at 90.15 GHz with a beam size of $14'' \times 4''$, Liu et al. (2001) found a beam-averaged column density of $1.1 \times 10^{17} \text{ cm}^{-2}$ for an assumed temperature of 200 K in the optically thin approximation. This translates into a column density of $1.5 \times 10^{17} \text{ cm}^{-2}$ for a source size of $4''$ and a temperature of 80 K. However, our model predicts an opacity of ~ 0.6 for this transition, which implies a higher column

density of $2.0 \times 10^{17} \text{ cm}^{-2}$. This is still about a factor 2 times lower than our estimate and suggests that, like in the case of formic acid, half of the single-dish flux may actually come from a region more extended than the size of our model and may be filtered out by the interferometer. This conclusion is further supported by the flux ratio of 1.7 between the 12 m telescope (*HPBW* = $71''$) and BIMA (*HPBW* = $25.2'' \times 6.3''$) measurements of Friedel et al. (2004) at 86–90 GHz, and the flux ratio of 2.3 we found between the measurements done with the 30 m telescope and the Plateau de Bure interferometer at 82.2 GHz (see Table 5 of Belloche et al. 2008b). As a result, the methyl formate column density of the compact sources listed in Table 5 may be overestimated by up to a factor 2.

Most lines of ethanol are optically thin at 3 mm ($\tau < 0.7$), except for three lines that are marginally optically thick ($\tau \sim 1 - 1.2$). As a result, the source size is not well constrained and we fixed it to $3''$. Nummelin et al. (2000) derived a beam-averaged column density of $4.2 \pm 0.2 \times 10^{15} \text{ cm}^{-2}$ for a temperature of 73_{-4}^{+5} K with the SEST telescope. This translates into a column density of $2.5 \times 10^{17} \text{ cm}^{-2}$ for a source size of $3''$, which is significantly lower than our measurement. However, Nummelin et al. (2000) used an earlier version of the JPL entry for ethanol that turned out to be inaccurate (J. Pearson, *private communication*). With this older version, we determined column densities of 2.8×10^{17} and $8.9 \times 10^{16} \text{ cm}^{-2}$ for both velocity components, which was consistent with the result of Nummelin et al. (2000). The column densities given in Table 5 were obtained with the latest JPL entry for ethanol (Pearson et al. 2008). The high-energy lines ($E_1/k_B \sim 40 - 80 \text{ K}$) detected by Friedel et al. (2004) with the NRAO 12 m telescope and the BIMA interferometer have the same fluxes with both instruments, implying that they are emitted by a compact region. Only the $4_{1,4} - 3_{0,3}$ line with $E_1/k_B = 5.0 \text{ K}$ has an interferometric flux significantly lower than the single-dish flux. Our LTE model is also too weak for this transition compared to the spectrum obtained with the 30 m telescope. However, it fits well the low-energy transitions at 84.595868 GHz ($E_1/k_B = 9.4 \text{ K}$) and 112.807174 GHz ($E_1/k_B = 2.1 \text{ K}$) detected in our survey. Therefore, it is unclear whether the BIMA missing flux of the $4_{1,4} - 3_{0,3}$ transition suggests an additional cold, extended component, or this line is heavily blended with a transition of another molecule.

Our model of dimethyl ether predicts line opacities up to 2. The size of the emitting region is thus reasonably well constrained for this molecule. Nummelin et al. (2000) derived a beam-averaged column density of $7.9_{-0.7}^{+0.8} \times 10^{15} \text{ cm}^{-2}$ for a temperature of $197_{-22}^{+31} \text{ K}$ with the SEST telescope. This translates into a column density of $6.8 \times 10^{17} \text{ cm}^{-2}$ for a source size of $2.5''$, which is a factor 4 lower than derived here. The discrepancy most likely comes from the beam filling factor of unity assumed by Nummelin et al. (2000) that leads to underestimating the line opacities. Our LTE model indeed predicts line optical depths up to 9 in the 1.3 mm window.

After rescaling to the same size of $3''$, the relative column densities of the three related molecules *t*-HCOOH / CH₃OCHO / C₂H₅OCHO are about 0.8 / 15 / 1 for the first velocity component, and 0.9 / 11 / 1 for the second velocity component using the upper limit found for ethyl formate. We discuss these ratios and the implications for the interstellar chemistry in Sect. 5.

4. Identification of *n*-propyl cyanide

4.1. *n*-Propyl cyanide frequencies

n-Butanenitrile, C₃H₇CN, is more commonly known as *n*-propyl cyanide or *n*-butyronitrile. Its rotational spectrum has been investigated in the microwave (Hirota 1962; Demaison & Dreizler 1982; Vormann & Dreizler 1988) and in the millimeter wave regions up to 284 GHz (Włodarczak et al. 1988). The *n* indicates the *normal* isomer with the carbon atoms forming a chain, in contrast to the *iso* isomer which has a branched structure. This isomer has been studied to a lesser extent. However, its rotational spectrum is currently under investigation in Cologne.

n-Propyl cyanide exists in two conformers, *anti* and *gauche*, just as does ethyl formate. Again, the *anti*-conformer is the lower energy form, is strongly prolate, and has a large *a*-dipole moment component of 3.60 D and a still sizable *b*-dipole moment component of 0.98 D. The *gauche*-conformer is 1.1 ± 0.3 kJ mol⁻¹ or 92 ± 25 cm⁻¹ or 132 ± 36 K higher in energy, more asymmetric, and has $\mu_a = 3.27$ and $\mu_b = 2.14$ D (Włodarczak et al. 1988). The energy difference has been estimated at room temperature and at 233 K from relative intensities in the ground state spectra. Since excited vibrational states have not been taken into consideration the error in the energy difference may well be slightly larger than mentioned above. The residuals quoted in the most recent study (Vormann & Dreizler 1988) for their measurements are frequently much larger than the suggested uncertainties of about 5 kHz suggesting an insufficient set of spectroscopic parameters was used. Moreover, only newly determined rotational and centrifugal distortion parameters were given for the *gauche*-conformer. Therefore, new sets of rotational and centrifugal distortion parameters were determined for both conformers in the present study.

In the initial fits transition frequencies were taken from all four studies (Hirota 1962; Demaison & Dreizler 1982; Włodarczak et al. 1988; Vormann & Dreizler 1988). Two *b*-type transitions from Włodarczak et al. (1988) were omitted from the fits as suggested in the erratum to this paper (Włodarczak et al. 1991). On the other hand, transition frequencies not given in Vormann & Dreizler (1988), but deposited at the library of the University of Kiel were obtained from there and included in the fits. Uncertainties of 200, 10, 50, and 5 kHz were assigned to the transitions from Hirota (1962), Demaison & Dreizler (1982), Włodarczak et al. (1988), and Vormann & Dreizler (1988), respectively. Demaison & Dreizler (1982) and Vormann & Dreizler (1988) resolved in part internal rotation of the methyl group or quadrupole splitting of the ¹⁴N nucleus in their laboratory measurements. The methyl internal rotation is unlikely to be resolved in astronomical observations. The quadrupole splitting may be resolvable for some low energy transitions, but these will be generally too weak. Therefore, only the unsplit frequencies were used from these two studies. In the unlikely event of detecting *n*-propyl cyanide in cold sources, quadrupole parameters published in Vormann & Dreizler (1988) would be adequate.

There were comparatively few transitions reported in Hirota (1962), and their uncertainties were fairly large. Trial fits with these transitions omitted from the fits caused essentially no change in the values and in the uncertainties of the spectroscopic parameters. Therefore, these transitions were omitted from the final fits. Two transitions, 36_{1,36} – 35_{0,35} of the *anti*-conformer and 31_{5,27} – 30_{5,26} of the *gauche*-conformer, had residuals between observed and calculated frequencies larger than four times the experimental uncertainties. Therefore, these transitions were omitted from the data sets. The final line list for the

Table 8. Spectroscopic parameters^a (MHz) of *n*-propyl cyanide.

Parameter	<i>anti</i>	<i>gauche</i>
<i>A</i>	23 668.319 31 (143)	10 060.416 49 (108)
<i>B</i>	2 268.146 892 (147)	3 267.662 408 (301)
<i>C</i>	2 152.963 946 (168)	2 705.459 572 (290)
<i>D_K</i> × 10 ³	240.653 (29)	60.235 (6)
<i>D_{JK}</i> × 10 ³	−10.826 31 (92)	−18.264 70 (117)
<i>D_J</i> × 10 ⁶	398.674 (69)	3 195.064 (207)
<i>d₁</i> × 10 ⁶	−46.637 (42)	−1 037.470 (55)
<i>d₂</i> × 10 ⁶	−0.590 1 (59)	−77.186 4 (183)
<i>H_K</i> × 10 ⁶	2.5	1.806 (18)
<i>H_{KJ}</i> × 10 ⁹	372.4 (24)	−517.3 (35)
<i>H_{JK}</i> × 10 ⁹	−20.67 (20)	9.92 (68)
<i>H_J</i> × 10 ⁹	0.353 (11)	4.486 (56)
<i>h₁</i> × 10 ⁹	0.117 (14)	2.505 (29)
<i>h₂</i> × 10 ¹²	–	524.6 (135)
<i>h₃</i> × 10 ¹²	–	111.3 (31)
<i>L_{KKJ}</i> × 10 ¹²	–	30.6 (31)
<i>L_{JK}</i> × 10 ¹²	–	−4.11 (78)

^a Watson’s *S*-reduction was used in the representation *I'*. Numbers in parentheses are one standard deviation in units of the least significant figures. Parameter values with no uncertainties given were estimated. A long dash indicates parameters that are determinable in theory, but could not be determined with significance here.

anti-conformer contained 4, 93, and 50 different transition frequencies from Demaison & Dreizler (1982), Włodarczak et al. (1988), and Vormann & Dreizler (1988), respectively. The total number of transitions is larger by 62 because of unresolved asymmetry splitting. The corresponding numbers of different transition frequencies for the *gauche*-conformer are 4, 119, and 46. Unresolved asymmetry splitting causes the total number of transitions to be larger by 46. The final line lists for both conformers are given in Tables 6 and 7 (*online material*).

The asymmetry parameter $\kappa = (2B - A - C)/(A - C)$ is −0.9893 for *anti*-*n*-propyl cyanide, rather close to the symmetric prolate limit of −1. In such cases it is advisable to avoid using Watson’s *A*-reduction and use the *S*-reduction instead. In the case of the *gauche*-conformer one finds $\kappa = -0.8471$. In this case both reductions may be used. In the present work the *S*-reduction was used throughout for consistency reason. The sextic distortion parameter *H_K* of the *anti*-conformer was initially estimated to be smaller than *D_K* by the same factor that that parameter is smaller than *A*. This is certainly only a crude estimate. Trial fits with *H_K* released suggested its value to be slightly larger than this estimate. But since the uncertainty was more than a third of its value and since the difference was smaller than the uncertainty, *H_K* was finally fixed to the estimated value. The final spectroscopic parameters are given in Table 8. Overall, the transition frequencies have been reproduced within experimental uncertainties as the dimensionless rms errors are 0.75 and 0.66 for the *anti* and *gauche*-conformer, respectively. The values for the individual data sets do not differ very much from these values. Moreover, this is reasonably close to 1.0 and suggests the ascribed uncertainties are quite appropriate.

The *gauche*-conformer is considerably more asymmetric than the *anti*-conformer. Therefore, it is probably not surprising that the distortion parameters describing the asymmetry splitting (the off-diagonal *d_i* and the *h_i*) are not only larger in magnitude for the former conformer, but also more of these terms are required in the fits. In addition, two octic centrifugal distortion parameters *L* were needed in the fit of the *gauche*-conformer

resulting in an overall much larger parameter set and thus a much slower converging Hamiltonian compared with the *anti*-conformer. A similar situation occurred in the recent investigation of ethyl formate (Medvedev et al. 2009) where also a much larger set of spectroscopic parameters was needed to fit the data of the *gauche*-conformer compared to the *anti*-conformer.

The predictions used for the current analysis will be made available in the CDMS (Müller et al. 2001, 2005, see footnote 4). The partition function of *n*-propyl cyanide is 5.608×10^4 at 150 K. In the course of the analysis, the two conformers again have been treated separately on occasion to evaluate if the abundance of either conformer is lower than would be expected under LTE conditions.

4.2. Detection of *n*-propyl cyanide in Sgr B2(N)

To identify *n*-propyl cyanide, we used the same method as for ethyl formate (see Sect. 3.2). In our spectral survey, 636 transitions of the *anti*-conformer and 706 transitions of the *gauche*-conformer are predicted above the threshold of 20 mK defined in Sect. 3.2. They are listed in Tables 9 and 10 (*online material*), respectively, which are presented in the same way as Tables 1 and 2. Again, as can be seen in these tables, most of the *n*-propyl cyanide lines covered by our survey of Sgr B2(N) are heavily blended with lines of other molecules and therefore cannot be identified in this source. Only 50 of the 636 transitions of the *anti*-conformer are relatively free of contamination from other molecules, known or still unidentified according to our modeling. They are marked “Detected” or “Group detected” in Col. 8 of Table 9, and are listed with more information in Table 11. We stress that all transitions of sufficient strength predicted in the frequency range of our spectral survey are either detected or blended, i.e. no predicted transition is missing in the observed spectrum. The 50 detected transitions correspond to 12 observed features that are shown in Fig. 3 (*online material*) and labeled in Col. 8 of Table 11. For reference, we show the spectrum observed toward Sgr B2(M) in these figures also. We identified the *n*-propyl cyanide lines and the blends affecting them with the LTE model of this molecule and the LTE model including all molecules (see Sect. 2.2). The parameters of our best-fit LTE model of *n*-propyl cyanide are listed in Table 12, and the model is overlaid in red on the spectrum observed toward Sgr B2(N) in Fig. 3. The best-fit LTE model including all molecules is shown in green in the same figures.

For the frequency range corresponding to each detected *n*-propyl cyanide feature, we list in Table 11 the integrated intensities of the observed spectrum (Col. 10), of the best-fit model of *n*-propyl cyanide (Col. 11), and of the best-fit model including all molecules (Col. 12). In these columns, the dash symbol indicates transitions belonging to the same feature. Columns 1 to 7 of Table 11 are the same as in Table 9. The 1σ uncertainty given for the integrated intensity in Col. 10 was computed using the estimated noise level of Col. 7.

As we did for ethyl formate, we show in Fig. 4a a population diagram derived from the integrated intensities of the detected features of the *anti*-conformer of *n*-propyl cyanide. Figure 4b displays the corresponding diagram after removing the expected contribution from contaminating molecules (see Sect. 3.2 for details). This figure is less helpful than in the case of ethyl formate because all features containing several transitions (6 out of 12) have transitions with different energy levels and cannot be shown in a population diagram. Therefore, this diagram does not help much for the determination of the temperature. Feature 3, which is a blend of transitions with upper energy levels from 61 to

Table 12. Parameters of our best-fit LTE model of *n*-propyl cyanide with two velocity components.

Size ^a (")	T_{rot} ^b (K)	N^c (cm^{-2})	ΔV^d (km s^{-1})	V_{off}^e (km s^{-1})
(1)	(2)	(3)	(4)	(5)
3.0	150	1.50×10^{16}	7.0	-1.0
3.0	150	6.60×10^{15}	7.0	9.0

Notes: ^a Source diameter (*FWHM*). ^b Temperature. ^c Column density. ^d Linewidth (*FWHM*). ^e Velocity offset with respect to the systemic velocity of Sgr B2(N) $V_{\text{lsr}} = 64 \text{ km s}^{-1}$.

147 K, is however reasonably well fitted by our 150 K model (see panel 2 of Fig. 3) and gives us some confidence in this high temperature. This is further confirmed by the high temperatures measured in our survey for chemically related molecules (see Sect. 4.4 below).

Our model for the *anti*-conformer of *n*-propyl cyanide consists of two components with different velocities. The need for a second component mainly comes from the shape of features 2, 9, and 12. Its velocity is consistent with the velocity of the second component we find for many other, more abundant molecules in our survey toward Sgr B2(N). It was shown interferometrically that this second velocity component is a physically distinct source located $\sim 5''$ to the North of the main hot core in Sgr B2(N) (see, e.g., Sect. 3.4 of Belloche et al. 2008a). Our data are consistent with a second component about half as strong in *n*-propyl cyanide as the first component (Table 12). This is also the ratio we found for the two components of ethyl cyanide ($\text{C}_2\text{H}_5\text{CN}$) with the IRAM Plateau de Bure interferometer and the 30 m telescope (see Table 5 of Belloche et al. 2008b). Finally, since all detected transitions are optically thin and the two regions emitting in *n*-propyl cyanide are most likely compact given their high temperature, column density and source size are degenerated. We fixed the source size to $3''$. This is approximately the size of the region emitting in the chemically related molecule ethyl cyanide that we measured with the IRAM Plateau de Bure interferometer (see Table 5 of Belloche et al. 2008b).

From this analysis, we conclude that our best-fit model for the *anti*-conformer of *n*-propyl cyanide is fully consistent with our 30 m data of Sgr B2(N). This is, to our knowledge, the first clear detection of this molecule in space⁸.

No feature of the *gauche*-conformer of *n*-propyl cyanide is clearly detected in our spectral survey of Sgr B2(N). Only one feature at 211.4 GHz is possibly detected but the baseline in this frequency range is very uncertain and this feature is blended with a transition of acetone. If we consider this feature as a detection, it implies a column density a factor 2 smaller than for the

⁸ Jones et al. (2007) tentatively identified two lines detected with the Australia Telescope Compact Array at ~ 86.9556 and ~ 90.0560 GHz as transitions of the *gauche*-conformer of *n*-propyl cyanide. However, our model predicts a peak temperature of the *n*-propyl cyanide transition at 86.955466 GHz 15 times smaller than the peak temperature (0.13 K) of the line detected with the 30 m telescope at this frequency. The tentative identification of Jones et al. (2007) at this frequency is therefore not confirmed. The origin of this line in our survey is still unknown. As far as the other transition is concerned, our model of *n*-propyl cyanide predicts a peak intensity equal to only one quarter of the peak intensity (0.07 K) of the line detected with the 30 m telescope at ~ 90.0560 GHz. Since this line is blended with a transition of $^{13}\text{CH}_3\text{CH}_2\text{CN}$ that has a stronger contribution according to our modeling, the tentative identification of Jones et al. (2007) should be viewed with caution too.

Table 11. Transitions of the *anti*-conformer of *n*-propyl cyanide detected toward Sgr B2(N) with the IRAM 30 m telescope.

N^a	Transition	Frequency (MHz)	Unc. ^b (kHz)	E_l^c (K)	$S\mu^2$ (D ²)	σ^d (mK)	F^e	τ^f	I_{obs}^g (K km s ⁻¹)	I_{mod}^g (K km s ⁻¹)	I_{all}^g (K km s ⁻¹)	Comments
(1)	(2)	(3)	(4)	(5)	(6)	(7)	(8)	(9)	(10)	(11)	(12)	(13)
5	19 _{6,14} – 18 _{6,13}	84021.555	4	73	221	19	1	0.06	3.27(13)	1.90	2.68	partial blend with C ₂ H ₅ CN
6	19 _{6,13} – 18 _{6,12}	84021.556	4	73	221	19	1	–	–	–	–	–
7	19 _{7,12} – 18 _{7,11}	84022.819	5	87	212	19	1	–	–	–	–	–
8	19 _{7,13} – 18 _{7,12}	84022.819	5	87	212	19	1	–	–	–	–	–
9	19 _{5,15} – 18 _{5,14}	84023.956	4	62	229	19	1	–	–	–	–	–
10	19 _{5,14} – 18 _{5,13}	84023.960	4	62	229	19	1	–	–	–	–	–
11	19 _{8,11} – 18 _{8,10}	84026.382	5	102	202	19	1	–	–	–	–	–
12	19 _{8,12} – 18 _{8,11}	84026.382	5	102	202	19	1	–	–	–	–	–
32	20 _{6,14} – 19 _{6,13}	88444.212	5	77	235	17	2	0.06	4.30(11)	2.31	3.28	partial blend with CH ₃ CH ₃ CO, C ₂ H ₅ OH, and U-line?
33	20 _{6,15} – 19 _{6,14}	88444.212	5	77	235	17	2	–	–	–	–	–
34	20 _{7,13} – 19 _{7,12}	88445.075	5	91	227	17	2	–	–	–	–	–
35	20 _{7,14} – 19 _{7,13}	88445.075	5	91	227	17	2	–	–	–	–	–
36	20 _{5,16} – 19 _{5,15}	88447.526	5	66	243	17	2	–	–	–	–	–
37	20 _{5,15} – 19 _{5,14}	88447.532	5	66	243	17	2	–	–	–	–	–
38	20 _{8,12} – 19 _{8,11}	88448.528	5	106	217	17	2	–	–	–	–	–
39	20 _{8,13} – 19 _{8,12}	88448.528	5	106	217	17	2	–	–	–	–	–
40	20 _{9,11} – 19 _{9,10}	88453.836	5	124	206	17	3	0.05	1.90(11)	1.40	2.42	partial blend with C ₂ H ₅ ¹³ CN, ¹³ CH ₃ CH ₂ CN, and CH ₂ (OH)CHO
41	20 _{9,12} – 19 _{9,11}	88453.836	5	124	206	17	3	–	–	–	–	–
42	20 _{4,17} – 19 _{4,16}	88458.794	5	57	248	17	3	–	–	–	–	–
43	20 _{4,16} – 19 _{4,15}	88459.387	5	57	248	17	3	–	–	–	–	–
44	20 _{10,10} – 19 _{10,9}	88460.625	5	143	194	17	3	–	–	–	–	–
45	20 _{10,11} – 19 _{10,10}	88460.625	5	143	194	17	3	–	–	–	–	–
53	20 _{1,19} – 19 _{1,18}	89391.938	5	42	258	16	4	0.03	0.65(08)	0.44	0.62	blend with CH ₃ OCHO, $v_t=1$
55	21 _{0,21} – 20 _{0,20}	92164.912	5	44	272	27	5	0.03	1.15(14)	0.49	0.66	blend with CH ₃ ¹³ CN, $v_8=1$ and U-line?
57	21 _{6,16} – 20 _{6,15}	92866.939	5	82	250	28	6	0.07	1.54(21)	3.17	3.21	uncertain baseline
58	21 _{6,15} – 20 _{6,14}	92866.939	5	82	250	28	6	–	–	–	–	–
59	21 _{7,14} – 20 _{7,13}	92867.332	5	95	242	28	6	–	–	–	–	–
60	21 _{7,15} – 20 _{7,14}	92867.332	5	95	242	28	6	–	–	–	–	–
61	21 _{8,13} – 20 _{8,12}	92870.627	5	110	232	28	6	–	–	–	–	–
62	21 _{8,14} – 20 _{8,13}	92870.627	5	110	232	28	6	–	–	–	–	–
63	21 _{5,17} – 20 _{5,16}	92871.289	5	70	256	28	6	–	–	–	–	–
64	21 _{5,16} – 20 _{5,15}	92871.298	5	70	256	28	6	–	–	–	–	–
65	21 _{9,12} – 20 _{9,11}	92875.977	5	128	222	28	6	–	–	–	–	–
66	21 _{9,13} – 20 _{9,12}	92875.977	5	128	222	28	6	–	–	–	–	–
77	21 _{2,19} – 20 _{2,18}	93376.934	5	49	269	22	7	0.03	0.52(11)	0.49	0.51	no blend
104	22 _{2,20} – 21 _{2,19}	97867.394	5	53	282	20	8	0.03	0.61(10)	0.58	0.63	uncertain baseline
108	10 _{4,6} – 11 _{3,9}	101512.348	5	23	1	16	9	0.03	0.67(08)	0.66	0.96	small blend with CH ₃ CH ₃ CO, $v_t=1$
109	23 _{2,22} – 22 _{2,21}	101515.201	5	58	295	16	9	–	–	–	–	–
110	23 _{7,16} – 22 _{7,15}	101711.846	5	104	270	16	10	0.08	5.74(11)	4.35	6.38	partial blend with ¹³ CH ₂ CHCN, uncertain baseline
111	23 _{7,17} – 22 _{7,16}	101711.846	5	104	270	16	10	–	–	–	–	–
112	23 _{6,18} – 22 _{6,17}	101712.624	5	91	277	16	10	–	–	–	–	–
113	23 _{6,17} – 22 _{6,16}	101712.624	5	91	277	16	10	–	–	–	–	–
114	23 _{8,15} – 22 _{8,14}	101714.680	5	120	262	16	10	–	–	–	–	–
115	23 _{8,16} – 22 _{8,15}	101714.680	5	120	262	16	10	–	–	–	–	–
116	23 _{5,19} – 22 _{5,18}	101719.429	5	79	283	16	10	–	–	–	–	–
117	23 _{5,18} – 22 _{5,17}	101719.450	5	79	283	16	10	–	–	–	–	–
118	23 _{9,14} – 22 _{9,13}	101720.011	5	137	252	16	10	–	–	–	–	–
119	23 _{9,15} – 22 _{9,14}	101720.011	5	137	252	16	10	–	–	–	–	–
161	24 _{3,22} – 23 _{3,21}	106188.197	5	68	306	25	11	0.03	0.97(11)	0.76	0.82	noisy
205	25 _{1,24} – 24 _{1,23}	111593.662	5	65	323	29	12	0.03	1.48(14)	0.90	1.08	no blend

Notes: ^a Numbering of the observed transitions associated with a modeled line stronger than 20 mK (see Table 9). ^b Frequency uncertainty. ^c Lower energy level in temperature units (E_l/k_B). ^d Calculated rms noise level in T_{mb} scale. ^e Numbering of the observed features. ^f Peak opacity of the modeled feature. ^g Integrated intensity in T_{mb} scale for the observed spectrum (Col. 10), the *n*-propyl cyanide model (Col. 11), and the model including all molecules (Col. 12). The uncertainty in Col. 10 is given in parentheses in units of the last digit.

model of the *anti*-conformer, which may suggest a non-thermal distribution of the molecules in the two conformers. However, we first have to evaluate the uncertainty on the ratio of the *anti*- and *gauche*-conformer populations coming from the uncertainty

on their energy difference ($\Delta E = 92 \pm 25 \text{ cm}^{-1}$, see Sect. 4.1). For $\Delta E = 92 \text{ cm}^{-1}$, the *anti* to *gauche* ratio is 0.51/0.49 at 150 K, and increases to 0.57/0.43 for $\Delta E = 117 \text{ cm}^{-1}$, i.e. a variation of $\sim 30\%$. This is not enough to explain the factor 2 mentioned

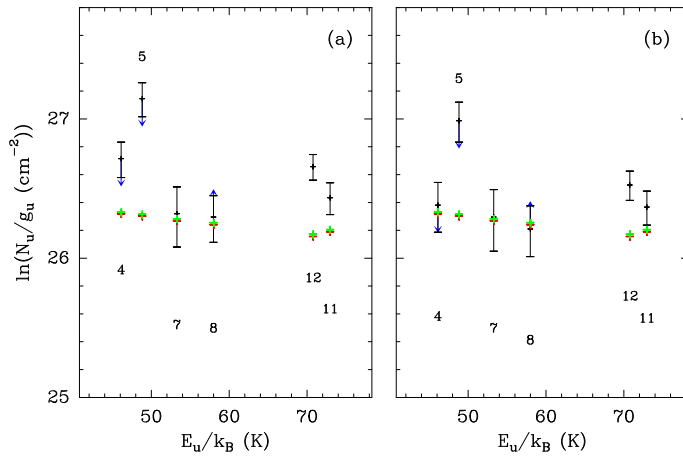


Fig. 4. Population diagram of the *anti*-conformer of *n*-propyl cyanide presented in the same way as for ethyl formate in Fig. 2 (see the caption of that figure for details). Panel **a**) shows the population diagram derived from the measured integrated intensities while panel **b**) presents the population diagram after correction for the expected contribution from contaminating molecules. Features 1, 2, 3, 6, 9, and 10 are blends of several transitions with different energy levels and were therefore omitted.

above, but it can have a significant contribution. Above all, the uncertainty on the baseline level at 211.4 GHz is quite large and the data are still consistent with a thermal distribution of the *gauche*- and *anti*-conformers.

4.3. Upper limit in Sgr B2(M)

We do not detect *n*-propyl cyanide in our spectral survey toward Sgr B2(M). Using the same source size, linewidth, and temperature as for Sgr B2(N) (see Table 12), we find a $\sim 3\sigma$ column density upper limit of $6 \times 10^{15} \text{ cm}^{-2}$ in the LTE approximation for both conformers. The column density of *n*-propyl cyanide is thus at least a factor ~ 2 lower toward Sgr B2(M) than toward Sgr B2(N), which is again consistent with the results of, e.g., Nummelin et al. (2000) for other molecules.

4.4. Comparison to related species

We easily detect the already known molecules methyl cyanide (CH_3CN) and ethyl cyanide ($\text{C}_2\text{H}_5\text{CN}$) in our survey toward Sgr B2(N) (see also, e.g., Miao et al. 1995; Liu & Snyder 1999; Nummelin et al. 2000). The parameters of our current best fit models of these two molecules are listed in Table 13. Our models use also constraints from the weaker isotopologues containing ^{13}C (see, e.g., Müller et al. 2008). The source size is constrained by the optically thick transitions, once the temperature has been fitted. For ethyl cyanide, we used in addition the constraints on the source size derived from our high angular resolution observations with the IRAM Plateau de Bure interferometer (see Table 5 of Belloche et al. 2008b). The first two velocity components detected in methyl cyanide and ethyl cyanide correspond to the two hot cores embedded in Sgr B2(N) (see, e.g., Hollis et al. 2003; Belloche et al. 2008a). They are also seen in *n*-propyl cyanide. In addition, methyl cyanide and ethyl cyanide show a third component that may arise from the blueshifted lobe of an outflow (see the cyanoacetylene $v_7 = 1$ emission in Fig. 5k to m of Belloche et al. 2008a). The redshifted counterpart

Table 13. Parameters of our best-fit LTE models of methyl cyanide, ethyl cyanide, vinyl cyanide, and aminoacetonitrile, and column density upper limit for cyanomethylidyne.

Molecule ^a	Size ^b ($''$)	T_{rot} ^c (K)	N^d (cm^{-2})	ΔV^e (km s^{-1})	V_{off}^f (km s^{-1})
(1)	(2)	(3)	(4)	(5)	(6)
CH_3CN	2.7	200	2.00×10^{18}	6.5	-1.0
	2.7	200	8.00×10^{17}	6.5	9.0
	2.7	200	1.00×10^{17}	8.0	-11.0
$\text{C}_2\text{H}_5\text{CN}$	3.0	170	1.20×10^{18}	6.5	-1.0
	2.3	170	1.40×10^{18}	6.5	9.0
	1.7	170	9.00×10^{17}	8.0	-11.0
$\text{C}_2\text{H}_3\text{CN}$	2.3	170	8.00×10^{17}	7.0	-1.0
	2.3	170	2.40×10^{17}	7.0	9.0
	2.3	170	1.00×10^{17}	10.0	-9.0
$\text{NH}_2\text{CH}_2\text{CN}$	2.0	100	2.80×10^{16}	7.0	0.0
CCN ^g	3.0	200	$< 1.20 \times 10^{17}$	6.5	-1.0
	3.0	200	$< 1.20 \times 10^{17}$	6.5	9.0

Notes: ^a We used the JPL entry for CH_3CN (version 3), and the CDMS entries for $\text{C}_2\text{H}_5\text{CN}$ (ver. 1), $\text{C}_2\text{H}_3\text{CN}$ (ver. 1), $\text{NH}_2\text{CH}_2\text{CN}$ (ver. 1), and CCN (ver. 1). See references to the laboratory data therein. ^b Source diameter (*FWHM*). ^c Temperature. ^d Column density. ^e Linewidth (*FWHM*). ^f Velocity offset with respect to the systemic velocity of Sgr B2(N) $V_{\text{lsr}} = 64 \text{ km s}^{-1}$. ^g The column density upper limit is $\sim 3\sigma$. The other parameters were fixed.

is blended with the northern component in the single-dish beam (see Fig. 3 of Hollis et al. 2003). The third velocity component is too faint to be detected in *n*-propyl cyanide.

The model parameters for the compact sources listed for methyl cyanide in Table 13 are mostly based on the ^{13}C isotopologues with a $^{12}\text{C}/^{13}\text{C}$ isotopic ratio of 20 because the transitions of the ^{12}C main isotopologue are very optically thick and most likely dominated by large scale emission (see maps of, e.g., de Vicente et al. 1997; Jones et al. 2008). de Vicente et al. (1997) analysed their maps of methyl cyanide emission in the Large Velocity Gradient approximation. They found that the emission consists of several components (hot core, warm envelope, diffuse and hot envelope), and mentioned that their modeling toward Sgr B2(N) is uncertain because of the large opacities. However, their figure 5 suggests that the temperature and column density of methyl cyanide are strongly centrally peaked toward Sgr B2(N). Therefore, the emission of the optically thin ^{13}C isotopologues should be dominated by the compact hot cores which gives us some confidence (within a factor of 2) in the column densities listed in Table 13. Friedel et al. (2004) measured similar intensities for $\text{CH}_3^{13}\text{CN}$ with the NRAO 12 m telescope and the BIMA interferometer toward Sgr B2(N), an additional evidence that the compact hot cores dominate the emission of the ^{13}C isotopologues we detected with the 30 m telescope. For a source size of $2.7''$, Nummelin et al. (2000) found column densities of $0.7 - 1.1 \times 10^{17} \text{ cm}^{-2}$ for the ^{13}C isotopologues, which translates into a column density of $1.4 - 2.2 \times 10^{18} \text{ cm}^{-2}$ for the main isotopologue assuming a $^{12}\text{C}/^{13}\text{C}$ isotopic ratio of 20. This is in very good agreement with our result (see Table 13).

Assuming a temperature of 200 K and optically thin emission, Liu et al. (2001) obtained a beam-averaged column density of $4.63 \pm 0.14 \times 10^{16} \text{ cm}^{-2}$ for ethyl cyanide with BIMA at 89.6 GHz (*HPBW* = $14'' \times 4''$). For a source size of $3''$, this translates into a column density of $2.9 \times 10^{17} \text{ cm}^{-2}$, which is a factor 4 smaller than the column density we derive for the main

velocity component. However, our model predicts peak line opacities of 4–6 for these transitions, which is supported by our simultaneous modeling of the ^{13}C isotopologues of ethyl cyanide (see Müller et al. 2008). As a result, Liu et al. (2001) most likely underestimated the column densities of ethyl cyanide by a factor of a few, which reconciles the single-dish and interferometric measurements and confirms that the source of ethyl cyanide emission is compact. This is also confirmed by the reasonable agreement between the 30 m and Plateau de Bure Interferometer fluxes published by Belloche et al. (2008b) at 81.7 GHz (see their Table 5). The compactness of the source of ethyl cyanide emission most likely explains the discrepancy with the column density found by Nummelin et al. (2000) with SEST in the 1.3 mm wavelength range ($HPBW \sim 23''$). These authors derived temperatures of 175_{-20}^{+25} K and 210_{-30}^{+30} K and beam-averaged column densities of $1.6_{-0.1}^{+0.2} \times 10^{15} \text{ cm}^{-2}$ and $1.5_{-0.3}^{+0.4} \times 10^{16} \text{ cm}^{-2}$ for the ethyl cyanide *a*- and *b*-type lines, respectively. While they find an order of magnitude difference between the column densities of the *a*- and *b*-type lines, we successfully reproduce the ethyl cyanide emission in our 3 mm survey with a single model for the two types of lines, the former being optically thick while the latter are optically thin. Our model with a small source size predicts line opacities on the order of 10–30 for the *a*-type lines in the 1.3 mm range. Hence, we believe that the column density derived by Nummelin et al. (2000) for these lines at 1.3 mm is underestimated by a large factor because they assumed a beam filling factor of 1, yielding opacities for these lines that were too low. On the other hand, since our model predicts opacities ≤ 1 for the *b*-type lines at 1.3 mm, we would expect the column density derived by these authors to match ours. For a source size of $3''$, their column density of the *b*-type lines translates into a column density of $9.0 \times 10^{17} \text{ cm}^{-2}$, which is about a factor 2 smaller than the sum of the column densities of the two main velocity components in Table 13 (after rescaling the second one to a source size of $3''$). As in Sect. 3.4, we think that the discrepancy arises from the uncertain baseline level and the partial dust absorption in the 1.3 mm wavelength range. Our current model, which suffers from the same problems, also over-predicts intensities for the lines detected in our partial 1.3 mm survey.

After rescaling to the same size of $3''$, the relative column densities of the three related molecules $\text{CH}_3\text{CN} / \text{C}_2\text{H}_5\text{CN} / \text{C}_3\text{H}_7\text{CN}$ are 108/80/1 for the first velocity component and 98/125/1 for the second velocity component. We discuss these ratios and the implications for the interstellar chemistry in Sect. 5.

In addition, we list in Table 13 the best-fit parameters we found for vinyl cyanide (Müller et al. 2008) and aminoacetonitrile (Belloche et al. 2008a), as well as an upper limit for the column density of cyanomethylidyne (CCN) for which the other parameters were fixed.

5. Chemical modeling and discussion

To better understand the observational results, we model the chemistry of Sgr B2(N) using a coupled gas-phase and grain-surface chemical code. Garrod et al. (2008) constructed a reaction network to account for the grain-surface formation of many complex molecules observed in hot cores. Surface formation was assumed to occur primarily by the addition of functional-group radicals derived from molecular ices or from other molecules formed in this way. Such reactions are viable when larger radicals become mobile at intermediate grain temperatures ($T_d \gtrsim 20$ K), achieved during the warm-up to typical hot-core temperatures (> 100 K). The network also includes destruction mecha-

nisms for all complex species, consisting of neutral–neutral reactions on the grain surfaces, ion–molecule reactions with simple ions in the gas phase, and cosmic ray-induced photodissociation both in the gas phase and on the grains. To this network we have added appropriate formation and destruction mechanisms for ethyl formate, ethyl and *n*-propyl cyanide, and also the recently identified aminoacetonitrile ($\text{NH}_2\text{CH}_2\text{CN}$, Belloche et al. 2008a,b), whose surface formation routes may be similar to the other cyanides. In addition, surface hydrogenation routes have been added to allow for the full hydrogenation of the carbon chains C_3 and C_4 , which was not previously considered, as well as the associated hydrogenated species and their destruction channels. The techniques used to construct the new reaction set are presented in detail by Garrod et al. (2008); the current model may be regarded as a consistent extension to that network.

We employ the single-point physical model used by Garrod & Herbst (2006), in which the isothermal collapse of a diffuse medium, to a density $n_H = 10^7 \text{ cm}^{-3}$, is followed by a warm-up from 10 to 200 K. Their T_2 warm-up profile is assumed, in which the hot-core temperature has a t^2 dependence on the time, t , elapsed in the warm-up phase. Dust and gas temperatures are assumed to be well coupled, hence we let $T = T_K = T_{dust}$. The warm-up timescale is representative of the time required for a parcel of gas to achieve a temperature of 200 K, as the hot core forms; it therefore does not relate directly to the *current* infall timescale.

This model traces the evolution of the chemistry up to a temperature of 200 K, associated with the central hot-core region. However, these time-dependent results may also be considered to represent differing spatial extents from the hot-core center, with the innermost regions being the most evolved and achieving the highest temperatures. As such, the time-dependent abundance profiles presented below also indicate a snapshot of the chemistry through the hot core.

Since we are interested mainly in specific features of the model, we choose not to fix the ice composition prior to the warm-up phase, but use the unadulterated composition computed in the collapse-phase.

Other details of the model may be found in Garrod et al. (2008). One important difference is the removal, in keeping with prior chemical networks, of the activation energy barrier for the surface reaction $\text{OH} + \text{H}_2\text{CO} \rightarrow \text{HCO} + \text{H}_2\text{O}$. Garrod et al. employed an activation energy merely for consistency with other hydrogen-abstraction reactions of OH. The available evidence, however, suggests there is no barrier⁹. This change makes HCO radicals somewhat more abundant on the grains, tending to increase the final abundances of species such as methyl formate, which is consistent with our observational results.

5.1. Surface Chemistry

Surface chemical routes for the formation of methyl cyanide, CH_3CN , were already present in the Garrod et al. (2008) network, including direct addition of methyl and nitrile groups, and repetitive surface hydrogenation of gas phase-produced C_2N . Formation of ethyl cyanide, $\text{C}_2\text{H}_5\text{CN}$, was limited to repetitive surface hydrogenation of cyanoacetylene HC_3N and vinyl cyanide, $\text{C}_2\text{H}_3\text{CN}$, both of which may be formed in the gas phase. *n*-Propyl cyanide and aminoacetonitrile were not present at all.

⁹ See the chemical kinetics database of the National Institute of Standards and Technology (NIST), <http://kinetics.nist.gov/kinetics>.

Table 14 shows the full set of surface reactions employed in the current model to form methyl cyanide, ethyl cyanide, *n*-propyl cyanide, aminoacetonitrile, and ethylformate, as well as a selection of significant cosmic ray-induced photodissociation processes that may occur on grain surfaces. (The same CR-induced processes are assumed also to occur in the gas phase, at the same rates). A cosmic-ray ionization rate of $\zeta_0 = 1.3 \times 10^{-17} \text{ s}^{-1}$ is assumed.

The new reactions allow each cyanide to be constructed by sequential formation of its carbon backbone by the addition of CH_2 , CH_3 , or yet larger hydrocarbon radicals; however, photodissociation also allows the break-down of these structures. The resultant radicals may further react with another functional-group radical, to extend the backbone, or with a hydrogen atom, to terminate this sequence. Similarly, aminoacetonitrile may be formed by the addition of NH or NH_2 groups, or by direct addition of CN to CH_2NH_2 , or CH_2NH (followed by hydrogenation). Different routes will dominate according to the relative mobilities of competing radicals, and their availabilities. Hence, the net direction of inter-conversion between cyanides may change with temperature, or as the abundances of molecular precursors vary.

Ethyl formate may be formed on grain surfaces by the addition of a CH_3 or HCO radical to a CH_2OCHO or $\text{C}_2\text{H}_5\text{O}$ radical, respectively. These latter species are formed directly by cosmic ray-induced photodissociation of methyl formate or ethanol on the grains; hence, methyl formate need not be the only precursor for ethyl formate, nor the most important one. We do not consider other routes to the formation of CH_2OCHO and $\text{C}_2\text{H}_5\text{O}$; radical addition to formaldehyde, H_2CO , would almost certainly be mediated by a substantial activation energy barrier. Alternatively, addition of an oxygen atom to C_2H_5 is unlikely to be important, due to the relative scarcity of atomic oxygen, which is mainly bound in the ice mantles as H_2O ; however, this route cannot be entirely ruled out.

When the grain surface-produced molecules evaporate, they are subject to gas-phase destruction mechanisms. Whilst cosmic ray-induced photodissociation in the gas phase is also included for consistency, the gas-phase destruction of these molecules is dominated by reaction with the ions C^+ , He^+ , H_3^+ , H_3O^+ and HCO^+ (followed by dissociative recombination, if a protonated molecule results). Ion-molecule and dissociative recombination reaction rates are of a similar order for all new species; see Garrod et al. (2008).

5.2. Results

We analyse the model results for ethyl formate and the cyanides in the context of a selection of complex molecules to which they are chemically or observationally related. We consider first the results of the basic model described above (called hereafter *Basic* model), using an intermediate warm-up timescale of $2 \times 10^5 \text{ yr}$. This timescale was found by Garrod et al. (2008) to be most appropriate to match the abundances of Sgr B2(N).

5.2.1. Ethyl formate and related species

Table 15 presents peak fractional abundances, and the temperatures at which they are achieved, derived from the chemical model. Model abundances are converted to values per mean particle with a mean molecular weight, μ , of 2.33, for comparison to the observations. Also listed are the observed rotational temperatures and abundances (Cols. 7 and 8, respectively). The latter were derived from the column densities given in Tables 4, 5, 12,

Table 14. Surface reactions and cosmic-ray induced surface photodissociation processes related to the formation of cyanides, and ethyl formate.

Reaction	Garrod et al. (2008)	<i>Basic</i> model	<i>Select</i> model
$\text{C}_2\text{N} + \text{H} \rightarrow \text{HCCN}$	•	•	•
$\text{HCCN} + \text{H} \rightarrow \text{CH}_2\text{CN}$	•	•	•
$\text{CH}_2\text{CN} + \text{H} \rightarrow \text{CH}_3\text{CN}$	•	•	•
$\text{HC}_3\text{N} + \text{H} \rightarrow \text{C}_2\text{H}_2\text{CN}$ (1210 K)	•	•	
$\text{C}_2\text{H}_2\text{CN} + \text{H} \rightarrow \text{C}_2\text{H}_3\text{CN}$	•	•	
$\text{C}_2\text{H}_3\text{CN} + \text{H} \rightarrow \text{C}_2\text{H}_4\text{CN}$ (750 K)	•	•	
$\text{C}_2\text{H}_4\text{CN} + \text{H} \rightarrow \text{C}_2\text{H}_5\text{CN}$	•	•	•
$\text{C}_3\text{H}_6\text{CN} + \text{H} \rightarrow \text{C}_3\text{H}_7\text{CN}$		•	•
$\text{CH}_2 + \text{CN} \rightarrow \text{CH}_2\text{CN}$	•	•	•
$\text{CH}_3 + \text{CN} \rightarrow \text{CH}_3\text{CN}$	•	•	•
$\text{CH}_2 + \text{CH}_2\text{CN} \rightarrow \text{C}_2\text{H}_4\text{CN}$		•	•
$\text{CH}_3 + \text{CH}_2\text{CN} \rightarrow \text{C}_2\text{H}_5\text{CN}$		•	•
$\text{CH}_2 + \text{C}_2\text{H}_4\text{CN} \rightarrow \text{C}_3\text{H}_6\text{CN}$		•	•
$\text{CH}_3 + \text{C}_2\text{H}_4\text{CN} \rightarrow \text{C}_3\text{H}_7\text{CN}$		•	•
$\text{C}_2\text{H}_5 + \text{CN} \rightarrow \text{C}_2\text{H}_5\text{CN}$		•	
$\text{C}_3\text{H}_7 + \text{CN} \rightarrow \text{C}_3\text{H}_7\text{CN}$		•	
$\text{NH} + \text{CH}_2\text{CN} \rightarrow \text{NHCH}_2\text{CN}$		•	•
$\text{NH}_2 + \text{CH}_2\text{CN} \rightarrow \text{NH}_2\text{CH}_2\text{CN}$		•	•
$\text{H} + \text{NHCH}_2\text{CN} \rightarrow \text{NH}_2\text{CH}_2\text{CN}$		•	•
$\text{CH}_2\text{NH} + \text{CN} \rightarrow \text{NHCH}_2\text{CN}$		•	
$\text{CH}_2\text{NH}_2 + \text{CN} \rightarrow \text{NH}_2\text{CH}_2\text{CN}$		•	
$\text{CH}_3\text{CN} + h\nu \rightarrow \text{CH}_2\text{CN} + \text{H}$		•	•
$\text{CH}_3\text{CN} + h\nu \rightarrow \text{CH}_3 + \text{CN}$	•	•	•
$\text{C}_2\text{H}_5\text{CN} + h\nu \rightarrow \text{C}_2\text{H}_4\text{CN} + \text{H}$		•	•
$\text{C}_2\text{H}_5\text{CN} + h\nu \rightarrow \text{CH}_3 + \text{CH}_2\text{CN}$		•	•
$\text{C}_2\text{H}_5\text{CN} + h\nu \rightarrow \text{C}_2\text{H}_5 + \text{CN}$	•	•	•
$\text{C}_3\text{H}_7\text{CN} + h\nu \rightarrow \text{CH}_3 + \text{C}_2\text{H}_4\text{CN}$		•	•
$\text{C}_3\text{H}_7\text{CN} + h\nu \rightarrow \text{C}_2\text{H}_5 + \text{CH}_2\text{CN}$		•	•
$\text{C}_3\text{H}_7\text{CN} + h\nu \rightarrow \text{C}_3\text{H}_7 + \text{CN}$		•	•
$\text{NH}_2\text{CH}_2\text{CN} + h\nu \rightarrow \text{NH}_2 + \text{CH}_2\text{CN}$		•	•
$\text{NH}_2\text{CH}_2\text{CN} + h\nu \rightarrow \text{NH}_2\text{CH}_2 + \text{CN}$		•	•
$\text{CH}_3 + \text{CH}_2\text{OCHO} \rightarrow \text{C}_2\text{H}_5\text{OCHO}$		•	•
$\text{H} + \text{CH}_2\text{OCHO} \rightarrow \text{CH}_3\text{OCHO}$		•	•
$\text{HCO} + \text{C}_2\text{H}_5\text{O} \rightarrow \text{C}_2\text{H}_5\text{OCHO}$		•	•
$\text{H} + \text{C}_2\text{H}_5\text{O} \rightarrow \text{C}_2\text{H}_5\text{OH}$		•	•
$\text{CH}_3\text{OCHO} + h\nu \rightarrow \text{CH}_2\text{OCHO} + \text{H}$		•	•
$\text{C}_2\text{H}_5\text{OH} + h\nu \rightarrow \text{C}_2\text{H}_5\text{O} + \text{H}$		•	•
$\text{C}_2\text{H}_5\text{OCHO} + h\nu \rightarrow \text{CH}_2\text{OCHO} + \text{CH}_3$		•	•
$\text{C}_2\text{H}_5\text{OCHO} + h\nu \rightarrow \text{C}_2\text{H}_5\text{O} + \text{HCO}$		•	•

Notes: Reactions that were present in the hot core model of Garrod et al. (2008) are indicated. Activation energies required for reaction are shown in brackets, where applicable.

and 13, assuming an H_2 column density of $1.8 \times 10^{25} \text{ cm}^{-2}$ for a source size of $2''$ (see Belloche et al. 2008b), and an H_2 column density profile proportional to $r^{-0.5}$ that corresponds to an H_2 density profile proportional to $r^{-1.5}$ in spherical symmetry¹⁰. Given that the dust properties are uncertain by a factor ~ 2 at least and that the contribution of the vibrationally or torsionally excited states of some molecules studied here (e.g. ethanol, see Pearson et al. 2008) to their partition function was not included, we estimate these observed abundances to be accurate within a factor ~ 3 .

Ethyl formate is clearly formed most significantly at late times (see Fig. 5a), and its grain-surface abundance (dotted red lines) scales well with that of methyl formate. Grain-surface methyl formate is, in fact, the primary source of precursor radicals (via photodissociation) for the formation of ethyl formate. When methyl formate evaporates, and ethanol is left as the dominant source of precursor radicals, ethyl formate production becomes dependent on the addition of HCO to C_2H_5O . The post-evaporation gas-phase abundance of ethyl formate relative to methyl formate and formic acid appears to match observational abundances and rotational temperatures reasonably well.

The gas-phase methyl formate peak abundance is also relatively close to the observed abundance (within a factor 5), and the model temperature at this peak is in very good agreement with the observed rotational temperature (see Table 5). However, the abundance quickly falls, and the ratio of gas phase CH_3OCHO to $HCOOH$, C_2H_5OH and CH_3OCH_3 at the higher temperatures most appropriate to the densest regions of the hot core is low compared to the observed values.

The *Basic* model uses the same binding energies for methyl formate and dimethyl ether as were employed by Garrod et al. (2008), appropriate to binding on amorphous water ice. These values cause relatively early evaporation of those species, resulting in significant destruction in the gas-phase, and low fractional abundances in comparison to observed values in the case of methyl formate. The binding energies of those molecules were obtained by simple interpolation of measured values obtained for other species. Laboratory data for methyl formate and dimethyl ether evaporation from appropriate ice surfaces are not currently available.

For species comprising at least one -OH functional group, binding-energy estimates take account of hydrogen-bonding interactions with the ice surface. Such species may act as both hydrogen-bond donors and acceptors, raising their binding strengths. However, both methyl formate and dimethyl ether have at least one unbonded electron pair attached to a strongly electro-negative atom (oxygen), allowing them to be hydrogen-bond acceptors. This may give them a somewhat stronger bond to the predominantly water-ice surface than has been assumed.

Here, the binding energy of methyl formate is raised beyond that of the *Basic* model, such that it falls approximately half way between its old value and that of ethanol, its most closely-matched counterpart with a single, fully hydrogen-bonding functional group. This augmentation constitutes an increase of approximately 1000 K, giving $E_D = 5200$ K. The binding energy of dimethyl ether is similarly raised by 1000 K.

Augmentation of methyl formate binding energy allows it to remain on grains for longer, reducing the time available for gas-phase destruction, before the majority of other species evaporate,

damping the effect of ion-molecule destruction pathways (see Fig. 5b). This allows gas-phase methyl formate fractional abundances to remain high for longer, although the resulting peak-abundance temperature is somewhat greater, at 112 K.

Dimethyl ether does have a viable gas-phase formation mechanism, and is largely produced in the gas phase, due to the large abundance of methanol ($\sim 10^{-5} n_H$); hence, the peak abundance is not strongly affected by the augmentation of its binding energy. Its gas-phase abundance in the model is consistent with the observed value (within a factor 2, see Table 15). The peak-abundance temperature of the model is somewhat higher than that derived observationally. A slightly lower grain-surface methanol abundance would remedy this, as post-evaporation gas-phase methanol abundances should diminish more rapidly, reducing the rate of dimethyl ether formation. A slower warm-up subsequent to methanol evaporation would also produce a similar effect. Nevertheless, the observed rotational temperature of dimethyl ether seems consistent with gas-phase formation.

Surface formation rates of ethyl formate, methyl formate and ethanol are not strictly dependent on methanol abundance in the ices, but rather on the rate of formation of its photodissociation products, CH_3O , CH_2OH , and CH_3 . These rates are not well constrained; however, they seem appropriate for this model. A lower grain-surface methanol abundance, as suggested above, would therefore necessitate slightly greater methanol photodissociation rates, in order to achieve appropriate abundances for methyl formate and other surface-formed species. Gas-phase and grain-surface ethyl formate abundances are largely unaffected by the changes in methyl formate binding energy. Both the gas-phase and grain-surface abundances of formic acid are strongly dependent on gas-phase processes (see Garrod et al. 2008). As a result, there appears to be no simple correlation with ethyl or methyl formate abundances. However, the low rotational temperature reported in Sect. 3.4 is qualitatively consistent with the low-temperature gas-phase formic acid peak at 40–60 K, a point noted by Garrod et al. (2008) in comparison to other hot-core observations. This “cold” peak presents a fractional abundance very close to the observed value (within a factor 4, see Table 15). In Sect 3.4, we modeled the spectrum of formic acid using a single temperature component; however, a two-component model with rotational temperatures (and inferred spatial extents) appropriate to the chemical models is not noticeably worse than the single-component fit. As discussed in Sect. 3.4, the existence of both hot, compact and cold, extended components would be consistent with the lower flux measured with the BIMA interferometer by Liu et al. (2001) compared to our lower-resolution single-dish measurement.

5.2.2. Cyanides

The *Basic* model is capable of producing cyanide species in appropriate absolute quantities (see Fig. 6a), however, their relative abundances are not well matched to the observationally determined values. In order to understand the behavior of the cyanide network, the different grain-surface formation mechanisms, and combinations, were isolated by artificially de-activating particular reaction routes. In fact, all combinations that include either the hydrogenation of the cyanopolyne HC_3N and of vinyl cyanide, C_2H_3CN , or the addition of large, pre-formed hydrocarbons directly to the CN radical, produce wildly inaccurate ratios. In some such cases, *n*-propyl cyanide is the most abundant of all, often with methyl cyanide abundances deeply depressed. The only combination in which the correct proportion is reproduced is that in which only the sequential addition of

¹⁰ Osorio et al. (1999) expect a density profile proportional to r^{-p} with $p = 1.5$ for the central region of a hot core. On larger scales in Sgr B2 (20–200''), Lis & Goldsmith (1989) derived a density profile $p \sim 2-2.5$ while de Vicente et al. (1997) found $p \sim 0.9$.

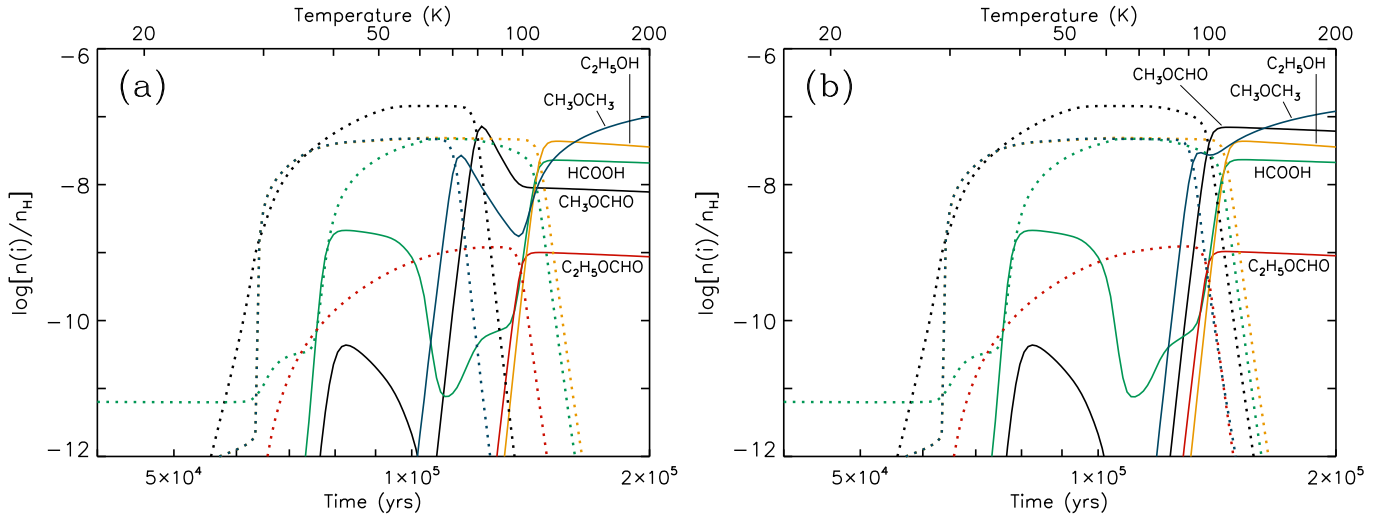


Fig. 5. **a)** *Basic* model, showing methyl formate, ethyl formate, formic acid, and related species. **b)** The same species, following augmentation of methyl formate and dimethyl ether binding energies. Solid lines indicate gas-phase species; dotted lines of the same color indicate the same species on the grain surfaces.

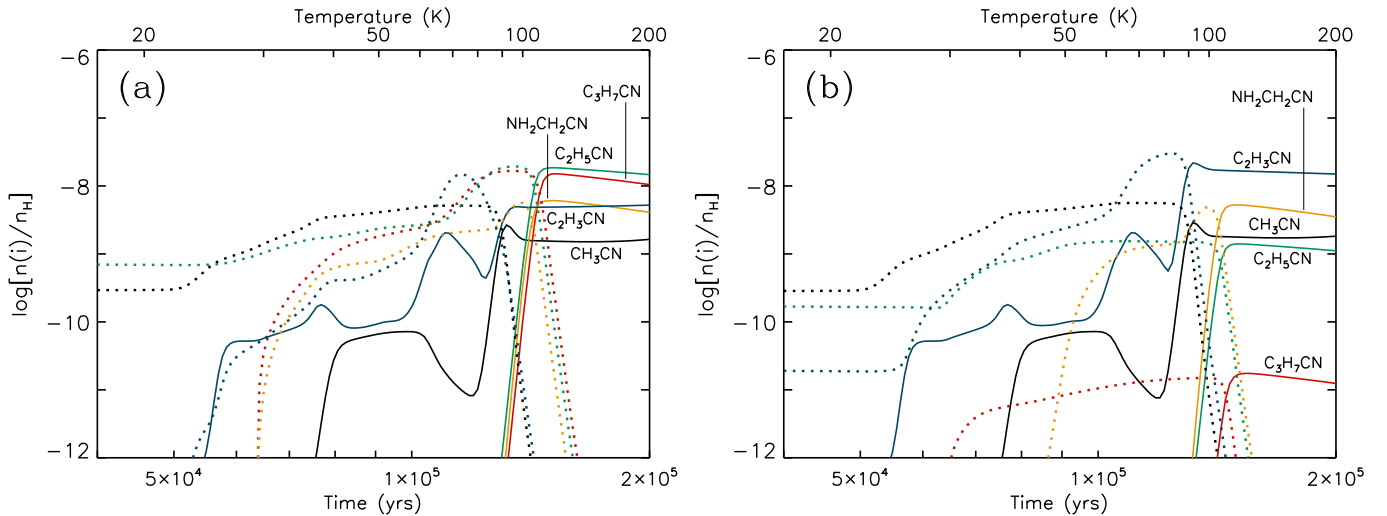


Fig. 6. **a)** *Basic* model, showing cyanides. **b)** The same species, using the *Select* model, in which selected grain-surface reactions are de-activated (see Table 14). Solid lines indicate gas-phase species; dotted lines of the same color indicate the same species on the grain surfaces.

grain-surface CH_2 and CH_3 functional groups is allowed (see Fig. 6b). We label this model, combined with the augmented binding energies of methyl formate and dimethyl ether, as the *Select* model. In this scheme, formation of the larger cyanides begins with cosmic ray-induced photodissociation of a smaller grain-surface alkyl cyanide molecule (resulting in the ejection of a hydrogen atom), or with the accretion of CH_2CN (which may be formed in the gas-phase following the evaporation of HCN). A methyl-group radical is then added to produce a larger alkyl cyanide molecule.

Methyl cyanide itself is mainly formed on the grains by addition of CH_3 and CN radicals, but it may also be formed by gas-phase processes fuelled by the evaporation of HCN. Methyl cyanide evaporates from the dust grains around 90 K, producing its greatest gas-phase abundance; however, the subsequent evaporation of all molecular material from the grains promotes rapid gas-phase formation, maintaining methyl cyanide abun-

dances for longer, and providing qualitative agreement with the large rotational temperature derived from the observational data.

The abundance obtained for aminoacetonitrile is in reasonable agreement with that obtained observationally (within a factor 8), suggesting that the addition of NH or NH_2 to CH_2CN on grain surfaces, similar to the suggested mechanism for ethyl cyanide, is a plausible route to its formation. There may therefore be some degree of correlation between these two species, which should be investigated in future. The removal of the other formation routes for aminoacetonitrile, comprising the addition of grain-surface CN to either CH_2NH or CH_2NH_2 , makes little difference to the results, mainly due to limited availability of the latter two radicals.

Vinyl cyanide, $\text{C}_2\text{H}_3\text{CN}$, a potential precursor of ethyl cyanide and *n*-propyl cyanide, is formed predominantly in the gas-phase in both the *Basic* and *Select* models. This occurs through the reaction of CN with ethylene (C_2H_4), which has been shown experimentally to be rapid over a range of temper-

Table 15. Peak gas-phase abundances from each model, with corresponding model temperatures, as well as source sizes, rotation temperatures, and gas-phase abundances derived from the observations of the main source in Sgr B2(N).

Species	<i>Basic</i> model		<i>Select</i> model		Observations			Abundance ratio
	$n[i]/n_{\text{H}_2}$	T^a (K)	$n[i]/n_{\text{H}_2}$	T^a (K)	Size (")	T_{rot} (K)	$n[i]/n_{\text{H}_2}$	<i>Select</i> model over observation
(1)	(2)	(3)	(4)	(5)	(6)	(7)	(8)	(9)
HCOOH (hot)	5.4e-08	120	5.4e-08	120	5.0	70	1.3e-09	42
HCOOH (cold)	4.9e-09	42	4.9e-09	42	5.0	70	1.3e-09	3.8
CH ₃ OCHO	1.7e-07	81	1.6e-07	112	4.0	80	3.5e-08	4.6
C ₂ H ₅ OCHO	2.3e-09	110	2.3e-09	110	3.0	100	3.6e-09	0.6
C ₂ H ₅ OH	1.0e-07	120	1.0e-07	120	3.0	100	5.7e-08	1.8
CH ₃ OCH ₃	2.3e-07	200	2.8e-07	200	2.5	130	1.4e-07	2.0
CH ₃ CN	6.3e-09	92	6.8e-09	92	2.7	200	1.3e-07	0.05
C ₂ H ₅ CN	4.4e-08	117	3.3e-09	117	3.0	170	8.1e-08	0.04
C ₃ H ₇ CN	3.5e-08	120	4.0e-11	123	3.0	150	1.0e-09	0.04
NH ₂ CH ₂ CN	1.4e-08	117	1.2e-08	117	2.0	100	1.5e-09	8.0
C ₂ H ₃ CN	1.2e-08	200	5.1e-08	92	2.3	170	4.7e-08	1.1

Notes: ^a The model temperatures are the temperatures at which the peak gas-phase abundances are achieved.

atures (Carty et al. 2001). The resultant gas-phase vinyl cyanide then accretes onto the grains until greater temperatures are achieved. Following evaporation of the ice mantles at $T > 100$ K, vinyl cyanide is again formed rapidly in the gas-phase by the same mechanism, allowing it, like methyl cyanide, to retain large fractional abundances longer than the other cyanides. This effect is also in qualitative agreement with its relatively high rotational temperature. Both models show good agreement with the observational abundance of this molecule, but the *Select* model produces an excellent match (see Table 15).

For the *Basic* model, ratios of peak abundance values are HCOOH / CH₃OCHO / C₂H₅OCHO = 23 / 72 / 1 and CH₃CN / C₂H₅CN / C₃H₇CN = 0.18 / 1.3 / 1. For the *Select* model, these ratios are HCOOH / CH₃OCHO / C₂H₅OCHO = 23 / 70 / 1 and CH₃CN / C₂H₅CN / C₃H₇CN = 171 / 82 / 1. These seem a fair match to the observed values of Sects. 3.4 and 4.4 (0.8 / 15 / 1 and 108 / 80 / 1, respectively). Consideration of only the low temperature formic acid peak in the models further improves its ratio with ethyl formate abundances.

The warm-up timescale of $t_{\text{max}} = 2 \times 10^5$ yr appears to yield the most appropriate reproduction of observed cyanide ratios, although longer timescales are also plausible; the *Select* model, with $t_{\text{max}} = 10^6$ yr, produces peak abundance ratios of HCOOH / CH₃OCHO / C₂H₅OCHO = 4.2 / 3.3 / 1 and CH₃CN / C₂H₅CN / C₃H₇CN = 258 / 106 / 1.

5.3. Discussion

Based on the abundance ratios of the model, the dominant formation mechanism for alkyl cyanides is probably the sequential addition of CH₂ or CH₃ radicals to CN, CH₂CN and C₂H₄CN on the grain surfaces. Both the alternative routes – the grain-surface hydrogenation of gas phase-formed HC₃N and C₂H₃CN, or the direct grain-surface addition of pre-formed large hydrocarbon radicals like C₂H₅ or C₃H₇ to a CN radical – appear to be very much too fast, resulting in excessive quantities of the two largest alkyl cyanides.

To achieve the appropriate ratios, those two formation routes must be artificially disabled within the model. Why should these mechanisms be less efficient in reality than they would appear from the model? Firstly, gas-phase HC₃N and C₂H₃CN may be less abundant than the model suggests. The evaporation, and subsequent reaction, of HCN from the grains is a primary cause of gas-phase formation for each of these molecules. Variation in the evaporation characteristics or the composition/structure of the ices may weaken such mechanisms. However, the agreement between observed and modeled abundances of vinyl cyanide is very good. Indeed, the *Select* model shows excellent agreement, providing further justification for the omission of its hydrogenation reactions.

Alternatively, surface hydrogenation of HC₃N and C₂H₃CN, once they have accreted onto the grains, may be less efficient than has been assumed here. Importantly, activation energies are required for hydrogenation of both these species, whose values are poorly constrained. The fact that it is these very reactions that must be disabled suggests strongly that their activation energies should be significantly higher than has been assumed here. Additionally, our use of a “deterministic” gas-grain model may also produce somewhat more efficient hydrogenation than is really the case (although a test-run using the rate-modification method of Garrod (2008) shows no great difference in this respect).

In the case of the addition of large hydrocarbon radicals to CN, the over-dominance of these channels is probably due to the incompleteness of the hydrocarbon chemistry as a whole, particularly on the grains. Whilst up to 10 carbon atoms in a chain are considered in this model, the hydrogenation states of the larger chains are typically limited to 4 hydrogen atoms. Crucially, hydrogenation is the only type of reaction included in the network for most hydrocarbons, aside from the newly-added CN addition reactions. The hydrocarbon reaction set was largely devised with cold dark clouds in mind, where hydrogenation dominates. By including only a single new reaction (addition to CN) for any particular hydrocarbon, that reaction can easily become the dominant channel. The completion of the hydrocarbon network

to include reactions with all major reactants would be beneficial, although this is not a trivial task.

The small hydrocarbons CH₂ and CH₃, on the other hand, as well as CN itself, have a much more comprehensive reaction network, making sequential addition and its apparent degree of efficiency more credible.

Ethyl formate and aminoacetonitrile also seem to be well reproduced with a similar addition scheme to that of the alkyl cyanides. Ethyl formate abundance may be dependent on ethanol as well as methyl formate, depending on the specific conditions.

The *Select* model reproduces well the abundance ratios for alkyl cyanides, but their absolute abundances are an order of magnitude lower than observational values. This also results in a poor match to abundance ratios relative to methyl formate and other methanol-related species. In fact, the chemistries of the cyanides and the methanol-related species do not strongly influence one another in the model. The overall abundances of each category of molecule are mainly influenced by different, independent parameters: the formation rate of the products of methanol photodissociation (i.e. the product of the photodissociation rate and absolute grain-surface abundance of methanol), and the quantity of HCN or related nitrile-group species in the ice mantles, respectively. Similarly, the modeled abundance of aminoacetonitrile relative to the alkyl cyanides is very high. The formation rate of this molecule is strongly dependent on the product of the abundance of NH₃ in the ices, and its rate of photodissociation. This indicates that one or both of these values may be too large, by at least an order of magnitude. A parameter search should yield the optimal values for all such quantities, but such is not the focus of this paper.

The augmentation of methyl formate binding energy allows its abundance to remain high at temperatures appropriate to the densest parts of the hot core. However, the low observed rotational temperatures suggest that methyl formate should still have a binding energy less than that of H₂O, which is indeed the case here, even with the highest value we use. A value somewhat lower than our maximum would also achieve quite acceptable results. Clearly, an experimental value for binding to astrophysically appropriate surfaces would be highly valuable for the chemical modeling of hot cores.

While certain crucial steps in the formation of these complex molecules occur only in the gas-phase or on the grain surfaces, processes in each phase are inter-dependent and cannot be understood in isolation.

6. Conclusions

We used the complete 3 mm and partial 2 and 1.3 mm line surveys obtained with the IRAM 30 m telescope toward the hot cores Sgr B2(N) and (M) to search for emission from the organic molecules ethyl formate and *n*-propyl cyanide. We report the detection of both molecules toward the hot core Sgr B2(N), which are the first detections of these molecules in the interstellar medium. Our main results and conclusions are the following:

1. New entries for the CDMS catalog have been created for *n*-propyl cyanide and ethyl formate.
2. 46 of the 711 significant transitions of the *anti*-conformer of ethyl formate covered by our 30 m line survey are relatively free of contamination from other molecules and are detected in the form of 24 observed features toward Sgr B2(N). The emission of the *gauche*-conformer is too weak to be clearly detected in our survey.
3. 50 of the 636 significant transitions of the *anti*-conformer of *n*-propyl cyanide covered by our 30 m line survey are relatively free of contamination from other molecules and are detected in the form of 12 observed features toward Sgr B2(N) with two velocity components. The emission of the *gauche*-conformer is too weak to be clearly detected in our survey.
4. With a source size of 3'', we derive an ethyl formate column density of $5.4 \times 10^{16} \text{ cm}^{-2}$ for a temperature of 100 K and a linewidth of 7 km s^{-1} in the LTE approximation. The abundance of ethyl formate relative to H₂ is estimated to be 3.6×10^{-9} .
5. The two velocity components detected in *n*-propyl cyanide have LTE column densities of 1.5×10^{16} and $6.6 \times 10^{15} \text{ cm}^{-2}$, respectively, with a temperature of 150 K, a linewidth of 7 km s^{-1} , and a source size of 3''. The fractional abundance of *n*-propyl cyanide in the main source is estimated to be 1.0×10^{-9} .
6. We detected neither ethyl formate nor *n*-propyl cyanide toward the more evolved source Sgr B2(M) and derived column density upper limits of 2×10^{16} and $6 \times 10^{15} \text{ cm}^{-2}$, respectively, for a source size of 3''.
7. We modeled the emission of chemically related species also detected in our survey of Sgr B2(N) and derived column density ratios of 0.8/15/1 for *t*-HCOOH/CH₃OCHO/C₂H₅OCHO and 108/80/1 for CH₃CN/C₂H₅CN/C₃H₇CN in the main hot core of Sgr B2(N).
8. The chemical models suggest that the sequential, piecewise construction of ethyl and *n*-propyl cyanide from their constituent functional groups on the grain surfaces is their most likely formation route. Aminoacetonitrile formation proceeds similarly, suggesting a possible correlation with ethyl cyanide abundance. Vinyl cyanide is formed predominantly in the gas-phase.
9. Comparison of the observational and model results suggests that the production of alkyl cyanides by the hydrogenation of less saturated species is much less efficient than functional-group addition.
10. Ethyl formate can be formed on the grains by addition of HCO or CH₃ to functional-group radicals derived from methyl formate and ethanol; however, methyl formate appears to be the dominant precursor.
11. Understanding of the complex interactions between gas-phase and grain-surface processes may be necessary to fully explain the observational features displayed by many complex molecules, including formic acid and methyl formate.
12. The detection in Sgr B2(N) of the next stage of complexity in two classes of complex molecule, esters and alkyl cyanides, suggests that greater complexity also may be present in other classes of molecule in the interstellar medium.

Our results have demonstrated the power of the "complete spectrum fitting" approach used by us as a technique that is mandatory today for the identification of new complex molecules by their generally weak signals. Ideally, one would want to verify identifications with interferometric observations as done for the case of aminoacetonitrile (Belloche et al. 2008a,b). However, given the limited collecting area, bandwidth and spatial resolution of today's interferometer arrays, this would be very time consuming or even prohibitive. It will, however, be a trivial exercise for the Atacama Large Millimeter Array (ALMA) once it is fully operational.

Acknowledgements. We thank the anonymous referee and the editor for their careful reading of the manuscript and for their suggestions that helped improve

the clarity of this article. H.S.P.M. thanks Dr. Jürgen Aschenbach from the library of the University of Kiel for providing the supplementary material to Vormann & Dreizler (1988). We are grateful to Eric Herbst for providing the ethyl formate spectroscopic line list as well as a preprint of the manuscript prior to publication. H.S.P.M. thanks the Deutsche Forschungsgemeinschaft (DFG) for initial support through the collaborative research grant SFB 494. He is grateful to the Bundesministerium für Bildung und Forschung (BMBF) for recent support which was administered through Deutsches Zentrum für Luft- und Raumfahrt (DLR). R.T.G. thanks the Alexander von Humboldt Foundation for a Research Fellowship.

References

- Belloche, A., Menten, K. M., Comito, C., Müller, H. S. P., Schilke, P., Ott, J., Thorwirth, S., & Hieret, C. 2008a, *A&A*, 482, 179
- Belloche, A., Menten, K. M., Comito, C., Müller, H. S. P., Schilke, P., Ott, J., Thorwirth, S., & Hieret, C. 2008b, *A&A*, 492, 769
- Bernstein, M. P., Dworkin, J. P., Sandford, S. A., Cooper, G. W., & Allamandola, L. J. 2002, *Nature*, 416, 401
- Carty, D., Le Page, V., Sims, I. R., & Sims, I. W. M. 2001, *Chem. Phys. Lett.*, 344, 310
- Comito, C., Schilke, P., Phillips, T. G., Lis, D. C., Motte, F., & Mehringer, D. 2005, *ApJS*, 156, 127
- Demaison, J., & Dreizler, H. 1982, *Z. Naturforsch. A*, 37, 199
- Demaison, J., Boucher, D., Burie, J., & Dubrulle, A. 1984, *Z. Naturforsch. A*, 39, 560
- de Vicente, P., Martin-Pintado, J., & Wilson, T. L. 1997, *A&A*, 320, 957
- Ehrenfreund, P., Glavin, D. P., Botta, O., Cooper, G., & Bada, J. L. 2001, *Proceedings of the National Academy of Science*, 98, 2138
- Elsila, J. E., Dworkin, J. P., Bernstein, M. P., Martin, M. P., & Sandford, S. A. 2007, *ApJ*, 660, 911
- Friedel, D. N., Snyder, L. E., Turner, B. E., & Remijan, A. 2004, *ApJ*, 600, 234
- Garrod, R. T., & Herbst, E. 2006, *A&A*, 457, 927
- Garrod, R. T., Widicus Weaver, S. L., & Herbst, E. 2008, *ApJ*, 682, 283
- Garrod, R. T. 2008, *A&A*, 491, 239
- Geppert, W. D., Hamberg, M., Thomas, R. D., Österdahl, F., et al. 2006, *Faraday Discuss.* 133, 177
- Goldsmith, P. F., & Langer, W. D. 1999, *ApJ*, 517, 209
- Gordon, M. A., Berkemann, U., Mezger, P. G., Zylka, R., Haslam, C. G. T., Kreysa, E., Sievers, A., & Lemke, R. 1993, *A&A*, 280, 208
- Hirota, E. 1962, *J. Chem. Phys.*, 37, 2918
- Hollis, J. M., Lovas, F. J., & Jewell, P. R. 2000, *ApJ*, 540, L107
- Hollis, J. M., Pedelty, J. A., Boboltz, D. A., Liu, S.-Y., Snyder, L. E., Palmer, P., Lovas, F. J., & Jewell, P. R. 2003, *ApJ*, 596, L235
- Hollis, J. M., Lovas, F. J., Remijan, A. J., Jewell, P. R., Ilyushin, V. V., & Kleiner, I. 2006, *ApJ*, 643, L25
- Horn, A., Møllendal, H., Sekiguchi, O., Uggerud, E., Roberts, H., Herbst, E., Viggiano, A. A., & Fridgen, T. D. 2004, *ApJ*, 611, 605
- Jones, P. A., Cunningham, M. R., Godfrey, P. D., & Cragg, D. M. 2007, *MNRAS*, 374, 579
- Jones, P. A., Burton, M. G., Cunningham, M. R., Menten, K. M., Schilke, P., Belloche, A., Leurini, S., Ott, J., Walsh, A. J. 2008, *MNRAS*, 386, 117
- Lis, D. C., & Goldsmith, P. F. 1989, *ApJ*, 337, 704
- Lis, D. C., Goldsmith, P. F., Carlstrom, J. E., & Scoville, N. Z. 1993, *ApJ*, 402, 238
- Liu, S.-Y., & Snyder, L. E. 1999, *ApJ*, 523, 683
- Liu, S.-Y., Mehringer, D. M., & Snyder, L. E. 2001, *ApJ*, 552, 654
- Medvedev, I. R., De Lucia, F. C., & Herbst, E. 2009, *ApJS*, in press
- Mehringer, D. M., Snyder, L. E., Miao, Y., & Lovas, F. J. 1997, *ApJ*, 480, L71
- Miao, Y., Mehringer, D. M., Kuan, Y.-J., & Snyder, L. E. 1995, *ApJ*, 445, L59
- Millar, T. J., Herbst, E., & Charnley, S. B. 1991, *ApJ*, 369, 147
- Müller, H. S. P., Thorwirth, S., Roth, D. A., & Winnewisser, G. 2001, *A&A*, 370, L49
- Müller, H. S. P., Schlöder, F., Stutzki, J., & Winnewisser, G. 2005, *J. Mol. Struct.* 742, 215
- Müller, H. S. P., Belloche, A., Menten, K. M., Comito, C., & Schilke, P. 2008, *J. Mol. Spectrosc.*, 251, 319
- Nummelin, A., Bergman, P., Hjalmarsen, Å., Friberg, P., Irvine, W. M., Millar, T. J., Ohishi, M., & Saito, S. 2000, *ApJS*, 128, 213
- Osorio, M., Lizano, S., & D'Alessio, P. 1999, *ApJ*, 525, 808
- Pearson, J. C., Brauer, C. S., Drouin, B. J. 2008, *J. Mol. Spectrosc.*, 251, 394
- Pickett, H. M., Poynter, I. R. L., Cohen, E. A., Delitsky, M. L., Pearson, J. C., & Müller, H. S. P. 1998, *J. Quant. Spectrosc. Radiat. Transfer*, 60, 883
- Reid, M. J. 1993, *ARA&A*, 31, 345
- Riveros, J. M., & Bright Wilson, E., Jr. 1967, *J. Chem. Phys.*, 46, 4605
- Snyder, L. E., Kuan, Y.-J., & Miao, Y. 1994, *The Structure and Content of Molecular Clouds*, ed. T. L. Wilson & K. J. Johnston (Springer-Verlag), Lecture Notes in Physics, 439, 187
- Snyder, L. E., Lovas, F. J., Hollis, J. M., Friedel, D. N., et al. 2005, *ApJ*, 619, 914
- Vormann, K., & Dreizler, H. 1988, *Z. Naturforsch. A*, 43, 338
- Włodarczak, G., Martinache, L., Demaison, J., Marstokk, K.-M., & Møllendal, H. 1988, *J. Mol. Spectrosc.*, 127, 178
- Włodarczak, G., Martinache, L., Demaison, J., Marstokk, K.-M., & Møllendal, H. 1991, *J. Mol. Spectrosc.*, 146, 224

Appendix A: *a*-Type and *b*-type lines of methyl formate

Both *A* and *E* symmetry species of methyl formate (CH_3OCHO) are easily detected in our spectral survey of Sgr B2(N) at 3 mm. Sixty four lines of the *A* species are detected in the form of 57 features in our 3 mm survey and 48 lines of the *E* species in the form of 43 features. We followed the same procedure as described in Sect. 3.2 for ethyl formate to compute the population diagrams shown in Fig. A.1. In these diagrams, the *a*-type lines of methyl formate (with $\Delta K_a = 0$ [2] and $\Delta K_c = 1$ [2]) are marked with an additional circle. As mentioned in Sect. 3.4, both *a*- and *b*-type lines are well fitted with the same physical model (see Table 5). Although many *a*-type transitions with $E_u/k_B < 50$ K look systematically too low in the population diagrams after removal of the contribution of contaminating lines (Fig. A.1b and d), this can be explained by the limitations of our radiative transfer modeling: these *a*-type transitions (of the *A* or *E* species) have optical depths on the order of unity, as indicated by the significant shift between the red and green crosses in the lower energy range, and overlap with *a*-type lines of the other symmetry species (*E* or *A*, respectively) that have significant optical depths too. Since our current complete model treats the two symmetry species as independent and our radiative transfer program computes the contributions of overlapping transitions of different species independently, the sum of the overlapping *A* and *E* transitions with significant optical depths is systematically overestimated. For a transition of, e.g., the *A* species, the “contamination” by the *E* species is overestimated and its removal in Fig. A.1b yields an underestimated residual flux. Our model could be improved by treating both symmetry species as a single molecule but this would not significantly change the physical parameters found for methyl formate and is beyond the scope of this article focused on ethyl formate and *n*-propyl cyanide.

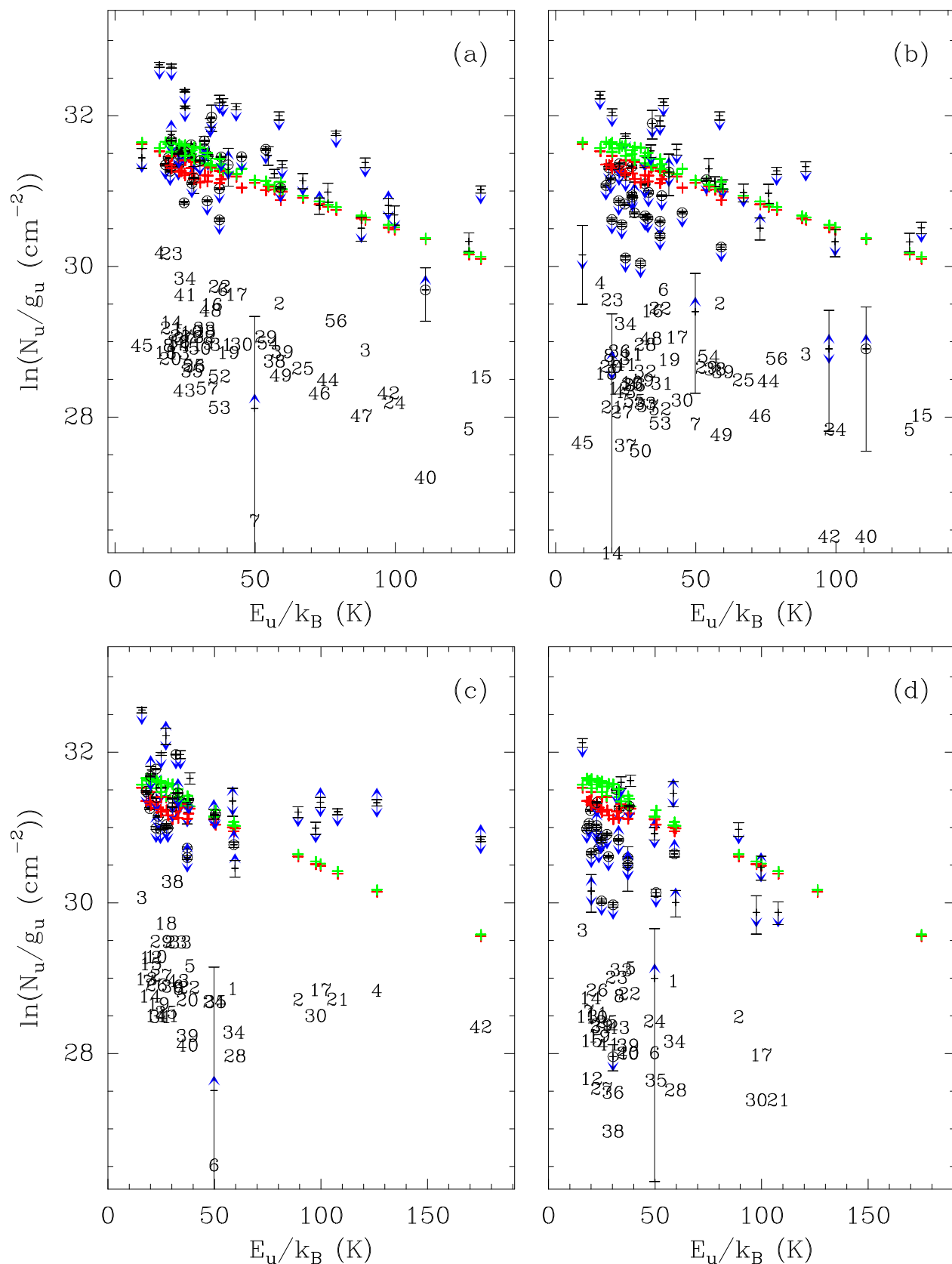


Fig. A.1. Population diagrams of the A and E symmetry species of methyl formate presented in the same way as for ethyl formate in Fig. 2 (see the caption of that figure for details). The *a*-type lines are marked with a circle. Panel a and c show the population diagrams derived from the measured integrated intensities for the A and E species, respectively, while panels b and d present the respective population diagrams after removing the expected contribution from contaminating molecules. Features 4 and 42 with $E_u/k_B > 120$ K (see panel c) are missing in panel d because the removal of the contaminating lines yields negative residuals. This is due to the uncertain level of the baseline that looks overestimated for both features in the observed spectrum.

Table 1. Transitions of the *anti*-conformer of ethyl formate observed with the IRAM 30 m telescope toward Sgr B2(N). The horizontal lines mark discontinuities in the observed frequency coverage. Only the transitions associated with a modeled line stronger than 20 mK are listed.

N^a	Transition ^b	Frequency (MHz)	Unc. ^c (kHz)	E_1^d (K)	$S\mu^2$ (D ²)	σ^e (mK)	Comments
(1)	(2)	(3)	(4)	(5)	(6)	(7)	(8)
1	15 _{2,14} – 14 _{2,13}	81779.567	4	30	50.5	13	Detected , blend with U-line
2	15 _{13,2} – 14 _{13,1} *	82297.815	4	149	12.8	19	Blend with C ₂ H ₅ CN, $v_{13}=1/v_{21}=1$ and absorption line of c-HC ¹³ CCH
4	15 _{14,1} – 14 _{14,0} *	82297.944	4	169	6.6	19	Blend with C ₂ H ₅ CN, $v_{13}=1/v_{21}=1$ and absorption line of c-HC ¹³ CCH
6	15 _{12,3} – 14 _{12,2} *	82298.480	4	131	18.5	19	Blend with C ₂ H ₅ CN, $v_{13}=1/v_{21}=1$ and absorption line of c-HC ¹³ CCH
8	15 _{10,5} – 14 _{10,4} *	82303.360	4	100	28.6	19	Blend with HC ₃ N, $v_6=v_7=1$ and absorption line of c-HC ¹³ CCH
10	15 _{9,6} – 14 _{9,5} *	82308.580	4	86	32.9	19	Strong HC ₃ N, $v_6=v_7=1$
12	15 _{8,7} – 14 _{8,6} *	82316.890	4	74	36.8	19	Strong HC ₃ N, $v_6=v_7=1$
14	15 _{7,8} – 14 _{7,7} *	82330.125	4	63	40.2	19	Blend with CH ₃ CHO and CH ₃ ¹⁸ OH
16	15 _{6,10} – 14 _{6,9} *	82351.854	4	54	43.2	19	Detected , partial blend with C ₂ H ₅ CN, $v_{13}=1/v_{21}=1$ and U-line
18	19 _{3,17} – 19 _{2,18}	82389.204	9	53	4.8	18	Blend with ¹³ CH ₃ OH
19	15 _{5,11} – 14 _{5,10}	82389.698	4	46	45.7	18	Blend with ¹³ CH ₃ OH
20	15 _{5,10} – 14 _{5,9}	82390.016	4	46	45.7	18	Blend with ¹³ CH ₃ OH
21	15 _{4,12} – 14 _{4,11}	82457.126	4	39	47.8	18	Strong CH ₃ OCH ₃
22	15 _{4,11} – 14 _{4,10}	82471.367	4	39	47.8	18	Blend with CH ₂ (OH)CHO and U-line
23	15 _{3,13} – 14 _{3,12}	82485.618	4	34	49.4	18	Blend with U-lines
24	15 _{3,12} – 14 _{3,11}	82802.132	4	34	49.4	17	Blend with C ₂ H ₅ CN
25	15 _{1,14} – 14 _{1,13}	83792.699	4	29	51.1	16	Blend with CH ₃ OH and U-lines
26	15 _{2,13} – 14 _{2,12}	84081.357	4	31	50.5	19	Detected , partial blend with CH ₃ CH ₃ CO, $v_t=1$
27	16 _{1,16} – 15 _{1,15}	84444.095	4	31	54.6	19	Blend with ¹³ CH ₃ OH and C ₂ H ₅ CN, $v_{13}=1/v_{21}=1$
28	16 _{0,16} – 15 _{0,15}	85065.106	4	31	54.7	22	Detected , partial blend with c-C ₂ H ₄ O
29	16 _{2,15} – 15 _{2,14}	87160.417	4	34	54.0	17	Strong CH ₃ OCHO
30	16 _{14,2} – 15 _{14,1} *	87785.462	4	173	12.9	17	Blend with C ₂ H ₅ CN, $v_{13}=1/v_{21}=1$, problem with baseline?
32	16 _{13,3} – 15 _{13,2} *	87785.683	4	153	18.7	17	Blend with C ₂ H ₅ CN, $v_{13}=1/v_{21}=1$, problem with baseline?
34	16 _{15,1} – 15 _{15,0} *	87785.966	4	193	6.6	17	Blend with C ₂ H ₅ CN, $v_{13}=1/v_{21}=1$, problem with baseline?
36	16 _{12,4} – 15 _{12,3} *	87786.848	4	135	24.0	17	Blend with C ₂ H ₅ CN, $v_{13}=1/v_{21}=1$, problem with baseline?
38	16 _{11,5} – 15 _{11,4} *	87789.267	4	119	28.9	17	Blend with U-line, uncertain baseline
40	16 _{10,6} – 15 _{10,5} *	87793.413	4	104	33.4	17	Blend with CH ₃ ¹³ CH ₂ CN and U-line
42	16 _{9,7} – 15 _{9,6} *	87800.031	4	90	37.5	17	Blend with CH ₃ ¹³ CH ₂ CN and HNC, $v_4=1$
44	16 _{8,8} – 15 _{8,7} *	87810.372	4	78	41.2	17	Group detected , partial blend with CH ₂ (OH)CHO and C ₂ H ₅ CN
46	16 _{7,9} – 15 _{7,8} *	87826.665	4	67	44.4	17	Group detected , partial blend with HNC, $v_5=1$
48	16 _{6,11} – 15 _{6,10} *	87853.244	4	58	47.2	17	Blend with NH ₂ CHO, problem with baseline?
50	16 _{5,12} – 15 _{5,11}	87899.302	4	50	49.5	17	Strong C ₂ H ₅ ¹³ CN, HNC, and HN ¹³ CO
51	16 _{5,11} – 15 _{5,10}	87899.879	4	50	49.5	17	Strong C ₂ H ₅ ¹³ CN, HNC, and HN ¹³ CO
52	16 _{4,13} – 15 _{4,12}	87979.119	4	43	51.4	19	Blend with U-lines
53	16 _{3,14} – 15 _{3,13}	87993.944	4	38	52.9	19	Detected , partial blend with CH ₃ CH ₃ CO and U-line
54	16 _{4,12} – 15 _{4,11}	88001.562	4	43	51.4	19	Detected , blend with C ₂ H ₅ CN, $v_{13}=1/v_{21}=1$
55	16 _{3,13} – 15 _{3,12}	88425.192	4	38	52.9	17	Blend with CH ₂ (OH)CHO
56	16 _{1,15} – 15 _{1,14}	89218.355	4	33	54.6	16	Strong HCO ⁺ in absorption
57	17 _{1,17} – 16 _{1,16}	89651.925	4	35	58.0	18	Blend with C ₂ H ₅ CN, $v_{13}=1/v_{21}=1$, CH ₃ OH, $v_t=2$, and C ₂ H ₅ CN, $v_{20}=1$
58	16 _{2,14} – 15 _{2,13}	89804.728	4	35	54.0	18	Blend with CH ₃ CH ₃ CO
59	17 _{0,17} – 16 _{0,16}	90190.497	5	35	58.1	17	Blend with CH ₂ (OH)CHO, C ₂ H ₅ CN, $v_{13}=1/v_{21}=1$, and U-line
60	17 _{2,16} – 16 _{2,15}	92528.452	4	39	57.4	22	Blend with CH ₃ CN, $v_8=2$
61	17 _{14,3} – 16 _{14,2} *	93273.169	4	177	18.8	22	Blend with U-lines
63	17 _{15,2} – 16 _{15,1} *	93273.377	5	198	12.9	22	Blend with U-lines
65	17 _{13,4} – 16 _{13,3} *	93273.813	4	157	24.2	22	Blend with U-lines
67	17 _{16,1} – 16 _{16,0} *	93274.251	5	220	6.7	22	Blend with U-lines
69	17 _{12,5} – 16 _{12,4} *	93275.564	4	139	29.3	22	Blend with U-lines
71	17 _{11,6} – 16 _{11,5} *	93278.797	4	123	33.9	22	Blend with U-lines
73	17 _{10,7} – 16 _{10,6} *	93284.077	4	108	38.1	22	Group detected , uncertain baseline
75	17 _{9,8} – 16 _{9,7} *	93292.297	4	94	42.0	22	Group detected , uncertain baseline
77	17 _{8,9} – 16 _{8,8} *	93304.955	4	82	45.4	22	Group detected , partial blend with U-line
79	17 _{7,11} – 16 _{7,10} *	93324.728	4	71	48.4	22	Group detected , partial blend with U-lines
81	17 _{6,12} – 16 _{6,11} *	93356.821	4	62	51.0	22	Group detected , blend with CH ₃ CH ₃ CO and U-line?
83	17 _{5,13} – 16 _{5,12}	93412.160	4	54	53.3	22	Group detected , partial blend with U-line?
84	17 _{5,12} – 16 _{5,11}	93413.168	4	54	53.3	22	Group detected , partial blend with U-line?
85	17 _{3,15} – 16 _{3,14}	93499.096	4	42	56.5	24	Blend with C ₂ H ₅ OH and U-line
86	17 _{4,14} – 16 _{4,13}	93504.972	4	47	55.1	24	Detected , blend with CH ₃ ¹⁸ OH
87	17 _{4,13} – 16 _{4,12}	93539.303	4	47	55.1	24	Detected
88	17 _{3,14} – 16 _{3,13}	94072.891	4	42	56.5	31	Blend with CH ₃ CH ₃ CO, $v_t=1$ and ¹³ CH ₃ OH, $v_t=1$
89	17 _{1,16} – 16 _{1,15}	94608.131	4	37	58.0	26	Blend with ¹³ CH ₃ CH ₂ CN and U-line
90	18 _{1,18} – 17 _{1,17}	94852.542	5	40	61.5	28	Weak
91	18 _{0,18} – 17 _{0,17}	95313.428	5	39	61.5	28	Weak, partial blend with C ₂ H ₅ CN, $v_{11}=1/v_{15}=1$, uncertain baseline
92	17 _{2,15} – 16 _{2,14}	95517.316	4	39	57.5	23	Blend with C ₂ H ₅ CN, $v_{11}=2$

Table 1. continued.

N^a	Transition ^b	Frequency (MHz)	Unc. ^c (kHz)	E_l^d (K)	$S\mu^2$ (D ²)	σ^e (mK)	Comments
(1)	(2)	(3)	(4)	(5)	(6)	(7)	(8)
93	18 _{2,17} – 17 _{2,16}	97883.281	4	43	60.9	20	Blend with CH ₃ OCHO, $v_t=1$ and NH ₂ CHO
94	18 _{15,3} – 17 _{15,2} *	98760.931	5	202	18.9	18	Group detected , blend with U-line
96	18 _{14,4} – 17 _{14,3} *	98761.079	5	181	24.4	18	Group detected , blend with U-line
98	18 _{16,2} – 17 _{16,1} *	98761.555	5	224	13.0	18	Group detected , blend with U-line
100	18 _{13,5} – 17 _{13,4} *	98762.218	5	162	29.5	18	Group detected , blend with U-line
102	18 _{17,1} – 17 _{17,0} *	98762.790	5	248	6.7	18	Group detected , blend with U-line
104	18 _{12,6} – 17 _{12,5} *	98764.650	5	144	34.3	18	Group detected
106	18 _{11,7} – 17 _{11,6} *	98768.818	5	127	38.7	18	Blend with U-line
108	18 _{10,8} – 17 _{10,7} *	98775.390	5	112	42.7	18	Blend with C ₂ H ₅ CN, $v_{20}=1$
110	18 _{9,9} – 17 _{9,8} *	98785.427	5	99	46.3	18	Blend with U-line, CH ₃ OCHO, and C ₂ H ₅ CN, $v_{13}=1/v_{21}=1$
112	18 _{8,10} – 17 _{8,9} *	98800.707	5	86	49.6	18	Blend with CH ₃ CH ₃ CO
114	18 _{7,12} – 17 _{7,11} *	98824.411	4	76	52.4	18	Blend with C ₂ H ₅ OH
116	18 _{6,13} – 17 _{6,12} *	98862.724	4	66	54.9	18	Blend with strong U-line
118	18 _{5,14} – 17 _{5,13}	98928.453	4	58	57.0	18	Group detected , blend with C ₂ H ₅ CN, $v_{13}=1/v_{21}=1$
119	18 _{5,13} – 17 _{5,12}	98930.153	4	58	57.0	18	Group detected , blend with C ₂ H ₅ CN, $v_{13}=1/v_{21}=1$
120	18 _{3,16} – 17 _{3,15}	98999.806	4	47	60.0	18	Blend with U-lines
121	18 _{4,15} – 17 _{4,14}	99034.515	4	52	58.7	19	Blend with ¹³ CH ₃ CH ₂ CN, CH ₃ CH ₃ CO, $v_t=1$, and U-lines
122	18 _{4,14} – 17 _{4,13}	99085.662	4	52	58.7	19	Blend with a(CH ₂ OH) ₂ and CH ₃ OCHO, $v_t=1$
123	18 _{3,15} – 17 _{3,14}	99746.684	5	47	60.0	14	Blend with NH ₂ CN and C ₂ H ₅ CN, $v_{20}=1$
124	18 _{1,17} – 17 _{1,16}	99959.814	4	42	61.4	14	Blend with NH ₂ CN and CH ₃ CH ₃ CO
125	19 _{1,19} – 18 _{1,18}	100046.587	5	44	64.9	14	Blend with HCC ¹³ CN, $v_7=1$ and U-line
126	19 _{0,19} – 18 _{0,18}	100436.418	5	44	64.9	24	Blend with CH ₃ OCH ₃ and C ₂ H ₅ OH
127	18 _{2,16} – 17 _{2,15}	101213.969	5	44	61.0	21	Blend with U-line
128	19 _{2,18} – 18 _{2,17}	103224.624	5	48	64.4	25	Blend with c-C ₂ H ₄ O, CH ₃ OCHO, and U-line
129	19 _{15,4} – 18 _{15,3} *	104248.635	5	207	24.6	48	Blend with SO ₂ and U-line?
131	19 _{16,3} – 18 _{16,2} *	104248.958	5	229	19.0	48	Blend with SO ₂ and U-line?
133	19 _{14,5} – 18 _{14,4} *	104249.203	5	186	29.8	48	Blend with SO ₂ and U-line?
135	19 _{17,2} – 18 _{17,1} *	104249.983	5	253	13.0	48	Blend with SO ₂ and U-line?
137	19 _{13,6} – 18 _{13,5} *	104250.916	5	167	34.7	48	Blend with SO ₂ and U-line?
139	19 _{18,1} – 18 _{18,0} *	104251.566	5	278	6.7	48	Blend with SO ₂ and U-line?
141	19 _{12,7} – 18 _{12,6} *	104254.128	5	149	39.2	48	Blend with CH ₃ OCHO
143	19 _{11,8} – 18 _{11,7} *	104259.358	5	132	43.3	48	Weak, baseline problem?
145	19 _{10,9} – 18 _{10,8} *	104267.390	5	117	47.1	48	Weak
147	19 _{9,10} – 18 _{9,9} *	104279.474	5	103	50.6	48	Blend with C ₂ H ₅ CN, $v_{13}=1/v_{21}=1$ and C ₂ H ₅ OH
149	19 _{8,11} – 18 _{8,10} *	104297.698	5	91	53.6	48	Strong ¹³ CH ₃ OH, CH ₃ OCHO, and CH ₃ OH
151	19 _{7,13} – 18 _{7,12} *	104325.811	5	80	56.3	48	Blend with C ₂ H ₃ CN, $v_{11}=3$, CH ₃ ¹⁸ OH, and U-lines
153	19 _{6,14} – 18 _{6,13} *	104371.094	5	71	58.7	48	Blend with U-lines
155	19 _{5,15} – 18 _{5,14}	104448.349	5	63	60.7	48	Blend with C ₂ H ₅ CN, $v_{13}=1/v_{21}=1$ and ¹³ CH ₃ CH ₂ CN
156	19 _{5,14} – 18 _{5,13}	104451.132	5	63	60.7	48	Blend with ¹³ CH ₃ CH ₂ CN, C ₂ H ₃ CN, and ¹³ CH ₃ OH
157	19 _{3,17} – 18 _{3,16}	104494.782	5	52	63.5	25	Blend with C ₂ H ₃ CN and C ₂ H ₃ CN, $v_{15}=2$
158	19 _{4,16} – 18 _{4,15}	104567.468	5	57	62.3	25	Blend with C ₂ H ₃ CN, $v_{15}=1$
159	19 _{4,15} – 18 _{4,14}	104641.877	5	57	62.3	25	Blend with C ₂ H ₃ CN, $v_{15}=1$, C ₂ H ₃ CN, $v_{11}=1/v_{15}=1$, and U-line
160	20 _{1,20} – 19 _{1,19}	105234.713	5	49	68.4	28	Detected , blend with C ₂ H ₅ OH and CH ₃ OCHO
161	19 _{1,18} – 18 _{1,17}	105272.047	5	47	64.8	28	Detected , blend with U-lines
162	19 _{3,16} – 18 _{3,15}	105447.141	5	52	63.5	37	Detected
163	20 _{0,20} – 19 _{0,19}	105561.113	5	49	68.4	37	Blend with CH ₃ OCH ₃ and CH ₃ CH ₃ CO
164	19 _{2,17} – 18 _{2,16}	106890.388	100	49	64.5	24	Blend with C ₂ H ₅ CN, $v_{13}=1/v_{21}=1$ and U-lines
165	20 _{2,19} – 19 _{2,18}	108552.378	100	53	67.8	20	Detected , partial blend with C ₂ H ₃ CN, $v_{15}=1$ and U-lines
166	20 _{16,4} – 19 _{16,3} *	109736.466	5	234	24.7	41	Strong HC ₃ N, $v_6=v_7=1$ and HCC ¹³ CN, $v_5=1/v_7=3$
168	20 _{15,5} – 19 _{15,4} *	109736.499	5	212	30.0	41	Strong HC ₃ N, $v_6=v_7=1$ and HCC ¹³ CN, $v_5=1/v_7=3$
170	20 _{17,3} – 19 _{17,2} *	109737.236	5	258	19.0	41	Strong HC ₃ N, $v_6=v_7=1$ and HCC ¹³ CN, $v_5=1/v_7=3$
172	20 _{14,6} – 19 _{14,5} *	109737.553	5	191	35.0	41	Strong HC ₃ N, $v_6=v_7=1$ and HCC ¹³ CN, $v_5=1/v_7=3$
174	20 _{18,2} – 19 _{18,1} *	109738.645	5	283	13.0	41	Strong HC ₃ N, $v_6=v_7=1$ and HCC ¹³ CN, $v_5=1/v_7=3$
176	20 _{13,7} – 19 _{13,6} *	109739.922	5	172	39.6	41	Strong HC ₃ N, $v_6=v_7=1$ and HCC ¹³ CN, $v_5=1/v_7=3$
178	20 _{19,1} – 19 _{19,0} *	109740.558	6	310	6.7	41	Strong HC ₃ N, $v_6=v_7=1$ and HCC ¹³ CN, $v_5=1/v_7=3$
180	20 _{12,8} – 19 _{12,7} *	109744.026	100	154	43.9	41	Strong HC ₃ N, $v_6=v_7=1$ and HCC ¹³ CN, $v_5=1/v_7=3$
182	20 _{11,9} – 19 _{11,8} *	109750.509	100	137	47.9	41	Strong HC ₃ N, $v_6=v_7=1$ and NH ₂ CHO
184	20 _{10,10} – 19 _{10,9} *	109760.033	100	122	51.4	41	Strong SO ₂ and CH ₃ OCHO, $v_t=1$
186	20 _{9,11} – 19 _{9,10} *	109774.484	100	108	54.7	41	Strong CH ₃ OCHO, $v_t=1$ and C ¹⁸ O
188	20 _{8,12} – 19 _{8,11} *	109796.006	100	96	57.6	41	Blend with CH ₃ CN, $v_4=1$, C ¹⁸ O? and U-line?, uncertain baseline
190	20 _{7,13} – 19 _{7,12} *	109829.206	100	85	60.2	41	Blend with CH ₃ CN, $v_4=1$ and HNC
192	20 _{6,15} – 19 _{6,14}	109882.071	5	76	62.4	41	Blend with C ₂ H ₅ CN
193	20 _{6,14} – 19 _{6,13}	109882.180	5	76	62.4	41	Blend with C ₂ H ₅ CN
194	20 _{5,16} – 19 _{5,15}	109971.950	100	68	64.3	41	Blend with U-lines

Table 1. continued.

N^a	Transition ^b	Frequency (MHz)	Unc. ^c (kHz)	E_l^d (K)	$S\mu^2$ (D ²)	σ^e (mK)	Comments
(1)	(2)	(3)	(4)	(5)	(6)	(7)	(8)
195	20 _{5,15} – 19 _{5,14}	109976.496	100	68	64.3	41	Blend with U-lines
196	20 _{3,18} – 19 _{3,17}	109982.754	100	57	67.0	41	Blend with U-lines
197	20 _{4,17} – 19 _{4,16}	110103.554	100	62	65.8	24	Blend with HNCO, $v_5=1$
198	20 _{4,16} – 19 _{4,15}	110209.376	5	62	65.8	24	Blend with ¹³ CO and HC ₃ N, $v_5=1/v_7=3$
199	21 _{1,21} – 20 _{1,20}	110417.565	5	54	71.8	24	Blend with HNCO, $v_5=1$
200	20 _{1,19} – 19 _{1,18}	110544.656	100	52	68.2	32	Blend with CH ₃ ¹³ CN, $v_8=1$, C ₂ H ₅ OH, CH ₃ OCHO, and U-line
201	21 _{0,21} – 20 _{0,20}	110688.469	100	54	71.8	32	Blend with CH ₃ CN, $v_8=1$
202	20 _{3,17} – 19 _{3,16}	111173.805	100	57	67.1	25	Blend with CH ₃ OCHO
203	20 _{2,18} – 19 _{2,17}	112542.864	100	54	67.9	31	Blend with U-lines
204	21 _{2,20} – 20 _{2,19}	113866.412	100	58	71.3	34	Blend with C ₂ H ₅ OH and U-lines
205	21 _{16,5} – 20 _{16,4} *	115224.084	5	239	30.2	60	Strong CO
207	21 _{15,6} – 20 _{15,5} *	115224.530	5	217	35.3	60	Strong CO
209	21 _{17,4} – 20 _{17,3} *	115224.552	5	263	24.8	60	Strong CO
211	21 _{18,3} – 20 _{18,2} *	115225.746	5	288	19.1	60	Strong CO
213	21 _{14,7} – 20 _{14,6} *	115226.140	5	196	40.0	60	Strong CO
215	21 _{19,2} – 20 _{19,1} *	115227.514	6	315	13.1	60	Strong CO
217	21 _{13,8} – 20 _{13,7} *	115229.252	5	177	44.4	60	Strong CO
219	21 _{20,1} – 20 _{20,0} *	115229.733	7	343	6.7	60	Strong CO
221	21 _{12,9} – 20 _{12,8} *	115234.500	100	159	48.5	60	Strong CO
223	21 _{11,10} – 20 _{11,9} *	115242.178	100	142	52.3	60	Strong CO
225	21 _{10,11} – 20 _{10,10} *	115253.747	100	127	55.7	60	Strong CO
227	21 _{9,12} – 20 _{9,11} *	115270.652	100	114	58.8	60	Strong CO
229	21 _{8,13} – 20 _{8,12} *	115295.734	100	101	61.6	60	Strong CO
231	21 _{7,14} – 20 _{7,13} *	115334.205	100	91	64.0	60	Strong CO
233	21 _{6,16} – 20 _{6,15}	115395.797	5	81	66.2	60	Group detected , partial blend with U-line
234	21 _{6,15} – 20 _{6,14}	115395.986	5	81	66.2	60	Group detected , partial blend with U-line
235	21 _{3,19} – 20 _{3,18} *	115462.453	100	62	70.5	60	Weak
237	21 _{5,16} – 20 _{5,15}	115506.424	100	73	68.0	60	Weak
238	22 _{1,22} – 21 _{1,21}	115595.764	5	59	75.2	79	Detected , blend with CH ₃ CH ₃ CO, $v_t=1$, uncertain baseline
239	21 _{4,18} – 20 _{4,17}	115641.781	100	67	69.4	79	Blend with U-line
240	21 _{1,20} – 20 _{1,19}	115778.715	100	57	71.6	79	Blend with CH ₃ OCH ₃
241	21 _{4,17} – 20 _{4,16}	115789.775	5	67	69.4	79	Weak
242	22 _{0,22} – 21 _{0,21}	115819.018	100	59	75.2	79	Weak
243	26 _{1,26} – 25 _{1,25}	136272.994	100	83	88.9	28	Blend with HC ₃ N, $v_4=1$ and CH ₃ OCHO
244	26 _{0,26} – 25 _{0,25}	136369.733	100	83	88.9	28	Blend with U-line
245	25 _{1,24} – 24 _{1,23}	136400.164	100	81	85.2	28	Blend with HC ¹³ CCN, $v_7=1$ and C ₂ H ₃ CN, $v_{11}=2$
246	27 _{2,26} – 26 _{2,25}	145476.697	100	94	91.9	25	Blend with C ₂ H ₅ CN, $v_{13}=1/v_{21}=1$ and O ¹³ CS
247	28 _{5,24} – 27 _{5,23}	154303.763	50	118	93.0	112	Blend with C ₂ H ₅ OH and CH ₃ OCH ₃
248	28 _{5,23} – 27 _{5,22}	154393.012	50	118	93.0	112	Blend with HCC ¹³ CN, $v_7=1$
249	28 _{4,25} – 27 _{4,24}	154410.681	50	111	94.1	112	Strong HNCO and CH ₃ OH
250	31 _{1,30} – 30 _{2,29}	163397.978	100	124	9.6	38	Blend with C ₂ H ₅ CN and CH ₃ COOH
251	31 _{2,30} – 30 _{2,29}	166330.213	100	124	105.7	66	Blend with ¹³ CH ₃ CH ₂ CN and U-lines
252	33 _{1,33} – 32 _{0,32}	172468.973	100	134	14.3	44	Strong C ₂ H ₅ CN and CH ₃ OCHO, $v_t=1$
253	31 _{4,27} – 30 _{4,26}	172707.869	100	135	104.6	44	Blend with H ¹³ CN in absorption and C ₂ H ₅ CN, $v_{13}=1/v_{21}=1$
254	32 _{7,26} – 31 _{7,25}	176045.797	4	166	104.5	365	Noisy
255	32 _{7,25} – 31 _{7,24}	176046.676	4	166	104.5	365	Noisy
256	32 _{6,27} – 31 _{6,26}	176266.224	100	157	105.9	365	Noisy
257	32 _{6,26} – 31 _{6,25}	176285.887	100	157	105.9	365	Noisy
258	38 _{1,37} – 37 _{2,36}	201872.699	100	185	13.2	138	Strong ¹³ CH ₃ CH ₂ CN
259	53 _{2,51} – 53 _{1,52}	201925.976	100	370	6.7	138	Strong CH ₂ CO
260	36 _{4,32} – 35 _{4,31}	201931.928	100	179	122.0	138	Strong CH ₂ CO
261	36 _{3,33} – 35 _{3,32}	202388.460	100	175	122.6	108	Blend with C ₂ H ₃ CN, $v_{11}=1$
262	53 _{3,51} – 53 _{2,52}	202394.525	28	370	6.7	108	Blend with C ₂ H ₃ CN, $v_{11}=1$
263	62 _{5,58} – 62 _{3,59}	202561.279	17	524	1.4	108	Strong C ₂ H ₃ CN, $v_{15}=1$
264	38 _{2,37} – 37 _{2,36}	202563.884	100	185	129.7	108	Strong C ₂ H ₃ CN, $v_{15}=1$
265	38 _{1,37} – 37 _{1,36}	202730.394	100	185	129.7	108	Blend with CH ₃ OCH ₃ and C ₂ H ₃ CN, $v_{15}=1$
266	37 _{23,14} – 36 _{23,13} *	203008.778	28	556	77.9	138	Blend with U-line
268	37 _{22,15} – 36 _{22,14} *	203008.823	19	523	82.0	138	Blend with U-line
270	37 _{24,13} – 36 _{24,12} *	203009.542	40	589	73.5	138	Blend with U-line
272	37 _{21,16} – 36 _{21,15} *	203009.945	13	492	86.0	138	Blend with U-line
274	37 _{25,12} – 36 _{25,11} *	203010.874	56	624	69.0	138	Blend with U-line
276	37 _{20,17} – 36 _{20,16} *	203012.456	9	463	89.8	138	Blend with U-line
278	37 _{26,11} – 36 _{26,10} *	203012.555	77	661	64.2	138	Blend with U-line
280	37 _{27,10} – 36 _{27,9} *	203014.377	104	699	59.3	138	Blend with U-line

Table 1. continued.

N^a	Transition ^b	Frequency (MHz)	Unc. ^c (kHz)	E_l^d (K)	$S\mu^2$ (D ²)	σ^e (mK)	Comments
(1)	(2)	(3)	(4)	(5)	(6)	(7)	(8)
282	37 _{28,9} – 36 _{28,8} *	203016.140	138	738	54.2	138	Blend with U-line
284	37 _{19,18} – 36 _{19,17} *	203016.766	100	435	93.4	138	Blend with U-line
286	37 _{29,8} – 36 _{29,7} *	203017.650	181	779	48.9	138	Blend with U-line
288	37 _{18,19} – 36 _{18,18} *	203023.193	6	408	96.9	138	Blend with CH ₃ OCH ₃
290	37 _{17,20} – 36 _{17,19} *	203032.356	100	383	100.1	138	Blend with CH ₃ OCH ₃ and CH ₃ ¹³ CN, $v_8=1$
292	37 _{16,21} – 36 _{16,20} *	203045.040	100	360	103.2	138	Blend with CH ₃ ¹³ CH ₂ CN and U-line
294	37 _{15,22} – 36 _{15,21} *	203062.173	100	337	106.1	138	Blend with ¹³ CH ₃ CH ₂ CN
296	37 _{14,23} – 36 _{14,22} *	203085.040	100	316	108.7	138	Blend with CH ₃ ¹³ CH ₂ CN
298	37 _{2,35} – 36 _{2,34}	203093.256	100	181	126.0	138	Blend with H ¹³ CCCN, $v_6=1$
299	37 _{13,24} – 36 _{13,23} *	203115.417	100	297	111.2	138	Blend with C ₂ H ₃ CN, $v_{11}=1/v_{15}=1$
301	37 _{12,25} – 36 _{12,24} *	203155.887	100	279	113.6	138	Strong CH ₃ CN, $v_8=1$
303	37 _{11,26} – 36 _{11,25} *	203210.265	100	263	115.7	138	Blend with U-line
305	39 _{0,39} – 38 _{1,38}	203277.722	100	187	17.2	161	Blend with C ₂ H ₃ CN, $v_{11}=1$
306	37 _{10,27} – 36 _{10,26} *	203284.465	100	247	117.6	161	Blend with C ₂ H ₃ CN, $v_{11}=1$ and U-line
308	39 _{1,39} – 38 _{1,38}	203293.314	100	187	133.5	161	Blend with CH ₃ CN, $v_8=2$
309	39 _{0,39} – 38 _{0,38}	203297.717	100	187	133.5	161	Blend with CH ₃ CN, $v_8=2$
310	39 _{1,39} – 38 _{0,38}	203313.274	100	187	17.2	161	Blend with U-line
311	37 _{9,29} – 36 _{9,28} *	203387.942	4	234	119.4	161	Strong C ₂ H ₃ CN, CH ₃ OCH ₃ , and SO ₂
313	7 _{6,2} – 6 _{5,1} *	203409.735	13	24	2.7	161	Strong C ₂ H ₃ CN, CH ₃ OCH ₃ , and ¹³ CH ₂ CHCN
315	38 _{2,37} – 37 _{1,36}	203421.857	4	185	13.2	161	Strong CH ₃ OCH ₃ and ¹³ CH ₂ CHCN
316	37 _{8,30} – 36 _{8,29}	203536.955	4	222	121.0	161	Blend with CH ₃ CN, $v_8=2$ and ¹³ CH ₂ CHCN
317	37 _{8,29} – 36 _{8,28}	203537.200	4	222	121.0	161	Blend with CH ₃ CN, $v_8=2$ and ¹³ CH ₂ CHCN
318	37 _{7,31} – 36 _{7,30}	203760.083	100	211	122.4	364	Blend with U-line
319	37 _{7,30} – 36 _{7,29}	203765.767	100	211	122.4	364	Blend with C ₃ H ₇ CN and ¹³ CH ₂ CHCN
320	37 _{4,34} – 36 _{4,33}	203781.525	4	188	125.4	364	Blend with ¹³ CH ₂ CHCN and U-line
321	18 _{4,14} – 17 _{3,15}	203899.881	11	47	2.8	364	Blend with C ₃ H ₇ CN and U-line
322	37 _{6,32} – 36 _{6,31}	204086.275	100	202	123.6	364	Blend with H ¹³ CCCN, $v_7=2$ and U-line
323	34 _{3,32} – 33 _{2,31}	204129.239	11	153	7.0	316	Blend with ³⁴ SO ₂
324	37 _{6,31} – 36 _{6,30}	204178.927	100	202	123.6	316	Blend with CH ₃ CH ₃ CO and U-line?
325	37 _{5,33} – 36 _{5,32}	204364.928	4	194	124.6	316	Blend with CH ₃ CH ₃ CO
326	82 _{8,75} – 81 _{9,72}	204369.553	82	938	5.1	316	Blend with CH ₃ CH ₃ CO and SO ₂
327	75 _{8,67} – 74 _{9,66}	205281.393	47	792	5.8	100	Blend with SO ₂
328	37 _{5,32} – 36 _{5,31}	205282.240	100	194	124.6	100	Blend with SO ₂
329	13 _{5,9} – 12 _{4,8}	206264.566	12	32	2.8	280	Strong C ₂ H ₃ CN and CH ₃ OCHO
330	13 _{5,8} – 12 _{4,9}	206270.541	12	32	2.8	280	Strong C ₂ H ₃ CN and CH ₃ OCHO
331	38 _{3,36} – 37 _{3,35}	206596.942	100	191	129.3	106	Strong C ₂ H ₃ CN, $v_{13}=1/v_{21}=1$
332	19 _{4,16} – 18 _{3,15}	206607.866	11	52	2.9	106	Strong C ₂ H ₃ CN
333	35 _{3,33} – 34 _{2,32}	207085.257	11	162	7.5	117	Strong C ₂ H ₃ CN
334	39 _{1,38} – 38 _{2,37}	207168.207	4	195	13.7	117	Blend with CH ₃ CH ₃ CO and U-line
335	39 _{2,38} – 38 _{2,37}	207723.987	100	195	133.1	282	Blend with U-line and C ₂ H ₃ CN, $v_{13}=1/v_{21}=1$
336	37 _{4,33} – 36 _{4,32}	207774.900	4	189	125.5	282	Blend with C ₂ H ₅ OH
337	37 _{3,34} – 36 _{3,33}	207820.202	100	185	126.0	173	Blend with C ₃ H ₇ CN and C ₂ H ₅ OH
338	39 _{1,38} – 38 _{1,37}	207859.555	4	195	133.1	173	Blend with C ₂ H ₃ CN, $v_{13}=1/v_{21}=1$
339	38 _{2,36} – 37 _{2,35}	208144.350	100	191	129.4	173	Blend with CH ₂ CH ¹³ CN and C ₂ H ₃ CN, $v_{11}=1$
340	39 _{2,38} – 38 _{1,37}	208415.332	4	195	13.7	168	Strong C ₂ H ₃ CN
341	40 _{0,40} – 39 _{1,39}	208431.560	5	197	17.7	168	Strong C ₂ H ₃ CN
342	40 _{1,40} – 39 _{1,39}	208443.521	100	197	137.0	168	Strong C ₂ H ₃ CN
343	40 _{0,40} – 39 _{0,39}	208447.014	100	197	137.0	168	Strong C ₂ H ₃ CN
344	40 _{1,40} – 39 _{0,39}	208459.081	5	197	17.7	168	Strong C ₂ H ₃ CN
345	38 _{23,15} – 37 _{23,14} *	208493.011	28	565	82.6	168	Strong C ₂ H ₃ CN
347	38 _{24,14} – 37 _{24,13} *	208493.410	41	599	78.3	168	Strong C ₂ H ₃ CN
349	38 _{22,16} – 37 _{22,15} *	208493.496	19	533	86.6	168	Strong C ₂ H ₃ CN
351	38 _{25,13} – 37 _{25,12} *	208494.438	57	634	73.9	168	Strong C ₂ H ₃ CN
353	38 _{21,17} – 37 _{21,16} *	208495.153	13	502	90.5	168	Strong C ₂ H ₃ CN
355	38 _{26,12} – 37 _{26,11} *	208495.863	79	671	69.3	168	Strong C ₂ H ₃ CN
357	38 _{27,11} – 37 _{27,10} *	208497.466	107	709	64.5	168	Strong C ₂ H ₃ CN
359	38 _{20,18} – 37 _{20,17} *	208498.313	9	473	94.2	168	Strong C ₂ H ₃ CN
361	38 _{28,10} – 37 _{28,9} *	208499.037	142	748	59.6	168	Strong C ₂ H ₃ CN
363	38 _{29,9} – 37 _{29,8} *	208500.372	185	789	54.4	168	Strong C ₂ H ₃ CN
365	38 _{19,19} – 37 _{19,18} *	208503.415	100	445	97.8	168	Strong C ₂ H ₃ CN, $v_{13}=1/v_{21}=1$
367	38 _{18,20} – 37 _{18,19} *	208510.857	100	418	101.1	168	Blend with C ₂ H ₅ OH and C ₂ H ₃ CN
369	38 _{17,21} – 37 _{17,20} *	208521.187	100	393	104.3	168	Blend with C ₂ H ₅ OH
371	38 _{16,22} – 37 _{16,21} *	208535.402	100	369	107.2	168	Blend with C ₂ H ₅ OH
373	38 _{15,23} – 37 _{15,22} *	208554.387	100	347	110.0	168	Blend with C ₂ H ₃ CN, $v_{13}=1/v_{21}=1$ and U-line

Table 1. continued.

N^a	Transition ^b	Frequency (MHz)	Unc. ^c (kHz)	E_l^d (K)	$S\mu^2$ (D ²)	σ^e (mK)	Comments
(1)	(2)	(3)	(4)	(5)	(6)	(7)	(8)
375	38 _{14,24} – 37 _{14,23} *	208579.484	100	326	112.6	168	Blend with CH ₃ CH ₃ CO, $v_l=1$ and U-line
377	38 _{13,25} – 37 _{13,24} *	208612.841	4	307	115.1	168	Strong C ₂ H ₅ CN, $v_{13}=1/v_{21}=1$
379	38 _{12,26} – 37 _{12,25} *	208657.029	4	289	117.3	168	Blend with CH ₃ OCHO and CH ₃ CH ₃ CO
381	38 _{11,27} – 37 _{11,26} *	208716.183	100	272	119.4	160	Blend with CH ₃ OCHO
383	38 _{10,29} – 37 _{10,28} *	208796.910	4	257	121.3	160	Blend with CH ₂ CH ¹³ CN and CH ₃ OCHO
385	8 _{6,3} – 7 _{5,2} *	208895.157	13	25	2.8	160	Strong CH ₃ OCHO and C ₂ H ₃ CN
387	38 _{8,31} – 37 _{8,30}	209071.357	4	231	124.6	160	Strong C ₂ H ₃ CN
388	38 _{8,30} – 37 _{8,29}	209071.723	4	231	124.6	160	Strong C ₂ H ₃ CN
389	38 _{4,35} – 37 _{4,34}	209201.665	4	197	128.8	58	Strong H ₂ CS and C ₂ H ₃ CN, $v_{15}=1$
390	38 _{7,32} – 37 _{7,31}	209313.439	4	221	125.9	58	Strong C ₂ H ₃ CN, $v_{15}=1$
391	38 _{7,31} – 37 _{7,30}	209321.499	4	221	125.9	58	Strong C ₂ H ₃ CN, $v_{15}=1$
392	19 _{4,15} – 18 _{3,16}	209541.953	11	52	2.9	58	Blend with C ₂ H ₃ CN
393	38 _{6,33} – 37 _{6,32}	209660.931	4	212	127.1	45	Blend with C ₂ H ₃ CN, $v_{11}=1$, HC ¹³ CCN, $v_7=2$, and HCC ¹³ CN, $v_7=2$
394	38 _{6,32} – 37 _{6,31}	209783.452	100	212	127.1	45	Blend with C ₂ H ₃ CN, $v_{11}=1/v_{15}=1$
395	38 _{5,34} – 37 _{5,33}	209918.890	4	204	128.1	45	Strong CH ₃ OCHO
396	36 _{3,34} – 35 _{2,33}	210218.541	10	172	8.0	64	Blend with C ₂ H ₃ CN, $v_{11}=2$
397	40 _{2,38} – 39 _{3,37}	210705.222	6	211	10.0	37	Blend with C ₂ H ₃ CN, $v_{11}=2$ and U-line
398	38 _{5,33} – 37 _{5,32}	211044.215	100	204	128.1	33	Blend with C ₂ H ₅ CN
399	20 _{4,17} – 19 _{3,16}	211264.158	11	57	3.0	33	Strong CH ₃ OCHO
400	14 _{5,10} – 13 _{4,9}	211717.651	12	35	2.9	47	Strong C ₂ H ₃ CN
401	14 _{5,9} – 13 _{4,10} *	211728.949	12	35	2.9	47	Strong C ₂ H ₃ CN
402	39 _{3,37} – 38 _{3,36}	211830.506	100	201	132.7	47	Blend with NH ₂ ¹³ CHO, $v_{12}=1$
403	51 _{1,50} – 51 _{0,51}	211833.125	40	333	3.3	47	Blend with NH ₂ ¹³ CHO, $v_{12}=1$
404	40 _{1,39} – 39 _{2,38}	212435.627	4	205	14.2	36	Strong NH ₂ CHO and CH ₃ OCHO
405	40 _{2,39} – 39 _{2,38}	212881.373	100	205	136.5	99	Blend with H ¹³ CCCN, $v_7=2$
406	40 _{1,39} – 39 _{1,38}	212991.436	100	205	136.5	99	Blend with ³⁴ SO ₂ and U-line?
407	39 _{2,37} – 38 _{2,36}	213191.655	100	201	132.8	48	Blend with CH ₂ (OH)CHO
408	38 _{3,35} – 37 _{3,34}	213203.256	100	195	129.4	48	Blend with CH ₂ (OH)CHO
409	40 _{2,39} – 39 _{1,38}	213437.154	5	205	14.2	48	Blend with C ₂ H ₅ OH and CH ₃ OCH ₃
410	37 _{3,35} – 36 _{2,34}	213536.157	9	181	8.5	48	Blend with C ₂ H ₃ CN, $v_{11}=2$
411	41 _{0,41} – 40 _{1,40}	213584.046	5	207	18.2	48	Blend with ¹³ CH ₂ CHCN
412	41 _{1,41} – 40 _{1,40}	213593.386	100	207	140.4	48	Partial blend with H ¹³ CCCN, $v_5=1/v_7=3$, uncertain baseline
413	41 _{0,41} – 40 _{0,40}	213596.056	100	207	140.4	48	Partial blend with H ¹³ CCCN, $v_5=1/v_7=3$, uncertain baseline
414	38 _{4,34} – 37 _{4,33}	213600.651	100	199	129.0	48	Partial blend with H ¹³ CCCN, $v_5=1/v_7=3$, uncertain baseline
415	41 _{1,41} – 40 _{0,40}	213605.377	5	207	18.2	48	Partial blend with H ¹³ CCCN, $v_5=1/v_7=3$, uncertain baseline
416	39 _{23,16} – 38 _{23,15} *	213977.041	29	575	87.2	48	Strong C ₂ H ₅ ¹³ CN and CH ₃ ¹³ CH ₂ CN
418	39 _{24,15} – 38 _{24,14} *	213977.045	42	609	83.1	48	Strong C ₂ H ₅ ¹³ CN and CH ₃ ¹³ CH ₂ CN
420	39 _{25,14} – 38 _{25,13} *	213977.743	59	644	78.8	48	Strong C ₂ H ₅ ¹³ CN and CH ₃ ¹³ CH ₂ CN
422	39 _{22,17} – 38 _{22,16} *	213978.002	20	543	91.2	48	Strong C ₂ H ₅ ¹³ CN and CH ₃ ¹³ CH ₂ CN
424	39 _{26,13} – 38 _{26,12} *	213978.888	81	681	74.3	48	Strong C ₂ H ₅ ¹³ CN and CH ₃ ¹³ CH ₂ CN
426	39 _{21,18} – 38 _{21,17} *	213980.233	13	512	95.0	48	Strong C ₂ H ₅ ¹³ CN and CH ₃ ¹³ CH ₂ CN
428	39 _{27,12} – 38 _{27,11} *	213980.250	109	719	69.7	48	Strong C ₂ H ₅ ¹³ CN and CH ₃ ¹³ CH ₂ CN
430	39 _{28,11} – 38 _{28,10} *	213981.610	145	758	64.8	48	Strong C ₂ H ₅ ¹³ CN and CH ₃ ¹³ CH ₂ CN
432	39 _{29,10} – 38 _{29,9} *	213982.754	190	799	59.8	48	Strong C ₂ H ₅ ¹³ CN and CH ₃ ¹³ CH ₂ CN
434	39 _{20,19} – 38 _{20,18} *	213984.089	9	483	98.6	48	Strong C ₂ H ₅ ¹³ CN and CH ₃ ¹³ CH ₂ CN
436	39 _{19,20} – 38 _{19,19} *	213989.994	7	455	102.0	48	Strong C ₂ H ₅ ¹³ CN and CH ₃ ¹³ CH ₂ CN
438	39 _{18,21} – 38 _{18,20} *	213998.464	6	428	105.3	48	Strong C ₂ H ₅ ¹³ CN and CH ₃ ¹³ CH ₂ CN
440	39 _{17,22} – 38 _{17,21} *	214010.151	5	403	108.3	48	Strong C ₂ H ₅ ¹³ CN and CH ₃ ¹³ CH ₂ CN
442	39 _{16,24} – 38 _{16,23} *	214025.894	5	379	111.3	48	Strong C ₂ H ₅ ¹³ CN and CH ₃ ¹³ CH ₂ CN
444	39 _{15,24} – 38 _{15,23} *	214046.781	100	357	114.0	48	Blend with ¹³ CH ₃ CN
446	39 _{14,25} – 38 _{14,24} *	214074.316	100	336	116.5	75	Strong CH ₃ OCH ₃ and CH ₃ ¹³ CH ₂ CN
448	39 _{13,26} – 38 _{13,25} *	214110.717	4	317	118.9	75	Blend with ¹³ CH ₃ CN
450	39 _{12,27} – 38 _{12,26} *	214158.803	100	299	121.1	75	Blend with C ₂ H ₅ ¹³ CN
452	39 _{11,28} – 38 _{11,27} *	214223.159	100	282	123.1	75	Strong CH ₂ NH and ¹³ CH ₃ CN
454	39 _{10,30} – 38 _{10,29} *	214310.764	4	267	125.0	75	Strong ¹³ CH ₃ CN
456	66 _{4,62} – 66 _{3,63}	214317.063	27	591	13.5	75	Strong ¹³ CH ₃ CN
457	9 _{6,4} – 8 _{5,3} *	214379.791	13	27	2.8	75	Strong ¹³ CH ₃ CN
459	39 _{9,31} – 38 _{9,30} *	214432.762	4	254	126.6	75	Blend with CH ₃ ¹³ CH ₂ CN and C ₂ H ₅ OH
461	22 _{3,19} – 21 _{2,20}	214433.988	14	63	1.7	75	Blend with CH ₃ ¹³ CH ₂ CN and C ₂ H ₅ OH
462	65 _{5,61} – 65 _{4,62}	214600.532	23	574	13.4	75	Blend with CH ₃ CH ₃ CO
463	39 _{4,36} – 38 _{4,35}	214605.781	4	207	132.3	75	Blend with CH ₃ CH ₃ CO and CH ₃ ¹³ CH ₂ CN
464	56 _{8,49} – 56 _{7,50}	214606.526	11	457	15.7	75	Blend with CH ₃ CH ₃ CO and CH ₃ ¹³ CH ₂ CN

Table 1. continued.

N^a	Transition ^b	Frequency (MHz)	Unc. ^c (kHz)	E_l^d (K)	$S\mu^2$ (D ²)	σ^e (mK)	Comments
(1)	(2)	(3)	(4)	(5)	(6)	(7)	(8)
465	39 _{8,32} – 38 _{8,31}	214608.530	4	241	128.1	75	Blend with CH ₃ ¹³ CH ₂ CN
466	39 _{8,31} – 38 _{8,30}	214609.070	4	241	128.1	75	Blend with CH ₃ ¹³ CH ₂ CN
467	39 _{7,33} – 38 _{7,32}	214870.593	100	231	129.5	75	Blend with ¹³ CH ₃ CN, $v_8=1$
468	39 _{7,32} – 38 _{7,31}	214881.820	4	231	129.5	75	Blend with ¹³ CH ₂ CHCN
469	39 _{6,34} – 38 _{6,33}	215238.445	100	222	130.6	74	Strong C ₂ H ₅ CN, $v_{13}=1/v_{21}=1$ and C ₂ H ₅ CN, $v_{20}=1$
470	20 _{4,16} – 19 _{3,17}	215256.547	11	57	2.9	74	Strong C ₂ H ₅ CN, $v_{13}=1/v_{21}=1$ and C ₂ H ₅ CN, $v_{20}=1$
471	39 _{6,33} – 38 _{6,32}	215399.020	100	222	130.6	74	Strong C ₂ H ₅ CN
472	39 _{5,35} – 38 _{5,34}	215467.027	4	214	131.6	74	Strong C ₂ H ₅ CN, $v_{13}=1/v_{21}=1$
473	21 _{4,18} – 20 _{3,17}	215732.383	12	62	3.0	74	Strong C ₂ H ₅ CN, $v_{13}=1/v_{21}=1$
474	39 _{5,34} – 38 _{5,33}	216832.944	100	214	131.6	50	Strong CH ₃ OCHO
475	61 _{3,58} – 61 _{3,59}	216833.377	28	498	1.2	50	Strong CH ₃ OCHO
476	41 _{2,39} – 40 _{3,38}	216942.926	5	222	10.6	50	Strong CH ₃ OH
477	38 _{3,36} – 37 _{2,35}	217039.712	8	191	9.0	50	Blend with ¹³ CH ₃ OH and ¹³ CN
478	40 _{3,38} – 39 _{3,37}	217052.822	100	211	136.1	50	Blend with ¹³ CH ₃ OH, ¹³ CN, and U-line
479	15 _{5,11} – 14 _{4,10}	217159.548	12	39	3.0	50	Blend with CH ₃ OCH ₃
480	15 _{5,10} – 14 _{4,11}	217179.901	12	39	3.0	50	Blend with CH ₃ OCH ₃ and U-line
481	41 _{1,40} – 40 _{2,39}	217679.824	4	215	14.7	50	Blend with U-line
482	39 _{4,35} – 38 _{4,34}	219402.429	4	209	132.5	92	Strong C ₂ H ₅ CN
483	40 _{24,16} – 39 _{24,15} *	219460.441	43	619	87.8	92	Strong C ₂ H ₅ CN
485	40 _{25,15} – 39 _{25,14} *	219460.780	60	655	83.6	92	Strong C ₂ H ₅ CN
487	40 _{23,17} – 39 _{23,16} *	219460.864	30	586	91.8	92	Strong C ₂ H ₅ CN
489	40 _{26,14} – 39 _{26,13} *	219461.621	83	691	79.2	92	Strong C ₂ H ₅ CN
491	40 _{22,18} – 39 _{22,17} *	219462.336	20	553	95.7	92	Strong C ₂ H ₅ CN
493	40 _{27,13} – 39 _{27,12} *	219462.721	112	729	74.7	92	Strong C ₂ H ₅ CN
495	40 _{28,12} – 39 _{28,11} *	219463.851	149	768	70.0	92	Strong C ₂ H ₅ CN
497	40 _{21,19} – 39 _{21,18}	219465.183	14	522	99.4	92	Strong C ₂ H ₅ CN
498	40 _{21,20} – 39 _{21,19}	219465.523	100	522	99.4	92	Strong C ₂ H ₅ CN
499	40 _{20,20} – 39 _{20,19}	219469.782	10	493	102.9	92	Strong NH ₂ CN
500	40 _{20,21} – 39 _{20,20}	219469.912	100	493	102.9	92	Strong NH ₂ CN
501	40 _{19,21} – 39 _{19,20} *	219476.588	7	465	106.3	92	Strong NH ₂ CN
503	40 _{18,22} – 39 _{18,21}	219486.155	6	438	109.4	92	Strong HC ₃ N, $v_6=v_7=1$
504	40 _{18,23} – 39 _{18,22}	219486.310	100	438	109.4	92	Strong HC ₃ N, $v_6=v_7=1$
505	40 _{17,23} – 39 _{17,22}	219499.182	5	413	112.4	92	Strong C ₂ H ₅ CN
506	40 _{17,24} – 39 _{17,23}	219499.329	100	413	112.4	92	Strong C ₂ H ₅ CN
507	40 _{16,25} – 39 _{16,24} *	219516.573	5	390	115.3	92	Strong HC ₃ N, $v_6=v_7=1$
509	40 _{15,25} – 39 _{15,24} *	219539.521	5	367	117.9	92	Strong HNCO and H ₂ CO, $v_5=1$
511	40 _{14,26} – 39 _{14,25} *	219569.648	5	346	120.4	92	Strong C ¹⁸ O
513	67 _{4,63} – 67 _{3,64}	219571.157	30	609	13.4	92	Strong C ¹⁸ O
514	40 _{13,27} – 39 _{13,26} *	219609.218	5	327	122.7	92	Strong C ₂ H ₅ CN, $v_{15}=1$ and CH ₂ CH ¹³ CN
516	40 _{12,28} – 39 _{12,27}	219661.381	100	309	124.8	92	Strong HNCO and HC ₃ N, $v_7=2$
517	40 _{12,29} – 39 _{12,28}	219661.485	5	309	124.8	92	Strong HNCO and HC ₃ N, $v_7=2$
518	40 _{11,30} – 39 _{11,29} *	219731.290	4	293	126.8	92	Strong HNCO
520	40 _{7,34} – 39 _{7,33}	220431.537	100	241	133.0	98	Strong CH ₃ ¹³ CN
521	40 _{7,33} – 39 _{7,32}	220446.964	100	241	133.0	98	Blend with U-line, uncertain baseline
522	41 _{7,35} – 40 _{7,34}	225996.244	100	252	136.5	278	Blend with CH ₃ CH ₃ CO, $v_7=1$, uncertain baseline
523	41 _{7,34} – 40 _{7,33}	226017.388	100	252	136.5	278	Blend with U-line?, uncertain baseline
524	63 _{3,60} – 63 _{2,61}	226393.597	33	530	10.0	278	Blend with CN in absorption, C ₂ H ₃ CN, and C ₂ H ₅ OH
525	41 _{6,36} – 40 _{6,35}	226400.096	100	243	137.6	278	Blend with CN in absorption and C ₂ H ₅ OH
526	41 _{5,37} – 40 _{5,36}	226540.631	4	235	138.5	278	Blend with CH ₂ NH
527	41 _{6,35} – 40 _{6,34}	226668.561	4	243	137.6	96	Strong CN absorption
528	22 _{4,18} – 21 _{3,19}	226986.056	11	67	3.0	96	Strong CN absorption
529	42 _{3,40} – 41 _{3,39}	227467.207	100	233	143.0	85	Blend with CH ₂ (OH)CHO, CH ₂ CH ¹³ CN, and C ₃ H ₇ CN
530	24 _{4,21} – 23 _{3,20}	227801.331	12	80	3.2	85	Strong CH ₃ OH
531	42 _{9,34} – 41 _{9,33} *	231015.633	5	285	137.4	183	Blend with CH ₃ OCHO, H ₂ ¹³ CS, and U-line
533	42 _{8,35} – 41 _{8,34}	231237.570	5	273	138.8	183	Strong ¹³ CH ₂ CHCN and C ₂ H ₃ CN, $v_{15}=1$
534	42 _{8,34} – 41 _{8,33}	231239.195	5	273	138.8	183	Strong ¹³ CH ₂ CHCN and C ₂ H ₃ CN, $v_{15}=1$
535	25 _{4,22} – 24 _{3,21}	231328.525	13	86	3.3	40	Blend with CH ₃ CHO and ¹³ CH ₂ CHCN
536	42 _{7,36} – 41 _{7,35}	231564.827	4	262	140.1	40	Blend with C ₂ H ₅ OH
537	42 _{7,35} – 41 _{7,34}	231593.484	100	263	140.1	40	Blend with CH ₃ ¹³ CH ₂ CN
538	43 _{3,41} – 42 _{3,40}	232661.017	5	243	146.4	19	Blend with C ₂ H ₅ CN, $v_{13}=1/v_{21}=1$
539	42 _{3,40} – 41 _{2,39}	232789.078	6	232	11.2	19	Strong CH ₃ OH, C ₂ H ₅ CN, and C ₂ H ₃ CN, $v_{11}=1$
540	43 _{26,17} – 42 _{26,16} *	235907.995	89	723	93.6	131	Blend with HCC ¹³ CN, $v_6=1$
542	43 _{27,16} – 42 _{27,15} *	235908.172	120	761	89.3	131	Blend with HCC ¹³ CN, $v_6=1$

Table 1. continued.

N^a	Transition ^b	Frequency (MHz)	Unc. ^c (kHz)	E_l^d (K)	$S\mu^2$ (D ²)	σ^e (mK)	Comments
(1)	(2)	(3)	(4)	(5)	(6)	(7)	(8)
544	43 _{25,18} – 42 _{25,17} *	235908.220	65	687	97.6	131	Blend with HCC ¹³ CN, $v_6=1$
546	43 _{24,19} – 42 _{24,18} *	235909.130	46	652	101.6	131	Blend with HCC ¹³ CN, $v_6=1$
548	43 _{23,20} – 42 _{23,19} *	235911.029	32	618	105.3	131	Blend with HCC ¹³ CN, $v_6=1$
550	43 _{22,22} – 42 _{22,21} *	235914.238	100	586	108.9	131	Strong CH ₃ OCHO
552	43 _{21,22} – 42 _{21,21} *	235919.208	15	555	112.3	131	Strong CH ₃ OCHO
554	43 _{20,23} – 42 _{20,22}	235926.335	10	525	115.6	131	Strong CH ₃ OCHO, C ₂ H ₃ CN, $v_{15}=1$, and ¹³ CH ₃ OH
555	43 _{20,24} – 42 _{20,23}	235926.477	100	525	115.6	131	Strong CH ₃ OCHO, C ₂ H ₃ CN, $v_{15}=1$, and ¹³ CH ₃ OH
556	43 _{19,24} – 42 _{19,23} *	235936.190	8	497	118.7	131	Strong CH ₃ OCHO, C ₂ H ₃ CN, $v_{15}=1$, and ¹³ CH ₃ OH
558	43 _{18,25} – 42 _{18,24} *	235949.452	6	471	121.6	131	Strong C ₂ H ₃ CN, $v_{15}=1$, ¹³ CH ₃ OH, and C ₂ H ₅ ¹³ CN
560	43 _{17,26} – 42 _{17,25} *	235966.980	6	446	124.4	131	Strong ¹³ CH ₃ OH and SiS
562	43 _{16,27} – 42 _{16,26} *	235989.879	100	422	127.1	131	Strong ¹³ CH ₃ OH
564	43 _{13,31} – 42 _{13,30} *	236108.561	100	359	134.0	37	Blend with C ₂ H ₅ CN, $v_{13}=1/v_{21}=1$ and NH ₂ CH ₂ CN
566	43 _{12,31} – 42 _{12,30} *	236174.724	5	342	136.0	37	Blend with ¹³ CH ₃ CH ₂ CN and CH ₃ ¹³ CHCN
568	43 _{11,32} – 42 _{11,31} *	236262.562	100	325	137.9	37	Blend with C ₂ H ₅ CN, $v_{13}=1/v_{21}=1$ and NH ₂ CH ₂ CN
570	13 _{6,8} – 12 _{5,7} *	236300.957	13	39	3.1	37	Strong CH ₂ ¹³ CHCN and C ₂ H ₅ OH
572	65 _{4,62} – 65 _{3,63}	236306.402	38	563	10.0	37	Strong ¹³ CH ₃ CH ₂ CN
573	43 _{10,33} – 42 _{10,32} *	236381.716	100	310	139.5	37	Blend with CH ₂ ¹³ CHCN
575	43 _{9,35} – 42 _{9,34}	236547.689	5	296	141.0	37	Blend with ¹³ CH ₃ CH ₂ CN
576	43 _{9,34} – 42 _{9,33}	236547.789	5	296	141.0	37	Blend with ¹³ CH ₃ CH ₂ CN
577	20 _{5,16} – 19 _{4,15}	244080.041	12	62	3.4	46	Blend with CH ₃ CH ₃ CO, $v_7=1$
578	20 _{5,15} – 19 _{4,16}	244307.468	12	62	3.4	46	Blend with CH ₃ OH and C ₂ H ₅ ¹³ CN
579	9 _{7,2} – 8 _{6,3} *	244368.037	13	35	3.2	46	Blend with C ₂ H ₅ CN
581	47 _{0,47} – 46 _{1,46}	244480.036	7	272	21.2	91	Blend with ³⁴ SO ₂
582	47 _{1,47} – 46 _{1,46}	244482.013	7	272	161.0	91	Blend with ³⁴ SO ₂
583	47 _{0,47} – 46 _{0,46}	244482.600	7	272	161.0	91	Blend with ³⁴ SO ₂
584	47 _{1,47} – 46 _{0,46}	244484.577	7	272	21.2	91	Blend with ³⁴ SO ₂
585	44 _{3,41} – 43 _{3,40}	244500.437	5	260	149.8	91	Blend with CH ₃ OCH ₃
586	30 _{4,27} – 29 _{3,26}	245163.234	16	123	3.8	72	Strong HCC ¹³ CN, $v_7=1$
587	25 _{4,21} – 24 _{3,22}	245723.730	11	86	3.0	53	Blend with CH ₂ ¹³ CHCN
588	45 _{17,28} – 44 _{17,27} *	246946.103	100	469	132.3	68	Strong C ₂ H ₃ CN
590	45 _{16,29} – 44 _{16,28} *	246973.216	6	445	134.8	68	Blend with C ₂ H ₅ CN and CH ₃ COOH
592	45 _{15,30} – 44 _{15,29} *	247008.106	100	423	137.2	68	Strong C ₂ H ₃ CN
594	45 _{14,31} – 44 _{14,30} *	247053.206	100	402	139.4	68	Strong CH ₃ OCHO
596	45 _{13,33} – 44 _{13,32} *	247111.643	100	382	141.5	68	Strong HC ₃ N, $v_7=2$ and CH ₃ OCHO
598	45 _{12,34} – 44 _{12,33} *	247188.187	5	364	143.4	68	Blend with C ₂ H ₃ CN, CH ₃ CH ₃ CO, $v_7=1$ and CH ₃ COOH
600	15 _{6,10} – 14 _{5,9}	247242.428	12	46	3.3	68	Strong C ₂ H ₃ CN, $v_{15}=1$ and CH ₃ ¹³ CH ₂ CN
601	15 _{6,9} – 14 _{5,10}	247242.754	12	46	3.3	68	Strong C ₂ H ₃ CN, $v_{15}=1$ and CH ₃ ¹³ CH ₂ CN
602	31 _{4,28} – 30 _{3,27}	247248.744	16	131	3.9	68	Strong C ₂ H ₃ CN, $v_{15}=1$ and CH ₃ ¹³ CH ₂ CN
603	45 _{11,35} – 44 _{11,34} *	247289.755	5	348	145.1	68	Blend with C ₂ H ₃ CN, $v_{15}=1$
605	56 _{9,48} – 56 _{8,49}	247291.902	12	468	15.2	68	Blend with C ₂ H ₃ CN, $v_{15}=1$
606	45 _{10,36} – 44 _{10,35} *	247427.317	5	333	146.7	68	Blend with H ¹³ CCCN, $v_6=1$ and t-HCOOH
608	46 _{4,43} – 45 _{4,42}	251970.749	5	285	156.4	42	Blend with CH ₃ OCH ₃ and CH ₃ OH
609	45 _{5,40} – 44 _{5,39}	252031.184	100	281	152.5	42	Blend with C ₂ H ₅ CN, $v_{13}=1/v_{21}=1$
610	46 _{21,25} – 45 _{21,24}	252371.919	16	590	124.9	42	Strong ¹³ CH ₃ OH
611	46 _{21,26} – 45 _{21,25}	252372.057	100	590	124.9	42	Strong ¹³ CH ₃ OH
612	46 _{20,26} – 45 _{20,25}	252382.043	11	560	128.0	42	Blend with ¹³ CH ₃ CH ₂ CN
613	46 _{20,27} – 45 _{20,26}	252382.165	100	560	128.0	42	Blend with ¹³ CH ₃ CH ₂ CN
614	46 _{19,27} – 45 _{19,26}	252395.494	8	532	130.9	42	Strong NH ₂ CHO and C ₂ H ₃ CN, $v_{11}=1$
615	46 _{19,28} – 45 _{19,27}	252395.596	100	532	130.9	42	Strong NH ₂ CHO and C ₂ H ₃ CN, $v_{11}=1$
616	26 _{4,22} – 25 _{3,23}	252401.668	100	92	3.0	42	Strong NH ₂ CHO and C ₂ H ₃ CN, $v_{11}=1$
617	46 _{18,28} – 45 _{18,27} *	252413.093	7	506	133.6	42	Blend with C ₂ H ₃ CN, $v_{11}=1$ and U-line
619	46 _{17,30} – 45 _{17,29} *	252435.886	6	480	136.2	42	Strong C ₂ H ₅ CN, $v_{13}=1/v_{21}=1$
621	46 _{16,31} – 45 _{16,30}	252465.229	6	457	138.7	42	Strong U-line
622	46 _{16,30} – 45 _{16,29}	252465.379	100	457	138.7	42	Strong U-line
623	93 _{7,86} – 93 _{6,87}	252466.454	90	1191	24.1	42	Strong U-line
624	34 _{9,25} – 34 _{8,26}	253951.681	13	203	8.3	32	Strong C ₂ H ₅ CN and SO ₂
625	34 _{9,26} – 34 _{8,27}	253951.859	13	203	8.3	32	Strong C ₂ H ₅ CN and SO ₂
626	46 _{7,39} – 45 _{7,38}	253965.040	5	309	154.1	32	Strong NS
627	48 _{1,47} – 47 _{2,46}	254009.911	6	293	18.1	32	Strong CH ₃ OH in absorption
628	35 _{4,32} – 34 _{3,31}	254021.313	17	166	4.6	32	Strong CH ₃ OH in absorption
629	46 _{5,42} – 45 _{5,41}	254033.953	5	292	155.8	32	Blend with HC ¹³ CCN, $v_6=1$ and C ₂ H ₅ OH
630	33 _{9,24} – 33 _{8,25}	254066.133	13	194	8.0	32	Blend with C ₂ H ₅ CN
631	33 _{9,25} – 33 _{8,26}	254066.244	13	194	8.0	32	Blend with C ₂ H ₅ CN

Table 1. continued.

N^a	Transition ^b	Frequency (MHz)	Unc. ^c (kHz)	E_l^d (K)	$S\mu^2$ (D ²)	σ^e (mK)	Comments
(1)	(2)	(3)	(4)	(5)	(6)	(7)	(8)
632	48 _{2,47} – 47 _{2,46}	254081.225	6	293	163.9	32	Strong CH ₃ CH ₃ CO and C ₂ H ₅ CN
633	86 _{6,80} – 86 _{5,81}	254082.060	64	1013	20.4	32	Strong CH ₃ CH ₃ CO and C ₂ H ₅ CN
634	48 _{1,47} – 47 _{1,46}	254100.087	6	293	164.0	32	Blend with SiS
635	32 _{9,23} – 32 _{8,24} *	254170.380	13	185	7.7	32	Blend with ¹³ CH ₃ CH ₂ CN
637	48 _{2,47} – 47 _{1,46}	254171.401	6	293	18.1	32	Blend with ¹³ CH ₃ CH ₂ CN
638	31 _{9,22} – 31 _{8,23} *	254265.069	13	177	7.4	32	Strong HCC ¹³ CN, $v_7=1$ and SO ₂
640	46 _{6,41} – 45 _{6,40}	254311.469	5	300	155.1	32	Strong C ₂ H ₅ CN and ¹³ CH ₃ CH ₂ CN
641	30 _{9,21} – 30 _{8,22} *	254350.818	13	169	7.2	32	Strong NH ₂ ¹³ CHO
643	89 _{8,82} – 89 _{7,83}	254352.623	46	1095	23.7	32	Strong NH ₂ ¹³ CHO
644	29 _{9,20} – 29 _{8,21} *	254428.220	13	161	6.9	32	Strong CH ₃ OH
646	11 _{7,5} – 10 _{6,4} *	255337.696	13	40	3.4	217	Strong HC ₃ N, $v_7=1$
648	47 _{3,45} – 46 _{2,44}	255440.594	6	289	13.8	217	Strong CH ₂ CH ¹³ CN
649	36 _{4,33} – 35 _{3,32}	255457.676	18	175	4.9	217	Strong C ₂ H ₅ CN, $v_{13}=1/v_{21}=1$ and CH ₂ ¹³ CHCN
650	47 _{18,29} – 46 _{18,28} *	257901.052	7	518	137.6	1127	Blend with CH ₃ CN, $v_8=1$
652	47 _{17,30} – 46 _{17,29} *	257925.778	6	493	140.1	1127	Noisy, blend with C ₂ H ₃ CN, $v_{11}=1/v_{15}=1$ and CH ₃ OCHO
654	46 _{5,41} – 45 _{5,40}	257933.505	5	293	156.0	1127	Noisy, blend with C ₂ H ₃ CN, $v_{11}=1/v_{15}=1$ and CH ₃ OCHO
655	47 _{16,31} – 46 _{16,30} *	257957.480	6	469	142.5	1127	Blend with C ₂ H ₅ ¹³ CN
657	47 _{15,32} – 46 _{15,31} *	257998.085	6	447	144.8	1127	Strong CH ₃ CN, $v_8=1$ and CH ₃ OCHO
659	47 _{14,33} – 46 _{14,32} *	258050.228	6	426	146.9	1127	Strong CH ₃ CN, $v_8=1$
661	47 _{13,34} – 46 _{13,33} *	258117.607	6	406	148.9	1127	Strong CH ₃ OCHO
663	17 _{6,12} – 16 _{5,11}	258162.597	12	54	3.5	1127	Strong ¹³ CH ₃ OH and HC ¹⁵ N
664	17 _{6,11} – 16 _{5,12}	258163.845	12	54	3.5	1127	Strong ¹³ CH ₃ OH and HC ¹⁵ N
665	47 _{12,35} – 46 _{12,34} *	258205.577	6	388	150.7	1127	Strong CH ₃ CN, $v_8=1$
667	38 _{4,35} – 37 _{3,34}	258232.157	17	195	5.4	1127	Strong CH ₃ CN, $v_8=1$
668	47 _{11,37} – 46 _{11,36} *	258322.177	6	372	152.4	1127	Strong CH ₃ CN, $v_8=1$
670	48 _{2,46} – 47 _{2,45}	258838.876	6	302	163.6	1609	Noisy
671	46 _{4,42} – 45 _{4,41}	258951.138	5	288	156.6	1609	Strong CH ₃ CN, $v_8=2$
672	70 _{4,67} – 70 _{3,68}	259007.596	58	650	10.0	1609	Blend with H ¹³ CN in absorption and CH ₃ CN, $v_8=2$
673	47 _{8,40} – 46 _{8,39}	259016.319	6	331	156.5	1609	Blend with H ¹³ CN in absorption and CH ₃ CN, $v_8=2$
674	96 _{11,85} – 96 _{10,86}	259022.243	75	1306	29.4	1609	Blend with H ¹³ CN in absorption, CH ₃ CN, $v_8=2$, and CH ₃ ¹³ CH ₂ CN
675	47 _{8,39} – 46 _{8,38}	259024.824	6	331	156.5	1609	Blend with H ¹³ CN in absorption, CH ₃ CN, $v_8=2$, and CH ₃ ¹³ CH ₂ CN
676	94 _{7,87} – 94 _{6,88}	259169.651	93	1215	24.0	1609	Noisy, blend with CH ₃ CH ₃ CO, $v_t=1$ and C ₂ H ₅ CN, $v_{13}=1/v_{21}=1$
677	49 _{1,48} – 48 _{2,47}	259170.075	6	306	18.6	1609	Noisy, blend with CH ₃ CH ₃ CO, $v_t=1$ and C ₂ H ₅ CN, $v_{13}=1/v_{21}=1$
678	49 _{2,48} – 48 _{2,47}	259226.397	6	306	167.4	1609	Strong C ₂ H ₅ ¹³ CN, ¹³ CH ₂ CHCN, and C ₂ H ₅ CN
679	49 _{1,48} – 48 _{1,47}	259241.389	6	306	167.4	1609	Strong C ₂ H ₅ ¹³ CN, ¹³ CH ₂ CHCN, and C ₂ H ₅ CN
680	75 _{4,71} – 75 _{3,72}	259244.206	58	756	13.4	1609	Strong C ₂ H ₅ ¹³ CN, ¹³ CH ₂ CHCN, and C ₂ H ₅ CN
681	48 _{3,46} – 47 _{2,45}	260229.609	6	302	14.3	413	Strong C ₂ H ₅ CN
682	23 _{5,18} – 22 _{4,19}	260510.203	11	78	3.6	413	Strong C ₂ H ₅ CN, $v_{13}=1/v_{21}=1$
683	48 _{20,28} – 47 _{20,27} *	263352.009	12	585	136.1	74	Blend with HCC ¹³ CN, $v_7=1$ and ¹³ CH ₃ CH ₂ CN
685	48 _{19,29} – 47 _{19,28} *	263368.180	9	557	138.9	74	Blend with NH ₂ CH ₂ CN
687	48 _{18,30} – 47 _{18,29} *	263389.051	7	530	141.5	74	Strong HNCO, $v_4=1$ and CH ₃ OCH ₃
689	48 _{17,31} – 47 _{17,30} *	263415.803	7	505	144.0	74	Strong CH ₃ OCH ₃
691	48 _{16,32} – 47 _{16,31} *	263449.974	6	481	146.4	74	Strong HNCO
693	48 _{15,33} – 47 _{15,32} *	263493.569	100	459	148.6	74	Blend with C ₂ H ₅ ¹³ CN and CH ₃ OCH ₃
695	48 _{14,34} – 47 _{14,33} *	263549.541	100	438	150.6	74	Strong NH ₂ CHO, SO ₂ , and NH ₂ CHO, $v_{12}=1$
697	18 _{6,13} – 17 _{5,12}	263612.153	12	58	3.6	74	Blend with NH ₂ CH ₂ CN and CH ₃ OCH ₃
698	18 _{6,12} – 17 _{5,13}	263614.442	12	58	3.6	74	Blend with NH ₂ CH ₂ CN and CH ₃ OCH ₃
699	48 _{13,35} – 47 _{13,34}	263621.701	6	419	152.5	74	Blend with CH ₃ OCH ₃
700	48 _{13,36} – 47 _{13,35}	263621.895	100	419	152.5	74	Blend with CH ₃ OCH ₃
701	49 _{3,47} – 48 _{3,46}	263687.072	100	314	167.0	108	Strong HNCO and HN ¹³ CO
702	48 _{12,36} – 47 _{12,35} *	263715.805	6	401	154.4	108	Blend with HCC ¹³ CN, $v_7=1$ and HNCO, $v_6=1$
704	47 _{5,42} – 46 _{5,41}	263828.012	6	305	159.5	108	Blend with HC ₃ N, $v_5=1/v_7=3$ and C ₂ H ₅ CN
705	48 _{11,38} – 47 _{11,37} *	263840.460	6	384	156.0	108	Blend with U-line and NH ₂ CHO
707	49 _{2,47} – 48 _{2,46}	263943.595	6	314	167.0	108	Blend with U-line and NH ₂ CHO
708	76 _{4,72} – 76 _{3,73}	264005.376	63	775	13.4	108	Strong CH ₃ ¹³ CH ₂ CN and C ₂ H ₅ CN
709	48 _{10,39} – 47 _{10,38} *	264009.192	6	369	157.5	108	Strong CH ₃ ¹³ CH ₂ CN and C ₂ H ₅ CN
711	48 _{6,42} – 47 _{6,41}	266696.771	100	324	162.1	91	Strong CH ₃ ¹³ CH ₂ CN, C ₂ H ₅ CN, and CH ₃ OH

Notes: ^a Numbering of the observed transitions associated with a modeled line stronger than 20 mK. ^b Transitions marked with a * are double with a frequency difference less than 0.1 MHz. The quantum numbers of the second one are not shown. ^c Frequency uncertainty. ^d Lower energy level in temperature units (E_l/k_B). ^e Calculated rms noise level in T_{mb} scale.

Table 2. Transitions of the *gauche*-conformer of ethyl formate observed with the IRAM 30 m telescope toward Sgr B2(N). The horizontal lines mark discontinuities in the observed frequency coverage. Only the transitions associated with a modeled line stronger than 20 mK are listed.

N^a	Transition ^b	Frequency (MHz)	Unc. ^c (kHz)	E_l^d (K)	$S\mu^2$ (D ²)	σ^e (mK)	Comments
(1)	(2)	(3)	(4)	(5)	(6)	(7)	(8)
1	14 _{7,8} – 13 _{7,7}	99252.267	9	140	43.9	19	Blend with a(CH ₂ OH) ₂ and C ₂ H ₅ CN
2	14 _{7,7} – 13 _{7,6}	99252.460	9	140	43.9	19	Blend with a(CH ₂ OH) ₂ and C ₂ H ₅ CN
3	16 _{1,16} – 15 _{1,15}	104834.473	10	132	66.3	25	Blend with C ₂ H ₅ CN, $v_{13}=1/v_{21}=1$ and U-line
4	16 _{0,16} – 15 _{0,15}	104848.839	10	132	66.3	25	Blend with C ₂ H ₅ CN, $v_{11}=1/v_{15}=1$
5	15 _{9,7} – 14 _{9,6} *	106216.238	9	154	40.2	25	Blend with C ₂ H ₅ CN, $v_{11}=1/v_{15}=1$
7	15 _{8,8} – 14 _{8,7} *	106286.532	9	149	44.9	25	Blend with U-line
9	15 _{7,9} – 14 _{7,8}	106400.093	9	144	49.1	25	Blend with U-line
10	15 _{7,8} – 14 _{7,7}	106400.593	9	144	49.1	25	Blend with U-line
11	15 _{2,13} – 14 _{2,12}	107933.484	100	131	60.9	46	Blend with C ₂ H ₅ CN, $v_{13}=1/v_{21}=1$, C ₃ H ₇ CN, and U-line
12	15 _{4,11} – 14 _{4,10}	108497.732	10	134	58.3	20	Blend with C ₂ H ₅ CN and U-line
13	16 _{2,15} – 15 _{2,14}	108858.373	9	135	65.2	20	Blend with ¹³ CN in absorption, CH ₃ CH ₃ CO, $v_i=1$, and U-line
14	16 _{1,15} – 15 _{1,14}	109206.256	100	135	65.3	29	Blend with C ₂ H ₅ CN, $v_{13}=1/v_{21}=1$ and U-line
15	15 _{3,12} – 14 _{3,11}	110117.142	10	133	60.4	24	Blend with U-lines
16	17 _{1,17} – 16 _{1,16}	111255.183	100	137	70.5	35	Blend with CH ₃ OH
17	17 _{0,17} – 16 _{0,16}	111263.830	100	137	70.5	35	Blend with C ₂ H ₅ CN, $v_{11}=1/v_{15}=1$ and ¹³ CH ₃ CH ₂ CN
18	16 _{3,14} – 15 _{3,13}	112186.512	8	137	64.2	42	Blend with CH ₂ ¹³ CHCN
19	16 _{10,6} – 15 _{10,5} *	113276.855	9	165	40.8	28	Blend with CH ₃ OCH ₃
21	16 _{9,8} – 15 _{9,7} *	113332.031	9	159	45.8	28	Blend with C ₂ H ₅ CN, $v_{13}=1/v_{21}=1$ and CH ₂ ¹³ CHCN
23	16 _{8,9} – 15 _{8,8} *	113419.845	9	154	50.2	28	Blend with C ₂ H ₅ CN, $v_{11}=1$
25	46 _{10,37} – 46 _{9,38}	113560.008	23	488	62.8	28	Strong CN in absorption
26	16 _{7,10} – 15 _{7,9}	113560.122	9	150	54.1	28	Strong CN in absorption
27	16 _{7,9} – 15 _{7,8}	113561.324	9	150	54.1	28	Strong CN in absorption
28	16 _{6,11} – 15 _{6,10}	113783.618	9	146	57.5	34	Blend with U-line
29	16 _{6,10} – 15 _{6,9}	113810.530	9	146	57.5	34	Blend with C ₂ H ₅ CN, $v_{15}=1$
30	16 _{4,13} – 15 _{4,12}	113866.411	9	139	62.7	34	Blend with a-C ₂ H ₅ OCHO and U-line
31	16 _{5,12} – 15 _{5,11}	114054.354	9	142	60.4	33	Blend with C ₂ H ₅ CN, $v_{15}=1$
32	16 _{2,14} – 15 _{2,13}	114356.265	100	137	64.9	33	Blend with CH ₃ CH ₃ CO and U-line
33	16 _{5,11} – 15 _{5,10}	114420.852	100	142	60.4	37	Blend with C ₂ H ₅ CN, $v_{11}=1/v_{15}=1$
34	42 _{6,36} – 42 _{5,37}	115318.413	41	411	44.6	60	Strong CO
35	17 _{2,16} – 16 _{2,15}	115319.089	9	140	69.4	60	Strong CO
36	17 _{1,16} – 16 _{1,15}	115551.954	100	140	69.4	60	Blend with C ₂ H ₅ CN
37	22 _{1,21} – 21 _{2,20}	147415.492	100	171	37.3	31	Blend with CH ₃ CH ₃ CO, $v_i=1$ and CH ₃ ¹³ CN, $v_8=1$
38	9 _{7,3} – 8 _{6,2} *	147431.313	18	117	14.5	31	Blend with C ₂ H ₅ OH and CH ₃ CN, $v_8=1$
40	9 _{7,3} – 8 _{6,3} *	147431.321	18	117	0.9	31	Blend with C ₂ H ₅ OH and CH ₃ CN, $v_8=1$
42	22 _{2,21} – 21 _{2,20}	147454.440	100	171	90.3	31	Blend with a(CH ₂ OH) ₂ , CH ₃ ¹³ CN, $v_8=1$, and CH ₃ OCH ₃
43	22 _{1,21} – 21 _{1,20}	147479.064	100	171	90.3	31	Blend with CH ₃ CN, $v_8=1$ and ¹³ CH ₃ CH ₂ CN
44	22 _{2,21} – 21 _{1,20}	147517.966	100	171	37.3	31	Blend with CH ₃ ¹³ CN, $v_8=1$ and CH ₃ CN, $v_8=1$
45	10 _{7,4} – 9 _{6,3} *	154495.310	18	120	14.6	112	Blend with C ₂ H ₅ CN
47	10 _{7,4} – 9 _{6,4} *	154495.348	18	120	0.9	112	Blend with C ₂ H ₅ CN
49	23 _{9,15} – 22 _{9,14}	163354.580	7	205	81.5	38	Group possibly detected, partial blend with c-C ₂ H ₄ O, uncertain baseline
50	23 _{9,14} – 22 _{9,13}	163355.083	7	205	81.5	38	Group possibly detected, partial blend with c-C ₂ H ₄ O, uncertain baseline
51	23 _{3,20} – 22 _{3,19}	163550.748	100	184	93.0	38	Blend with CH ₃ OCHO, $v_i=1$ and CH ₂ CH ¹³ CN
52	23 _{8,16} – 22 _{8,15}	163648.730	7	199	84.6	38	Blend with C ₃ H ₇ CN and NH ₂ ¹³ CHO
53	23 _{8,15} – 22 _{8,14}	163658.516	7	199	84.6	38	Blend with C ₃ H ₇ CN, uncertain baseline
54	24 _{5,19} – 23 _{5,18}	176014.876	9	196	96.4	365	Blend with CH ₃ OCHO, CH ₂ CH ¹³ CN, and HNCO, $v_5=1$
55	19 _{6,14} – 18 _{5,13}	202061.374	15	160	13.8	138	Blend with CH ₃ ¹³ CN
56	15 _{8,8} – 14 _{7,7} *	202643.074	17	144	17.5	108	Blend with CH ₃ CN, $v_8=1$ and CH ₃ ¹³ CN, $v_8=1$
58	15 _{8,8} – 14 _{7,8} *	202643.365	17	144	1.1	108	Blend with CH ₃ CN, $v_8=1$ and CH ₃ ¹³ CN, $v_8=1$
60	30 _{2,28} – 29 _{3,27}	202805.197	7	241	47.3	138	Blend with C ₂ H ₅ CN and CH ₃ ¹³ CN, $v_8=1$
61	30 _{3,28} – 29 _{3,27}	202824.924	100	241	122.7	138	Strong CH ₃ CN, $v_8=1$
62	30 _{2,28} – 29 _{2,27}	202837.051	100	241	122.6	138	Strong CH ₃ CN, $v_8=1$
63	45 _{9,37} – 44 _{10,34}	202856.742	41	463	10.5	138	Blend with CH ₃ CN, $v_8=1$
64	30 _{3,28} – 29 _{2,27}	202856.967	7	241	47.3	138	Blend with CH ₃ CN, $v_8=1$
65	65 _{8,58} – 65 _{7,59}	202857.921	214	828	52.8	138	Blend with CH ₃ CN, $v_8=1$
66	17 _{7,11} – 16 _{6,10}	203524.096	16	151	15.9	161	Blend with CH ₃ CN, $v_8=2$
67	17 _{7,10} – 16 _{6,10}	203528.806	16	151	1.1	161	Blend with CH ₃ CN, $v_8=2$
68	17 _{7,11} – 16 _{6,11}	203574.259	16	151	1.1	161	Blend with CH ₃ CN, $v_8=2$
69	17 _{7,10} – 16 _{6,11}	203578.970	16	151	15.9	161	Blend with CH ₃ CN, $v_8=2$ and C ₂ H ₅ CN, $v_{20}=1$
70	29 _{5,25} – 28 _{5,24}	204412.101	7	240	116.8	316	Blend with ¹³ CH ₃ CH ₂ CN and U-lines
71	19 _{6,14} – 18 _{5,14}	204417.969	16	160	1.2	316	Blend with ¹³ CH ₃ CH ₂ CN and U-lines

Table 2. continued.

N^a	Transition ^b	Frequency (MHz)	Unc. ^c (kHz)	E_l^d (K)	$S\mu^2$ (D ²)	σ^e (mK)	Comments
(1)	(2)	(3)	(4)	(5)	(6)	(7)	(8)
72	59 _{17,43} – 59 _{16,44}	205092.813	17	774	72.3	100	Strong C ₂ H ₅ CN, CH ₃ OCH ₃ , and CH ₃ ¹³ CH ₂ CN
73	28 _{5,23} – 27 _{5,22}	205093.048	8	232	113.5	100	Strong C ₂ H ₅ CN, CH ₃ OCH ₃ , and CH ₃ ¹³ CH ₂ CN
74	31 _{1,30} – 30 _{2,29}	205095.436	11	245	57.4	100	Strong CH ₃ ¹³ CH ₂ CN and CH ₃ OCH ₃
75	31 _{2,30} – 30 _{2,29}	205095.823	11	245	127.9	100	Strong CH ₃ ¹³ CH ₂ CN and CH ₃ OCH ₃
76	31 _{1,30} – 30 _{1,29}	205096.091	11	245	127.9	100	Strong CH ₃ ¹³ CH ₂ CN and CH ₃ OCH ₃
77	31 _{2,30} – 30 _{1,29}	205096.478	11	245	57.4	100	Strong CH ₃ ¹³ CH ₂ CN and CH ₃ OCH ₃
78	29 _{18,11} – 28 _{18,10} *	205308.386	8	332	74.6	100	Strong SO ₂
80	29 _{17,12} – 28 _{17,11} *	205313.243	8	321	79.7	100	Strong SO ₂ and U-line?
82	54 _{14,40} – 53 _{15,39} *	205317.032	22	650	15.2	100	Strong SO ₂ and U-line?
84	29 _{19,11} – 28 _{19,10}	205317.035	9	343	69.3	100	Strong SO ₂ and U-line?
85	29 _{16,13} – 28 _{16,12} *	205334.455	8	311	84.4	100	Strong CH ₃ ¹³ CH ₂ CN
87	29 _{20,9} – 28 _{20,8} *	205337.037	9	355	63.6	100	Strong CH ₃ ¹³ CH ₂ CN
89	29 _{21,8} – 28 _{21,7} *	205366.726	10	368	57.7	100	Blend with C ₂ H ₅ ¹³ CN
91	29 _{15,14} – 28 _{15,13} *	205375.865	8	301	88.9	100	Strong C ₂ H ₅ CN
93	29 _{14,15} – 28 _{14,14} *	205442.791	7	292	93.1	100	Blend with CH ₃ ¹³ CH ₂ CN and C ₂ H ₅ ¹³ CN
95	29 _{13,17} – 28 _{13,16} *	205542.814	7	284	97.0	271	Blend with U-line
97	29 _{12,18} – 28 _{12,17} *	205687.132	7	276	100.6	271	Blend with C ₂ H ₃ CN, $v_{11}=1$, uncertain baseline
99	29 _{27,2} – 28 _{27,1} *	205690.300	20	456	16.2	271	Blend with C ₂ H ₃ CN, $v_{11}=1$, uncertain baseline
101	29 _{11,19} – 28 _{11,18} *	205893.033	7	269	103.9	271	Blend with C ₂ H ₅ ¹³ CN
103	29 _{10,20} – 28 _{10,19}	206188.338	7	263	106.9	280	Blend with SO and ¹³ CH ₂ CHCN
104	29 _{10,19} – 28 _{10,18}	206190.002	7	263	106.9	280	Blend with SO and ¹³ CH ₂ CHCN
105	29 _{4,25} – 28 _{4,24}	206280.705	100	240	117.1	280	Blend with C ₂ H ₅ CN and C ₂ H ₅ CN, $v_{20}=1$
106	29 _{9,21} – 28 _{9,20}	206614.666	7	257	109.6	106	Strong C ₂ H ₅ CN and CH ₃ OCHO
107	29 _{9,20} – 28 _{9,19}	206639.557	7	257	109.6	106	Blend with U-lines
108	56 _{17,40} – 56 _{16,40}	206650.461	14	715	2.7	106	Blend with C ₂ H ₅ CN
109	56 _{17,39} – 56 _{16,40}	206650.601	14	715	67.2	106	Blend with C ₂ H ₅ CN
110	56 _{17,40} – 56 _{16,41}	206652.471	14	715	67.2	106	Blend with C ₂ H ₅ CN
111	56 _{17,39} – 56 _{16,41}	206652.612	14	715	2.7	106	Blend with C ₂ H ₅ CN
112	30 _{3,27} – 29 _{4,26}	206654.482	7	246	38.8	106	Blend with C ₂ H ₅ CN
113	29 _{6,24} – 28 _{6,23}	206929.917	8	244	115.8	117	Strong C ₂ H ₅ CN, $v_{20}=1$ and C ₂ H ₅ CN
114	30 _{4,27} – 29 _{4,26}	206996.130	100	246	121.8	117	Blend with OCS, $v_2=1$ and NH ₂ ¹³ CHO
115	28 _{5,24} – 27 _{4,23}	207002.205	100	230	24.1	117	Blend with OCS, $v_2=1$ and NH ₂ ¹³ CHO
116	30 _{3,27} – 29 _{3,26}	207175.063	100	246	121.8	117	Blend with U-line
117	29 _{8,22} – 28 _{8,21}	207183.249	7	252	112.1	117	Blend with U-line
118	12 _{10,2} – 11 _{9,3} *	207240.583	16	141	21.0	117	Blend with CH ₃ OCHO and U-line
120	12 _{10,2} – 11 _{9,2} *	207240.583	16	141	1.2	117	Blend with CH ₃ OCHO and U-line
122	32 _{0,32} – 31 _{0,31} *	207408.086	100	249	133.2	282	Blend with C ₂ H ₅ CN, $v_{13}=1/v_{21}=1$
124	32 _{0,32} – 31 _{1,31} *	207408.141	17	249	67.2	282	Blend with C ₂ H ₅ CN, $v_{13}=1/v_{21}=1$
126	29 _{8,21} – 28 _{8,20}	207451.586	7	252	112.1	282	Blend with C ₂ H ₅ CN, $v_{13}=1/v_{21}=1$ and C ₂ H ₅ OH
127	30 _{4,27} – 29 _{3,26}	207516.619	7	246	38.8	282	Blend with CH ₃ CH ₃ CO, $v_7=1$ and U-line
128	29 _{7,23} – 28 _{7,22}	207601.807	8	247	114.2	282	Strong NH ₂ CHO, $v_{12}=1$ and C ₂ H ₃ CN
129	20 _{6,15} – 19 _{5,14}	207703.938	15	166	13.7	282	Blend with CH ₃ OCH ₃
130	14 _{9,6} – 13 _{8,5} *	208513.304	16	144	19.3	168	Blend with C ₂ H ₅ OH and C ₂ H ₃ CN
132	14 _{9,5} – 13 _{8,6} *	208513.306	16	144	19.3	168	Blend with C ₂ H ₅ OH and C ₂ H ₃ CN
134	31 _{2,29} – 30 _{3,28}	209205.202	8	251	49.5	58	Strong H ₂ CS and C ₂ H ₃ CN, $v_{15}=1$
135	31 _{3,29} – 30 _{3,28}	209217.484	100	251	126.8	58	Strong C ₂ H ₃ CN, $v_{15}=1$, CH ₃ OCHO, and HC ₃ N
136	31 _{2,29} – 30 _{2,28}	209225.073	100	251	126.8	58	Strong CH ₃ OCHO and HC ₃ N
137	31 _{3,29} – 30 _{2,28}	209237.276	8	251	49.5	58	Strong HC ₃ N
138	74 _{18,56} – 74 _{17,57} *	209239.716	197	1125	97.1	58	Strong HC ₃ N
140	29 _{7,22} – 28 _{7,21}	209426.660	9	248	114.3	58	Strong CH ₃ OCH ₃ and CH ₃ CH ₃ CO
141	16 _{8,9} – 15 _{7,8} *	209662.326	16	150	17.7	45	Strong C ₂ H ₃ CN, $v_{11}=1$, HC ¹³ CCN, $v_7=2$, and HCC ¹³ CN, $v_7=2$
143	16 _{8,9} – 15 _{7,9} *	209663.117	16	150	1.2	45	Strong C ₂ H ₃ CN, $v_{11}=1$, HC ¹³ CCN, $v_7=2$, and HCC ¹³ CN, $v_7=2$
145	18 _{7,12} – 17 _{6,11}	210394.041	16	157	16.0	64	Blend with C ₂ H ₅ OH and CH ₃ OCHO
146	18 _{7,11} – 17 _{6,12}	210507.031	16	157	16.0	64	Strong HC ₃ N, $v_7=2$
147	41 _{17,24} – 41 _{16,25} *	210945.438	10	465	43.1	37	Strong NH ₂ ¹³ CHO and C ₂ H ₅ CN, $v_{13}=1/v_{21}=1$
149	41 _{17,25} – 41 _{16,26} *	210945.438	10	465	43.1	37	Strong NH ₂ ¹³ CHO and C ₂ H ₅ CN, $v_{13}=1/v_{21}=1$
151	30 _{5,26} – 29 _{5,25}	210948.194	7	250	121.0	37	Strong NH ₂ ¹³ CHO and C ₂ H ₅ CN, $v_{13}=1/v_{21}=1$
152	29 _{5,25} – 28 _{4,24}	211213.126	100	240	26.6	33	Strong H ₂ CO in absorption
153	32 _{1,31} – 31 _{2,30}	211492.742	12	255	59.6	33	Strong CH ₃ OCH ₃
154	32 _{2,31} – 31 _{2,30}	211492.971	12	255	132.0	33	Strong CH ₃ OCH ₃
155	32 _{1,31} – 31 _{1,30}	211493.129	12	255	132.0	33	Strong CH ₃ OCH ₃
156	32 _{2,31} – 31 _{1,30}	211493.358	12	255	59.6	33	Strong CH ₃ OCH ₃
157	29 _{5,24} – 28 _{5,23}	211817.880	100	242	117.5	47	Blend with CH ₃ OH, $v_7=1$ and U-line

Table 2. continued.

N^a	Transition ^b	Frequency (MHz)	Unc. ^c (kHz)	E_l^d (K)	$S\mu^2$ (D ²)	σ^e (mK)	Comments
(1)	(2)	(3)	(4)	(5)	(6)	(7)	(8)
158	18 _{17,1} – 18 _{16,2} *	211857.177	16	231	4.4	47	Blend with C ₂ H ₃ CN, $v_{15}=1$ and U-line
160	29 _{17,12} – 29 _{16,13} *	211859.692	10	320	24.2	47	Blend with C ₂ H ₃ CN, $v_{15}=1$ and U-line
162	29 _{17,12} – 29 _{16,14} *	211859.692	10	320	1.2	47	Blend with C ₂ H ₃ CN, $v_{15}=1$ and U-line
164	28 _{17,11} – 28 _{16,12} *	211880.904	10	311	22.6	47	Blend with CH ₂ CH ¹³ CN
166	28 _{17,11} – 28 _{16,13} *	211880.904	10	311	1.1	47	Blend with CH ₂ CH ¹³ CN
168	27 _{17,10} – 27 _{16,11} *	211896.387	11	301	20.9	47	Strong C ₂ H ₃ CN, $v_{11}=1$ and C ₂ H ₅ OH
170	27 _{17,10} – 27 _{16,12} *	211896.387	11	301	1.0	47	Strong C ₂ H ₃ CN, $v_{11}=1$ and C ₂ H ₅ OH
172	21 _{17,4} – 21 _{16,5} *	211896.595	13	251	10.4	47	Strong C ₂ H ₃ CN, $v_{11}=1$ and C ₂ H ₅ OH
174	21 _{17,4} – 21 _{16,6} *	211896.595	13	251	0.5	47	Strong C ₂ H ₃ CN, $v_{11}=1$ and C ₂ H ₅ OH
176	22 _{17,5} – 22 _{16,6} *	211905.280	13	259	12.2	47	Blend with CH ₃ CH ₃ CO, $v_7=1$, C ₂ H ₃ CN, $v_{11}=1$, and U-line
178	22 _{17,5} – 22 _{16,7} *	211905.280	13	259	0.6	47	Blend with CH ₃ CH ₃ CO, $v_7=1$, C ₂ H ₃ CN, $v_{11}=1$, and U-line
180	26 _{17,10} – 26 _{16,11} *	211906.656	11	292	19.2	47	Blend with CH ₃ CH ₃ CO, $v_7=1$, C ₂ H ₃ CN, $v_{11}=1$, and U-line
182	26 _{17,10} – 26 _{16,10}	211906.656	11	292	0.9	47	Blend with CH ₃ CH ₃ CO, $v_7=1$, C ₂ H ₃ CN, $v_{11}=1$, and U-line
183	26 _{17,9} – 26 _{16,10}	211906.776	100	292	19.2	47	Blend with CH ₃ CH ₃ CO, $v_7=1$, C ₂ H ₃ CN, $v_{11}=1$, and U-line
184	23 _{17,6} – 23 _{16,7} *	211911.066	12	266	14.0	47	Blend with CH ₃ CH ₃ CO, $v_7=1$, C ₂ H ₃ CN, $v_{11}=1$, and U-line
186	23 _{17,6} – 23 _{16,8} *	211911.066	12	266	0.7	47	Blend with CH ₃ CH ₃ CO, $v_7=1$, C ₂ H ₃ CN, $v_{11}=1$, and U-line
188	25 _{17,8} – 25 _{16,9} *	211912.208	11	283	17.5	47	Blend with CH ₃ CH ₃ CO, $v_7=1$, C ₂ H ₃ CN, $v_{11}=1$, and U-line
190	25 _{17,8} – 25 _{16,10} *	211912.208	11	283	0.9	47	Blend with CH ₃ CH ₃ CO, $v_7=1$, C ₂ H ₃ CN, $v_{11}=1$, and U-line
192	24 _{17,8} – 24 _{16,9} *	211913.523	12	275	15.8	47	Blend with CH ₃ CH ₃ CO, $v_7=1$, C ₂ H ₃ CN, $v_{11}=1$, and U-line
194	24 _{17,8} – 24 _{16,8}	211913.523	12	275	0.8	47	Blend with CH ₃ CH ₃ CO, $v_7=1$, C ₂ H ₃ CN, $v_{11}=1$, and U-line
195	24 _{17,7} – 24 _{16,8}	211913.626	100	275	15.8	47	Blend with CH ₃ CH ₃ CO, $v_7=1$, C ₂ H ₃ CN, $v_{11}=1$, and U-line
196	20 _{6,14} – 19 _{5,15}	212146.465	17	166	13.4	36	Strong NH ₂ CHO, $v_{12}=1$
197	30 _{4,26} – 29 _{4,25}	212369.981	100	249	121.2	36	Blend with U-line, NH ₂ ¹³ CHO, $v_{12}=1$, and C ₃ H ₇ CN, uncertain baseline
198	30 _{18,12} – 29 _{18,11} *	212385.195	8	341	80.3	36	Strong NH ₂ CHO, $v_{12}=1$
200	71 _{18,54} – 71 _{17,55}	212386.233	123	1051	91.5	36	Strong NH ₂ CHO, $v_{12}=1$
201	30 _{19,11} – 29 _{19,10} *	212390.341	8	353	75.2	36	Strong NH ₂ CHO, $v_{12}=1$
203	30 _{17,13} – 29 _{17,12} *	212394.782	8	331	85.2	36	Strong NH ₂ CHO, $v_{12}=1$
205	30 _{20,11} – 29 _{20,10} *	212407.836	9	365	69.7	36	Blend with NH ₂ ¹³ CHO, $v_{12}=1$ and CH ₃ CH ₃ CO, $v_7=1$
207	30 _{16,14} – 29 _{16,13} *	212422.256	8	320	89.8	36	Strong NH ₂ CHO
209	30 _{21,9} – 29 _{21,8} *	212435.843	9	377	64.0	36	Strong NH ₂ CHO
211	30 _{15,15} – 29 _{15,14} *	212471.882	8	311	94.1	99	Blend with C ₂ H ₅ OH, CH ₃ OCHO, and C ₃ H ₇ CN
213	30 _{22,8} – 29 _{22,7} *	212472.920	10	391	58.0	99	Blend with C ₂ H ₅ OH, CH ₃ OCHO, and C ₃ H ₇ CN
215	30 _{14,17} – 29 _{14,16} *	212549.578	7	302	98.2	99	Blend with NH ₂ ¹³ CHO and U-line
217	29 _{6,23} – 28 _{6,22}	212550.033	10	244	116.6	99	Blend with NH ₂ ¹³ CHO and U-line
218	30 _{13,17} – 29 _{13,16} *	212663.809	7	294	102.0	99	Blend with C ₂ H ₅ OH and ¹³ CH ₂ CHCN
220	30 _{12,19} – 29 _{12,18} *	212827.135	7	286	105.4	99	Strong ¹³ CH ₂ CHCN and NH ₂ CHO
222	30 _{28,3} – 29 _{28,2} *	212834.203	100	482	16.2	99	Strong ¹³ CH ₂ CHCN and NH ₂ CHO
224	21 _{6,16} – 20 _{5,15}	212845.604	15	173	13.7	99	Blend with ¹³ CH ₂ CHCN, uncertain baseline
225	11 _{11,1} – 10 _{10,0} *	212997.517	100	143	23.2	99	Blend with C ₂ H ₅ CN
227	11 _{11,0} – 10 _{10,0} *	212997.572	16	143	1.3	99	Blend with C ₂ H ₅ CN
229	30 _{11,20} – 29 _{11,19}	213059.055	7	279	108.7	48	Strong SO ₂
230	30 _{11,19} – 29 _{11,18}	213059.228	7	279	108.7	48	Strong SO ₂
231	31 _{3,28} – 30 _{4,27}	213169.983	7	255	41.1	48	Strong C ₂ H ₃ CN, $v_{11}=1$
232	30 _{10,21} – 29 _{10,20}	213390.877	7	273	111.6	48	Blend with CH ₃ CH ₃ CO, $v_7=1$, uncertain baseline
233	31 _{4,28} – 30 _{4,27}	213392.357	7	255	125.9	48	Blend with CH ₃ CH ₃ CO, $v_7=1$, uncertain baseline
234	30 _{10,20} – 29 _{10,19}	213394.012	7	273	111.6	48	Blend with CH ₃ CH ₃ CO, $v_7=1$, uncertain baseline
235	16 _{4,13} – 15 _{1,14}	213509.497	41	135	0.8	48	Blend with C ₂ H ₅ CN, $v_{13}=1/v_{21}=1$ and U-line
236	31 _{3,28} – 30 _{3,27} *	213511.580	100	255	125.9	48	Blend with C ₂ H ₅ CN, $v_{13}=1/v_{21}=1$ and U-line
237	31 _{4,28} – 30 _{3,27}	213733.932	7	255	41.1	48	Blend with C ₂ H ₅ CN, $v_{13}=1/v_{21}=1$
238	30 _{6,25} – 29 _{6,24}	213791.953	100	253	120.1	48	Blend with CH ₃ CH ₃ CO, $v_7=1$, C ₂ H ₃ CN, $v_{15}=1$, and U-line
239	33 _{0,33} – 32 _{1,32} *	213807.575	17	259	69.4	48	Blend with C ₂ H ₅ CN
241	33 _{0,33} – 32 _{0,32} *	213807.621	100	259	137.4	48	Blend with C ₂ H ₅ CN
243	30 _{9,22} – 29 _{9,21}	213865.943	7	267	114.2	48	Blend with C ₂ H ₅ OH and C ₂ H ₅ ¹³ CN
244	30 _{9,21} – 29 _{9,20}	213909.016	7	267	114.2	48	Blend with C ₃ H ₇ CN and ¹³ CH ₃ OH
245	13 _{10,3} – 12 _{9,4} *	214314.472	16	145	21.1	75	Strong ¹³ CH ₃ CN and C ₂ H ₅ ¹³ CN
247	13 _{10,3} – 12 _{9,3} *	214314.472	16	145	1.2	75	Strong ¹³ CH ₃ CN and C ₂ H ₅ ¹³ CN
249	30 _{8,23} – 29 _{8,22}	214467.553	8	262	116.6	75	Blend with CH ₃ OCH ₃
250	30 _{7,24} – 29 _{7,23}	214783.566	8	257	118.6	75	Strong CH ₃ OCHO
251	30 _{8,22} – 29 _{8,21}	214889.514	8	262	116.6	74	Blend with ¹³ CH ₂ CHCN
252	31 _{4,27} – 30 _{5,26}	214982.375	100	260	31.4	74	Strong C ₂ H ₅ ¹³ CN and ¹³ CH ₃ CN, $v_8=1$
253	15 _{9,7} – 14 _{8,6} *	215567.674	16	149	19.5	74	Strong C ₂ H ₅ CN, $v_{20}=1$ and C ₂ H ₅ CN, $v_{13}=1/v_{21}=1$
255	15 _{9,7} – 14 _{8,7} *	215567.680	16	149	1.2	74	Strong C ₂ H ₅ CN, $v_{20}=1$ and C ₂ H ₅ CN, $v_{13}=1/v_{21}=1$

Table 2. continued.

N^a	Transition ^b	Frequency (MHz)	Unc. ^c (kHz)	E_l^d (K)	$S\mu^2$ (D ²)	σ^e (mK)	Comments
(1)	(2)	(3)	(4)	(5)	(6)	(7)	(8)
257	32 _{2,30} – 31 _{3,29}	215600.637	8	261	51.8	74	Strong C ₂ H ₅ CN
258	32 _{3,30} – 31 _{3,29}	215608.230	100	261	131.0	74	Strong C ₂ H ₅ CN
259	32 _{2,30} – 31 _{2,29}	215612.952	100	261	131.0	74	Strong C ₂ H ₅ CN
260	32 _{3,30} – 31 _{2,29}	215620.426	8	261	51.8	74	Strong C ₂ H ₅ CN
261	36 _{9,27} – 36 _{6,30}	215623.049	44	336	2.1	74	Strong C ₂ H ₅ CN
262	30 _{5,26} – 29 _{4,25}	215880.577	100	249	29.1	55	Strong ¹³ CH ₃ OH
263	17 _{8,10} – 16 _{7,9}	216663.426	16	155	17.9	55	Blend with C ₂ H ₅ OH, C ₃ H ₇ CN, and U-line
264	17 _{8,9} – 16 _{7,9}	216663.574	16	155	1.2	55	Blend with C ₂ H ₅ OH, C ₃ H ₇ CN, and U-line
265	17 _{8,10} – 16 _{7,10}	216665.420	16	155	1.2	55	Blend with C ₂ H ₅ OH, C ₃ H ₇ CN, and U-line
266	17 _{8,9} – 16 _{7,10}	216665.567	16	155	17.9	55	Blend with C ₂ H ₅ OH, C ₃ H ₇ CN, and U-line
267	61 _{4,57} – 61 _{4,58} *	216666.695	128	715	4.3	55	Blend with C ₂ H ₅ OH, C ₃ H ₇ CN, and U-line
269	61 _{5,57} – 61 _{4,58} *	216666.699	128	715	29.9	55	Blend with C ₂ H ₅ OH, C ₃ H ₇ CN, and U-line
271	19 _{7,13} – 18 _{6,12}	217192.379	16	163	16.1	50	Strong CH ₃ OCH ₃
272	30 _{7,23} – 29 _{7,22}	217285.278	10	258	118.8	50	Blend with ¹³ CN, CH ₂ ¹³ CHCN, and U-line
273	22 _{6,17} – 21 _{5,16}	217407.902	17	181	13.6	50	Strong HC ¹³ CCN, ¹³ CH ₃ OH, HCC ¹³ CN, and ¹³ CN in absorption
274	21 _{2,20} – 20 _{1,20}	217409.248	52	160	0.3	50	Strong HC ¹³ CCN, ¹³ CH ₃ OH, HCC ¹³ CN, and ¹³ CN in absorption
275	19 _{7,12} – 18 _{6,13}	217414.071	16	163	16.1	50	Strong HCC ¹³ CN and ¹³ CN in absorption
276	31 _{5,27} – 30 _{5,26}	217441.193	100	260	125.2	50	Strong ¹³ CN in absorption, CH ₂ ¹³ CHCN, and CH ₂ CH ¹³ CN
277	31 _{18,13} – 30 _{18,12} *	219461.424	8	352	86.0	92	Strong C ₂ H ₅ CN
279	31 _{19,12} – 30 _{19,11} *	219462.695	8	363	81.0	92	Strong C ₂ H ₅ CN
281	31 _{17,14} – 30 _{17,13} *	219476.189	8	341	90.7	92	Strong NH ₂ CN
283	31 _{20,11} – 30 _{20,10} *	219477.375	9	375	75.7	92	Strong NH ₂ CN
285	31 _{21,10} – 30 _{21,9} *	219503.439	9	388	70.2	92	Strong C ₂ H ₅ CN
287	31 _{16,15} – 30 _{16,14} *	219510.475	8	331	95.1	92	Strong C ₂ H ₅ CN
289	31 _{22,9} – 30 _{22,8} *	219539.304	9	401	64.4	92	Strong HNCO, $v_5=1$ and HNCO
291	31 _{15,16} – 30 _{15,15} *	219569.004	8	321	99.3	92	Strong C ¹⁸ O
293	62 _{17,46} – 61 _{18,43}	219569.366	161	836	17.0	92	Strong C ¹⁸ O
294	62 _{17,45} – 61 _{18,44}	219572.725	161	836	17.0	92	Strong C ¹⁸ O
295	31 _{24,7} – 30 _{24,6} *	219635.627	11	429	52.0	92	Blend with C ₂ H ₅ CN, $v_{20}=1$ and CH ₃ CN, $v_4=1$
297	32 _{3,29} – 31 _{4,28}	219637.655	7	266	43.4	92	Blend with C ₂ H ₅ CN, $v_{20}=1$ and CH ₃ CN, $v_4=1$
298	31 _{14,17} – 30 _{14,16} *	219658.346	7	312	103.2	92	Strong NH ₂ CN and HNCO
300	32 _{4,29} – 31 _{4,28}	219781.349	100	266	130.1	92	Strong HNCO, $v_6=1$ and HNCO
301	31 _{13,19} – 30 _{13,18} *	219787.930	7	304	106.9	92	Strong HNCO
303	21 _{6,15} – 20 _{5,16}	219793.028	100	173	13.1	92	Strong HNCO
304	34 _{1,34} – 33 _{0,33} *	220205.386	100	270	71.6	98	Strong HNCO, $v_5=1$ and C ₂ H ₅ CN, $v_{13}=1/v_{21}=1$
306	34 _{1,34} – 33 _{1,33} *	220205.400	17	270	141.6	98	Strong HNCO, $v_5=1$ and C ₂ H ₅ CN, $v_{13}=1/v_{21}=1$
308	58 _{18,41} – 58 _{17,41} *	220209.432	15	764	2.8	98	Strong HNCO, $v_5=1$ and C ₂ H ₅ CN, $v_{13}=1/v_{21}=1$
310	58 _{18,41} – 58 _{17,42} *	220209.852	15	764	68.8	98	Strong HNCO, $v_5=1$ and C ₂ H ₅ CN, $v_{13}=1/v_{21}=1$
312	31 _{11,21} – 30 _{11,20}	220231.977	7	289	113.4	98	Blend with CH ₃ CN and U-line
313	31 _{11,20} – 30 _{11,19}	220232.321	7	289	113.4	98	Blend with CH ₃ CN and U-line
314	31 _{6,26} – 30 _{6,25}	220580.985	100	264	124.3	98	Strong CH ₃ ¹³ CN and HNCO
315	31 _{10,22} – 30 _{10,21}	220603.352	7	283	116.2	98	Strong CH ₃ CN, CH ₃ ¹³ CN, and C ₂ H ₅ OH
316	62 _{4,58} – 62 _{3,59} *	220606.847	154	735	30.0	98	Strong CH ₃ ¹³ CN and C ₂ H ₅ OH
318	62 _{5,58} – 62 _{4,59} *	220606.849	154	735	30.0	98	Strong CH ₃ ¹³ CN and C ₂ H ₅ OH
320	31 _{10,21} – 30 _{10,20}	220609.106	7	283	116.2	98	Strong CH ₃ ¹³ CN and C ₂ H ₅ OH
321	33 _{3,30} – 32 _{4,29}	226072.922	7	276	45.7	278	Blend with c-C ₂ H ₄ O and ¹³ CH ₃ OH
322	33 _{4,30} – 32 _{4,29}	226165.300	7	276	134.3	278	Blend with CN in absorption and CH ₃ CH ₃ CO, $v_t=1$
323	33 _{3,30} – 32 _{3,29}	226216.618	100	276	134.3	278	Blend with CH ₃ CH ₃ CO and CN in absorption
324	33 _{4,30} – 32 _{3,29}	226309.069	7	276	45.8	278	Strong CN in absorption
325	32 _{5,28} – 31 _{4,27}	226357.720	9	270	34.1	278	Strong CN in absorption
326	32 _{19,13} – 31 _{19,12} *	226534.021	8	373	86.7	278	Blend with CH ₂ NH
328	32 _{18,15} – 31 _{18,14} *	226537.002	100	362	91.5	278	Blend with CH ₂ NH
330	32 _{20,13} – 31 _{20,12} *	226545.568	8	385	81.6	278	Blend with CH ₂ NH
332	32 _{17,15} – 31 _{17,14} *	226557.411	8	351	96.1	278	Blend with C ₂ H ₅ CN, $v_{13}=1/v_{21}=1$
334	32 _{21,11} – 31 _{21,10} *	226569.424	9	398	76.2	278	Blend with CH ₃ COOH, C ₂ H ₅ OH, and CN in absorption
336	32 _{16,16} – 31 _{16,15} *	226599.078	8	341	100.4	278	Blend with C ₂ H ₅ ¹³ CN
338	35 _{0,35} – 34 _{1,34} *	226601.560	18	280	73.8	278	Blend with C ₂ H ₅ ¹³ CN
340	35 _{0,35} – 34 _{0,34} *	226601.561	18	280	145.8	278	Blend with C ₂ H ₅ ¹³ CN
342	32 _{22,10} – 31 _{22,9} *	226603.850	9	411	70.6	278	Blend with C ₂ H ₅ ¹³ CN
344	32 _{15,17} – 31 _{15,16} *	226667.222	8	332	104.5	96	Strong CN in absorption and C ₂ H ₅ OH
346	32 _{14,18} – 31 _{14,17} *	226769.121	8	323	108.3	96	Strong CN in absorption
348	32 _{13,20} – 31 _{13,19} *	226915.261	8	314	111.8	96	Strong CN in absorption
350	32 _{12,21} – 31 _{12,20} *	227121.372	7	307	115.1	96	Blend with C ₂ H ₅ CN, uncertain baseline

Table 2. continued.

N^a	Transition ^b	Frequency (MHz)	Unc. ^c (kHz)	E_l^d (K)	$S\mu^2$ (D ²)	σ^e (mK)	Comments
(1)	(2)	(3)	(4)	(5)	(6)	(7)	(8)
352	32 _{11,22} – 31 _{11,21}	227412.121	7	300	118.1	85	Strong HC ₃ N
353	32 _{11,21} – 31 _{11,20}	227412.786	7	300	118.1	85	Strong HC ₃ N
354	31 _{6,25} – 30 _{6,24}	227600.701	10	265	125.4	85	Strong C ₂ H ₅ OH and NH ₂ CHO
355	32 _{10,23} – 31 _{10,22}	227826.118	8	293	120.8	85	Blend with CH ₃ OH
356	32 _{10,22} – 31 _{10,21}	227836.414	8	293	120.8	85	Blend with CH ₃ CH ₃ CO
357	22 _{6,16} – 21 _{5,17}	227855.315	20	180	12.7	85	Blend with HC ¹³ CCN, $v_7=2$, HCC ¹³ CN, $v_7=2$, and U-line
358	81 _{10,71} – 81 _{9,72} *	231205.772	1715	1244	77.8	183	Strong ¹³ CS and U-line
360	34 _{3,31} – 33 _{4,30}	232486.365	7	287	48.0	19	Strong C ₂ H ₅ ¹³ CN and C ₂ H ₅ OH
361	34 _{4,31} – 33 _{4,30}	232545.336	50	287	138.4	19	Blend with C ₂ H ₅ CN and C ₂ H ₅ OH
362	34 _{3,31} – 33 _{3,30}	232578.686	50	287	138.4	19	Blend with CH ₃ ¹³ CH ₂ CN and ¹³ CH ₂ CHCN
363	34 _{4,31} – 33 _{3,30}	232637.775	8	287	48.0	19	Blend with CH ₃ OH, $v_t=1$, CH ₃ CH ₃ CO, and ¹³ CH ₂ CO
364	12 _{12,0} – 11 _{11,1} *	232895.717	15	153	25.4	19	Blend with C ₂ H ₅ CN and ¹³ CH ₃ CN, $v_8=1$
366	12 _{12,0} – 11 _{11,0} *	232895.717	15	153	1.4	19	Blend with C ₂ H ₅ CN and ¹³ CH ₃ CN, $v_8=1$
368	33 _{10,24} – 32 _{10,23}	235059.537	50	304	125.4	131	Strong CH ₃ OCHO and C ₂ H ₅ CN
369	33 _{10,23} – 32 _{10,22}	235077.408	8	304	125.4	131	Strong CH ₃ CH ₃ CO and C ₂ H ₅ OH
370	16 _{10,7} – 15 _{9,6} *	235511.949	15	159	21.6	131	Strong HC ¹³ CCN
372	16 _{10,6} – 15 _{9,7} *	235511.949	15	159	21.6	131	Strong HC ¹³ CCN
374	33 _{9,25} – 32 _{9,24}	235683.207	50	299	127.8	131	Blend with HCC ¹³ CN, $v_5=1/v_7=3$
375	33 _{9,24} – 32 _{9,23}	235875.700	8	299	127.8	131	Strong ¹³ CH ₃ OH and CH ₃ OCHO
376	34 _{4,30} – 33 _{5,29}	235952.121	100	292	39.0	131	Strong C ₂ H ₅ ¹³ CN, ¹³ CH ₃ OH, and SiS
377	33 _{7,27} – 32 _{7,26}	236011.028	50	289	131.6	131	Strong ¹³ CH ₃ OH
378	66 _{4,62} – 66 _{3,63} *	236269.468	357	816	30.1	37	Blend with NH ₂ CH ₂ CN and H ₂ C ³⁴ S
380	66 _{5,62} – 66 _{4,63} *	236269.469	357	816	30.1	37	Blend with NH ₂ CH ₂ CN and H ₂ C ³⁴ S
382	33 _{8,26} – 32 _{8,25}	236274.518	50	294	130.0	37	Blend with NH ₂ CH ₂ CN and H ₂ C ³⁴ S
383	23 _{6,17} – 22 _{5,18}	236483.115	100	188	12.0	37	Blend with NH ₂ CH ₂ CN and CH ₂ ¹³ CHCN
384	34 _{23,11} – 33 _{23,10} *	240768.473	9	447	77.2	216	Strong CH ₃ ¹³ CH ₂ CN, CH ₃ CH ₃ CO, and C ₂ H ₅ OH
386	34 _{16,18} – 33 _{16,17} *	240777.277	8	363	110.8	216	Strong CH ₃ ¹³ CH ₂ CN, CH ₃ CH ₃ CO, and C ₂ H ₅ OH
388	34 _{15,19} – 33 _{15,18} *	240866.895	8	354	114.6	216	Strong C ₂ H ₅ CN and HNCO
390	34 _{14,21} – 33 _{14,20} *	240996.801	8	345	118.2	216	Strong C ₂ H ₅ ¹³ CN, CH ₃ CH ₃ CO, and C ³⁴ S
392	33 _{7,26} – 32 _{7,25}	241104.938	12	290	132.3	216	Blend with CH ₃ ¹³ CH ₂ CN and U-line
393	36 _{2,34} – 35 _{3,33}	241154.165	10	304	60.8	216	Strong CH ₃ OH, $v_t=1$
394	36 _{3,34} – 35 _{3,33}	241155.214	10	304	147.7	216	Strong CH ₃ OH, $v_t=1$
395	36 _{2,34} – 35 _{2,33}	241155.889	10	304	147.7	216	Strong CH ₃ OH, $v_t=1$
396	36 _{3,34} – 35 _{2,33}	241156.938	10	304	60.8	216	Strong CH ₃ OH, $v_t=1$
397	34 _{29,5} – 33 _{29,4} *	241179.811	17	543	38.8	216	Strong CH ₃ OH, $v_t=1$
399	34 _{13,22} – 33 _{13,21} *	241179.912	8	337	121.5	216	Strong CH ₃ OH, $v_t=1$
401	65 _{3,62} – 65 _{2,63} *	241187.055	355	784	22.6	216	Strong CH ₃ OH, $v_t=1$
403	65 _{3,62} – 65 _{3,63} *	241187.055	355	784	3.4	216	Strong CH ₃ OH, $v_t=1$
405	21 _{8,14} – 20 _{7,13}	244391.993	15	180	18.5	46	Strong ¹³ CH ₃ CH ₂ CN and C ₂ H ₅ CN
406	21 _{8,13} – 20 _{7,13}	244396.589	15	180	1.4	46	Strong ¹³ CH ₃ CH ₂ CN and C ₂ H ₅ CN
407	23 _{5,18} – 22 _{4,19}	244399.583	45	185	5.5	46	Strong ¹³ CH ₃ CH ₂ CN and C ₂ H ₅ CN
408	21 _{8,14} – 20 _{7,14}	244437.241	15	180	1.4	46	Blend with C ₂ H ₅ CN, C ₂ H ₅ OH, and U-line
409	21 _{8,13} – 20 _{7,14}	244441.837	15	180	18.5	46	Blend with C ₂ H ₅ CN, C ₂ H ₅ OH, and U-line
410	23 _{7,16} – 22 _{6,17}	245129.808	16	191	16.1	72	Strong CH ₂ NH
411	36 _{3,33} – 35 _{4,32}	245273.854	100	310	52.6	72	Strong HC ₃ N, $v_4=1$ and C ₂ H ₅ ¹³ CN
412	36 _{4,33} – 35 _{4,32}	245297.601	100	310	146.7	72	Blend with CH ₃ CH ₃ CO and ³⁴ SO ₂
413	36 _{3,33} – 35 _{3,32}	245311.367	100	310	146.7	72	Blend with C ₂ H ₅ OH and SO ₂
414	36 _{4,33} – 35 _{3,32}	245335.158	100	310	52.6	72	Strong SO ₂
415	34 _{8,26} – 33 _{8,25}	245447.840	11	305	134.4	72	Strong C ₂ H ₅ OH, C ₂ H ₅ CN, $v_{13}=1/v_{21}=1$, and ¹³ CH ₃ CH ₂ CN
416	38 _{0,38} – 37 _{0,37} *	245779.482	100	314	158.3	53	Strong CH ₂ ¹³ CHCN and C ₂ H ₅ CN, $v_{13}=1/v_{21}=1$
418	38 _{0,38} – 37 _{1,37} *	245779.550	18	314	80.5	53	Strong CH ₂ ¹³ CHCN and C ₂ H ₅ CN, $v_{13}=1/v_{21}=1$
420	24 _{6,18} – 23 _{5,19}	245842.016	26	196	11.2	53	Blend with C ₂ H ₃ CN, $v_{11}=1/v_{15}=1$
421	14 _{12,2} – 13 _{11,3} *	247059.416	14	162	25.4	68	Strong CH ₃ OCHO
423	14 _{12,2} – 13 _{11,2} *	247059.416	14	162	1.5	68	Strong CH ₃ OCHO
425	35 _{6,30} – 34 _{6,29}	247073.069	100	308	141.1	68	Strong C ₂ H ₃ CN and CH ₂ ¹³ CHCN
426	39 _{0,39} – 38 _{0,38} *	252168.489	100	326	162.5	42	Blend with C ₂ H ₅ CN, $v_{13}=1/v_{21}=1$
428	39 _{0,39} – 38 _{1,38} *	252168.541	18	326	82.7	42	Blend with C ₂ H ₅ CN, $v_{13}=1/v_{21}=1$
430	24 _{7,17} – 23 _{6,18}	252254.714	16	199	16.0	42	Strong CH ₃ OH
431	25 _{7,19} – 24 _{6,18}	254026.124	15	207	16.1	32	Strong CH ₃ OH in absorption, C ₂ H ₅ CN, $v_{13}=1/v_{21}=1$, and HC ¹³ CCN, $v_6=1$
432	15 _{12,3} – 14 _{11,4} *	254139.046	14	167	25.5	32	Strong C ₂ H ₃ CN
434	15 _{12,3} – 14 _{11,3} *	254139.046	14	167	1.5	32	Strong C ₂ H ₃ CN

Table 2. continued.

N^a	Transition ^b	Frequency (MHz)	Unc. ^c (kHz)	E_l^d (K)	$S\mu^2$ (D ²)	σ^e (mK)	Comments
(1)	(2)	(3)	(4)	(5)	(6)	(7)	(8)
436	36 _{14,23} – 35 _{14,22} *	255232.834	8	368	127.8	217	Strong CH ₃ OH
438	17 _{11,6} – 16 _{10,7} *	255442.928	14	171	23.8	217	Strong CH ₂ CH ¹³ CN
440	17 _{11,6} – 16 _{10,6} *	255442.928	14	171	1.4	217	Strong CH ₂ CH ¹³ CN
442	36 _{13,24} – 35 _{13,23} *	255458.533	8	360	131.0	217	Strong C ₂ H ₅ CN, $v_{13}=1/v_{21}=1$ and CH ₂ ¹³ CHCN
444	37 _{4,33} – 36 _{5,32}	255646.981	8	327	46.2	217	Strong H ¹³ CCCN and NH ₂ CHO, $v_{12}=1$
445	23 _{8,16} – 22 _{7,15}	257978.249	15	195	18.7	1127	Strong CH ₃ CN, $v_8=1$
446	56 _{11,46} – 55 _{12,43}	258029.375	88	664	12.8	1127	Strong CH ₃ CN, $v_8=1$
447	38 _{3,35} – 37 _{4,34}	258032.591	9	334	57.1	1127	Strong CH ₃ CN, $v_8=1$
448	38 _{4,35} – 37 _{4,34}	258042.009	9	334	155.1	1127	Strong CH ₃ CN, $v_8=1$
449	38 _{3,35} – 37 _{3,34}	258047.578	9	334	155.1	1127	Strong CH ₃ CN, $v_8=1$
450	38 _{4,35} – 37 _{3,34}	258056.996	9	334	57.1	1127	Strong CH ₃ CN, $v_8=1$
451	23 _{8,15} – 22 _{7,16}	258162.637	15	195	18.7	1127	Strong ¹³ CH ₃ OH and HC ¹⁵ N
452	36 _{9,27} – 35 _{9,26}	258237.747	10	334	141.2	1127	Strong CH ₃ CN, $v_8=1$ and SO
453	36 _{6,31} – 35 _{5,30}	258252.184	13	320	33.8	1127	Strong CH ₃ CN, $v_8=1$ and SO
454	26 _{7,20} – 25 _{6,19}	258801.772	16	216	15.9	1609	Strong CH ₃ ¹³ CH ₂ CN
455	37 _{6,32} – 36 _{6,31}	260009.847	8	332	149.4	413	Strong C ₂ H ₅ OH, CH ₂ ¹³ CHCN, and CH ₃ OCH ₃
456	39 _{2,37} – 38 _{3,36}	260297.586	10	340	67.4	413	Strong C ₂ H ₅ CN, $v_{13}=1/v_{21}=1$
457	39 _{3,37} – 38 _{3,36}	260297.819	10	340	160.2	413	Strong C ₂ H ₅ CN, $v_{13}=1/v_{21}=1$
458	39 _{2,37} – 38 _{2,36}	260297.972	10	340	160.2	413	Strong C ₂ H ₅ CN, $v_{13}=1/v_{21}=1$
459	39 _{3,37} – 38 _{2,36}	260298.205	10	340	67.4	413	Strong C ₂ H ₅ CN, $v_{13}=1/v_{21}=1$
460	37 _{7,31} – 36 _{7,30}	263345.617	9	337	148.6	74	Blend with HCC ¹³ CN, $v_7=1$
461	37 _{6,32} – 36 _{5,31}	263354.897	11	332	36.3	74	Blend with NH ₂ CH ₂ CN
462	37 _{11,27} – 36 _{11,26}	263432.848	8	358	141.1	74	Strong HNCO, $v_5=1$ and HNCO
463	37 _{11,26} – 36 _{11,25}	263445.456	8	358	141.2	74	Strong HNCO, $v_5=1$ and HNCO
464	20 _{10,11} – 19 _{9,10} *	263669.118	14	183	22.4	108	Strong CH ₃ OCH ₃ , HNCO, and HC ¹³ CCN, $v_7=1$
466	20 _{10,11} – 19 _{9,11} *	263669.145	14	183	1.4	108	Strong CH ₃ OCH ₃ , HNCO, and HC ¹³ CCN, $v_7=1$
468	36 _{7,29} – 35 _{7,28}	264087.850	11	326	145.6	108	Blend with H ₂ ¹³ CS and U-line
469	37 _{10,28} – 36 _{10,27}	264094.028	9	351	143.5	108	Blend with H ₂ ¹³ CS and U-line
470	40 _{2,38} – 39 _{3,37}	266674.808	10	352	69.7	91	Blend with O ¹³ CS and C ₂ H ₅ ¹³ CN
471	40 _{3,38} – 39 _{3,37} *	266674.948	10	352	164.4	91	Blend with O ¹³ CS and C ₂ H ₅ ¹³ CN
473	40 _{3,38} – 39 _{2,37}	266675.181	10	352	69.7	91	Blend with O ¹³ CS and C ₂ H ₅ ¹³ CN
474	15 _{13,2} – 14 _{12,3} *	266949.479	14	174	27.6	91	Blend with SO ₂ and U-line
476	15 _{13,2} – 14 _{12,2} *	266949.479	14	174	1.6	91	Blend with SO ₂ and U-line
478	38 _{5,33} – 37 _{5,32}	267143.852	100	344	153.6	91	Strong NH ₂ ¹³ CHO, CH ₃ CH ₃ CO, and C ₂ H ₅ CN, $v_{13}=1/v_{21}=1$

Notes: ^a Numbering of the observed transitions associated with a modeled line stronger than 20 mK. ^b Transitions marked with a * are double with a frequency difference less than 0.1 MHz. The quantum numbers of the second one are not shown. ^c Frequency uncertainty. ^d Lower energy level in temperature units (E_l/k_B). ^e Calculated rms noise level in T_{mb} scale.

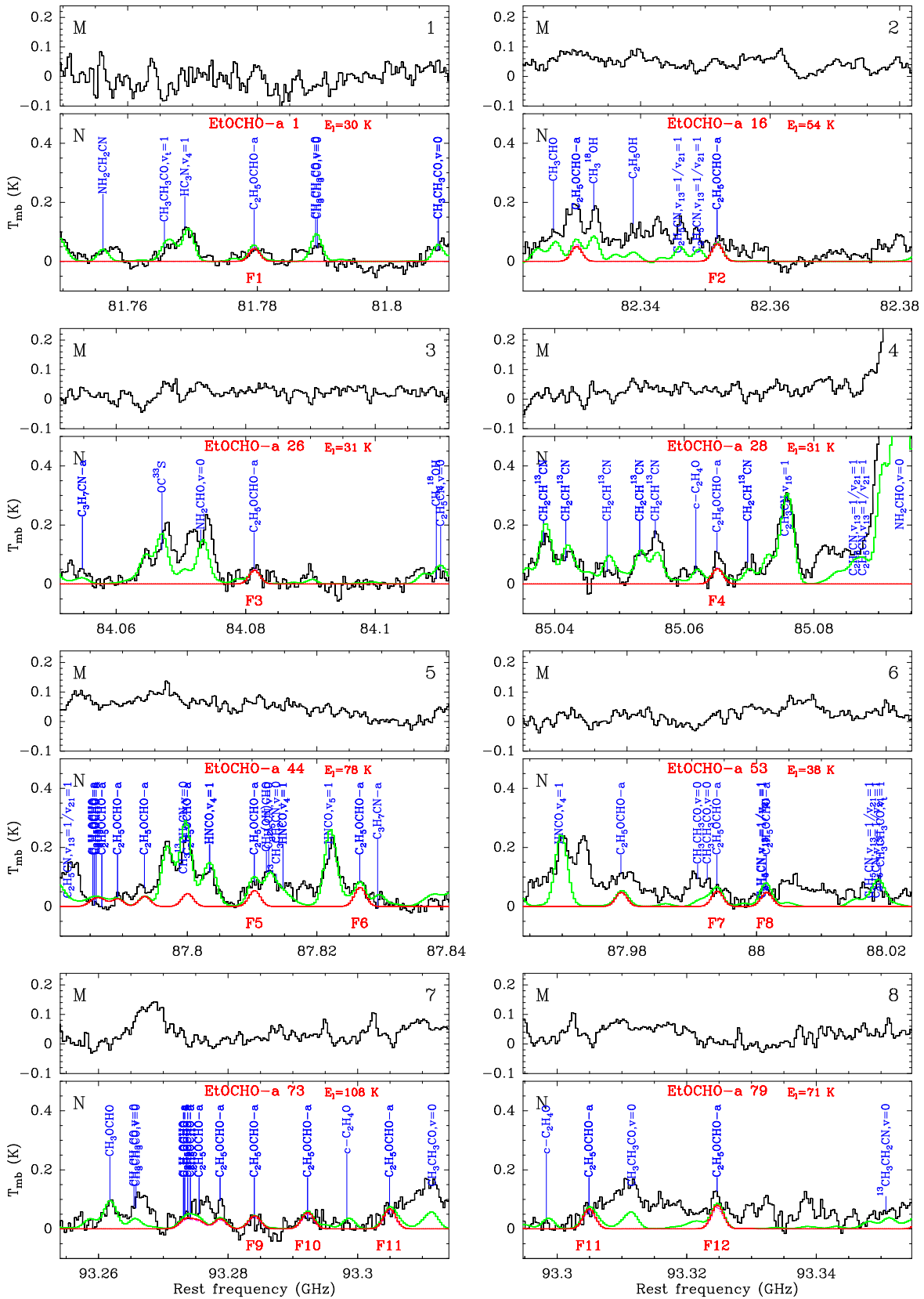


Fig. 1. Transitions of the *anti*-conformer of ethyl formate (EtOCHO-a) detected with the IRAM 30 m telescope. Each panel consists of two plots and is labeled in black in the upper right corner. The lower plot shows in black the spectrum obtained toward Sgr B2(N) in main-beam brightness temperature scale (K), while the upper plot shows the spectrum toward Sgr B2(M). The rest frequency axis is labeled in GHz. The systemic velocities assumed for Sgr B2(N) and (M) are 64 and 62 km s⁻¹, respectively. The lines identified in the Sgr B2(N) spectrum are labeled in blue. The top red label indicates the EtOCHO-a transition centered in each plot (numbered like in Col. 1 of Table 3), along with the energy of its lower level in K (E_l/k_B). The other EtOCHO-a lines are labeled in blue only. The bottom red label is the feature number (see Col. 8 of Table 3). The green spectrum shows our LTE model containing all identified molecules, including EtOCHO-a. The LTE synthetic spectrum of EtOCHO-a alone is overlaid in red, and its opacity in dashed violet. All observed lines which have no counterpart in the green spectrum are still unidentified in Sgr B2(N).

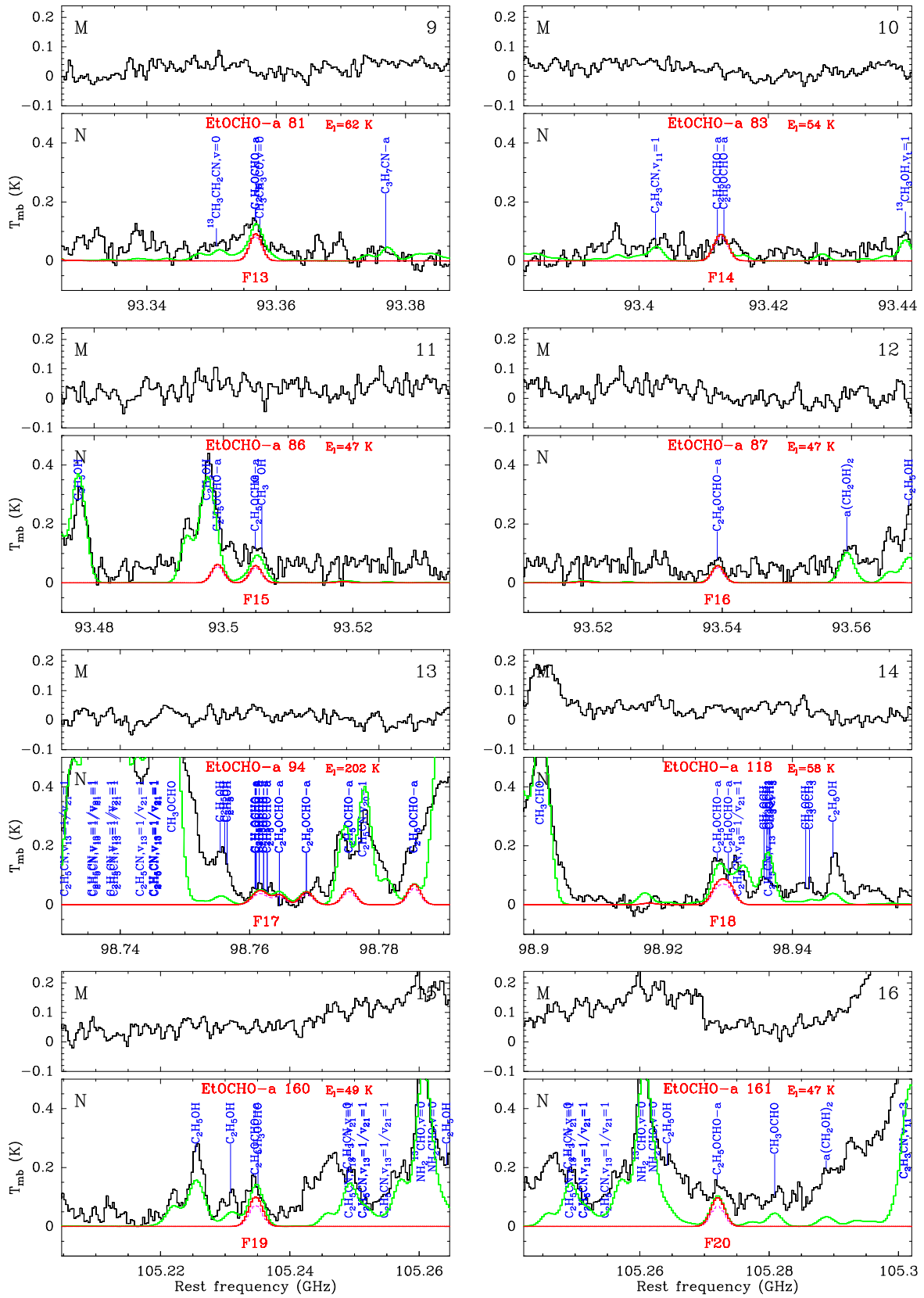


Fig. 1. (continued)

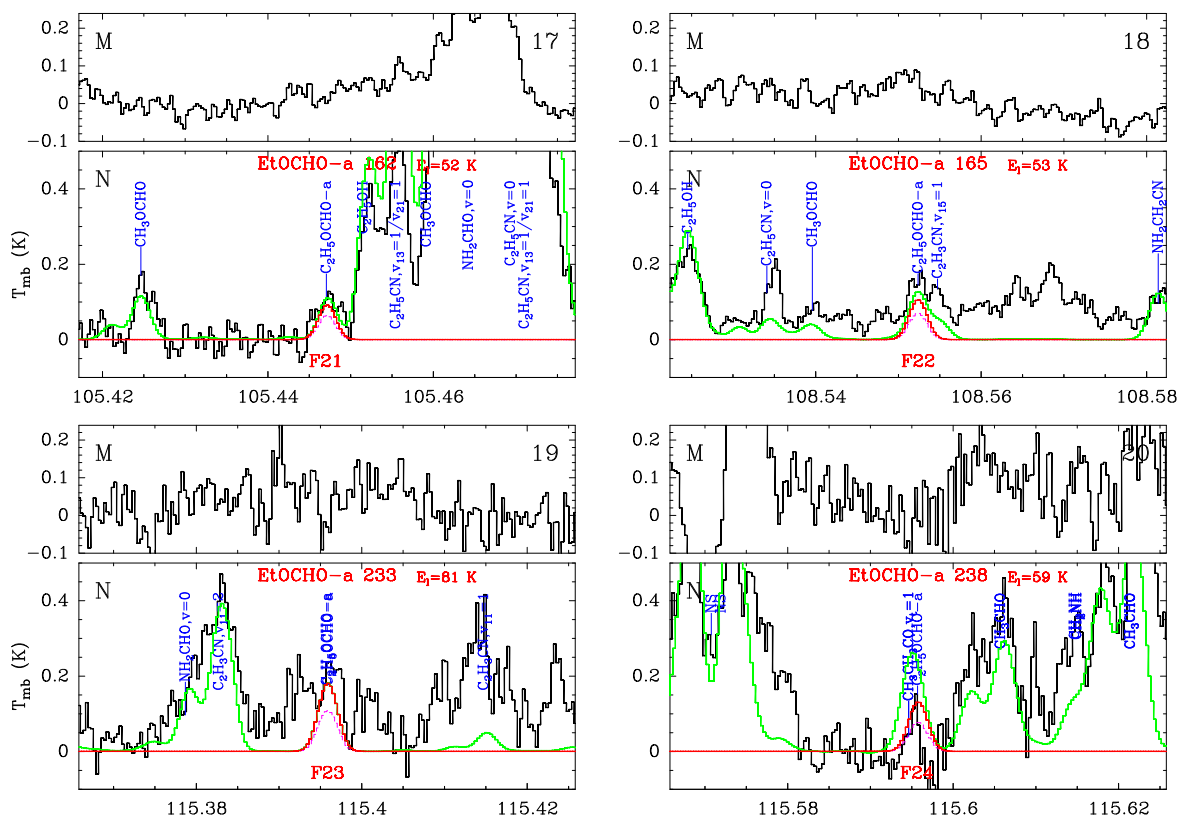


Fig. 1. (continued)

Table 9. Transitions of the *anti*-conformer of *n*-propyl cyanide observed with the IRAM 30 m telescope toward Sgr B2(N). The horizontal lines mark discontinuities in the observed frequency coverage. Only the transitions associated with a modeled line stronger than 20 mK are listed.

N^a	Transition ^b	Frequency (MHz)	Unc. ^c (kHz)	E_l^d (K)	$S\mu^2$ (D ²)	σ^e (mK)	Comments
(1)	(2)	(3)	(4)	(5)	(6)	(7)	(8)
1	18 _{1,17} – 17 _{1,16}	80486.371	5	34	232.1	24	Blend with C ₂ H ₅ CN, $v_{13}=1/v_{21}=1$ and U-line
2	19 _{1,19} – 18 _{1,18}	82778.264	4	37	245.1	17	Blend with HC ₃ N, $v_5=1/v_7=3$ and C ₂ H ₅ CN
3	19 _{0,19} – 18 _{0,18}	83487.658	4	36	245.7	17	Blend with C ₂ H ₃ CN and U-line
4	19 _{2,18} – 18 _{2,17}	83906.011	5	40	243.1	16	Weak, blend with U-lines
5	19 _{6,14} – 18 _{6,13} *	84021.555	4	73	221.3	19	Group detected , partial blend with C ₂ H ₅ CN
7	19 _{7,12} – 18 _{7,11} *	84022.819	5	87	212.5	19	Group detected , partial blend with C ₂ H ₅ CN
9	19 _{5,15} – 18 _{5,14} *	84023.956	4	62	228.8	19	Group detected , partial blend with C ₂ H ₅ CN
11	19 _{8,11} – 18 _{8,10} *	84026.382	5	102	202.2	19	Group detected , partial blend with C ₂ H ₅ CN
13	19 _{9,10} – 18 _{9,9} *	84031.619	5	120	190.6	19	Blend with C ₂ H ₅ CN
15	19 _{4,16} – 18 _{4,15}	84033.299	4	53	234.9	19	Blend with C ₂ H ₅ CN
16	19 _{4,15} – 18 _{4,14}	84033.712	4	53	234.9	19	Blend with C ₂ H ₅ CN
17	19 _{10,9} – 18 _{10,8} *	84038.206	5	139	177.7	19	Blend with C ₂ H ₅ CN
19	19 _{11,8} – 18 _{11,7} *	84045.967	5	161	163.4	19	Blend with U-line
21	19 _{3,17} – 18 _{3,16}	84050.001	4	46	239.7	19	Blend with CH ₃ CH ₃ CO
22	57 _{3,54} – 57 _{2,55} *	84073.432	63	358	44.1	19	Blend with NH ₂ CHO
24	19 _{14,5} – 18 _{14,4} *	84075.429	7	238	112.4	19	Blend with NH ₂ CHO
26	19 _{2,17} – 18 _{2,16}	84408.080	4	40	243.1	19	Blend with ³⁴ SO
27	19 _{1,18} – 18 _{1,17}	84940.688	5	38	245.1	22	Blend with C ₂ H ₃ CN
28	20 _{1,20} – 19 _{1,19}	87121.605	4	41	258.1	16	Blend with HN ¹³ C in absorption
29	40 _{1,39} – 40 _{1,40}	87829.125	82	172	0.8	17	Weak, partial blend with C ₂ H ₅ OCHO
30	20 _{0,20} – 19 _{0,19}	87829.384	5	40	258.6	17	Weak, partial blend with C ₂ H ₅ OCHO
31	20 _{2,19} – 19 _{2,18}	88310.935	5	44	256.2	17	Blend with H ¹³ CCCN, $v_6=1$ and CH ₃ CH ₃ CO
32	20 _{6,14} – 19 _{6,13} *	88444.212	5	77	235.5	17	Group detected , partial blend with CH ₃ CH ₃ CO, C ₂ H ₅ OH, and U-line?
34	20 _{7,13} – 19 _{7,12} *	88445.075	5	91	227.0	17	Group detected , partial blend with CH ₃ CH ₃ CO, C ₂ H ₅ OH, and U-line?
36	20 _{5,16} – 19 _{5,15} *	88447.526	5	66	242.6	17	Group detected , partial blend with CH ₃ CH ₃ CO, C ₂ H ₅ OH, and U-line?
38	20 _{8,12} – 19 _{8,11} *	88448.528	5	106	217.4	17	Group detected , partial blend with CH ₃ CH ₃ CO, C ₂ H ₅ OH, and U-line?
40	20 _{9,11} – 19 _{9,10} *	88453.836	5	124	206.4	17	Group detected , partial blend with C ₂ H ₅ ¹³ CN, ¹³ CH ₃ CH ₂ CN, and CH ₂ (OH)CHO
42	20 _{4,17} – 19 _{4,16}	88458.794	5	57	248.4	17	Group detected , partial blend with C ₂ H ₅ ¹³ CN, ¹³ CH ₃ CH ₂ CN, and CH ₂ (OH)CHO
43	20 _{4,16} – 19 _{4,15}	88459.387	5	57	248.4	17	Group detected , partial blend with C ₂ H ₅ ¹³ CN, ¹³ CH ₃ CH ₂ CN, and CH ₂ (OH)CHO
44	20 _{10,10} – 19 _{10,9} *	88460.625	5	143	194.1	17	Group detected , partial blend with C ₂ H ₅ ¹³ CN, ¹³ CH ₃ CH ₂ CN, and CH ₂ (OH)CHO
46	20 _{11,9} – 19 _{11,8} *	88468.687	5	165	180.5	17	Weak
48	20 _{3,18} – 19 _{3,17}	88477.246	5	50	252.9	17	Blend with HNCO, $v_4=1$ and C ₂ H ₅ CN
49	20 _{12,8} – 19 _{12,7} *	88477.898	6	188	165.6	17	Blend with HNCO, $v_4=1$ and C ₂ H ₅ CN
51	20 _{3,17} – 19 _{3,16}	88507.586	5	50	252.9	17	Blend with C ₂ H ₅ CN, $v_{13}=1/v_{21}=1$ and H ¹³ CCCN, $v_7=1$
52	20 _{2,18} – 19 _{2,17}	88890.385	5	45	256.2	21	Blend with CH ₂ (OH)CHO and U-line
53	20 _{1,19} – 19 _{1,18}	89391.938	5	42	258.1	16	Detected , blend with CH ₃ OCHO, $v_l=1$
54	21 _{1,21} – 20 _{1,20}	91463.179	5	45	271.1	24	Blend with HC ₃ N, $v_6=v_7=1$ and U-line
55	21 _{0,21} – 20 _{0,20}	92164.912	5	44	271.6	27	Detected , blend with CH ₃ ¹³ CN, $v_8=1$ and U-line?
56	21 _{2,20} – 20 _{2,19}	92714.159	5	49	269.2	28	Blend with CH ₃ OCH ₃ and CH ₃ CH ₃ CO, $v_l=1$
57	21 _{6,16} – 20 _{6,15} *	92866.939	5	82	249.5	28	Group detected , uncertain baseline
59	21 _{7,14} – 20 _{7,13} *	92867.332	5	95	241.5	28	Group detected , uncertain baseline
61	21 _{8,13} – 20 _{8,12} *	92870.627	5	110	232.2	28	Group detected , uncertain baseline
63	21 _{5,17} – 20 _{5,16} *	92871.289	5	70	256.3	28	Group detected , uncertain baseline
65	21 _{9,12} – 20 _{9,11} *	92875.977	5	128	221.8	28	Group detected , uncertain baseline
67	21 _{10,11} – 20 _{10,10} *	92882.945	5	147	210.1	28	Blend with CH ₃ OCHO
69	21 _{4,18} – 20 _{4,17}	92884.684	5	61	261.8	28	Blend with CH ₃ OCHO
70	21 _{4,17} – 20 _{4,16}	92885.520	5	61	261.8	28	Blend with CH ₃ OCHO
71	21 _{11,10} – 20 _{11,9} *	92891.291	6	169	197.1	28	Noisy
73	21 _{12,9} – 20 _{12,8} *	92900.873	6	193	183.0	28	Blend with U-line
75	21 _{3,19} – 20 _{3,18}	92904.745	5	54	266.1	28	Blend with CH ₃ CH ₃ CO, $v_l=1$ and CH ₃ CH ₃ CO
76	21 _{3,18} – 20 _{3,17}	92943.421	5	54	266.2	28	Blend with CH ₃ OCHO
77	21 _{2,19} – 20 _{2,18}	93376.934	5	49	269.2	22	Detected
78	21 _{1,20} – 20 _{1,19}	93839.887	5	46	271.1	24	Blend with U-line
79	22 _{1,22} – 21 _{1,21}	95802.965	5	49	284.0	23	Blend with ¹³ CH ₃ CH ₂ CN and C ₂ H ₅ CN, $v_{13}=1/v_{21}=1$
80	22 _{0,22} – 21 _{0,21}	96494.470	5	49	284.5	32	Blend with CH ₃ OH, $v_l=1$ and CH ₃ CH ₃ CO

Table 9. continued.

N^a	Transition ^b	Frequency (MHz)	Unc. ^c (kHz)	E_l^d (K)	$S\mu^2$ (D ²)	σ^e (mK)	Comments
(1)	(2)	(3)	(4)	(5)	(6)	(7)	(8)
81	22 _{2,21} – 21 _{2,20}	97115.607	5	53	282.3	21	Blend with U-line
82	22 _{7,15} – 21 _{7,14} *	97289.589	5	99	255.8	21	Blend with C ₂ H ₃ CN and OCS
84	22 _{6,17} – 21 _{6,16} *	97289.742	5	86	263.5	21	Blend with C ₂ H ₃ CN and OCS
86	22 _{8,14} – 21 _{8,13} *	97292.679	5	115	247.0	21	Blend with OCS
88	22 _{5,18} – 21 _{5,17} *	97295.253	5	75	269.9	21	Strong OCS
90	22 _{9,13} – 21 _{9,12} *	97298.036	5	132	237.0	21	Strong OCS
92	22 _{10,12} – 21 _{10,11} *	97305.160	5	152	225.8	21	Strong OCS
94	22 _{4,19} – 21 _{4,18}	97310.983	5	66	275.2	21	Blend with OCS and C ₂ H ₃ CN, $v_{11}=1$
95	22 _{4,18} – 21 _{4,17}	97312.143	5	66	275.2	21	Blend with OCS and C ₂ H ₃ CN, $v_{11}=1$
96	22 _{11,11} – 21 _{11,10} *	97313.773	6	173	213.5	21	Blend with OCS and C ₂ H ₃ CN, $v_{11}=1$
98	22 _{12,10} – 21 _{12,9} *	97323.712	6	197	199.9	21	Blend with CH ₃ OCHO
100	22 _{3,20} – 21 _{3,19}	97332.446	5	58	279.4	21	Blend with U-line
101	22 _{13,9} – 21 _{13,8} *	97334.877	7	223	185.2	21	Blend with U-line and CH ₃ OCHO
103	22 _{3,19} – 21 _{3,18}	97381.167	5	58	279.4	20	Blend with CH ₃ CH ₃ CO, $v_t=1$, uncertain baseline
104	22 _{2,20} – 21 _{2,19}	97867.394	5	53	282.3	20	Detected , uncertain baseline
105	22 _{1,21} – 21 _{1,20}	98284.291	5	51	284.0	18	Blend with CH ₃ OCH ₃ , CH ₃ OCHO, and U-line
106	23 _{1,23} – 22 _{1,22}	100140.951	5	54	296.9	14	Blend with CH ₃ OCHO, $v_t=1$ and HC ₃ N, $v_5=1/v_7=3$
107	23 _{0,23} – 22 _{0,22}	100818.358	5	53	297.4	20	Blend with CH ₃ ¹³ CH ₂ CN and U-line
108	10 _{4,6} – 11 _{3,9}	101512.348	5	23	1.2	16	Detected , small blend with CH ₃ CH ₃ CO, $v_t=1$
109	23 _{2,22} – 22 _{2,21}	101515.201	5	58	295.3	16	Detected , small blend with CH ₃ CH ₃ CO, $v_t=1$
110	23 _{7,16} – 22 _{7,15} *	101711.846	5	104	270.0	16	Group detected , partial blend with ¹³ CH ₂ CHCN, uncertain baseline
112	23 _{6,18} – 22 _{6,17} *	101712.624	5	91	277.3	16	Group detected , partial blend with ¹³ CH ₂ CHCN, uncertain baseline
114	23 _{8,15} – 22 _{8,14} *	101714.680	5	120	261.5	16	Group detected , uncertain baseline
116	23 _{5,19} – 22 _{5,18} *	101719.429	5	79	283.5	16	Group detected , small blend with ¹³ CH ₂ CHCN
118	23 _{9,14} – 22 _{9,13} *	101720.011	5	137	252.0	16	Group detected , small blend with ¹³ CH ₂ CHCN
120	23 _{10,13} – 22 _{10,12} *	101727.266	5	157	241.3	16	Blend with CH ₃ OCHO and U-line?
122	23 _{11,12} – 22 _{11,11} *	101736.128	6	178	229.5	16	Blend with CH ₃ OH
124	23 _{4,20} – 22 _{4,19}	101737.702	5	70	288.6	16	Blend with CH ₃ OH
125	23 _{4,19} – 22 _{4,18}	101739.288	5	70	288.6	16	Blend with CH ₃ OH
126	23 _{12,11} – 22 _{12,10} *	101746.410	6	202	216.6	16	Blend with U-line and C ₂ H ₅ CN, $v_{13}=1/v_{21}=1$
128	23 _{13,10} – 22 _{13,9} *	101757.997	7	227	202.5	16	Blend with U-line
130	23 _{3,21} – 22 _{3,20}	101760.286	5	63	292.5	16	Blend with U-line
131	23 _{17,6} – 22 _{17,5} *	101816.271	10	350	135.0	34	Blend with CH ₃ CH ₃ CO, $v_t=1$ and $v_t=0$, and U-line
133	23 _{3,20} – 22 _{3,19}	101820.997	5	63	292.5	34	Blend with CH ₃ CH ₃ CO, $v_t=1$ and $v_t=0$, and U-line
134	25 _{3,22} – 25 _{2,23}	102358.115	5	73	13.4	30	Blend with U-line
135	23 _{2,21} – 22 _{2,20}	102361.359	5	58	295.3	30	Blend with U-line
136	23 _{1,22} – 22 _{1,21}	102724.897	5	55	296.9	37	Noisy, baseline problem
137	24 _{1,24} – 23 _{1,23}	104477.131	5	59	309.9	48	Blend with U-line
138	24 _{0,24} – 23 _{0,23}	105136.938	5	58	310.3	28	Blend with U-line
139	24 _{2,23} – 23 _{2,22}	105912.868	5	63	308.3	43	Blend with ¹³ CH ₃ OH
140	24 _{7,17} – 23 _{7,16} *	106134.103	5	109	284.1	25	Blend with NH ₂ CHO
142	37 _{2,36} – 37 _{1,37}	106135.161	50	148	12.1	25	Blend with NH ₂ CHO
143	24 _{6,19} – 23 _{6,18} *	106135.587	5	96	291.1	25	Blend with NH ₂ CHO
145	24 _{8,16} – 23 _{8,15} *	106136.628	5	124	276.0	25	Blend with NH ₂ CHO
147	24 _{9,15} – 23 _{9,14} *	106141.897	5	142	266.9	25	Blend with NH ₂ CHO
149	24 _{5,20} – 23 _{5,19} *	106143.824	5	84	297.0	25	Blend with NH ₂ CHO and C ₂ H ₅ CN, $v_{13}=1/v_{21}=1$
151	24 _{10,14} – 23 _{10,13} *	106149.258	5	161	256.6	25	Blend with C ₂ H ₅ CN, $v_{13}=1/v_{21}=1$
153	24 _{11,13} – 23 _{11,12} *	106158.350	6	183	245.3	25	Blend with CH ₃ CH ₃ CO and CH ₂ CH ¹³ CN
155	24 _{4,21} – 23 _{4,20}	106164.853	5	75	301.9	25	Blend with CH ₂ CH ¹³ CN and C ₂ H ₅ CN, $v_{13}=1/v_{21}=1$
156	24 _{4,20} – 23 _{4,19}	106166.991	5	75	301.9	25	Blend with CH ₂ CH ¹³ CN and C ₂ H ₅ CN, $v_{13}=1/v_{21}=1$
157	24 _{12,12} – 23 _{12,11} *	106168.961	6	207	232.9	25	Blend with C ₂ H ₅ CN, $v_{13}=1/v_{21}=1$
159	24 _{13,11} – 23 _{13,10} *	106180.959	7	232	219.4	25	Blend with C ₂ H ₅ CN, $v_{13}=1/v_{21}=1$
161	24 _{3,22} – 23 _{3,21}	106188.197	5	68	305.7	25	Detected , noisy
162	24 _{14,10} – 23 _{14,9} *	106194.262	7	260	204.8	25	Blend with CH ₃ CH ₃ CO, $v_t=1$ and U-line
164	24 _{18,6} – 23 _{18,5} *	106259.676	12	391	135.8	25	Blend with ¹³ CH ₃ CH ₂ CN
166	24 _{3,21} – 23 _{3,20}	106263.099	5	68	305.6	25	Blend with ¹³ CH ₃ CH ₂ CN and U-line
167	24 _{2,22} – 23 _{2,21}	106858.357	5	63	308.4	24	Blend with U-line, C ₂ H ₅ OH, and CH ₃ CH ₃ CO, $v_t=1$
168	24 _{1,23} – 23 _{1,22}	107161.444	5	60	309.9	24	Blend with CH ₃ OH and ¹³ CH ₃ CN
169	25 _{1,25} – 24 _{1,24}	108811.506	5	64	322.9	20	Blend with ¹³ CN in absorption and C ₂ H ₃ CN
170	25 _{0,25} – 24 _{0,24}	109450.626	5	63	323.2	36	Blend with HC ₃ N, $v_7=1$ and OCS
171	78 _{4,74} – 78 _{3,75}	109452.759	321	668	59.9	36	Blend with HC ₃ N, $v_7=1$ and OCS
172	25 _{2,24} – 24 _{2,23}	110308.536	5	68	321.3	24	Strong CH ₃ ¹³ CN

Table 9. continued.

N^a	Transition ^b	Frequency (MHz)	Unc. ^c (kHz)	E_l^d (K)	$S\mu^2$ (D ²)	σ^e (mK)	Comments
(1)	(2)	(3)	(4)	(5)	(6)	(7)	(8)
173	25 _{7,18} – 24 _{7,17} *	110556.359	5	114	298.1	32	Blend with U-lines and CH ₃ OCHO
175	25 _{8,17} – 24 _{8,16} *	110558.521	5	130	290.3	32	Blend with U-lines and CH ₃ OCHO
177	25 _{6,20} – 24 _{6,19} *	110558.636	5	101	304.8	32	Blend with U-lines and CH ₃ OCHO
179	25 _{9,16} – 24 _{9,15} *	110563.690	5	147	281.5	32	Blend with U-line
181	25 _{5,21} – 24 _{5,20} *	110568.450	5	89	310.5	32	Blend with CH ₃ OCHO, $v_t=1$
183	25 _{10,15} – 24 _{10,14} *	110571.130	6	167	271.7	32	Blend with CH ₃ OCHO, $v_t=1$
185	25 _{11,14} – 24 _{11,13} *	110580.433	6	188	260.8	32	Blend with CH ₃ CH ₃ CO and U-line, uncertain baseline
187	86 _{6,80} – 85 _{7,79}	110581.350	563	826	15.9	32	Blend with CH ₃ CH ₃ CO and U-line, uncertain baseline
188	25 _{12,13} – 24 _{12,12} *	110591.357	6	212	248.9	32	Blend with U-line, CH ₃ ¹³ CN, $v_8=1$, and HNCO, $v_4=1$
190	25 _{4,22} – 24 _{4,21}	110592.442	5	80	315.2	32	Blend with U-line, CH ₃ ¹³ CN, $v_8=1$, and HNCO, $v_4=1$
191	28 _{3,26} – 28 _{2,27}	110593.409	5	90	14.3	32	Blend with U-line, CH ₃ ¹³ CN, $v_8=1$, and HNCO, $v_4=1$
192	25 _{4,21} – 24 _{4,20}	110595.288	5	80	315.1	32	Blend with CH ₃ ¹³ CN, $v_8=1$ and HNCO, $v_4=1$
193	46 _{1,45} – 46 _{1,46}	110603.457	123	227	0.8	32	Blend with CH ₃ CN, $v_8=1$ and U-line
194	25 _{13,12} – 24 _{13,11} *	110603.755	7	237	236.0	32	Blend with CH ₃ CN, $v_8=1$ and U-line
196	25 _{3,23} – 24 _{3,22}	110616.104	5	73	318.8	32	Blend with CH ₃ CN, $v_8=1$ and CH ₃ ¹³ CN, $v_8=1$
197	25 _{14,11} – 24 _{14,10} *	110617.532	7	265	222.0	32	Blend with CH ₃ CN, $v_8=1$ and CH ₃ ¹³ CN, $v_8=1$
199	25 _{15,10} – 24 _{15,9} *	110632.625	8	295	207.0	32	Blend with CH ₃ ¹³ CN, $v_8=1$ and CH ₃ CN, $v_8=1$
201	25 _{19,6} – 24 _{19,5} *	110705.543	14	434	136.6	32	Strong CH ₃ CN, $v_8=1$
203	25 _{3,22} – 24 _{3,21}	110707.662	5	73	318.8	32	Strong CH ₃ CN, $v_8=1$
204	25 _{2,23} – 24 _{2,22}	111357.863	5	68	321.4	35	Noisy
205	25 _{1,24} – 24 _{1,23}	111593.662	5	65	322.9	29	Detected
206	26 _{1,26} – 25 _{1,25}	113144.084	5	69	335.9	40	Strong CN in absorption
207	26 _{0,26} – 25 _{0,25}	113759.873	5	69	336.1	34	Blend with CH ₃ OCHO and U-line
208	26 _{2,25} – 25 _{2,24}	114702.134	5	73	334.4	37	Blend with CH ₃ OCH ₃
209	26 _{7,19} – 25 _{7,18} *	114978.615	5	119	312.0	59	Blend with C ₂ H ₃ CN, $v_{11}=3$ and ¹³ CH ₃ OH
211	26 _{8,18} – 25 _{8,17} *	114980.356	5	135	304.5	59	Blend with C ₂ H ₃ CN, $v_{11}=3$ and ¹³ CH ₃ OH
213	26 _{6,21} – 25 _{6,20} *	114981.774	5	106	318.5	59	Blend with C ₂ H ₃ CN, $v_{11}=3$, ¹³ CH ₃ OH, and C ₂ H ₃ CN, $v_{11}=3$
215	26 _{9,17} – 25 _{9,16} *	114985.387	5	152	296.1	59	Blend with C ₂ H ₃ CN, $v_{11}=3$ and CH ₃ CH ₃ CO
217	26 _{10,16} – 25 _{10,15} *	114992.878	6	172	286.6	59	Blend with CH ₃ CH ₃ CO
219	26 _{5,22} – 25 _{5,21} *	114993.314	5	95	323.9	59	Blend with CH ₃ CH ₃ CO
221	26 _{11,15} – 25 _{11,14} *	115002.371	6	193	276.2	59	Blend with C ₂ H ₅ CN, $v_{13}=1/v_{21}=1$ and C ₂ H ₃ CN, $v_{11}=1$
223	26 _{12,14} – 25 _{12,13} *	115013.593	6	217	264.7	59	Blend with C ₂ H ₅ CN, $v_{13}=1/v_{21}=1$, CH ₂ ¹³ CHCN, and U-line
225	26 _{4,23} – 25 _{4,22}	115020.476	5	85	328.4	59	Blend with U-line
226	26 _{4,22} – 25 _{4,21}	115024.221	5	85	328.4	59	Blend with U-line
227	26 _{13,13} – 25 _{13,12} *	115026.378	7	243	252.3	59	Blend with U-line and C ₂ H ₅ OH
229	26 _{14,12} – 25 _{14,11} *	115040.619	8	270	238.9	59	Blend with U-line
231	26 _{3,24} – 25 _{3,23}	115043.924	5	78	331.9	59	Blend with U-line
232	26 _{15,11} – 25 _{15,10} *	115056.245	8	300	224.4	59	Blend with H ¹³ CCCN, $v_7=1$
234	64 _{4,60} – 64 _{3,61}	115150.722	157	453	43.9	59	Blend with C ₂ H ₃ CN, CH ₃ OCHO, $v_t=1$, NS, and CH ₃ CH ₃ CO, $v_t=1$
235	26 _{20,6} – 25 _{20,5} *	115154.006	17	479	137.3	59	Blend with CH ₃ OCHO, $v_t=1$, NS, and CH ₃ CH ₃ CO, $v_t=1$
237	26 _{3,23} – 25 _{3,22}	115154.885	5	78	331.9	59	Blend with CH ₃ OCHO, $v_t=1$, NS, and CH ₃ CH ₃ CO, $v_t=1$
238	26 _{2,24} – 25 _{2,23}	115859.309	5	73	334.4	79	Weak, blend with a(CH ₂ OH) ₂ and C ₂ H ₅ OH
239	33 _{2,32} – 32 _{2,31}	145394.105	5	116	425.3	25	Blend with U-line and NH ₂ CH ₂ CN
240	34 _{1,34} – 33 _{1,33}	147742.893	6	118	439.5	31	Partial blend with C ₂ H ₅ CN and CH ₃ CN, $v_8=1$, uncertain baseline
241	37 _{8,29} – 36 _{8,28} *	163616.044	6	207	456.4	38	Blend with SO ₂
243	37 _{9,28} – 36 _{9,27} *	163616.543	6	225	450.4	38	Blend with SO ₂
245	65 _{4,62} – 65 _{3,63}	163620.536	185	464	33.9	38	Blend with SO ₂
246	37 _{10,27} – 36 _{10,26} *	163622.456	6	244	443.8	38	Blend with U-line, uncertain baseline
248	37 _{7,31} – 36 _{7,30} *	163623.355	5	192	461.6	38	Blend with U-line, uncertain baseline
250	37 _{11,26} – 36 _{11,25} *	163632.454	7	266	436.4	38	Blend with NH ₂ CH ₂ CN, uncertain baseline
252	37 _{6,32} – 36 _{6,31} *	163643.143	5	178	466.1	38	Blend with NH ₂ CH ₂ CN, uncertain baseline
254	37 _{12,25} – 36 _{12,24} *	163645.748	7	289	428.3	38	Blend with NH ₂ CH ₂ CN, uncertain baseline
256	37 _{13,24} – 36 _{13,23} *	163661.850	8	315	419.6	38	Blend with C ₂ H ₅ OCHO, uncertain baseline
258	37 _{14,23} – 36 _{14,22} *	163680.443	8	343	410.2	38	Blend with C ₂ H ₅ CN, $v_{13}=1/v_{21}=1$ and HC ¹³ CCN, $v_7=1$
260	37 _{5,33} – 36 _{5,32}	163684.984	5	167	470.0	38	Blend with HC ¹³ CCN, $v_7=1$ and C ₂ H ₅ CN
261	37 _{5,32} – 36 _{5,31}	163686.545	5	167	470.0	38	Blend with HC ¹³ CCN, $v_7=1$ and C ₂ H ₅ CN
262	37 _{15,22} – 36 _{15,21} *	163701.318	9	373	400.1	38	Blend with HC ¹³ CCN, $v_7=1$
264	37 _{3,35} – 36 _{3,34}	163715.634	5	151	475.5	38	Blend with CH ₃ CH ₃ CO, $v_t=1$
265	37 _{16,21} – 36 _{16,20} *	163724.332	9	404	389.2	38	Blend with g-C ₃ H ₇ CN and U-line
267	39 _{9,30} – 38 _{9,29} *	172456.851	6	241	477.7	44	Strong C ₂ H ₅ CN and CH ₃ OCHO, $v_t=1$
269	39 _{8,31} – 38 _{8,30} *	172457.861	6	223	483.3	44	Strong C ₂ H ₅ CN and CH ₃ OCHO, $v_t=1$
271	39 _{10,29} – 38 _{10,28} *	172461.990	7	260	471.4	44	Strong C ₂ H ₅ CN and CH ₃ OCHO, $v_t=1$
273	39 _{7,33} – 38 _{7,32} *	172467.829	6	208	488.4	44	Strong CH ₃ OCHO, $v_t=1$ and C ₂ H ₃ CN

Table 9. continued.

N^a	Transition ^b	Frequency (MHz)	Unc. ^c (kHz)	E_l^d (K)	$S\mu^2$ (D ²)	σ^e (mK)	Comments
(1)	(2)	(3)	(4)	(5)	(6)	(7)	(8)
275	39 _{11,28} – 38 _{11,27} *	172471.720	7	282	464.4	44	Strong CH ₃ OCHO, $v_1=1$ and C ₂ H ₃ CN
277	39 _{12,27} – 38 _{12,26} *	172485.116	8	305	456.8	44	Blend with C ₂ H ₅ CN
279	39 _{6,34} – 38 _{6,33} *	172492.223	5	194	492.7	44	Blend with C ₂ H ₅ CN
281	39 _{13,26} – 38 _{13,25} *	172501.606	8	331	448.5	44	Blend with C ₂ H ₅ CN, $v_{13}=1/v_{21}=1$
283	52 _{2,50} – 51 _{3,49}	172516.550	77	291	14.0	44	Blend with C ₂ H ₅ CN, $v_{13}=1/v_{21}=1$ and CH ₃ OCHO, $v_1=1$
284	39 _{14,25} – 38 _{14,24} *	172520.819	8	359	439.6	44	Blend with CH ₃ OCHO, $v_1=1$, HC ¹³ CCN, $v_7=1$, and HC ¹³ CCN, $v_6=1$
286	39 _{5,35} – 38 _{5,34}	172542.025	5	183	496.3	44	Blend with NH ₂ CH ₂ CN and HCC ¹³ CN, $v_6=1$
287	39 _{15,24} – 38 _{15,23} *	172542.509	9	388	429.9	44	Blend with NH ₂ CH ₂ CN and HCC ¹³ CN, $v_6=1$
289	39 _{5,34} – 38 _{5,33}	172544.526	5	183	496.3	44	Blend with HCC ¹³ CN, $v_6=1$ and HCC ¹³ CN, $v_7=1$
290	39 _{3,37} – 38 _{3,36}	172551.469	5	167	501.6	44	Blend with HCC ¹³ CN, $v_6=1$ and HCC ¹³ CN, $v_7=1$
291	39 _{16,23} – 38 _{16,22} *	172566.508	9	420	419.6	44	Blend with NH ₂ CH ₂ CN
293	39 _{17,22} – 38 _{17,21} *	172592.700	10	454	408.7	44	Blend with CH ₂ (OH)CHO and U-line
295	39 _{18,21} – 38 _{18,20} *	172621.005	11	490	397.1	44	Blend with NH ₂ CH ₂ CN, t-HCOOH, and U-line?
297	39 _{4,36} – 38 _{4,35}	172622.501	5	174	499.2	44	Blend with NH ₂ CH ₂ CN, t-HCOOH, and U-line?
298	39 _{19,20} – 38 _{19,19} *	172651.366	13	528	384.8	44	Blend with C ₂ H ₅ CN, $v_{20}=1$ and U-line
300	39 _{20,19} – 38 _{20,18} *	172683.745	16	568	371.8	44	Strong H ¹³ CN in absorption and CH ₃ OCHO
302	39 _{4,35} – 38 _{4,34}	172684.518	5	174	499.2	44	Strong H ¹³ CN in absorption and CH ₃ OCHO
303	46 _{2,45} – 45 _{2,44}	202062.851	7	223	593.9	138	Blend with CH ₃ ¹³ CN
304	46 _{1,45} – 45 _{1,44}	203271.058	6	222	594.2	161	Strong H ¹³ CCCN, $v_7=1$ and C ₂ H ₃ CN, $v_{11}=1$
305	46 _{9,37} – 45 _{9,36} *	203392.918	7	303	572.3	161	Strong SO ₂ and C ₂ H ₅ CN
307	46 _{10,36} – 45 _{10,35} *	203393.942	8	323	567.0	161	Strong SO ₂ and C ₂ H ₅ CN
309	46 _{8,39} – 45 _{8,38} *	203401.192	7	286	577.1	161	Strong C ₂ H ₅ CN and CH ₃ OCH ₃
311	46 _{11,35} – 45 _{11,34} *	203401.696	8	344	561.1	161	Strong C ₂ H ₅ CN and CH ₃ OCH ₃
313	46 _{12,34} – 45 _{12,33} *	203414.661	9	368	554.6	161	Strong CH ₃ OCH ₃ and ¹³ CH ₂ CHCN
315	46 _{3,44} – 45 _{3,43}	203419.779	6	229	592.5	161	Blend with ¹³ CH ₂ CHCN
316	46 _{7,40} – 45 _{7,39} *	203423.393	6	270	581.4	161	Blend with ¹³ CH ₂ CHCN
318	46 _{13,33} – 45 _{13,32} *	203431.894	9	393	547.6	161	Blend with CH ₃ CN, $v_8=2$
320	46 _{14,32} – 45 _{14,31} *	203452.784	9	421	540.0	161	Blend with CH ₃ CN, $v_8=2$
322	46 _{6,41} – 45 _{6,40}	203468.489	6	257	585.0	161	Blend with CH ₃ CN, $v_8=2$ and CH ₃ OCHO
323	46 _{6,40} – 45 _{6,39}	203468.859	6	257	585.0	161	Blend with CH ₃ CN, $v_8=2$ and CH ₃ OCHO
324	46 _{15,31} – 45 _{15,30} *	203476.924	9	451	531.9	161	Blend with CH ₃ OCHO and CH ₃ CN, $v_8=2$
326	46 _{16,30} – 45 _{16,29} *	203504.034	9	483	523.1	161	Blend with ³⁴ SO ₂ and CH ₃ CN, $v_8=2$
328	46 _{17,29} – 45 _{17,28} *	203533.921	10	517	513.8	161	Blend with CH ₃ CN, $v_8=2$
330	16 _{7,9} – 17 _{6,12} *	203535.308	25	70	1.6	161	Blend with CH ₃ CN, $v_8=2$ and C ₂ H ₅ OCHO
332	46 _{5,42} – 45 _{5,41}	203552.152	6	245	588.1	161	Blend with CH ₃ CN, $v_8=2$ and H ¹³ CCCN, $v_7=1$
333	46 _{5,41} – 45 _{5,40}	203562.997	6	245	588.2	161	Strong CH ₃ CN, $v_8=2$, CH ₃ OCH ₃ , and ¹³ CH ₂ CHCN
334	46 _{18,28} – 45 _{18,27} *	203566.446	10	552	504.0	161	Strong CH ₃ CN, $v_8=2$, CH ₃ OCH ₃ , and ¹³ CH ₂ CHCN
336	46 _{19,27} – 45 _{19,26} *	203601.513	11	590	493.6	161	Blend with CH ₃ OCHO and CH ₃ CH ₃ CO
338	46 _{20,26} – 45 _{20,25} *	203639.052	14	630	482.7	161	Blend with C ₂ H ₅ CN
340	46 _{4,43} – 45 _{4,42}	203653.642	6	236	590.6	161	Blend with C ₂ H ₅ CN, C ₂ H ₅ OH, and U-line
341	46 _{21,25} – 45 _{21,24} *	203679.015	17	672	471.1	161	Blend with CH ₃ CN, $v_8=2$
343	46 _{23,23} – 45 _{23,22} *	203766.086	29	762	446.4	364	Blend with C ₂ H ₅ OCHO
345	47 _{1,47} – 46 _{1,46}	203773.957	14	227	607.7	364	Blend with ¹³ CH ₂ CHCN
346	46 _{4,42} – 45 _{4,41}	203841.799	6	236	590.6	364	Blend with C ₂ H ₅ CN and CH ₃ OCHO
347	47 _{0,47} – 46 _{0,46}	203894.538	14	227	607.7	364	Blend with U-line
348	46 _{2,44} – 45 _{2,43}	205486.337	8	226	594.0	100	Blend with CH ₃ OCHO
349	41 _{2,40} – 40 _{1,39}	205486.671	20	176	17.7	100	Blend with CH ₃ OCHO
350	47 _{2,46} – 46 _{2,45}	206403.502	7	233	606.8	106	Strong C ₂ H ₅ CN
351	47 _{1,46} – 46 _{1,45}	207565.934	6	232	607.1	282	Blend with C ₂ H ₅ OH and U-line?
352	47 _{9,38} – 46 _{9,37} *	207811.666	7	313	585.8	173	Blend with ¹³ CH ₃ OH and C ₂ H ₅ CN
354	47 _{10,37} – 46 _{10,36} *	207811.909	8	332	580.5	173	Blend with ¹³ CH ₃ OH and C ₂ H ₅ CN
356	47 _{11,36} – 46 _{11,35} *	207819.239	8	354	574.7	173	Blend with C ₂ H ₅ CN and C ₂ H ₅ OCHO
358	47 _{3,45} – 46 _{3,44}	207820.872	6	239	605.5	173	Blend with C ₂ H ₅ CN and C ₂ H ₅ OCHO
359	47 _{8,40} – 46 _{8,39} *	207821.249	7	295	590.5	173	Blend with C ₂ H ₅ CN, C ₂ H ₅ OCHO, and C ₂ H ₅ OH
361	47 _{12,35} – 46 _{12,34} *	207832.034	9	378	568.5	173	Strong NS, CH ₂ ¹³ CHCN, and C ₂ H ₅ CN
363	47 _{7,41} – 46 _{7,40} *	207845.603	7	280	594.7	173	Strong C ₂ H ₅ CN, $v_{13}=1/v_{21}=1$
365	47 _{13,34} – 46 _{13,33} *	207849.289	9	403	561.6	173	Strong C ₂ H ₅ CN, $v_{13}=1/v_{21}=1$
367	47 _{14,33} – 46 _{14,32} *	207870.351	9	431	554.2	173	Blend with C ₂ H ₅ OH, uncertain baseline
369	47 _{6,42} – 46 _{6,41}	207894.282	6	267	598.2	173	Blend with C ₂ H ₅ OH and CH ₂ ¹³ CHCN
370	47 _{6,41} – 46 _{6,40} *	207894.750	6	267	598.2	173	Blend with C ₂ H ₅ OH and CH ₂ ¹³ CHCN
372	47 _{15,33} – 46 _{15,32}	207894.786	10	461	546.2	173	Blend with C ₂ H ₅ OH and CH ₂ ¹³ CHCN
373	47 _{16,31} – 46 _{16,30} *	207922.295	10	492	537.6	173	Blend with C ₂ H ₃ CN, $v_{15}=1$, C ₂ H ₅ ¹³ CN, and CH ₃ CH ₃ CO, $v_7=1$
375	47 _{17,30} – 46 _{17,29} *	207952.671	10	526	528.5	173	Blend with C ₂ H ₅ CN and CH ₂ ¹³ CHCN

Table 9. continued.

N^a	Transition ^b	Frequency (MHz)	Unc. ^c (kHz)	E_l^d (K)	$S\mu^2$ (D ²)	σ^e (mK)	Comments
(1)	(2)	(3)	(4)	(5)	(6)	(7)	(8)
377	15 _{7,8} – 16 _{6,11} *	207955.703	25	66	1.4	173	Blend with C ₂ H ₅ CN and CH ₂ ¹³ CHCN
379	47 _{5,43} – 46 _{5,42}	207983.470	6	255	601.2	173	Blend with C ₂ H ₅ OH and CH ₂ ¹³ CHCN
380	47 _{18,29} – 46 _{18,28} *	207985.767	10	562	518.9	173	Blend with C ₂ H ₅ OH and CH ₂ ¹³ CHCN
382	47 _{5,42} – 46 _{5,41}	207996.582	6	255	601.2	173	Blend with C ₂ H ₅ CN, C ₂ H ₅ OH, and CH ₂ CH ¹³ CN
383	47 _{19,28} – 46 _{19,27} *	208021.478	11	600	508.7	173	Blend with CH ₂ ¹³ CHCN
385	47 _{20,27} – 46 _{20,26} *	208059.729	14	640	498.0	173	Blend with C ₂ H ₅ CN
387	48 _{1,48} – 47 _{1,47}	208076.611	16	236	620.6	173	Blend with C ₂ H ₅ CN and CH ₃ CH ₃ CO
388	47 _{4,44} – 46 _{4,43}	208085.930	6	246	603.7	173	Blend with CH ₃ CH ₃ CO and CH ₂ CH ¹³ CN
389	47 _{21,26} – 46 _{21,25} *	208100.469	17	682	486.7	173	Blend with CH ₂ CH ¹³ CN, C ₂ H ₅ CN, $v_{13}=1/v_{21}=1$, and CH ₂ ¹³ CHCN
391	48 _{0,48} – 47 _{0,47}	208185.442	16	236	620.6	173	Blend with C ₂ H ₅ OH and CH ₂ ¹³ CHCN
392	47 _{23,24} – 46 _{23,23} *	208189.277	29	771	462.5	173	Blend with C ₂ H ₅ OH and CH ₂ ¹³ CHCN
394	47 _{25,22} – 46 _{25,21} *	208287.742	46	869	436.0	168	Blend with C ₂ H ₅ OH
396	47 _{4,43} – 46 _{4,42}	208302.740	7	246	603.7	168	Blend with C ₂ H ₅ CN
397	47 _{3,44} – 46 _{3,43}	209390.960	9	239	605.7	58	Blend with C ₂ H ₅ OH and C ₂ H ₃ CN, $v_{15}=1$
398	47 _{2,45} – 46 _{2,44}	209918.318	9	235	607.0	45	Strong ¹³ CH ₃ CH ₂ CN, C ₂ H ₅ OH, and CH ₃ OCHO
399	48 _{2,47} – 47 _{2,46}	210741.480	50	243	619.6	37	Blend with C ₂ H ₃ CN, $v_{11}=3$ and C ₂ H ₅ CN, $v_{13}=1/v_{21}=1$, uncertain baseline
400	48 _{1,47} – 47 _{1,46}	211856.190	50	242	620.1	47	Blend with U-line
401	48 _{3,46} – 47 _{3,45}	212219.540	50	249	618.5	36	Blend with C ₂ H ₅ CN, $v_{20}=1$
402	48 _{10,38} – 47 _{10,37} *	212229.670	50	342	594.1	36	Strong C ₂ H ₅ CN, $v_{20}=1$ and NH ₂ CHO
404	48 _{9,39} – 47 _{9,38} *	212230.190	50	323	599.2	36	Strong C ₂ H ₅ CN, $v_{20}=1$ and NH ₂ CHO
406	48 _{11,37} – 47 _{11,36} *	212236.507	9	364	588.4	36	Strong C ₂ H ₅ CN, $v_{20}=1$ and NH ₂ CHO
408	48 _{8,40} – 47 _{8,39} *	212241.200	50	305	603.8	36	Strong NH ₂ CHO
410	48 _{12,36} – 47 _{12,35} *	212249.060	50	388	582.2	36	Strong NH ₂ CHO and NH ₂ CHO, $v_{12}=1$
412	48 _{13,35} – 47 _{13,34} *	212266.320	50	413	575.5	36	Strong C ₂ H ₅ OH, NH ₂ ¹³ CHO, and NH ₂ CHO
414	48 _{7,41} – 47 _{7,40} *	212267.790	50	290	607.8	36	Strong C ₂ H ₅ OH, NH ₂ ¹³ CHO, and NH ₂ CHO
416	48 _{14,34} – 47 _{14,33} *	212287.590	50	441	568.2	36	Blend with C ₂ H ₅ CN, $v_{13}=1/v_{21}=1$ and $v=0$, and U-line
418	48 _{15,33} – 47 _{15,32} *	212312.290	50	471	560.4	36	Strong C ₂ H ₃ CN, $v_{11}=1$ and NH ₂ CHO
420	48 _{6,43} – 47 _{6,42}	212320.280	50	276	611.3	36	Strong C ₂ H ₃ CN, $v_{11}=1$ and NH ₂ CHO
421	48 _{6,42} – 47 _{6,41}	212320.770	50	276	611.3	36	Strong C ₂ H ₃ CN, $v_{11}=1$ and NH ₂ CHO
422	48 _{16,32} – 47 _{16,31} *	212340.190	50	502	552.0	36	Strong C ₂ H ₃ CN
424	48 _{17,31} – 47 _{17,30} *	212371.060	50	536	543.1	36	Blend with NH ₂ ¹³ CHO, $v_{12}=1$, uncertain baseline
426	14 _{7,7} – 15 _{6,10} *	212375.891	25	63	1.2	36	Blend with NH ₂ ¹³ CHO, $v_{12}=1$, uncertain baseline
428	49 _{1,49} – 48 _{1,48}	212378.480	50	246	633.5	36	Blend with NH ₂ ¹³ CHO, $v_{12}=1$, uncertain baseline
429	48 _{18,30} – 47 _{18,29} *	212404.720	50	572	533.7	36	Strong NH ₂ CHO, $v_{12}=1$ and H ¹³ CCCN, $v_7=1$
431	48 _{5,44} – 47 _{5,43}	212415.060	50	265	614.2	36	Blend with NH ₂ CHO
432	48 _{5,43} – 47 _{5,42}	212430.890	50	265	614.3	36	Strong NH ₂ CHO
433	48 _{19,29} – 47 _{19,28} *	212441.110	50	610	523.7	99	Blend with NH ₂ CHO and CH ₃ OCHO
435	49 _{0,49} – 48 _{0,48}	212476.620	50	246	633.6	99	Blend with C ₂ H ₅ OH and CH ₃ OCHO
436	48 _{20,28} – 47 _{20,27} *	212480.030	50	650	513.3	99	Blend with ¹³ CH ₃ OH, $v_i=1$ and CH ₃ CHO
438	48 _{4,45} – 47 _{4,44}	212517.790	50	256	616.8	99	Blend with C ₂ H ₅ CN and C ₂ H ₅ OH, uncertain baseline
439	48 _{21,27} – 47 _{21,26} *	212521.490	50	692	502.1	99	Blend with C ₂ H ₅ CN and C ₂ H ₅ OH, uncertain baseline
441	48 _{26,22} – 47 _{26,21} *	212766.374	57	931	438.8	99	Blend with ¹³ CH ₃ OH and C ₂ H ₅ CN, uncertain baseline
443	48 _{4,44} – 47 _{4,43}	212766.640	50	256	616.7	99	Blend with ¹³ CH ₃ OH and C ₂ H ₅ CN, uncertain baseline
444	48 _{3,45} – 47 _{3,44}	213912.029	10	249	618.6	48	Blend with ¹³ CH ₃ OH
445	48 _{2,46} – 47 _{2,45}	214343.680	50	245	619.9	75	Strong ¹³ CH ₃ CN and C ₂ H ₅ ¹³ CN
446	49 _{2,48} – 48 _{2,47}	215077.170	50	253	632.6	74	Strong C ₂ H ₅ CN
447	49 _{1,48} – 48 _{1,47}	216142.273	8	252	632.9	55	Blend with OCS and U-line
448	49 _{3,47} – 48 _{3,46}	216615.615	6	259	631.5	55	Blend with CH ₃ COOH and CH ₃ CHO
449	49 _{10,39} – 48 _{10,38} *	216647.130	8	352	607.5	55	Strong SO ₂ and C ₂ H ₅ OH
451	49 _{9,40} – 48 _{9,39} *	216648.604	8	333	612.6	55	Strong SO ₂ and C ₂ H ₅ OH
453	49 _{11,38} – 48 _{11,37} *	216653.496	9	374	602.0	55	Strong SO ₂ and C ₂ H ₅ OH
455	49 _{8,42} – 48 _{8,41} *	216661.026	7	315	617.0	55	Strong SO ₂ and C ₂ H ₅ OH
457	49 _{12,37} – 48 _{12,36} *	216665.865	9	398	596.0	55	Strong SO ₂ and C ₂ H ₅ OH
459	50 _{1,50} – 49 _{1,49}	216679.385	20	257	646.5	55	Blend with H ₂ S
460	49 _{13,36} – 48 _{13,35} *	216683.096	10	423	589.3	55	Blend with H ₂ S
462	49 _{7,43} – 48 _{7,42} *	216690.012	7	300	621.0	55	Strong H ₂ S
464	49 _{14,35} – 48 _{14,34} *	216704.448	10	451	582.2	55	Strong H ₂ S
466	49 _{15,34} – 48 _{15,33} *	216729.429	10	481	574.6	50	Strong H ₂ S and C ₂ H ₅ CN, $v_{13}=1/v_{21}=1$
468	49 _{6,44} – 48 _{6,43}	216746.358	7	287	624.5	50	Strong C ₂ H ₅ CN
469	49 _{6,43} – 48 _{6,42}	216747.094	7	287	624.5	50	Strong C ₂ H ₅ CN
470	49 _{16,33} – 48 _{16,32} *	216757.710	50	513	566.3	50	Strong C ₂ H ₅ CN
472	50 _{0,50} – 49 _{0,49}	216767.700	50	256	646.5	50	Blend with C ₂ H ₅ CN and U-line

Table 9. continued.

N^a	Transition ^b	Frequency (MHz)	Unc. ^c (kHz)	E_l^d (K)	$S\mu^2$ (D ²)	σ^e (mK)	Comments
(1)	(2)	(3)	(4)	(5)	(6)	(7)	(8)
473	49 _{17,32} – 48 _{17,31} *	216789.070	50	546	557.7	50	Blend with CH ₃ CH ₃ CO, $v_t=1$
475	13 _{7,6} – 14 _{6,9} *	216795.931	26	59	1.0	50	Blend with CH ₃ CH ₃ CO, $v_t=1$
477	49 _{18,31} – 48 _{18,30} *	216823.235	10	582	548.3	50	Strong CH ₃ OCHO
479	49 _{5,45} – 48 _{5,44}	216847.000	7	275	627.3	50	Strong C ₂ H ₅ CN, $v_{13}=1/v_{21}=1$
480	49 _{19,30} – 48 _{19,29} *	216860.211	11	620	538.7	50	Blend with C ₂ H ₅ CN, $v_{13}=1/v_{21}=1$ and U-line
482	49 _{5,44} – 48 _{5,43}	216865.924	7	275	627.4	50	Blend with C ₂ H ₅ CN, $v_{13}=1/v_{21}=1$ and U-line
483	49 _{20,29} – 48 _{20,28} *	216899.870	50	660	528.3	50	Blend with U-line
485	49 _{21,28} – 48 _{21,27} *	216942.142	17	702	517.5	50	Strong CH ₃ OH
487	49 _{4,46} – 48 _{4,45}	216949.090	50	266	629.7	50	Strong CH ₃ OH
488	42 _{10,32} – 43 _{9,35} *	216956.684	77	284	6.3	50	Strong CH ₃ OH
490	49 _{4,45} – 48 _{4,44}	217233.695	7	266	629.8	50	Strong CH ₂ ¹³ CHCN
491	45 _{2,44} – 44 _{1,43}	217511.675	25	213	21.1	50	Blend with ¹³ CN in absorption and U-line
492	50 _{1,50} – 49 _{0,49}	217512.520	22	256	41.1	50	Blend with ¹³ CN in absorption and U-line
493	50 _{2,49} – 49 _{2,48}	219410.228	10	263	645.7	92	Strong HC ₃ N, $v_6=v_7=1$
494	65 ₂ – 5 _{4,1} *	219563.799	11	20	4.4	92	Strong C ¹⁸ O
496	50 _{1,49} – 49 _{1,48}	220424.730	8	262	645.9	98	Strong CH ₃ ¹³ CN
497	51 _{4,47} – 50 _{4,46}	226177.852	9	287	655.8	278	Noisy
498	51 _{3,48} – 50 _{3,47}	227473.842	14	281	657.7	85	Blend with CH ₂ CH ¹³ CN and C ₂ H ₅ OCHO, uncertain baseline
499	51 _{2,49} – 50 _{2,48}	227577.811	11	277	658.7	85	Strong CH ₃ OCHO and C ₂ H ₅ OH
500	29 _{3,27} – 28 _{2,26}	227580.141	9	91	7.6	85	Strong CH ₃ OCHO and C ₂ H ₅ OH
501	53 _{2,52} – 52 _{2,51}	232395.004	14	295	684.5	19	Blend with C ₂ H ₅ OH
502	9 _{5,5} – 8 _{4,4} *	232831.850	11	24	4.9	19	Blend with CH ₃ CH ₃ CO, $v_t=1$ and U-line
504	62 _{6,57} – 62 _{5,58}	232836.738	28	440	32.6	19	Blend with CH ₃ CH ₃ CO, $v_t=1$ and U-line
505	44 _{6,39} – 44 _{5,40}	235131.269	9	236	22.2	131	Strong C ₂ H ₅ OH
506	53 _{4,49} – 52 _{4,48}	235136.432	11	309	681.8	131	Strong C ₂ H ₅ OH
507	39 _{6,33} – 39 _{5,34}	235437.401	9	191	19.4	131	Blend with ¹³ CH ₃ OH, $v_t=1$
508	38 _{6,32} – 38 _{5,33}	235489.643	9	183	18.9	131	Blend with CH ₃ CH ₃ CO and HC ¹³ CCN
509	37 _{6,31} – 37 _{5,32}	235537.303	9	175	18.4	131	Strong HCC ¹³ CN
510	37 _{6,32} – 37 _{5,33}	235543.778	9	175	18.4	131	Strong HCC ¹³ CN and CH ₃ CH ₃ CO
511	36 _{6,30} – 36 _{5,31}	235580.671	9	167	17.8	131	Blend with C ₂ H ₅ CN, uncertain baseline
512	36 _{6,31} – 36 _{5,32}	235585.618	9	167	17.8	131	Blend with C ₂ H ₅ CN, uncertain baseline
513	35 _{6,29} – 35 _{5,30}	235620.022	9	159	17.3	131	Blend with C ₂ H ₅ CN, $v_{13}=1/v_{21}=1$
514	35 _{6,30} – 35 _{5,31}	235623.773	9	159	17.3	131	Blend with C ₂ H ₅ CN, $v_{13}=1/v_{21}=1$
515	34 _{6,28} – 34 _{5,29}	235655.616	9	152	16.7	131	Blend with C ₂ H ₅ CN, $v_{13}=1/v_{21}=1$, HC ¹³ CCN, $v_5=1/v_7=3$, and C ₂ H ₃ CN, $v_{11}=1$
516	34 _{6,29} – 34 _{5,30}	235658.436	9	152	16.7	131	Blend with C ₂ H ₅ CN, $v_{13}=1/v_{21}=1$, HC ¹³ CCN, $v_5=1/v_7=3$, and C ₂ H ₃ CN, $v_{11}=1$
517	33 _{6,27} – 33 _{5,28}	235687.700	10	145	16.2	131	Blend with HCC ¹³ CN, $v_5=1/v_7=3$, uncertain baseline
518	33 _{6,28} – 33 _{5,29}	235689.803	10	145	16.2	131	Blend with HCC ¹³ CN, $v_5=1/v_7=3$, uncertain baseline
519	32 _{6,26} – 32 _{5,27}	235716.510	10	138	15.7	131	Blend with CH ₃ OCH ₃
520	32 _{6,27} – 32 _{5,28}	235718.063	10	138	15.7	131	Blend with CH ₃ OCH ₃
521	31 _{6,25} – 31 _{5,26}	235742.268	10	131	15.1	131	Blend with U-line in absorption or baseline problem?
522	31 _{6,26} – 31 _{5,27}	235743.404	10	131	15.1	131	Blend with U-line in absorption or baseline problem?
523	30 _{6,24} – 30 _{5,25}	235765.188	10	124	14.6	131	Blend with U-line in absorption or baseline problem?
524	30 _{6,25} – 30 _{5,26}	235766.010	10	124	14.6	131	Blend with U-line in absorption or baseline problem?
525	29 _{6,23} – 29 _{5,24}	235785.473	10	118	14.1	131	Blend with CH ₃ OCH ₃ and ¹³ CH ₃ CH ₂ CN
526	29 _{6,24} – 29 _{5,25}	235786.062	10	118	14.1	131	Blend with CH ₃ OCH ₃ and ¹³ CH ₃ CH ₂ CN
527	28 _{6,22} – 28 _{5,23}	235803.318	11	112	13.6	131	Blend with CH ₃ CH ₃ CO, $v_t=1$
528	28 _{6,23} – 28 _{5,24}	235803.734	11	112	13.6	131	Blend with CH ₃ CH ₃ CO, $v_t=1$
529	27 _{6,21} – 27 _{5,22}	235818.908	11	106	13.0	131	Blend with CH ₃ CHO, uncertain baseline
530	27 _{6,22} – 27 _{5,23}	235819.199	11	106	13.0	131	Blend with CH ₃ CHO, uncertain baseline
531	26 _{6,20} – 26 _{5,21}	235832.420	11	100	12.5	131	Blend with CH ₃ OCHO
532	26 _{6,21} – 26 _{5,22}	235832.620	11	100	12.5	131	Blend with CH ₃ OCHO
533	25 _{6,19} – 25 _{5,20}	235844.025	11	95	12.0	131	Strong CH ₃ OCHO
534	25 _{6,20} – 25 _{5,21}	235844.161	11	95	12.0	131	Strong CH ₃ OCHO
535	24 _{6,18} – 24 _{5,19} *	235853.884	12	89	11.4	131	Blend with CH ₃ OCHO
537	23 _{6,17} – 23 _{5,18} *	235862.152	12	84	10.9	131	Strong CH ₃ OCHO and C ₂ H ₅ CN, $v_{13}=1/v_{21}=1$
539	22 _{6,16} – 22 _{5,17} *	235868.978	12	79	10.4	131	Strong CH ₃ OCHO and C ₂ H ₅ CN, $v_{13}=1/v_{21}=1$
541	21 _{6,15} – 21 _{5,16} *	235874.503	13	75	9.9	131	Strong ¹³ CH ₃ OH, CH ₃ OCHO, and HC ¹³ CCN, $v_6=1$
543	6 _{6,0} – 6 _{5,1} *	235877.922	15	30	0.9	131	Strong ¹³ CH ₃ OH, CH ₃ OCHO, and HC ¹³ CCN, $v_6=1$
545	20 _{6,14} – 20 _{5,15} *	235878.862	13	70	9.3	131	Strong ¹³ CH ₃ OH, CH ₃ OCHO, and HC ¹³ CCN, $v_6=1$
547	7 _{6,1} – 7 _{5,2} *	235879.246	15	32	1.7	131	Strong ¹³ CH ₃ OH, CH ₃ OCHO, and HC ¹³ CCN, $v_6=1$
549	8 _{6,2} – 8 _{5,3} *	235880.638	15	33	2.4	131	Strong ¹³ CH ₃ OH, CH ₃ OCHO, and HC ¹³ CCN, $v_6=1$
551	9 _{6,3} – 9 _{5,4} *	235882.048	15	35	3.1	131	Strong ¹³ CH ₃ OH, CH ₃ OCHO, and HC ¹³ CCN, $v_6=1$

Table 9. continued.

N^a	Transition ^b	Frequency (MHz)	Unc. ^c (kHz)	E_l^d (K)	$S\mu^2$ (D ²)	σ^e (mK)	Comments
(1)	(2)	(3)	(4)	(5)	(6)	(7)	(8)
553	19 _{6,13} – 19 _{5,14} *	235882.182	13	66	8.8	131	Strong ¹³ CH ₃ OH, CH ₃ OCHO, and HC ¹³ CCN, $v_6=1$
555	10 _{6,4} – 10 _{5,5} *	235883.423	15	37	3.7	131	Strong ¹³ CH ₃ OH, CH ₃ OCHO, and HC ¹³ CCN, $v_6=1$
557	18 _{6,12} – 18 _{5,13} *	235884.587	13	62	8.2	131	Strong ¹³ CH ₃ OH, CH ₃ OCHO, and HC ¹³ CCN, $v_6=1$
559	11 _{6,5} – 11 _{5,6} *	235884.702	15	40	4.3	131	Strong ¹³ CH ₃ OH, CH ₃ OCHO, and HC ¹³ CCN, $v_6=1$
561	12 _{6,6} – 12 _{5,7} *	235885.818	15	42	4.9	131	Strong ¹³ CH ₃ OH, CH ₃ OCHO, and HC ¹³ CCN, $v_6=1$
563	17 _{6,11} – 17 _{5,12} *	235886.191	14	58	7.7	131	Strong ¹³ CH ₃ OH, CH ₃ OCHO, and HC ¹³ CCN, $v_6=1$
565	13 _{6,7} – 13 _{5,8} *	235886.698	14	45	5.5	131	Strong ¹³ CH ₃ OH, CH ₃ OCHO, and HC ¹³ CCN, $v_6=1$
567	16 _{6,10} – 16 _{5,11} *	235887.104	14	55	7.2	131	Strong ¹³ CH ₃ OH, CH ₃ OCHO, and HC ¹³ CCN, $v_6=1$
569	14 _{6,8} – 14 _{5,9} *	235887.263	14	48	6.1	131	Strong ¹³ CH ₃ OH, CH ₃ OCHO, and HC ¹³ CCN, $v_6=1$
571	15 _{6,9} – 15 _{5,10} *	235887.429	14	51	6.6	131	Strong ¹³ CH ₃ OH, CH ₃ OCHO, and HC ¹³ CCN, $v_6=1$
573	53 _{2,51} – 52 _{2,50}	236363.740	13	299	684.6	37	Strong CH ₂ CH ¹³ CN
574	53 _{3,50} – 52 _{3,49}	236507.754	18	303	683.6	37	Strong HC ₃ N
575	54 _{3,51} – 53 _{3,50}	241020.744	20	314	696.6	216	Strong C ³⁴ S
576	55 _{2,54} – 54 _{2,53}	241040.003	19	318	710.3	216	Strong C ₂ H ₃ CN, $v_{11}=2$ and CH ₃ OH
577	55 _{4,51} – 54 _{4,50}	244110.418	14	332	707.8	46	Blend with CH ₃ CH ₃ CO, $v_t=1$, C ₂ H ₃ CN, $v_{11}=1$, and U-line
578	55 _{2,53} – 54 _{2,52}	245118.648	14	322	710.4	72	Blend with CH ₂ NH
579	56 _{2,55} – 55 _{2,54}	245359.219	21	329	723.3	72	Strong ¹³ CH ₃ CH ₂ CN
580	55 _{3,52} – 54 _{3,51}	245530.359	22	326	709.6	72	Strong HCC ¹³ CN, $v_7=1$ and ¹³ CH ₃ CH ₂ CN
581	58 _{1,57} – 57 _{2,56}	247309.555	23	353	33.7	68	Blend with C ₂ H ₃ CN, $v_{15}=1$
582	56 _{3,54} – 55 _{3,53}	247311.322	10	336	722.3	68	Blend with C ₂ H ₃ CN, $v_{15}=1$
583	57 _{10,47} – 56 _{10,46} *	251977.746	9	442	714.8	42	Strong CH ₃ OH
585	57 _{11,46} – 56 _{11,45} *	251978.622	9	463	709.9	42	Strong CH ₃ OH
587	57 _{12,45} – 56 _{12,44} *	251988.044	9	487	704.7	42	Strong CH ₃ OH
589	57 _{9,49} – 56 _{9,48} *	251988.316	8	422	719.0	42	Strong CH ₃ OH
591	57 _{13,44} – 56 _{13,43} *	252004.207	10	512	699.1	42	Strong C ₂ H ₅ CN
593	57 _{8,50} – 56 _{8,49} *	252015.263	9	405	722.9	42	Strong C ₂ H ₅ CN and ¹³ CH ₂ CO
595	57 _{14,43} – 56 _{14,42} *	252025.947	10	540	692.9	42	Strong C ₂ H ₅ CN, $v_{13}=1/v_{21}=1$
597	57 _{15,42} – 56 _{15,41} *	252052.483	11	570	686.4	42	Blend with CH ₃ ¹³ CH ₂ CN and U-line
599	57 _{7,51} – 56 _{7,50}	252067.511	9	389	726.4	42	Blend with t-HCOOH
600	57 _{7,50} – 56 _{7,49}	252067.645	9	389	726.4	42	Blend with t-HCOOH
601	57 _{16,41} – 56 _{16,40} *	252083.278	11	602	679.4	42	Strong t-HCOOH and CH ₃ OH
603	57 _{17,40} – 56 _{17,39} *	252117.956	11	636	671.9	42	Blend with C ₂ H ₅ CN, $v_{13}=1/v_{21}=1$ and CH ₂ (OH)CHO
605	57 _{18,39} – 56 _{18,38} *	252156.248	12	671	664.0	42	Strong C ₂ H ₅ CN, $v_{13}=1/v_{21}=1$
607	57 _{6,52} – 56 _{6,51}	252161.456	10	376	729.2	42	Strong C ₂ H ₅ CN, $v_{13}=1/v_{21}=1$
608	57 _{6,51} – 56 _{6,50}	252165.248	10	376	729.2	42	Strong C ₂ H ₅ CN, $v_{13}=1/v_{21}=1$
609	59 _{1,58} – 58 _{2,57}	252195.854	23	365	34.8	42	Strong C ₂ H ₅ CN, $v_{13}=1/v_{21}=1$
610	57 _{19,38} – 56 _{19,37} *	252197.960	12	709	655.6	42	Strong C ₂ H ₅ CN, $v_{13}=1/v_{21}=1$
612	57 _{20,37} – 56 _{20,36} *	252242.951	14	749	646.7	42	Strong C ₂ H ₅ CN and CH ₃ OH
614	57 _{21,36} – 56 _{21,35} *	252291.118	17	791	637.4	42	Blend with U-line and CH ₃ CH ₃ CO, $v_t=1$
616	57 _{5,53} – 56 _{5,52}	252310.240	11	365	731.8	42	Blend with CH ₃ CH ₃ CO, $v_t=1$ and ¹³ CH ₃ CH ₂ CN, uncertain baseline
617	57 _{4,54} – 56 _{4,53}	252367.776	11	355	733.8	42	Strong CH ₃ OCH ₃ and ¹³ CH ₃ OH
618	57 _{5,52} – 56 _{5,51}	252380.765	11	365	731.8	42	Blend with ¹³ CH ₃ CH ₂ CN
619	58 _{2,57} – 57 _{2,56}	253991.392	28	353	749.1	32	Blend with NS and CH ₃ OH in absorption
620	59 _{1,59} – 58 _{1,58}	255355.480	56	358	762.9	217	Strong ¹³ CH ₃ OH
621	59 _{0,59} – 58 _{0,58}	255388.370	56	358	762.8	217	Strong OCS, CH ₂ ¹³ CHCN, and CH ₂ CH ¹³ CN
622	58 _{2,56} – 57 _{2,55}	258190.922	16	358	749.2	1127	Strong CH ₃ CN, $v_8=1$ and C ₂ H ₃ CN, $v_{15}=1$
623	59 _{2,58} – 58 _{2,57}	258304.475	32	365	762.1	1127	Blend with CH ₃ CN, $v_8=1$
624	59 _{1,58} – 58 _{1,57}	258877.691	30	365	762.2	1609	Noisy
625	58 _{3,55} – 57 _{3,54}	259034.024	30	362	748.4	1609	Strong ¹³ CH ₃ OH and ¹³ CH ₂ CHCN
626	59 _{3,57} – 58 _{3,56}	260422.403	15	372	761.3	413	Strong CH ₃ OCHO and C ₂ H ₅ CN
627	60 _{1,59} – 59 _{1,58}	263146.854	35	377	775.1	74	Blend with ¹³ CH ₃ CH ₂ CN, baseline problem
628	59 _{3,56} – 58 _{3,55}	263525.388	34	374	761.5	74	Strong CH ₃ OCH ₃
629	16 _{5,12} – 15 _{4,11}	263780.394	11	42	6.3	108	Strong HC ₃ N and CH ₃ OH, $v_t=1$
630	16 _{5,11} – 15 _{4,12}	263780.579	11	42	6.3	108	Strong HC ₃ N and CH ₃ OH, $v_t=1$
631	61 _{1,61} – 60 _{1,60}	263943.020	70	382	788.7	108	Blend with C ₂ H ₅ CN and CH ₃ CH ₃ CO
632	61 _{0,61} – 60 _{0,60}	263969.205	70	382	788.7	108	Blend with HC ₃ N, $v_5=1/v_7=3$, C ₂ H ₅ CN, $v_{20}=1$, and CH ₃ ¹³ CH ₂ CN
633	7 _{6,1} – 6 _{5,2} *	266831.913	15	30	5.4	91	Strong CH ₃ OCHO, CH ₂ ¹³ CHCN, and CH ₃ OH
635	60 _{2,58} – 59 _{2,57}	266865.326	17	383	775.0	91	Strong CH ₃ OH, $v_t=1$
636	61 _{2,60} – 60 _{2,59}	266924.955	41	390	787.9	91	Blend with CH ₃ OCHO, C ₂ H ₅ CN, C ₂ H ₃ CN, SO ₂ , and U-line

Notes: ^a Numbering of the observed transitions associated with a modeled line stronger than 20 mK. ^b Transitions marked with a * are double with a frequency difference less than 0.1 MHz. The quantum numbers of the second one are not shown. ^c Frequency uncertainty. ^d Lower energy level in temperature units (E_l/k_B). ^e Calculated rms noise level in T_{mb} scale.

Table 10. Transitions of the *gauche*-conformer of *n*-propyl cyanide observed with the IRAM 30 m telescope toward Sgr B2(N). The horizontal lines mark discontinuities in the observed frequency coverage. Only the transitions associated with a modeled line stronger than 20 mK are listed.

N^a	Transition ^b	Frequency (MHz)	Unc. ^c (kHz)	E_l^d (K)	$S\mu^2$ (D ²)	σ^e (mK)	Comments
(1)	(2)	(3)	(4)	(5)	(6)	(7)	(8)
1	17 _{9,9} – 16 _{9,8} *	101965.911	6	199	262.1	34	Blend with U-line
3	17 _{8,10} – 16 _{8,9} *	102048.097	6	193	283.5	34	Blend with NH ₂ CHO, $v_{12}=1$
5	29 _{2,27} – 29 _{1,28}	102048.362	6	253	66.0	34	Blend with NH ₂ CHO, $v_{12}=1$
6	34 _{5,30} – 34 _{3,31}	102175.037	5	308	17.0	30	Blend with C ₂ H ₅ CN, $v_{13}=1/v_{21}=1$, ¹³ CH ₂ CHCN, and CH ₃ OCHO, $v_t=1$
7	17 _{7,11} – 16 _{7,10}	102176.110	6	188	302.4	30	Blend with C ₂ H ₅ CN, $v_{13}=1/v_{21}=1$, ¹³ CH ₂ CHCN, and CH ₃ OCHO, $v_t=1$
8	17 _{7,10} – 16 _{7,9}	102176.872	6	188	302.3	30	Blend with C ₂ H ₅ CN, $v_{13}=1/v_{21}=1$, ¹³ CH ₂ CHCN, and CH ₃ OCHO, $v_t=1$
9	19 _{0,19} – 18 _{0,18}	104811.610	6	179	403.9	25	Blend with C ₂ H ₅ CN, $v_{13}=1/v_{21}=1$ and C ₂ H ₅ OH
10	20 _{8,12} – 20 _{7,13}	104813.646	6	210	89.8	25	Blend with C ₂ H ₅ OH, C ₂ H ₃ CN, $v_{11}=1$, CH ₃ ¹³ CH ₂ CN, and C ₂ H ₅ CN, $v_{13}=1/v_{21}=1$
11	18 _{10,8} – 17 _{10,7} *	107933.825	6	210	266.5	46	Blend with CH ₃ CH ₃ CO, $v_t=1$, C ₂ H ₅ CN, $v_{13}=1/v_{21}=1$, and U-line
13	18 _{9,10} – 17 _{9,9} *	107999.345	6	204	289.1	46	Blend with U-line
15	18 _{8,11} – 17 _{8,10} *	108098.501	6	198	309.4	48	Blend with U-line
17	18 _{7,12} – 17 _{7,11}	108252.103	6	193	327.2	48	Blend with U-line
18	18 _{7,11} – 17 _{7,10}	108253.743	6	193	327.2	48	Blend with U-line
19	18 _{4,15} – 17 _{4,14}	108520.203	7	182	365.9	20	Blend with C ₂ H ₅ OH
20	18 _{2,16} – 17 _{2,15}	108793.066	7	179	375.5	20	Blend with ¹³ CN in absorption and C ₂ H ₅ CN, $v_{13}=1/v_{21}=1$
21	19 _{2,18} – 18 _{2,17}	108827.746	7	182	399.0	20	Blend with ¹³ CN in absorption and U-line?
22	19 _{1,18} – 18 _{1,17}	109039.231	7	182	399.0	29	Blend with C ₂ H ₃ CN and U-line?
23	20 _{1,20} – 19 _{1,19}	110209.409	6	184	425.4	24	Blend with ¹³ CO and HC ₃ N, $v_5=1/v_7=3$
24	20 _{0,20} – 19 _{0,19}	110214.195	6	184	425.4	24	Blend with ¹³ CO and HC ₃ N, $v_5=1/v_7=3$
25	18 _{4,14} – 17 _{4,13}	111109.974	6	182	366.9	25	Blend with U-line
26	18 _{3,15} – 17 _{3,14}	112088.070	7	181	375.2	42	Blend with U-line
27	19 _{3,17} – 18 _{3,16}	112370.034	7	185	394.3	42	Blend with CH ₃ CH ₃ CO and CH ₃ OCH ₃
28	19 _{15,4} – 18 _{15,3} *	113832.488	7	258	153.3	34	Blend with C ₂ H ₃ CN and U-line
30	19 _{16,3} – 18 _{16,2} *	113833.361	7	268	118.4	34	Blend with C ₂ H ₃ CN and U-line
32	19 _{12,7} – 18 _{12,6} *	113872.326	6	230	244.6	34	Blend with C ₂ H ₅ OH and U-line
34	19 _{11,8} – 18 _{11,7} *	113907.356	6	223	270.5	34	Strong C ₂ H ₃ CN
36	19 _{10,10} – 18 _{10,9} *	113960.196	6	216	294.2	33	Blend with C ₂ H ₃ CN
38	19 _{9,11} – 18 _{9,10} *	114038.886	6	209	315.7	33	Blend with U-line
40	19 _{2,17} – 18 _{2,16}	114077.162	7	184	396.3	33	Blend with C ₂ H ₃ CN, $v_{15}=1$ and U-line
41	19 _{8,12} – 18 _{8,11}	114157.197	6	203	334.8	33	Blend with U-line
42	19 _{8,11} – 18 _{8,10}	114157.321	6	203	334.8	33	Blend with U-line
43	20 _{2,19} – 19 _{2,18}	114255.098	6	187	420.4	33	Blend with C ₂ H ₃ CN, $v_{11}=1$
44	19 _{7,13} – 18 _{7,12}	114339.524	6	198	351.7	33	Blend with C ₂ H ₃ CN, $v_{11}=1$ and NH ₂ CHO
45	20 _{1,19} – 19 _{1,18}	114399.053	6	187	420.3	33	Blend with C ₂ H ₃ CN, $v_{13}=1/v_{21}=1$ and U-line?
46	19 _{4,16} – 18 _{4,15}	114451.328	7	187	388.1	37	Blend with C ₂ H ₃ CN, $v_{11}=1/v_{15}=1$ and c-C ₂ H ₄ O
47	19 _{6,14} – 18 _{6,13}	114615.647	6	194	366.3	37	Strong H ¹³ CCCN and C ₂ H ₃ CN
48	19 _{6,13} – 18 _{6,12}	114676.990	6	194	366.4	37	Blend with H ¹³ CCCN, $v_5=1/v_7=3$ and U-line
49	20 _{2,19} – 19 _{1,18}	114679.259	7	187	130.0	37	Blend with H ¹³ CCCN, $v_5=1/v_7=3$ and U-line
50	19 _{5,15} – 18 _{5,14}	114881.716	6	190	378.6	59	Blend with C ₂ H ₃ CN, $v_{11}=3$ and CH ₂ (OH)CHO
51	19 _{5,14} – 18 _{5,13}	115556.072	6	190	378.7	60	Blend with C ₂ H ₃ CN, NS, and CH ₃ OCHO, $v_t=1$
52	21 _{0,21} – 20 _{1,20}	115609.125	6	189	174.8	79	Blend with CH ₂ NH and U-line?
53	21 _{1,21} – 20 _{1,20}	115613.838	6	189	446.8	79	Blend with CH ₂ NH and CH ₃ CHO
54	21 _{0,21} – 20 _{0,20}	115616.804	6	189	446.8	79	Blend with CH ₂ NH and CH ₃ CHO
55	24 _{5,20} – 23 _{5,19}	145147.268	6	221	491.0	25	Strong C ₂ H ₃ CN
56	25 _{3,23} – 24 _{3,22}	145354.256	6	221	522.8	25	Blend with HC ₃ N, $v_4=1$
57	24 _{6,19} – 23 _{6,18}	145359.467	6	224	481.8	25	Blend with HC ₃ N, $v_4=1$
58	26 _{4,23} – 25 _{4,22}	154516.394	5	232	540.1	112	Blend with NH ₂ CH ₂ CN and C ₂ H ₅ CN, $v_{13}=1/v_{21}=1$
59	27 _{7,21} – 26 _{7,20}	163471.366	5	250	539.4	38	Blend with HCC ¹³ CN, $v_7=1$ and NH ₂ CH ₂ CN
60	12 _{7,6} – 11 _{6,5}	163626.490	12	164	62.4	38	Blend with a-C ₃ H ₇ CN and U-line
61	12 _{7,5} – 11 _{6,6}	163626.670	12	164	62.4	38	Blend with a-C ₃ H ₇ CN and U-line
62	27 _{6,22} – 26 _{6,21}	163729.422	5	246	549.4	38	Blend with a-C ₃ H ₇ CN and U-line
63	28 _{3,25} – 27 _{3,24}	166501.674	5	247	583.3	66	Blend with C ₂ H ₅ CN, $v_{13}=1/v_{21}=1$ and CH ₃ CN, $v_8=2$
64	30 _{3,28} – 29 _{2,27}	172509.803	5	258	186.7	44	Strong C ₂ H ₅ CN, $v_{13}=1/v_{21}=1$
65	24 _{13,11} – 24 _{12,12} *	176027.815	8	268	88.7	365	Blend with HNCO, $v_5=1$ and ¹³ CH ₂ CO
67	23 _{13,10} – 23 _{12,11} *	176085.591	8	261	82.2	365	Blend with CH ₃ OCH ₃
69	22 _{13,9} – 22 _{12,10} *	176134.711	8	254	75.7	365	Blend with HNCO, $v_6=1$ and HNCO, $v_5=1$
71	37 _{0,37} – 36 _{1,36} *	201966.900	11	309	321.5	138	Blend with CH ₃ CN
73	37 _{0,37} – 36 _{0,36} *	201966.902	11	309	789.3	138	Blend with CH ₃ CN
75	33 _{5,29} – 32 _{4,28}	201985.474	6	293	131.9	138	Blend with CH ₃ OH

Table 10. continued.

N^a	Transition ^b	Frequency (MHz)	Unc. ^c (kHz)	E_l^d (K)	$S\mu^2$ (D ²)	σ^e (mK)	Comments
(1)	(2)	(3)	(4)	(5)	(6)	(7)	(8)
76	34 _{5,30} – 33 _{5,29}	202090.888	6	303	707.1	138	Strong CH ₂ CO
77	56 _{3,53} – 56 _{3,54} *	202474.090	224	572	15.7	108	Blend with U-line and H ₂ CS
79	56 _{4,53} – 56 _{3,54} *	202474.109	224	572	100.1	108	Blend with U-line and H ₂ CS
81	41 _{15,26} – 41 _{14,27} *	202477.934	26	447	185.2	108	Blend with U-line and H ₂ CS
83	40 _{15,25} – 40 _{14,26} *	202689.659	25	435	178.9	108	Blend with C ₂ H ₃ CN, $v_{15}=1$ and NH ₂ CHO
85	33 _{7,26} – 32 _{7,25}	202881.421	5	302	675.4	138	Blend with C ₂ H ₃ CN, $v_{11}=1$
86	39 _{15,24} – 39 _{14,25} *	202883.694	24	423	172.6	138	Blend with C ₂ H ₃ CN, $v_{11}=1$
88	38 _{15,23} – 38 _{14,24} *	203061.073	23	412	166.3	138	Blend with ¹³ CH ₃ CH ₂ CN and C ₂ H ₅ OCHO
90	34 _{4,30} – 33 _{4,29}	203180.785	6	303	707.8	138	Blend with C ₂ H ₃ CN, $v_{11}=2$
91	37 _{15,22} – 37 _{14,23} *	203222.780	23	401	160.0	138	Blend with ³⁴ SO ₂
93	35 _{3,32} – 34 _{4,31}	203290.077	6	308	195.3	161	Blend with C ₂ H ₅ OCHO, CH ₃ CN, $v_8=2$, and U-line
94	36 _{15,21} – 36 _{14,22} *	203369.755	22	390	153.7	161	Strong CH ₃ OCH ₃
96	35 _{4,32} – 34 _{4,31}	203466.519	6	308	732.0	161	Blend with CH ₃ CN, $v_8=2$ and CH ₃ OCHO
97	35 _{15,20} – 35 _{14,21} *	203502.897	22	380	147.5	161	Blend with ³⁴ SO ₂
99	35 _{3,32} – 34 _{3,31}	203552.465	6	308	732.0	161	Blend with CH ₃ CN, $v_8=2$ and H ¹³ CCCN, $v_7=1$
100	34 _{15,19} – 34 _{14,20} *	203623.068	22	370	141.2	161	Blend with CH ₃ OCH ₃
102	35 _{4,32} – 34 _{3,31}	203728.907	6	308	195.4	364	Blend with C ₂ H ₅ CN, $v_{13}=1/v_{21}=1$ and U-line
103	33 _{15,18} – 33 _{14,19} *	203731.092	21	360	135.0	364	Blend with C ₂ H ₅ CN, $v_{13}=1/v_{21}=1$ and U-line
105	34 _{20,14} – 33 _{20,13} *	203795.929	10	429	476.3	364	Strong C ₂ H ₃ CN
107	34 _{21,13} – 33 _{21,12} *	203796.393	10	443	450.5	364	Strong C ₂ H ₃ CN
109	34 _{22,12} – 33 _{22,11} *	203805.898	11	457	423.4	364	Strong C ₂ H ₃ CN
111	34 _{19,15} – 33 _{19,14} *	203805.992	10	416	500.8	364	Strong C ₂ H ₃ CN
113	34 _{23,11} – 33 _{23,10} *	203823.272	12	473	395.0	364	Blend with C ₂ H ₃ CN, ¹³ CH ₃ CH ₂ CN, and C ₂ H ₅ CN
115	32 _{15,17} – 32 _{14,18} *	203827.761	21	351	128.7	364	Blend with C ₂ H ₃ CN, ¹³ CH ₃ CH ₂ CN, and C ₂ H ₅ CN
117	34 _{18,16} – 33 _{18,15} *	203828.503	10	403	524.2	364	Blend with C ₂ H ₃ CN, ¹³ CH ₃ CH ₂ CN, and C ₂ H ₅ CN
119	14 _{9,6} – 13 _{8,5} *	203835.897	12	180	80.1	364	Blend with C ₂ H ₃ CN, ¹³ CH ₃ CH ₂ CN, and C ₂ H ₅ CN
121	34 _{24,10} – 33 _{24,9} *	203847.587	14	488	365.4	364	Blend with CH ₃ OCHO and C ₂ H ₅ OH
123	65 _{14,52} – 64 _{15,49}	203856.381	379	809	80.4	364	Blend with C ₂ H ₅ OH and CH ₃ OCHO
124	34 _{17,17} – 33 _{17,16} *	203865.981	10	392	546.2	364	Blend with CH ₃ OCHO
126	34 _{25,9} – 33 _{25,8} *	203878.090	15	505	334.5	364	Blend with CH ₃ CH ₃ CO and U-line
128	31 _{15,16} – 31 _{14,17} *	203913.834	21	342	122.4	364	Strong C ₂ H ₅ CN, $v_{13}=1/v_{21}=1$
130	34 _{26,8} – 33 _{26,7} *	203914.173	17	522	302.4	364	Strong C ₂ H ₅ CN, $v_{13}=1/v_{21}=1$
132	34 _{16,18} – 33 _{16,17} *	203921.785	10	380	567.0	364	Strong C ₂ H ₃ CN, $v_{13}=1/v_{21}=1$
134	34 _{27,7} – 33 _{27,6} *	203955.332	20	540	269.0	364	Blend with U-line
136	33 _{5,28} – 32 _{5,27}	203957.407	6	296	687.9	364	Blend with U-line
137	30 _{15,15} – 30 _{14,16} *	203990.040	20	333	116.1	364	Blend with C ₂ H ₅ CN and C ₂ H ₃ CN, $v_{11}=3$
139	34 _{15,19} – 33 _{15,18} *	204000.498	9	370	586.5	364	Strong C ₂ H ₃ CN, $v_{11}=3$ and C ₂ H ₃ CN, $v_{11}=2$
141	34 _{28,6} – 33 _{28,5} *	204001.151	22	558	234.3	364	Strong C ₂ H ₃ CN, $v_{11}=3$ and C ₂ H ₃ CN, $v_{11}=2$
143	34 _{29,5} – 33 _{29,4} *	204051.281	26	577	198.4	364	Blend with H ¹³ CCCN, $v_7=2$ and U-line
145	29 _{15,14} – 29 _{14,15} *	204057.079	20	324	109.7	364	Blend with H ¹³ CCCN, $v_7=2$ and U-line
147	64 _{6,58} – 64 _{6,59}	204063.746	316	734	27.7	364	Blend with H ¹³ CCCN, $v_7=2$ and U-line
148	64 _{6,58} – 64 _{5,59}	204064.065	316	734	201.8	364	Blend with H ¹³ CCCN, $v_7=2$ and U-line
149	34 _{30,4} – 33 _{30,3} *	204105.426	30	597	161.3	316	Blend with U-line
151	34 _{14,20} – 33 _{14,19} *	204108.522	9	360	604.7	316	Blend with U-line
153	28 _{15,13} – 28 _{14,14} *	204115.622	20	316	103.3	316	Blend with U-line
155	34 _{31,3} – 33 _{31,2} *	204163.336	36	618	122.8	316	Strong CH ₃ OCH ₃ , C ₂ H ₃ CN, $v_{11}=1$, and ¹³ CH ₂ CHCN
157	27 _{15,12} – 27 _{14,13} *	204166.316	20	308	96.9	316	Strong CH ₃ OCH ₃ , C ₂ H ₃ CN, $v_{11}=1$, and ¹³ CH ₂ CHCN
159	22 _{6,17} – 21 _{5,16}	204205.122	12	208	60.2	316	Blend with CH ₃ CH ₃ CO and U-line
160	26 _{15,11} – 26 _{14,12} *	204209.781	20	300	90.4	316	Blend with CH ₃ CH ₃ CO and U-line
162	25 _{15,10} – 25 _{14,11} *	204246.611	20	292	83.8	316	Strong SO ₂
164	34 _{13,22} – 33 _{13,21} *	204255.076	8	351	621.9	316	Strong SO ₂
166	24 _{15,9} – 24 _{14,10} *	204277.378	20	285	77.2	316	Blend with CH ₃ CH ₃ CO and U-line
168	52 _{1,51} – 52 _{0,52} *	204278.834	248	495	33.4	316	Blend with CH ₃ CH ₃ CO and U-line
170	52 _{2,51} – 52 _{1,52} *	204278.834	248	495	33.4	316	Blend with CH ₃ CH ₃ CO and U-line
172	23 _{15,8} – 23 _{14,9} *	204302.630	20	278	70.4	316	Strong C ₂ H ₅ CN
174	22 _{15,7} – 22 _{14,8} *	204322.890	20	272	63.5	316	Blend with C ₂ H ₅ CN and U-line
176	21 _{15,6} – 21 _{14,7} *	204338.662	20	265	56.5	316	Blend with C ₂ H ₅ CN, $v_{13}=1/v_{21}=1$ and U-line
178	20 _{15,5} – 20 _{14,6} *	204350.423	21	259	49.3	316	Blend with CH ₃ CH ₃ CO, $v_l=1$
180	19 _{15,4} – 19 _{14,5} *	204358.632	21	253	41.9	316	Blend with CH ₃ CH ₃ CO
182	18 _{15,3} – 18 _{14,4} *	204363.725	21	248	34.2	316	Blend with CH ₃ CH ₃ CO and C ₂ H ₅ OCHO
184	15 _{15,0} – 15 _{14,1} *	204364.340	22	233	9.2	316	Blend with CH ₃ CH ₃ CO and C ₂ H ₅ OCHO
186	17 _{15,2} – 17 _{14,3} *	204366.116	21	243	26.3	316	Blend with CH ₃ CH ₃ CO and C ₂ H ₅ OCHO
188	16 _{15,1} – 16 _{14,2} *	204366.197	22	238	18.0	316	Blend with CH ₃ CH ₃ CO and C ₂ H ₅ OCHO
190	60 _{12,49} – 59 _{13,46}	204450.542	260	701	72.3	316	Blend with CH ₃ CH ₃ CO and U-line

Table 10. continued.

N^a	Transition ^b	Frequency (MHz)	Unc. ^c (kHz)	E_l^d (K)	$S\mu^2$ (D ²)	σ^e (mK)	Comments
(1)	(2)	(3)	(4)	(5)	(6)	(7)	(8)
191	34 _{12,23} – 33 _{12,22} *	204453.939	8	343	637.5	316	Blend with CH ₃ CH ₃ CO and U-line
193	34 _{10,25} – 33 _{10,24}	205107.534	6	328	665.3	100	Strong CH ₃ OCH ₃ , C ₂ H ₅ ¹³ CN, and CH ₃ ¹³ CH ₂ CN
194	34 _{10,24} – 33 _{10,23}	205113.060	6	328	665.2	100	Strong CH ₃ OCH ₃ , C ₂ H ₅ ¹³ CN, and CH ₃ ¹³ CH ₂ CN
195	34 _{6,29} – 33 _{6,28}	205176.196	6	307	703.2	100	Blend with CH ₃ CHO and CH ₃ ¹³ CH ₂ CN
196	35 _{4,31} – 34 _{5,30}	205501.651	7	313	152.2	100	Strong CH ₃ OCHO and c-C ₂ H ₄ O
197	34 _{9,26} – 33 _{9,25}	205639.058	6	322	677.2	271	Strong CH ₃ ¹³ CH ₂ CN and C ₂ H ₅ CN
198	34 _{9,25} – 33 _{9,24}	205708.710	6	322	677.2	271	Strong C ₂ H ₅ ¹³ CN and CH ₃ OCH ₃
199	33 _{6,27} – 32 _{6,26}	205773.682	6	299	685.9	271	Blend with U-line and CH ₃ OH in absorption
200	12 _{10,2} – 11 _{9,3} *	205968.115	12	179	87.1	271	Blend with CH ₃ CH ₃ CO, $v_t=1$ and CH ₃ COOH
202	37 _{1,36} – 36 _{2,35}	206014.847	7	315	287.3	280	Strong CH ₃ OH and C ₂ H ₅ CN, $v_{13}=1/v_{21}=1$
203	37 _{2,36} – 36 _{2,35} *	206014.958	7	315	783.9	280	Strong CH ₃ OH and C ₂ H ₅ CN, $v_{13}=1/v_{21}=1$
205	37 _{2,36} – 36 _{1,35}	206015.138	7	315	287.3	280	Strong CH ₃ OH and C ₂ H ₅ CN, $v_{13}=1/v_{21}=1$
206	34 _{5,30} – 33 _{4,29}	206035.987	6	303	142.4	280	Strong C ₂ H ₅ CN, $v_{13}=1/v_{21}=1$ and C ₂ H ₅ CN
207	34 _{8,27} – 33 _{8,26}	206266.954	6	316	687.9	280	Strong C ₂ H ₅ CN, $v_{20}=1$, C ₂ H ₅ CN, and CH ₃ OCHO
208	34 _{7,28} – 33 _{7,27}	206461.559	6	312	696.8	106	Strong C ₂ H ₅ CN, $v_{13}=1/v_{21}=1$
209	34 _{8,26} – 33 _{8,25}	206887.489	6	316	687.9	106	Blend with C ₂ H ₅ CN
210	38 _{0,38} – 37 _{1,37} *	207355.545	13	318	330.6	117	Blend with ¹³ CH ₂ CHCN and CH ₃ COOH
212	38 _{0,38} – 37 _{0,37} *	207355.546	13	318	810.7	117	Blend with ¹³ CH ₂ CHCN and CH ₃ COOH
214	35 _{5,31} – 34 _{5,30}	207543.638	6	313	728.4	282	Blend with CH ₃ OCHO and U-line
215	17 _{8,10} – 16 _{7,9}	207551.813	12	188	75.2	282	Blend with U-line
216	17 _{8,9} – 16 _{7,10}	207552.401	12	188	75.2	282	Blend with U-line
217	35 _{4,31} – 34 _{4,30}	208356.853	6	313	728.8	168	Strong HC ¹³ CCN and HCC ¹³ CN
218	36 _{3,33} – 35 _{4,32}	208729.722	6	318	204.9	160	Blend with CH ₃ OCHO and U-line
219	36 _{4,33} – 35 _{4,32}	208847.713	6	318	753.3	160	Strong HC ¹³ CCN, $v_6=1$
220	36 _{3,33} – 35 _{3,32}	208906.164	6	318	753.4	160	Strong C ₂ H ₅ CN and CH ₃ OCHO
221	36 _{4,33} – 35 _{3,32}	209024.156	6	318	204.9	160	Strong C ₂ H ₅ CN and CH ₃ OCHO
222	34 _{5,29} – 33 _{5,28}	209279.146	6	306	708.3	58	Blend with NH ₂ CH ₂ CN and CH ₃ CH ₃ CO
223	34 _{7,27} – 33 _{7,26}	209670.004	6	312	698.1	45	Blend with HCC ¹³ CN, $v_7=2$ and C ₂ H ₃ CN, $v_{11}=1$
224	35 _{21,14} – 34 _{21,13} *	209787.936	10	453	479.8	45	Blend with C ₂ H ₃ CN, $v_{11}=1/v_{15}=1$
226	35 _{20,15} – 34 _{20,14} *	209790.453	10	439	504.9	45	Blend with C ₂ H ₃ CN, $v_{11}=1/v_{15}=1$
228	35 _{22,13} – 34 _{22,12} *	209795.133	11	467	453.5	45	Blend with C ₂ H ₃ CN, $v_{11}=1/v_{15}=1$
230	35 _{19,16} – 34 _{19,15} *	209804.307	10	426	528.7	45	Strong C ₂ H ₃ CN, $v_{11}=1$ and CH ₃ OCH ₃
232	15 _{9,7} – 14 _{8,6} *	209810.239	12	184	81.0	45	Strong C ₂ H ₃ CN, $v_{11}=1$ and CH ₃ OCH ₃
234	35 _{23,12} – 34 _{23,11} *	209810.767	12	482	425.9	45	Strong C ₂ H ₃ CN, $v_{11}=1$ and CH ₃ OCH ₃
236	35 _{18,17} – 34 _{18,16} *	209831.596	10	413	551.4	45	Blend with ¹³ CH ₃ CH ₂ CN
238	35 _{24,11} – 34 _{24,10} *	209833.824	13	498	397.2	45	Blend with ¹³ CH ₃ CH ₂ CN
240	35 _{25,10} – 34 _{25,9} *	209863.488	15	515	367.2	45	Strong C ₂ H ₅ OH, CH ₃ OCHO, and ¹³ CH ₃ CH ₂ CN
242	35 _{17,18} – 34 _{17,17} *	209875.072	10	401	572.9	45	Strong CH ₃ OCHO, ¹³ CH ₃ CH ₂ CN, and C ₂ H ₅ CN
244	35 _{26,9} – 34 _{26,8} *	209899.094	17	532	336.0	45	Blend with C ₂ H ₃ CN, $v_{11}=1$ and ¹³ CH ₃ CH ₂ CN
246	35 _{16,19} – 34 _{16,18} *	209938.416	10	390	593.0	45	Strong CH ₃ OCHO and SO ₂
248	35 _{27,8} – 34 _{27,7} *	209940.094	19	550	303.6	45	Strong CH ₃ OCHO and SO ₂
250	35 _{15,20} – 34 _{15,19} *	210026.654	10	380	612.0	45	Strong HC ₃ N, $v_7=1$
252	37 _{2,35} – 36 _{3,34}	210086.448	6	322	251.9	45	Blend with C ₂ H ₃ CN, $v_{11}=2$
253	37 _{3,35} – 36 _{3,34}	210090.303	6	322	779.0	45	Blend with C ₂ H ₃ CN, $v_{11}=2$
254	35 _{30,5} – 34 _{30,4} *	210091.291	29	607	198.9	45	Blend with C ₂ H ₃ CN, $v_{11}=2$
256	37 _{2,35} – 36 _{2,34}	210092.485	6	322	779.0	45	Blend with C ₂ H ₃ CN, $v_{11}=2$
257	37 _{3,35} – 36 _{2,34}	210096.339	6	322	251.9	45	Blend with C ₂ H ₃ CN, $v_{11}=2$
258	35 _{14,22} – 34 _{14,21} *	210146.825	9	370	629.7	64	Blend with ¹³ CH ₃ CH ₂ CN
260	35 _{31,4} – 34 _{31,3} *	210150.008	35	628	161.6	64	Blend with ¹³ CH ₃ CH ₂ CN
262	35 _{13,23} – 34 _{13,22} *	210309.100	9	361	646.3	64	Strong HC ₃ N, $v_6=v_7=1$ and C ₂ H ₅ CN, $v_{13}=1/v_{21}=1$
264	35 _{5,31} – 34 _{4,30}	210398.840	6	313	152.8	64	Blend with C ₂ H ₅ OH and CH ₃ OCHO
265	35 _{12,24} – 34 _{12,23} *	210528.754	8	353	661.6	64	Strong HC ₃ N, $v_7=2$ and C ₂ H ₅ OH
267	20 _{7,14} – 19 _{6,13}	210694.282	12	199	69.5	37	Blend with C ₂ H ₃ CN, $v_{11}=2$
268	35 _{11,25} – 34 _{11,24}	210829.766	7	345	675.7	37	Blend with ¹³ CH ₃ OH and NH ₂ CHO
269	35 _{11,24} – 34 _{11,23}	210830.374	7	345	675.6	37	Blend with ¹³ CH ₃ OH and NH ₂ CHO
270	20 _{7,13} – 19 _{6,14}	210837.991	12	199	69.5	37	Blend with ¹³ CH ₃ OH and NH ₂ CHO
271	35 _{6,30} – 34 _{6,29}	210871.662	6	317	724.7	37	Blend with U-line and C ₂ H ₅ OH
272	20 _{5,15} – 19 _{5,16}	210878.636	15	192	2.3	37	Blend with CH ₃ OCHO, ¹³ CH ₃ CH ₂ CN, and U-line
273	35 _{10,26} – 34 _{10,25}	211249.809	7	338	688.5	33	Strong CH ₃ OCHO
274	35 _{10,25} – 34 _{10,24}	211259.223	7	338	688.5	33	Strong CH ₃ OCHO
275	38 _{1,37} – 37 _{2,36} *	211401.390	50	325	296.5	33	Blend with C ₂ H ₅ CN and CH ₃ CH ₃ CO, $v_t=1$, uncertain baseline
277	38 _{1,37} – 37 _{1,36} *	211401.444	9	325	805.2	33	Blend with C ₂ H ₅ CN and CH ₃ CH ₃ CO, $v_t=1$, uncertain baseline
279	36 _{4,32} – 35 _{5,31}	211527.010	50	323	162.7	47	Blend with C ₂ H ₃ CN and CH ₃ OCHO
280	35 _{9,27} – 34 _{9,26}	211828.060	50	332	700.1	47	Blend with U-line, C ₂ H ₅ OCHO, and NH ₂ ¹³ CHO, $v_{12}=1$

Table 10. continued.

N^a	Transition ^b	Frequency (MHz)	Unc. ^c (kHz)	E_l^d (K)	$S\mu^2$ (D ²)	σ^e (mK)	Comments
(1)	(2)	(3)	(4)	(5)	(6)	(7)	(8)
281	35 _{9,26} – 34 _{9,25}	211938.010	50	332	700.1	36	Strong NH ₂ ¹³ CHO and NH ₂ ¹³ CHO, $v_{12}=1$
282	13 _{10,3} – 12 _{9,4} *	211955.981	12	182	87.6	36	Strong NH ₂ ¹³ CHO, $v_{12}=1$ and NH ₂ ¹³ CHO
284	34 _{6,28} – 33 _{6,27}	212120.060	50	309	708.0	36	Strong CH ₃ CHO and NH ₂ ¹³ CHO
285	35 _{8,28} – 34 _{8,27}	212458.290	50	326	710.4	99	Blend with C ₂ H ₃ CN and C ₂ H ₅ OH
286	35 _{7,29} – 34 _{7,28}	212483.750	50	321	719.0	99	Blend with CH ₃ OCHO, a-C ₃ H ₇ CN, and ¹³ CH ₃ OH, $v_7=1$
287	39 _{1,39} – 38 _{1,38} *	212743.017	15	328	832.1	99	Strong CH ₃ OCH ₃ and C ₂ H ₅ OH
289	39 _{1,39} – 38 _{0,38} *	212743.018	15	328	339.8	99	Strong CH ₃ OCH ₃ and C ₂ H ₅ OH
291	36 _{5,32} – 35 _{5,31}	212972.357	6	323	749.7	99	Blend with ¹³ CH ₃ CH ₂ CN and ³⁴ SO ₂
292	35 _{8,27} – 34 _{8,26}	213353.646	6	326	710.6	48	Blend with ¹³ CH ₃ CHCN, C ₂ H ₅ CN, and U-line
293	18 _{8,11} – 17 _{7,10}	213473.443	12	193	76.1	48	Blend with C ₂ H ₅ ¹³ CN
294	50 _{11,40} – 50 _{9,41}	213474.581	160	532	6.1	48	Blend with C ₂ H ₅ ¹³ CN
295	18 _{8,10} – 17 _{7,11}	213474.845	12	193	76.1	48	Blend with C ₂ H ₅ ¹³ CN
296	36 _{4,32} – 35 _{4,31}	213568.985	6	323	749.9	48	Blend with C ₂ H ₃ CN, $v_{11}=1/v_{15}=1$ and ¹³ CH ₂ CHCN
297	11 _{11,0} – 10 _{10,1} *	214056.089	12	182	95.9	48	Strong ¹³ CH ₃ CN, C ₂ H ₅ ¹³ CN, and CH ₃ ¹³ CH ₂ CN
299	37 _{3,34} – 36 _{4,33}	214147.290	50	328	214.4	75	Strong C ₂ H ₅ ¹³ CN and CH ₃ ¹³ CH ₂ CN
300	37 _{4,34} – 36 _{4,33}	214225.810	50	328	774.6	75	Strong CH ₂ NH, ¹³ CH ₃ CN, and C ₂ H ₅ CN
301	37 _{3,34} – 36 _{3,33}	214265.300	50	328	774.6	75	Strong C ₂ H ₅ CN and C ₂ H ₅ OH
302	37 _{4,34} – 36 _{3,33}	214343.817	6	328	214.4	75	Strong ¹³ CH ₃ CN and C ₂ H ₅ ¹³ CN
303	35 _{5,30} – 34 _{5,29}	214468.257	6	316	728.6	75	Blend with CH ₃ OCH ₃
304	51 _{16,35} – 51 _{15,36}	214470.968	53	591	243.9	75	Blend with CH ₃ OCH ₃
305	51 _{16,36} – 51 _{15,37}	214471.118	53	591	243.9	75	Blend with CH ₃ OCH ₃
306	36 _{5,32} – 35 _{4,31}	215014.344	6	323	163.1	74	Blend with ¹³ CH ₃ CN, $v_8=1$
307	38 _{2,36} – 37 _{3,35}	215469.850	50	332	261.1	74	Strong C ₂ H ₅ CN, $v_{13}=1/v_{21}=1$
308	38 _{3,36} – 37 _{3,35}	215472.342	7	332	800.3	74	Strong C ₂ H ₅ CN, $v_{13}=1/v_{21}=1$
309	38 _{2,36} – 37 _{2,35}	215473.742	7	332	800.3	74	Strong C ₂ H ₅ CN, $v_{13}=1/v_{21}=1$
310	38 _{3,36} – 37 _{2,35}	215476.230	50	332	261.1	74	Strong C ₂ H ₅ CN, $v_{13}=1/v_{21}=1$
311	21 _{5,16} – 20 _{3,17}	215480.099	15	198	2.7	74	Strong C ₂ H ₅ CN, $v_{13}=1/v_{21}=1$
312	16 _{9,8} – 15 _{8,7} *	215778.326	12	189	82.0	74	Blend with C ₂ H ₅ CN, $v_{20}=1$
314	36 _{21,15} – 35 _{21,14} *	215779.220	50	463	508.7	74	Blend with C ₂ H ₅ CN, $v_{20}=1$
316	36 _{22,14} – 35 _{22,13} *	215783.850	50	477	483.1	74	Blend with C ₂ H ₅ CN, $v_{20}=1$
318	36 _{20,16} – 35 _{20,15} *	215784.950	50	449	533.2	74	Blend with C ₂ H ₅ CN, $v_{20}=1$
320	36 _{23,13} – 35 _{23,12} *	215797.530	50	492	456.3	74	Blend with C ₂ H ₅ CN, $v_{13}=1/v_{21}=1$
322	36 _{19,17} – 35 _{19,16} *	215802.872	10	436	556.3	74	Blend with C ₂ H ₅ CN, $v_{13}=1/v_{21}=1$
324	36 _{24,12} – 35 _{24,11} *	215819.220	50	508	428.4	55	Strong C ₂ H ₅ CN, $v_{13}=1/v_{21}=1$
326	36 _{18,18} – 35 _{18,17} *	215835.300	50	423	578.4	55	Strong C ₂ H ₅ CN, $v_{13}=1/v_{21}=1$ and ³⁴ SO
328	36 _{25,11} – 35 _{25,10} *	215847.810	50	525	399.2	55	Strong ³⁴ SO
330	36 _{26,10} – 35 _{26,9} *	215882.850	50	542	368.9	55	Strong ¹³ CH ₃ OH
332	36 _{17,19} – 35 _{17,18} *	215885.180	50	411	599.1	55	Strong ¹³ CH ₃ OH and C ₂ H ₅ OH
334	36 _{27,9} – 35 _{27,8} *	215923.600	50	560	337.4	55	Blend with C ₂ H ₅ OH, CH ₃ COOH, and U-line
336	36 _{16,20} – 35 _{16,19} *	215956.570	50	400	618.7	55	Strong C ₂ H ₅ CN
338	36 _{15,21} – 35 _{15,20} *	216055.006	10	390	637.2	55	Strong C ₂ H ₅ CN, $v_{13}=1/v_{21}=1$
340	36 _{14,22} – 35 _{14,21} *	216188.170	50	380	654.5	55	Blend with C ₂ H ₅ CN
342	36 _{32,4} – 35 _{32,3} *	216198.450	50	659	161.8	55	Blend with CH ₃ OCHO
344	36 _{13,23} – 35 _{13,22} *	216367.230	50	371	670.6	55	Strong CH ₃ OCHO and ¹³ CH ₃ OH
346	21 _{7,15} – 20 _{6,14}	216386.644	12	205	70.1	55	Blend with U-line
347	35 _{7,28} – 34 _{7,27}	216489.383	6	322	720.8	55	Blend with C ₂ H ₅ CN, $v_{13}=1/v_{21}=1$ and U-line
348	36 _{6,31} – 35 _{6,30}	216511.289	7	327	746.2	55	Strong CH ₃ CH ₂ CO, $v_7=1$ and C ₂ H ₅ CN, $v_{13}=1/v_{21}=1$
349	36 _{12,24} – 35 _{12,23} *	216609.170	50	363	685.5	55	Blend with CH ₃ COOH
351	21 _{7,14} – 20 _{6,15}	216649.055	12	205	70.1	55	Strong SO ₂
352	39 _{1,38} – 38 _{2,37} *	216786.652	10	335	305.7	50	Blend with U-line and CH ₃ CH ₂ CO, $v_7=1$
354	39 _{1,38} – 38 _{1,37} *	216786.721	10	335	826.7	50	Blend with U-line and CH ₃ CH ₂ CO, $v_7=1$
356	42 _{16,26} – 42 _{15,27} *	216853.893	37	469	186.2	50	Strong C ₂ H ₅ CN, $v_{13}=1/v_{21}=1$
358	36 _{11,26} – 35 _{11,25}	216940.590	50	355	699.1	50	Strong C ₂ H ₅ CN and CH ₃ OH
359	36 _{11,25} – 35 _{11,24}	216941.740	50	355	699.1	50	Strong C ₂ H ₅ CN and CH ₃ OH
360	41 _{16,25} – 41 _{15,26} *	217028.389	36	456	179.9	50	Blend with CH ₃ CH ₂ CO and ¹³ CN in absorption
362	40 _{16,24} – 40 _{15,25} *	217188.266	36	445	173.6	50	Strong CH ₃ OCH ₃
364	39 _{16,23} – 39 _{15,24} *	217334.340	35	433	167.4	50	Blend with CH ₂ ¹³ CHCN
366	37 _{4,33} – 36 _{5,32}	217368.200	8	333	173.0	50	Blend with ¹³ CN in absorption, C ₂ H ₅ ¹³ CN, and U-line?
367	36 _{10,27} – 35 _{10,26}	217402.380	50	348	711.7	50	Strong HC ¹³ CCN and ¹³ CH ₃ OH
368	36 _{10,26} – 35 _{10,25}	217418.120	50	348	711.6	50	Strong HCC ¹³ CN
369	38 _{16,22} – 38 _{15,23} *	217467.396	35	422	161.1	50	Blend with ¹³ CN in absorption
371	37 _{16,21} – 37 _{15,22} *	217588.187	34	411	154.8	50	Blend with (CH ₂ OH) ₂ and U-line
373	36 _{16,20} – 36 _{15,21} *	217697.439	34	400	148.6	50	Blend with CH ₂ CH ¹³ CN and U-line

Table 10. continued.

N^a	Transition ^b	Frequency (MHz)	Unc. ^c (kHz)	E_l^d (K)	$S\mu^2$ (D ²)	σ^e (mK)	Comments
(1)	(2)	(3)	(4)	(5)	(6)	(7)	(8)
375	39 _{8,31} – 39 _{5,34}	219371.585	37	370	11.6	92	Blend with C ₂ H ₃ CN, $v_{11}=1/v_{15}=1$
376	19 _{8,12} – 18 _{7,11}	219376.897	12	198	77.1	92	Blend with C ₂ H ₃ CN, $v_{11}=1/v_{15}=1$ and C ₂ H ₅ OH
377	19 _{8,11} – 18 _{7,12}	219380.063	12	198	77.1	92	Blend with C ₂ H ₃ CN, $v_{11}=1/v_{15}=1$ and C ₂ H ₅ OH
378	38 _{3,35} – 37 _{4,34}	219549.670	50	338	223.9	92	Strong C ¹⁸ O
379	36 _{5,31} – 35 _{5,30}	219565.844	7	327	748.9	92	Strong C ¹⁸ O
380	38 _{4,35} – 37 _{4,34}	219601.640	50	338	796.0	92	Blend with CH ₃ CN, $v_4=1$ and NH ₂ CN
381	38 _{3,35} – 37 _{3,34}	219628.210	50	338	796.0	92	Strong C ₂ H ₅ CN, $v_{20}=1$ and CH ₃ CN, $v_4=1$
382	58 _{2,56} – 58 _{1,57} *	219628.923	369	593	66.8	92	Strong C ₂ H ₅ CN, $v_{20}=1$ and CH ₃ CN, $v_4=1$
384	58 _{3,56} – 58 _{2,57} *	219628.923	369	593	66.8	92	Strong C ₂ H ₅ CN, $v_{20}=1$ and CH ₃ CN, $v_4=1$
386	63 _{11,53} – 62 _{12,50}	219678.339	347	748	53.1	92	Strong HC ₃ N, $v_7=2$
387	38 _{4,35} – 37 _{3,34}	219680.190	7	338	223.9	92	Strong HC ₃ N, $v_7=2$
388	13 _{11,2} – 12 _{10,3} *	226038.817	12	189	96.1	278	Blend with c-C ₂ H ₄ O
390	40 _{2,38} – 39 _{3,37}	226232.383	9	353	279.7	278	Noisy, blend with U-line?
391	40 _{3,38} – 39 _{3,37}	226233.371	9	353	843.2	278	Noisy, blend with U-line?
392	40 _{2,38} – 39 _{2,37}	226233.942	9	353	843.2	278	Noisy, blend with U-line?
393	40 _{3,38} – 39 _{2,37}	226234.930	9	353	279.6	278	Noisy, blend with U-line?
394	59 _{17,42} – 59 _{16,43}	226530.302	99	729	290.8	278	Blend with C ₂ H ₅ CN
395	59 _{17,43} – 59 _{16,44}	226530.999	99	729	290.8	278	Blend with C ₂ H ₅ CN
396	37 _{8,29} – 36 _{8,28}	226531.433	7	347	755.6	278	Blend with C ₂ H ₅ CN
397	62 _{3,59} – 62 _{3,60} *	226531.914	447	668	15.8	278	Blend with C ₂ H ₅ CN
399	62 _{4,59} – 62 _{3,60} *	226531.915	447	668	100.4	278	Blend with C ₂ H ₅ CN
401	23 _{7,17} – 22 _{6,16}	227460.224	12	218	70.9	85	Blend with CH ₃ COOH, CH ₂ (OH)CHO, and CH ₂ CH ¹³ CN
402	41 _{1,40} – 40 _{2,39} *	227553.664	14	357	324.0	85	Strong C ₂ H ₅ CN and CH ₃ OCHO
404	41 _{1,40} – 40 _{1,39} *	227553.690	14	357	869.6	85	Strong C ₂ H ₅ CN and CH ₃ OCHO
406	60 _{2,58} – 60 _{1,59} *	227625.680	458	624	66.9	85	Strong C ₂ H ₅ CN, $v_{13}=1/v_{21}=1$
408	60 _{2,58} – 60 _{2,59} *	227625.680	458	624	10.9	85	Strong C ₂ H ₅ CN, $v_{13}=1/v_{21}=1$
410	38 _{6,33} – 37 _{6,32}	227639.839	9	348	788.8	85	Strong C ₂ H ₅ CN, $v_{13}=1/v_{21}=1$ and CH ₃ OCHO
411	18 _{9,10} – 17 _{8,9} *	227689.981	12	198	84.0	85	Blend with U-line
413	23 _{5,18} – 22 _{3,19}	227691.505	14	210	3.5	85	Blend with U-line
414	38 _{22,16} – 37 _{22,15} *	227759.604	11	498	541.1	85	Blend with H ₂ ¹³ CS and C ₂ H ₅ OH
416	38 _{21,17} – 37 _{21,16} *	227760.667	11	484	565.4	85	Blend with H ₂ ¹³ CS and C ₂ H ₅ OH
418	38 _{23,15} – 37 _{23,14} *	227768.859	12	513	515.7	85	Strong C ₂ H ₅ CN
420	38 _{20,18} – 37 _{20,17} *	227773.682	11	470	588.4	85	Strong C ₂ H ₅ CN
422	38 _{24,14} – 37 _{24,13} *	227787.136	12	529	489.3	85	Strong C ₂ H ₅ CN and HC ₃ N, $v_6=1$
424	38 _{19,19} – 37 _{19,18} *	227800.733	11	457	610.4	85	Strong ¹³ CH ₃ CH ₂ CN and CH ₃ OH
426	38 _{25,13} – 37 _{25,12} *	227813.392	14	546	461.7	85	Strong CH ₃ OH
428	56 _{17,39} – 56 _{16,40}	227818.866	80	679	270.6	85	Strong CH ₃ OH
429	56 _{17,40} – 56 _{16,41}	227819.010	80	679	270.6	85	Strong CH ₃ OH
430	38 _{18,20} – 37 _{18,19} *	227844.521	11	444	631.3	85	Blend with CH ₃ CH ₃ CO, HC ¹³ CCN, $v_7=2$, and HCC ¹³ CN, $v_7=2$
432	38 _{26,12} – 37 _{26,11} *	227846.781	15	563	432.9	85	Blend with CH ₃ CH ₃ CO, HC ¹³ CCN, $v_7=2$, and HCC ¹³ CN, $v_7=2$
434	38 _{27,11} – 37 _{27,10} *	227886.609	17	581	403.0	85	Strong C ₂ H ₅ OH
436	38 _{17,21} – 37 _{17,20} *	227908.603	11	432	651.0	85	Strong CH ₃ ¹³ CH ₂ CN and C ₂ H ₃ CN
438	44 _{17,27} – 44 _{16,28} *	231002.504	54	504	193.5	183	Noisy
440	21 _{8,14} – 20 _{7,13}	231114.753	12	210	78.8	183	Blend with C ₂ H ₃ CN, $v_{11}=1$, CH ₃ CHO, and U-line
441	21 _{8,13} – 20 _{7,14}	231128.746	12	210	78.8	183	Blend with U-line and H ₂ ¹³ CS
442	43 _{17,26} – 43 _{16,27} *	231159.401	54	491	187.2	183	Strong ¹³ CH ₂ CHCN
444	42 _{17,25} – 42 _{16,26} *	231303.368	53	479	180.9	40	Strong ¹³ CH ₃ CH ₂ CN and C ₂ H ₅ CN
446	41 _{17,24} – 41 _{16,25} *	231435.094	53	467	174.7	40	Blend with ¹³ CH ₂ CHCN
448	40 _{17,23} – 40 _{16,24} *	231555.240	53	455	168.4	40	Blend with C ₂ H ₅ OH
450	41 _{2,39} – 40 _{3,38}	231611.663	10	364	288.9	40	Blend with HNCO, $v_5=1$, CH ₃ OCHO, ¹³ CH ₃ CN, and U-line
451	41 _{3,39} – 40 _{3,38}	231612.288	10	364	864.4	40	Blend with HNCO, $v_5=1$, CH ₃ OCHO, ¹³ CH ₃ CN, and U-line
452	41 _{2,39} – 40 _{2,38}	231612.651	10	364	864.6	40	Blend with HNCO, $v_5=1$, CH ₃ OCHO, ¹³ CH ₃ CN, and U-line
453	41 _{3,39} – 40 _{2,38}	231613.276	10	364	288.9	40	Blend with HNCO, $v_5=1$, CH ₃ OCHO, ¹³ CH ₃ CN, and U-line
454	61 _{2,59} – 61 _{1,60} *	231619.484	508	640	66.9	40	Blend with CH ₃ OCHO, ¹³ CH ₃ CN, and U-line
456	61 _{3,59} – 61 _{2,60} *	231619.484	508	640	66.9	40	Blend with CH ₃ OCHO, ¹³ CH ₃ CN, and U-line
458	58 _{11,47} – 57 _{12,46}	231619.899	325	659	71.0	40	Blend with CH ₃ OCHO, ¹³ CH ₃ CN, and U-line
459	39 _{17,22} – 39 _{16,23} *	231664.446	53	444	162.2	40	Blend with ¹³ CH ₃ CH ₂ CN and C ₂ H ₅ OH
461	37 _{6,32} – 36 _{5,31}	232675.249	9	337	125.2	19	Blend with CH ₃ CH ₃ CO, $v_l=1$ and U-line
462	24 _{7,18} – 23 _{6,17}	232766.448	12	224	71.1	19	Blend with ¹³ CH ₃ CN, $v_8=1$ and CH ₃ CH ₃ CO
463	40 _{5,36} – 39 _{4,35}	235023.563	9	365	203.0	131	Blend with CH ₃ OCHO
464	39 _{11,29} – 38 _{11,28}	235323.229	8	387	768.9	131	Blend with CH ₃ CHO and U-line
465	23 _{4,19} – 22 _{3,20}	235326.210	10	208	11.1	131	Blend with CH ₃ CHO and U-line
466	39 _{11,28} – 38 _{11,27}	235328.787	8	387	769.0	131	Blend with CH ₃ CHO and U-line

Table 10. continued.

N^a	Transition ^b	Frequency (MHz)	Unc. ^c (kHz)	E_l^d (K)	$S\mu^2$ (D ²)	σ^e (mK)	Comments
(1)	(2)	(3)	(4)	(5)	(6)	(7)	(8)
467	40 _{5,35} – 39 _{6,34}	235342.332	14	370	156.8	131	Blend with U-line and CH ₃ CH ₃ CO
468	62 _{2,60} – 62 _{1,61} *	235610.226	562	656	67.0	131	Blend with CH ₃ CH ₃ CO, ¹³ CH ₃ OH, $v_t=1$, and C ₂ H ₅ CN, $v_{13}=1/v_{21}=1$
470	62 _{2,60} – 62 _{2,61} *	235610.226	562	656	10.9	131	Blend with CH ₃ CH ₃ CO, ¹³ CH ₃ OH, $v_t=1$, and C ₂ H ₅ CN, $v_{13}=1/v_{21}=1$
472	38 _{6,32} – 37 _{6,31}	235612.906	10	351	792.6	131	Blend with CH ₃ CH ₃ CO, ¹³ CH ₃ OH, $v_t=1$, and C ₂ H ₅ CN, $v_{13}=1/v_{21}=1$
473	38 _{6,33} – 37 _{5,32}	235699.420	8	348	136.0	131	Blend with CH ₃ OCH ₃ , uncertain baseline
474	41 _{3,38} – 40 _{4,37}	235705.579	10	370	252.1	131	Blend with CH ₃ OCH ₃ , uncertain baseline
475	41 _{4,38} – 40 _{4,37}	235720.329	10	370	860.1	131	Blend with CH ₃ OCH ₃ , uncertain baseline
476	41 _{3,38} – 40 _{3,37}	235728.110	10	370	860.0	131	Blend with U-line, uncertain baseline
477	67 _{13,55} – 66 _{14,52}	235732.617	481	838	79.3	131	Blend with U-line, uncertain baseline
478	41 _{4,38} – 40 _{3,37}	235742.860	10	370	252.1	131	Baseline problem, or absorption line?
479	17 _{10,8} – 16 _{9,7} *	235876.754	12	199	90.8	131	Strong CH ₃ OCHO, C ₂ H ₅ CN, $v_{13}=1/v_{21}=1$, and ¹³ CH ₃ OH
481	39 _{10,30} – 38 _{10,29}	235923.054	8	380	780.4	131	Blend with CH ₃ OCHO
482	39 _{10,29} – 38 _{10,28}	235988.744	8	380	780.5	131	Strong C ₂ H ₅ OH and ¹³ CH ₃ OH
483	68 _{4,64} – 68 _{3,65} *	240990.966	671	784	134.4	216	Strong CH ₃ OCH ₃ , C ₂ H ₅ ¹³ CN, and CH ₃ CH ₃ CO
485	68 _{5,64} – 68 _{4,65} *	240990.969	671	784	134.4	216	Strong CH ₃ OCH ₃ , C ₂ H ₅ ¹³ CN, and CH ₃ CH ₃ CO
487	40 _{12,29} – 39 _{12,28}	240992.017	9	406	779.7	216	Strong CH ₃ OCH ₃ , C ₂ H ₅ ¹³ CN, and CH ₃ CH ₃ CO
488	40 _{12,28} – 39 _{12,27}	240992.663	9	406	779.7	216	Strong CH ₃ OCH ₃ , C ₂ H ₅ ¹³ CN, and CH ₃ CH ₃ CO
489	39 _{6,33} – 38 _{6,32}	241002.693	11	363	812.9	216	Strong C ₂ H ₅ ¹³ CN, CH ₃ CH ₃ CO, and C ³⁴ S
490	42 _{3,39} – 41 _{4,38}	241081.365	11	382	261.4	216	Blend with CH ₃ ¹³ CH ₂ CN and U-line
491	42 _{4,39} – 41 _{4,38}	241090.991	11	382	881.3	216	Blend with CH ₃ ¹³ CH ₂ CN and U-line
492	42 _{3,39} – 41 _{3,38}	241096.116	11	382	881.3	216	Blend with CH ₃ ¹³ CH ₂ CN and U-line
493	42 _{4,39} – 41 _{3,38}	241105.742	11	382	261.4	216	Blend with U-line and C ₂ H ₅ CN
494	16 _{11,5} – 15 _{10,6} *	244001.794	12	201	97.9	46	Blend with C ₂ H ₅ OH
496	41 _{6,36} – 40 _{6,35}	244037.948	12	382	852.7	46	Strong H ₂ CS
497	41 _{5,36} – 40 _{5,35}	244944.066	12	382	853.1	39	Strong CS
498	45 _{0,45} – 44 _{1,44} *	245041.483	39	394	394.8	39	Blend with C ₂ H ₅ CN and C ₂ H ₅ ¹³ CN
500	45 _{1,45} – 44 _{1,44} *	245041.483	39	394	960.6	39	Blend with C ₂ H ₅ CN and C ₂ H ₅ ¹³ CN
502	42 _{4,38} – 41 _{5,37}	245115.653	12	388	222.4	72	Strong CH ₂ NH
503	42 _{5,38} – 41 _{5,37}	245270.702	12	388	877.3	72	Strong HC ₃ N, $v_4=1$ and C ₂ H ₅ ¹³ CN
504	45 _{18,27} – 45 _{17,28} *	245277.970	79	528	194.5	72	Strong C ₂ H ₅ ¹³ CN
506	42 _{4,38} – 41 _{4,37}	245344.019	12	388	877.3	72	Strong SO ₂ and CH ₃ CH ₃ CO
507	44 _{18,26} – 44 _{17,27} *	245407.219	79	515	188.3	72	Blend with CH ₃ CH ₃ CO
509	21 _{9,13} – 20 _{8,12}	245470.669	12	215	86.9	72	Strong C ₂ H ₅ CN, $v_{13}=1/v_{21}=1$ and C ₂ H ₃ CN, $v_{11}=1$
510	21 _{9,12} – 20 _{8,13}	245471.188	12	215	86.9	72	Strong C ₂ H ₅ CN, $v_{13}=1/v_{21}=1$ and C ₂ H ₃ CN, $v_{11}=1$
511	86 _{10,76} – 86 _{9,77}	245475.958	1519	1239	344.4	72	Strong C ₂ H ₅ CN, $v_{13}=1/v_{21}=1$ and C ₂ H ₃ CN, $v_{11}=1$
512	42 _{5,38} – 41 _{4,37}	245499.068	12	388	222.4	72	Strong HC ¹³ CCN, $v_7=1$
513	43 _{18,25} – 43 _{17,26} *	245525.550	78	502	182.0	72	Strong HCC ¹³ CN, $v_7=1$
515	42 _{18,24} – 42 _{17,25} *	245633.528	78	490	175.7	53	Blend with CH ₂ ¹³ CHCN and C ₂ H ₃ CN, $v_{15}=2$
517	77 _{7,70} – 77 _{7,71} *	245718.043	974	998	32.3	53	Blend with CH ₂ ¹³ CHCN and HNCO, $v_5=1$
519	77 _{8,70} – 77 _{7,71} *	245718.533	974	998	237.4	53	Blend with CH ₂ ¹³ CHCN and HNCO, $v_5=1$
521	41 _{22,19} – 40 _{22,18} *	245718.666	11	532	625.3	53	Blend with CH ₂ ¹³ CHCN and HNCO, $v_5=1$
523	41 _{23,18} – 40 _{23,17} *	245719.705	12	547	601.8	53	Blend with CH ₂ ¹³ CHCN and HNCO, $v_5=1$
525	41 _{21,20} – 40 _{21,19} *	245730.112	12	517	647.8	53	Blend with HNCO, $v_5=1$
527	41 _{24,17} – 40 _{24,16} *	245731.600	12	563	577.2	53	Blend with HNCO, $v_5=1$
529	41 _{18,23} – 41 _{17,24} *	245731.700	78	478	169.5	53	Blend with HNCO, $v_5=1$
531	42 _{8,34} – 42 _{5,37}	245748.107	35	405	8.6	53	Strong CH ₂ ¹³ CHCN and CH ₃ OCHO
532	41 _{25,16} – 40 _{25,15} *	245753.043	13	579	551.6	53	Strong CH ₂ ¹³ CHCN, CH ₃ OCHO, and HC ₃ N, $v_5=1/v_7=3$
534	41 _{20,21} – 40 _{20,20} *	245756.100	12	504	669.2	53	Strong CH ₃ OCHO and HC ₃ N, $v_5=1/v_7=3$
536	41 _{26,15} – 40 _{26,14} *	245782.976	14	597	525.1	53	Strong CH ₂ ¹³ CHCN and C ₂ H ₅ CN, $v_{13}=1/v_{21}=1$
538	41 _{19,22} – 40 _{19,21} *	245799.265	12	490	689.7	53	Blend with CH ₂ CH ¹³ CN
540	48 _{8,40} – 47 _{9,39}	245812.073	103	487	81.9	53	Strong CH ₂ CH ¹³ CN and CH ₂ ¹³ CHCN
541	41 _{27,14} – 40 _{27,13} *	245820.530	15	614	497.4	53	Strong CH ₂ CH ¹³ CN and CH ₂ ¹³ CHCN
543	40 _{18,22} – 40 _{17,23} *	245820.595	78	466	163.2	53	Strong CH ₂ CH ¹³ CN and CH ₂ ¹³ CHCN
545	41 _{18,23} – 40 _{18,22} *	245863.030	12	478	708.9	53	Blend with CH ₂ CH ¹³ CN
547	41 _{28,13} – 40 _{28,12} *	245864.987	16	633	468.6	53	Blend with CH ₂ CH ¹³ CN
549	39 _{18,21} – 39 _{17,22} *	245900.727	78	455	157.0	53	Strong CH ₃ OCHO and CH ₂ CH ¹³ CN
551	41 _{29,12} – 40 _{29,11} *	245915.751	17	652	438.9	53	Strong CH ₂ CH ¹³ CN and CH ₂ ¹³ CHCN
553	26 _{7,19} – 25 _{6,20}	245927.818	12	239	70.3	53	Blend with CH ₂ CH ¹³ CN
554	41 _{17,24} – 40 _{17,23} *	245951.925	12	466	727.2	53	Blend with CH ₃ CH ₃ CO, $v_t=1$

Table 10. continued.

N^a	Transition ^b	Frequency (MHz)	Unc. ^c (kHz)	E_l^d (K)	$S\mu^2$ (D ²)	σ^e (mK)	Comments
(1)	(2)	(3)	(4)	(5)	(6)	(7)	(8)
556	41 _{30,11} – 40 _{30,10} *	245972.316	19	672	408.0	53	Blend with C ₂ H ₅ CN, $v_{13}=1/v_{21}=1$ and $v=0$, and U-line
558	38 _{18,20} – 38 _{17,21} *	245972.593	78	443	150.7	53	Blend with C ₂ H ₅ CN, $v_{13}=1/v_{21}=1$ and $v=0$, and U-line
560	41 _{31,10} – 40 _{31,9} *	246034.256	22	692	376.2	53	Blend with C ₂ H ₅ CN, $v_{13}=1/v_{21}=1$ and CH ₃ OCHO
562	37 _{18,19} – 37 _{17,20} *	246036.674	78	432	144.4	53	Blend with C ₂ H ₅ CN, $v_{13}=1/v_{21}=1$ and CH ₃ OCHO
564	27 _{7,21} – 26 _{6,20}	247058.498	12	246	70.8	68	Strong CH ₃ OCHO
565	63 _{12,51} – 62 _{13,50}	247101.751	518	754	76.5	68	Blend with C ₂ H ₅ CN and HC ₃ N, $v_7=2$
566	41 _{12,30} – 40 _{12,29}	247104.436	10	418	803.0	68	Blend with C ₂ H ₅ CN and HC ₃ N, $v_7=2$
567	41 _{12,29} – 40 _{12,28}	247105.557	10	418	803.0	68	Blend with C ₂ H ₅ CN and HC ₃ N, $v_7=2$
568	41 _{6,36} – 40 _{5,35}	247299.045	10	382	168.3	68	Blend with C ₂ H ₅ CN, $v_{15}=1$
569	41 _{7,35} – 40 _{7,34}	247432.588	13	387	849.3	68	Blend with C ₂ H ₅ OCHO, t-HCOOH, and ³⁴ SO ₂
570	42 _{17,25} – 41 _{17,24} *	251968.635	13	478	752.3	42	Blend with CH ₃ OCH ₃
572	27 _{7,20} – 26 _{6,21}	252059.917	12	246	69.6	42	Blend with CH ₃ ¹³ CH ₂ CN, C ₂ H ₅ CN, $v_{20}=1$, a-C ₃ H ₇ CN, and U-line
573	42 _{32,10} – 41 _{32,9} *	252075.949	25	725	377.4	42	Blend with a-C ₃ H ₇ CN and t-HCOOH
575	15 _{12,3} – 14 _{11,4} *	252090.157	12	204	105.6	42	Strong t-HCOOH and CH ₃ OH
577	42 _{16,27} – 41 _{16,26} *	252100.361	12	467	769.0	42	Strong CH ₃ OH and C ₂ H ₅ CN, $v_{13}=1/v_{21}=1$
579	42 _{15,28} – 41 _{15,27} *	252274.857	12	456	784.8	42	Strong C ₂ H ₅ CN, $v_{13}=1/v_{21}=1$
581	64 _{1,63} – 64 _{0,64} *	252277.352	860	678	33.6	42	Strong C ₂ H ₅ CN, $v_{13}=1/v_{21}=1$
583	64 _{1,63} – 64 _{1,64} *	252277.352	860	678	5.7	42	Strong C ₂ H ₅ CN, $v_{13}=1/v_{21}=1$
585	25 _{8,18} – 24 _{7,17}	254150.394	12	236	81.3	32	Blend with CH ₃ CH ₃ CO and U-line
586	13 _{13,0} – 12 _{12,1} *	254156.954	13	204	114.2	32	Blend with CH ₃ CH ₃ CO and U-line
588	25 _{8,17} – 24 _{7,18}	254324.253	12	236	81.3	32	Strong ¹³ CH ₃ OH
589	42 _{9,34} – 41 _{9,33}	255230.622	14	409	858.3	217	Strong C ₂ H ₅ CN, $v_{20}=1$ and NH ₂ CHO
590	43 _{5,38} – 42 _{5,37}	255329.346	15	405	895.6	217	Strong C ₂ H ₅ CN, $v_{13}=1/v_{21}=1$ and HC ₃ N, $v_7=1$
591	41 _{7,34} – 40 _{7,33}	255562.496	16	389	855.2	217	Strong SO ₂ and CH ₂ CH ¹³ CN
592	46 _{7,39} – 45 _{8,38}	257971.741	60	454	112.3	1127	Strong t-HCOOH and CH ₃ CN, $v_8=1$
593	43 _{31,12} – 42 _{31,11} *	257980.769	18	716	442.3	1127	Strong t-HCOOH and CH ₃ CN, $v_8=1$
595	43 _{17,26} – 42 _{17,25} *	257986.516	13	490	777.1	1127	Strong t-HCOOH and CH ₃ CN, $v_8=1$
597	55 _{19,36} – 55 _{18,37} *	258045.723	118	685	252.3	1127	Strong CH ₃ CN, $v_8=1$
599	43 _{32,11} – 42 _{32,10} *	258048.624	22	737	410.9	1127	Strong CH ₃ CN, $v_8=1$
601	16 _{12,4} – 15 _{11,5} *	258080.161	12	208	106.2	1127	Strong CH ₃ OCHO, CH ₃ ¹³ CN, $v_8=1$, and NH ₂ CN
603	43 _{33,10} – 42 _{33,9} *	258121.617	31	759	378.5	1127	Strong CH ₃ CN, $v_8=1$ and CH ₃ OCHO
605	43 _{16,28} – 42 _{16,27} *	258130.483	13	479	793.5	1127	Strong CH ₃ OCHO and CH ₃ CN, $v_8=1$
607	43 _{15,29} – 42 _{15,28} *	258320.451	13	469	809.0	1127	Strong CH ₃ CN, $v_8=1$
609	43 _{13,31} – 42 _{13,30}	258903.344	12	450	836.8	1609	Noisy, blend with ¹³ CH ₂ CHCN
610	43 _{13,30} – 42 _{13,29}	258903.558	12	450	836.8	1609	Noisy, blend with ¹³ CH ₂ CHCN
611	43 _{11,32} – 42 _{11,31}	260000.636	13	434	860.9	413	Strong CH ₃ OCH ₃ and CH ₂ ¹³ CHCN
612	40 _{19,21} – 40 _{18,22} *	260004.028	112	478	158.0	413	Strong CH ₃ OCH ₃ and CH ₂ ¹³ CHCN
614	26 _{8,18} – 25 _{7,19}	260060.358	12	243	81.7	413	Strong C ₂ H ₅ CN, $v_{20}=1$ and CH ₃ OH
615	39 _{19,20} – 39 _{18,21} *	260060.729	112	466	151.7	413	Strong C ₂ H ₅ CN, $v_{20}=1$ and CH ₃ OH
617	38 _{19,19} – 38 _{18,20} *	260110.774	112	455	145.4	413	Strong C ₂ H ₅ OH and C ₂ H ₅ CN, $v_{20}=1$
619	14 _{13,1} – 13 _{12,2} *	260151.979	13	207	114.1	413	Strong C ₂ H ₅ CN, $v_{20}=1$ and C ₂ H ₅ CN
621	37 _{19,18} – 37 _{18,19} *	260154.562	113	444	139.0	413	Strong C ₂ H ₅ CN, $v_{20}=1$ and C ₂ H ₅ CN
623	36 _{19,17} – 36 _{18,18} *	260192.478	113	434	132.7	413	Strong NH ₂ CHO and CH ₂ CO
625	44 _{6,39} – 43 _{6,38}	260216.245	17	418	916.5	413	Strong C ₂ H ₅ CN and C ₂ H ₅ CN, $v_{20}=1$
626	35 _{19,16} – 35 _{18,17} *	260224.898	113	423	126.2	413	Strong C ₂ H ₅ CN, $v_{20}=1$ and C ₂ H ₅ CN
628	34 _{19,15} – 34 _{18,16} *	260252.187	113	413	119.8	413	Strong C ₂ H ₅ OH, CH ₃ OCHO, H ¹³ CO ⁺ , and C ₂ H ₅ CN, $v_{13}=1/v_{21}=1$
630	73 _{14,60} – 72 _{15,57}	260255.958	771	968	86.0	413	Strong C ₂ H ₅ OH, CH ₃ OCHO, H ¹³ CO ⁺ , and C ₂ H ₅ CN, $v_{13}=1/v_{21}=1$
631	19 _{19,0} – 19 _{18,1} *	260262.738	117	297	9.3	413	Strong H ¹³ CO ⁺ and C ₂ H ₅ CN, $v_{13}=1/v_{21}=1$
633	33 _{19,14} – 33 _{18,15} *	260274.699	113	403	113.3	413	Strong C ₂ H ₅ CN, $v_{13}=1/v_{21}=1$, C ₂ H ₅ CN, $v_{20}=1$, and H ₂ ¹³ CS
635	20 _{19,1} – 20 _{18,2} *	260275.506	117	302	18.2	413	Strong C ₂ H ₅ CN, $v_{13}=1/v_{21}=1$, C ₂ H ₅ CN, $v_{20}=1$, and H ₂ ¹³ CS
637	21 _{19,2} – 21 _{18,3} *	260287.415	116	309	26.7	413	Strong H ₂ ¹³ CS and C ₂ H ₅ CN, $v_{13}=1/v_{21}=1$
639	32 _{19,13} – 32 _{18,14} *	260292.777	113	394	106.7	413	Strong H ₂ ¹³ CS and C ₂ H ₅ CN, $v_{13}=1/v_{21}=1$
641	22 _{19,3} – 22 _{18,4} *	260298.247	116	315	34.9	413	Strong H ₂ ¹³ CS and C ₂ H ₅ CN, $v_{13}=1/v_{21}=1$
643	31 _{19,12} – 31 _{18,13} *	260306.755	113	385	100.0	413	Strong C ₂ H ₅ CN, $v_{13}=1/v_{21}=1$
645	23 _{19,4} – 23 _{18,5} *	260307.776	116	321	42.8	413	Strong C ₂ H ₅ CN, $v_{13}=1/v_{21}=1$
647	24 _{19,5} – 24 _{18,6} *	260315.766	115	328	50.5	413	Strong C ₂ H ₅ CN, $v_{13}=1/v_{21}=1$
649	30 _{19,11} – 30 _{18,12} *	260316.958	114	376	93.3	413	Strong C ₂ H ₅ CN, $v_{13}=1/v_{21}=1$, CH ₃ OCH ₃ , and C ₂ H ₅ CN
651	25 _{19,6} – 25 _{18,7} *	260321.972	115	336	58.0	413	Strong C ₂ H ₅ CN, $v_{13}=1/v_{21}=1$, CH ₃ OCH ₃ , and C ₂ H ₅ CN
653	29 _{19,10} – 29 _{18,11} *	260323.698	114	367	86.5	413	Strong C ₂ H ₅ CN, $v_{13}=1/v_{21}=1$, CH ₃ OCH ₃ , and C ₂ H ₅ CN
655	26 _{19,7} – 26 _{18,8} *	260326.138	115	343	65.4	413	Strong CH ₃ OCH ₃ and C ₂ H ₅ CN

Table 10. continued.

N^a	Transition ^b	Frequency (MHz)	Unc. ^c (kHz)	E_l^d (K)	$S\mu^2$ (D ²)	σ^e (mK)	Comments
(1)	(2)	(3)	(4)	(5)	(6)	(7)	(8)
657	28 _{19,9} – 28 _{18,10} *	260327.281	114	359	79.6	413	Strong CH ₃ OCH ₃ and C ₂ H ₅ CN
659	27 _{19,8} – 27 _{18,9} *	260327.999	114	351	72.5	413	Strong CH ₃ OCH ₃ and C ₂ H ₅ CN
661	43 _{9,34} – 42 _{9,33}	263500.082	18	422	881.1	74	Blend with C ₂ H ₅ ¹³ CN and CH ₃ OCH ₃
662	37 _{7,31} – 36 _{6,30}	263656.862	14	340	85.0	108	Strong CH ₃ OCH ₃
663	44 _{23,21} – 43 _{23,20} *	263662.413	12	583	684.9	108	Strong CH ₃ OCH ₃ , HNCO, and HC ¹³ CCN, $v_7=1$
665	44 _{24,20} – 43 _{24,19} *	263666.216	12	599	662.1	108	Strong CH ₃ OCH ₃ , HNCO, and HC ¹³ CCN, $v_7=1$
667	44 _{22,22} – 43 _{22,21} *	263671.555	13	568	706.8	108	Strong CH ₃ OCH ₃ , HNCO, and HC ¹³ CCN, $v_7=1$
669	44 _{25,19} – 43 _{25,18} *	263681.350	13	616	638.2	108	Strong HC ¹³ CCN, $v_7=1$, HNCO, and HN ¹³ CO
671	44 _{21,23} – 43 _{21,22} *	263695.661	13	554	727.7	108	Strong HCC ¹³ CN, $v_7=1$ and C ₂ H ₅ OH
673	44 _{26,18} – 43 _{26,17} *	263706.506	13	633	613.4	108	Strong HCC ¹³ CN, $v_7=1$
675	44 _{20,24} – 43 _{20,23} *	263737.291	14	540	747.7	108	Strong HNCO
677	44 _{27,17} – 43 _{27,16} *	263740.615	14	651	587.6	108	Strong HNCO
679	44 _{28,16} – 43 _{28,15} *	263782.797	15	669	560.8	108	Strong HC ₃ N and CH ₃ OH, $v_t=1$
681	44 _{19,25} – 43 _{19,24} *	263799.727	14	527	766.8	108	Strong HC ₃ N, CH ₃ OH, $v_t=1$, and HC ₃ N, $v_5=1/v_7=3$
683	44 _{29,15} – 43 _{29,14} *	263832.314	16	688	533.0	108	Blend with NH ₂ CHO and U-line?
685	38 _{7,32} – 37 _{6,31}	263847.676	14	351	91.4	108	Blend with NH ₂ CHO
686	47 _{2,45} – 46 _{3,44} *	263860.484	28	434	344.1	108	Blend with C ₂ H ₅ OH and C ₂ H ₅ ¹³ CN
688	47 _{2,45} – 46 _{2,44} *	263860.546	28	434	992.8	108	Blend with C ₂ H ₅ OH and C ₂ H ₅ ¹³ CN
690	44 _{18,26} – 43 _{18,25} *	263887.257	14	514	784.7	108	Strong CH ₃ CH ₃ CO and HNCO, $v_4=1$
692	44 _{30,14} – 43 _{30,13} *	263888.552	16	708	504.4	108	Strong CH ₃ CH ₃ CO and HNCO, $v_4=1$
694	44 _{17,27} – 43 _{17,26} *	264005.588	14	502	801.8	108	Strong CH ₃ ¹³ CH ₂ CN
696	17 _{12,5} – 16 _{11,6} *	264068.075	12	213	106.9	108	Blend with CH ₃ CH ₃ CO, $v_t=1$
698	46 _{4,42} – 45 _{5,41}	266675.648	20	436	260.6	91	Strong O ¹³ CS and C ₂ H ₅ ¹³ CN
699	46 _{5,42} – 45 _{5,41}	266707.175	20	436	962.7	91	Strong CH ₃ OH
700	29 _{6,23} – 28 _{5,24}	266722.756	11	258	39.0	91	Blend with C ₂ H ₅ CN, $v_{13}=1/v_{21}=1$, CH ₃ CH ₃ CO, $v_t=1$, and U-line
701	46 _{4,42} – 45 _{4,41}	266722.874	20	436	962.6	91	Blend with C ₂ H ₅ CN, $v_{13}=1/v_{21}=1$, CH ₃ CH ₃ CO, $v_t=1$, and U-line
702	46 _{5,42} – 45 _{4,41}	266754.401	20	436	260.6	91	Blend with U-line
703	44 _{8,37} – 43 _{8,36}	266788.303	20	429	909.3	91	Blend with U-line
704	44 _{10,35} – 43 _{10,34}	266958.528	17	440	893.9	91	Blend with C ₂ H ₅ OH and U-line
705	44 _{10,34} – 44 _{7,37}	267152.855	100	440	8.9	91	Strong NH ₂ ¹³ CHO, CH ₃ CH ₃ CO, and C ₂ H ₅ CN, $v_{13}=1/v_{21}=1$
706	43 _{7,36} – 42 _{7,35}	267157.130	20	414	897.1	91	Strong NH ₂ ¹³ CHO, CH ₃ CH ₃ CO, and C ₂ H ₅ CN, $v_{13}=1/v_{21}=1$

Notes: ^a Numbering of the observed transitions associated with a modeled line stronger than 20 mK. ^b Transitions marked with a * are double with a frequency difference less than 0.1 MHz. The quantum numbers of the second one are not shown. ^c Frequency uncertainty. ^d Lower energy level in temperature units (E_l/k_B). ^e Calculated rms noise level in T_{mb} scale.

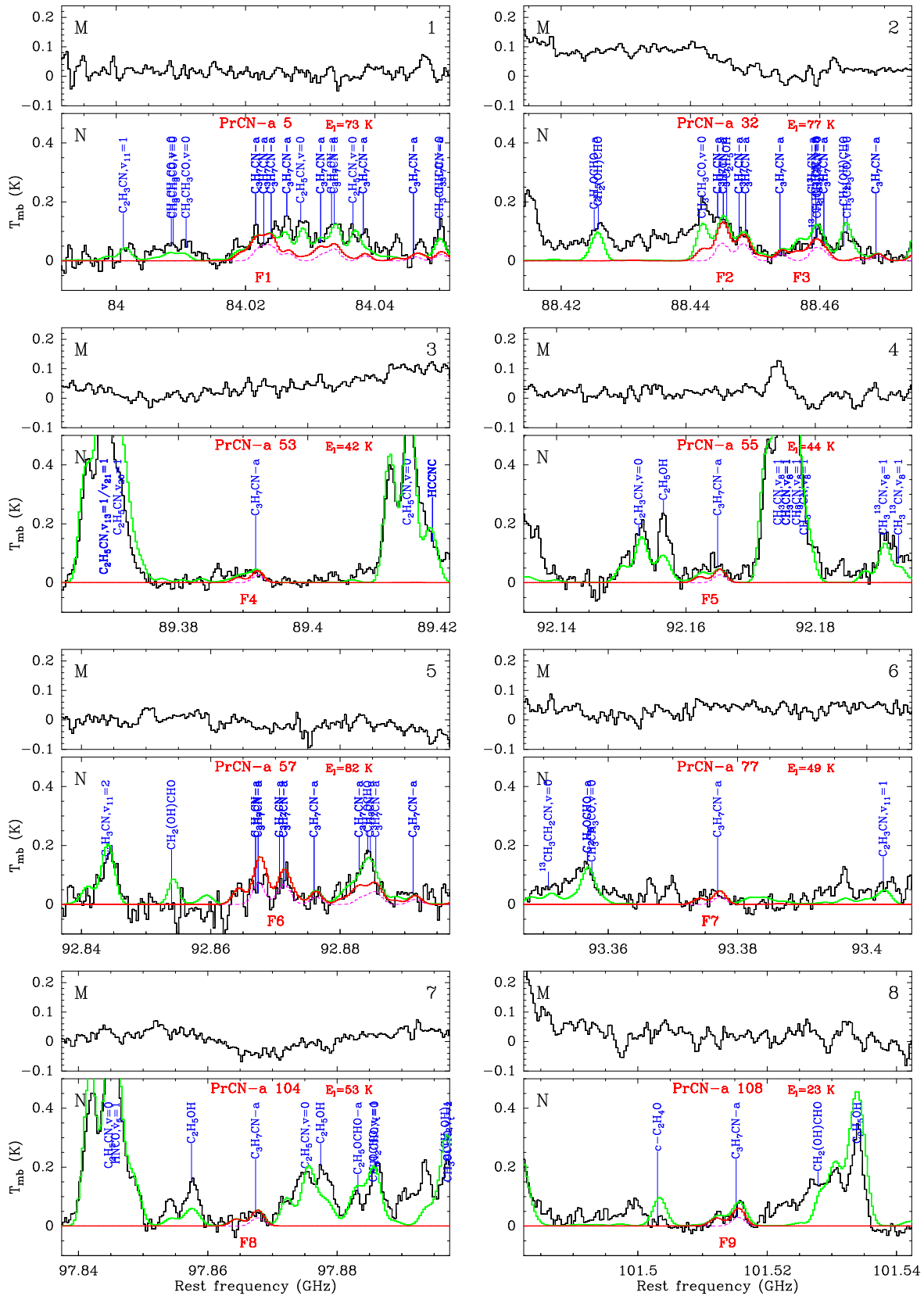


Fig. 3. Transitions of the *anti*-conformer of *n*-propyl cyanide (PrCN-a) detected with the IRAM 30 m telescope. Each panel consists of two plots and is labeled in black in the upper right corner. The lower plot shows in black the spectrum obtained toward Sgr B2(N) in main-beam brightness temperature scale (K), while the upper plot shows the spectrum toward Sgr B2(M). The rest frequency axis is labeled in GHz. The systemic velocities assumed for Sgr B2(N) and (M) are 64 and 62 km s⁻¹, respectively. The lines identified in the Sgr B2(N) spectrum are labeled in blue. The top red label indicates the PrCN-a transition centered in each plot (numbered like in Col. 1 of Table 11), along with the energy of its lower level in K (E_l/k_B). The other PrCN-a lines are labeled in blue only. The bottom red label is the feature number (see Col. 8 of Table 11). The green spectrum shows our LTE model containing all identified molecules, including PrCN-a. The LTE synthetic spectrum of PrCN-a alone is overlaid in red, and its opacity in dashed violet. All observed lines which have no counterpart in the green spectrum are still unidentified in Sgr B2(N).

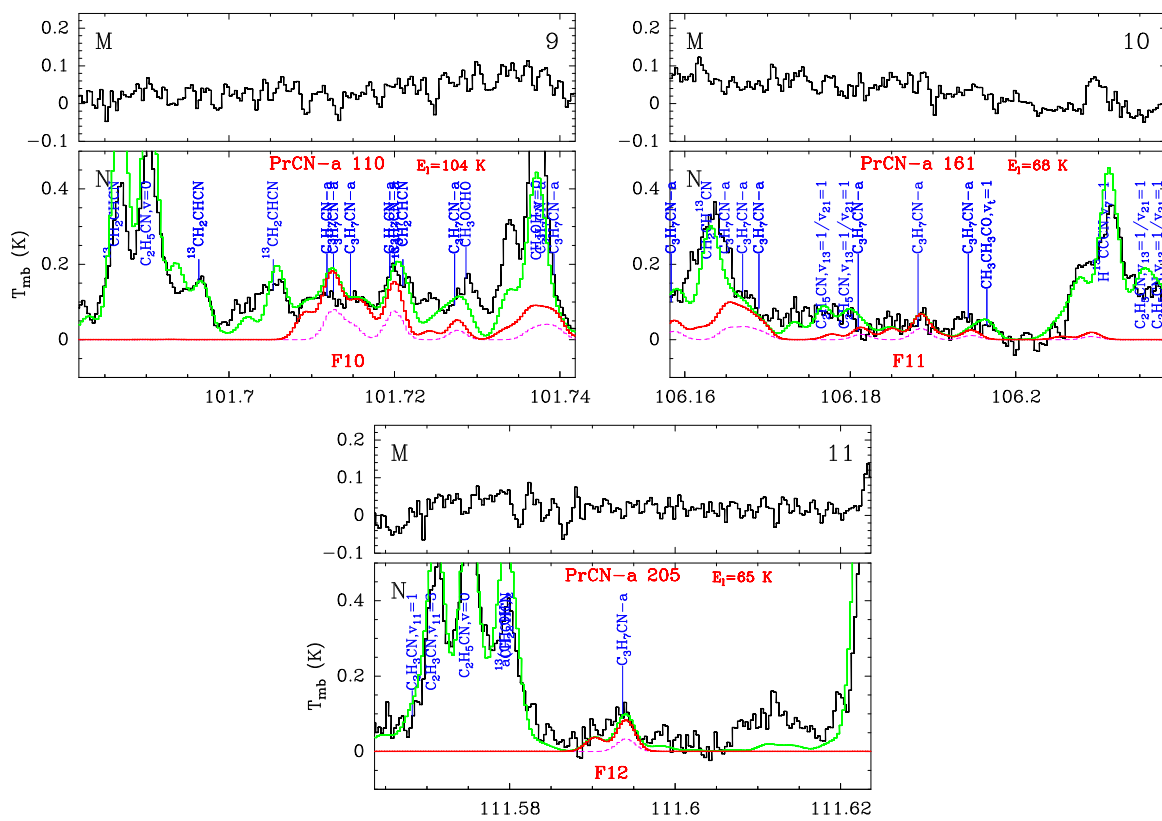


Fig. 3. (continued)

Table 6. Transitions of *anti-n*-propyl cyanide, employed in the present fits, their frequencies (MHz), uncertainties Unc. (kHz), and residuals O–C (kHz) between frequencies measured in the laboratory and those calculated from the final spectroscopic parameters. Unresolved asymmetry splitting (two transitions having the same K_a and the same transition frequency) has been treated as intensity-weighted average of the two lines.

J', K'_a, K'_c	–	J'', K''_a, K''_c	Frequency	Unc.	O–C
2, 1, 2	–	1, 1, 1	8727.068	10	–3
2, 0, 2	–	1, 0, 1	8841.749	10	4
2, 1, 1	–	1, 1, 0	8957.437	10	3
4, 1, 4	–	3, 1, 3	17453.162	10	12
3, 0, 3	–	2, 0, 2	13261.436	5	1
3, 1, 3	–	2, 1, 2	13090.304	5	8
3, 1, 2	–	2, 1, 1	13435.836	5	3
3, 2, 2	–	2, 2, 1	13263.547	5	–2
3, 2, 1	–	2, 2, 0	13265.404	5	–0
4, 2, 3	–	3, 2, 2	17684.317	5	–10
4, 3, 2	–	3, 3, 1	17686.050	5	2
4, 3, 1	–	3, 3, 0	17686.050	5	2
4, 2, 2	–	3, 2, 1	17688.965	5	2
5, 3, 3	–	4, 3, 2	22107.924	5	1
5, 3, 2	–	4, 3, 1	22107.924	5	1
5, 4, 2	–	4, 4, 1	22108.119	5	1
5, 4, 1	–	4, 4, 0	22108.119	5	1
9, 1, 8	–	9, 0, 9	24166.242	5	7
10, 1, 9	–	10, 0, 10	24799.350	5	3
11, 1, 10	–	11, 0, 11	25508.602	5	0
12, 1, 11	–	12, 0, 12	26297.469	5	–2
11, 2, 10	–	12, 1, 11	6897.938	5	–4
16, 1, 15	–	15, 2, 14	13992.090	5	–1
17, 1, 16	–	16, 2, 15	19339.460	5	1
19, 1, 19	–	18, 2, 16	6197.075	5	–1
17, 3, 15	–	18, 2, 16	26095.072	5	–3
18, 3, 16	–	19, 2, 17	21310.053	5	1
19, 3, 16	–	20, 2, 19	19831.330	5	5
20, 3, 18	–	21, 2, 19	11569.979	5	–1
21, 3, 19	–	22, 2, 20	6607.331	5	–0
22, 3, 19	–	23, 2, 22	7318.534	5	2
26, 2, 25	–	25, 3, 22	4813.248	5	–1
26, 2, 24	–	25, 3, 23	13932.516	5	–7
28, 2, 26	–	27, 3, 25	24644.757	5	–0
28, 2, 27	–	27, 3, 24	12629.848	5	4
29, 2, 28	–	28, 3, 25	16441.572	5	–1
30, 2, 29	–	29, 3, 26	20181.553	5	–0
31, 2, 30	–	30, 3, 27	23843.940	5	0
27, 4, 24	–	28, 3, 25	25160.533	5	3
27, 4, 23	–	28, 3, 26	26014.363	5	–8
28, 4, 25	–	29, 3, 26	20523.876	5	5
28, 4, 24	–	29, 3, 27	21572.582	5	–10
29, 4, 26	–	30, 3, 27	15856.700	5	6
29, 4, 25	–	30, 3, 28	17135.390	5	–4
30, 4, 27	–	31, 3, 28	11155.783	5	2
30, 4, 26	–	31, 3, 29	12704.192	5	–2
31, 4, 28	–	32, 3, 29	6417.726	5	3
31, 4, 27	–	32, 3, 30	8280.581	5	2
36, 3, 33	–	35, 4, 32	12979.624	5	4
36, 3, 34	–	35, 4, 31	9299.790	5	–2
37, 3, 35	–	36, 4, 32	13655.067	5	–4
38, 3, 35	–	37, 4, 34	22999.972	5	6
39, 3, 37	–	38, 4, 34	22299.091	5	3
37, 5, 32	–	38, 4, 35	24129.041	5	4
38, 5, 34	–	39, 4, 35	19274.638	5	–2
38, 5, 33	–	39, 4, 36	19621.858	5	1
39, 5, 34	–	40, 4, 37	15110.833	5	0
35, 0, 35	–	34, 0, 34	152420.07	50	10
35, 2, 33	–	34, 2, 32	156362.10	50	–19

Table 6. continued.

J', K'_a, K'_c	–	J'', K''_a, K''_c	Frequency	Unc.	O–C
35, 6, 29	–	34, 6, 28	154794.60	50	5
35, 6, 30	–	34, 6, 29	154794.60	50	5
35, 7, 28	–	34, 7, 27	154778.85	50	–24
35, 7, 29	–	34, 7, 28	154778.85	50	–24
35, 8, 27	–	34, 8, 26	154773.84	50	–40
35, 8, 28	–	34, 8, 27	154773.84	50	–40
35, 9, 26	–	34, 9, 25	154775.62	50	–38
35, 9, 27	–	34, 9, 26	154775.62	50	–38
35, 10, 26	–	34, 10, 25	154782.18	50	–3
35, 10, 25	–	34, 10, 24	154782.18	50	–3
35, 11, 25	–	34, 11, 24	154792.35	50	22
35, 11, 24	–	34, 11, 23	154792.35	50	22
35, 12, 24	–	34, 12, 23	154805.40	50	–28
35, 12, 23	–	34, 12, 22	154805.40	50	–28
36, 0, 36	–	35, 0, 35	156709.22	50	–7
36, 1, 36	–	35, 1, 35	156376.78	50	–9
36, 2, 34	–	35, 2, 33	160851.40	50	–55
36, 2, 35	–	35, 2, 34	158511.09	50	15
36, 3, 33	–	35, 3, 32	159816.09	50	–55
36, 3, 34	–	35, 3, 33	159295.56	50	–7
36, 4, 32	–	35, 4, 31	159360.35	50	–6
36, 4, 33	–	35, 4, 32	159324.49	50	–4
36, 5, 31	–	35, 5, 30	159258.14	50	–38
36, 5, 32	–	35, 5, 31	159256.97	50	14
36, 6, 31	–	35, 6, 30	159218.77	50	–44
36, 6, 30	–	35, 6, 29	159218.77	50	–44
36, 7, 30	–	35, 7, 29	159201.12	50	4
36, 7, 29	–	35, 7, 28	159201.12	50	4
36, 8, 29	–	35, 8, 28	159194.99	50	–15
36, 8, 28	–	35, 8, 27	159194.99	50	–15
36, 13, 24	–	35, 13, 23	159241.59	50	7
36, 13, 23	–	35, 13, 22	159241.59	50	7
36, 14, 23	–	35, 14, 22	159259.85	50	6
36, 14, 22	–	35, 14, 21	159259.85	50	6
36, 15, 22	–	35, 15, 21	159280.32	50	26
36, 15, 21	–	35, 15, 20	159280.32	50	26
36, 16, 21	–	35, 16, 20	159302.83	50	28
36, 16, 20	–	35, 16, 19	159302.83	50	28
36, 17, 20	–	35, 17, 19	159327.32	50	42
36, 17, 19	–	35, 17, 18	159327.32	50	42
36, 18, 19	–	35, 18, 18	159353.76	50	100
36, 18, 18	–	35, 18, 17	159353.76	50	100
37, 0, 37	–	36, 0, 36	160998.16	50	12
37, 1, 37	–	36, 1, 36	160691.64	50	25
48, 1, 47	–	47, 1, 46	211856.19	50	11
48, 2, 47	–	47, 2, 46	210741.48	50	–115
48, 2, 46	–	47, 2, 45	214343.68	50	15
48, 3, 46	–	47, 3, 45	212219.54	50	25
48, 4, 45	–	47, 4, 44	212517.79	50	5
48, 4, 44	–	47, 4, 43	212766.64	50	–12
48, 5, 44	–	47, 5, 43	212415.06	50	–32
48, 5, 43	–	47, 5, 42	212430.89	50	12
48, 6, 43	–	47, 6, 42	212320.28	50	40
48, 6, 42	–	47, 6, 41	212320.77	50	–59
48, 7, 42	–	47, 7, 41	212267.79	50	–29
48, 7, 41	–	47, 7, 40	212267.79	50	–29
48, 8, 41	–	47, 8, 40	212241.20	50	2
48, 8, 40	–	47, 8, 39	212241.20	50	2
48, 9, 40	–	47, 9, 39	212230.19	50	–42
48, 9, 39	–	47, 9, 38	212230.19	50	–42
48, 10, 39	–	47, 10, 38	212229.67	50	28

Table 6. continued.

J', K'_a, K'_c	–	J'', K''_a, K''_c	Frequency	Unc.	O–C
48, 10, 38	–	47, 10, 37	212229.67	50	28
48, 12, 37	–	47, 12, 36	212249.06	50	–46
48, 12, 36	–	47, 12, 35	212249.06	50	–46
48, 13, 36	–	47, 13, 35	212266.32	50	–39
48, 13, 35	–	47, 13, 34	212266.32	50	–39
48, 14, 35	–	47, 14, 34	212287.59	50	14
48, 14, 34	–	47, 14, 33	212287.59	50	14
48, 15, 34	–	47, 15, 33	212312.29	50	–1
48, 15, 33	–	47, 15, 32	212312.29	50	–1
48, 16, 33	–	47, 16, 32	212340.19	50	3
48, 16, 32	–	47, 16, 31	212340.19	50	3
48, 17, 32	–	47, 17, 31	212371.06	50	18
48, 17, 31	–	47, 17, 30	212371.06	50	18
48, 18, 31	–	47, 18, 30	212404.72	50	21
48, 18, 30	–	47, 18, 29	212404.72	50	21
48, 19, 30	–	47, 19, 29	212441.11	50	64
48, 19, 29	–	47, 19, 28	212441.11	50	64
48, 20, 29	–	47, 20, 28	212480.03	50	26
48, 20, 28	–	47, 20, 27	212480.03	50	26
48, 21, 28	–	47, 21, 27	212521.49	50	–24
48, 21, 27	–	47, 21, 26	212521.49	50	–24
48, 22, 27	–	47, 22, 26	212565.54	50	2
48, 22, 26	–	47, 22, 25	212565.54	50	2
48, 23, 26	–	47, 23, 25	212611.99	50	–58
48, 23, 25	–	47, 23, 24	212611.99	50	–58
49, 0, 49	–	48, 0, 48	212476.62	50	100
49, 1, 49	–	48, 1, 48	212378.48	50	62
49, 2, 48	–	48, 2, 47	215077.17	50	14
49, 4, 46	–	48, 4, 45	216949.09	50	–14
49, 16, 34	–	48, 16, 33	216757.71	50	9
49, 16, 33	–	48, 16, 32	216757.71	50	9
49, 17, 33	–	48, 17, 32	216789.07	50	45
49, 17, 32	–	48, 17, 31	216789.07	50	45
49, 20, 30	–	48, 20, 29	216899.87	50	3
49, 20, 29	–	48, 20, 28	216899.87	50	3
50, 0, 50	–	49, 0, 49	216767.70	50	–21
50, 3, 48	–	49, 3, 47	221009.11	50	7
50, 7, 44	–	49, 7, 43	221112.20	50	–26
50, 7, 43	–	49, 7, 42	221112.20	50	–26
50, 8, 43	–	49, 8, 42	221080.73	50	–13
50, 8, 42	–	49, 8, 41	221080.73	50	–13
50, 9, 42	–	49, 9, 41	221066.76	50	–28
50, 9, 41	–	49, 9, 40	221066.76	50	–28
50, 10, 41	–	49, 10, 40	221064.35	50	–25
50, 10, 40	–	49, 10, 39	221064.35	50	–25
50, 11, 40	–	49, 11, 39	221070.19	50	–11
50, 11, 39	–	49, 11, 38	221070.19	50	–11
50, 12, 39	–	49, 12, 38	221082.34	50	28
50, 12, 38	–	49, 12, 37	221082.34	50	28
50, 13, 38	–	49, 13, 37	221099.49	50	–5
50, 13, 37	–	49, 13, 36	221099.49	50	–5
50, 14, 37	–	49, 14, 36	221121.05	50	85
50, 14, 36	–	49, 14, 35	221121.05	50	85
50, 20, 31	–	49, 20, 30	221319.17	50	–141
50, 20, 30	–	49, 20, 29	221319.17	50	–141
51, 0, 51	–	50, 0, 50	221059.01	50	–5
51, 1, 51	–	50, 1, 50	220979.61	50	32
64, 6, 59	–	63, 6, 58	283158.51	50	–21
64, 6, 58	–	63, 6, 57	283171.68	50	33
64, 7, 58	–	63, 7, 57	283022.98	50	14
64, 7, 57	–	63, 7, 56	283022.98	50	14

Table 6. continued.

J', K'_a, K'_c	–	J'', K''_a, K''_c	Frequency	Unc.	O–C
64, 8, 57	–	63, 8, 56	282943.15	50	24
64, 8, 56	–	63, 8, 55	282943.15	50	24
64, 9, 56	–	63, 9, 55	282898.81	50	1
64, 9, 55	–	63, 9, 54	282898.81	50	1
64, 10, 55	–	63, 10, 54	282877.00	50	–26
64, 10, 54	–	63, 10, 53	282877.00	50	–26
64, 11, 54	–	63, 11, 53	282870.71	50	–11
64, 11, 53	–	63, 11, 52	282870.71	50	–11
64, 12, 53	–	63, 12, 52	282875.72	50	–41
64, 12, 52	–	63, 12, 51	282875.72	50	–41
64, 13, 52	–	63, 13, 51	282889.55	50	–38
64, 13, 51	–	63, 13, 50	282889.55	50	–38
64, 14, 51	–	63, 14, 50	282910.51	50	–38
64, 14, 50	–	63, 14, 49	282910.51	50	–38
64, 15, 50	–	63, 15, 49	282937.54	50	6
64, 15, 49	–	63, 15, 48	282937.54	50	6
64, 16, 49	–	63, 16, 48	282969.81	50	25
64, 16, 48	–	63, 16, 47	282969.81	50	25
64, 17, 48	–	63, 17, 47	283006.76	50	–3
64, 17, 47	–	63, 17, 46	283006.76	50	–3
64, 18, 47	–	63, 18, 46	283048.15	50	64
64, 18, 46	–	63, 18, 45	283048.15	50	64
64, 19, 46	–	63, 19, 45	283093.46	50	–14
64, 19, 45	–	63, 19, 44	283093.46	50	–14
64, 20, 45	–	63, 20, 44	283142.77	50	47
64, 20, 44	–	63, 20, 43	283142.77	50	47
64, 21, 44	–	63, 21, 43	283195.66	50	–22
64, 21, 43	–	63, 21, 42	283195.66	50	–22

Table 7. Transitions of *gauche-n*-propyl cyanide, employed in the present fits, their frequencies (MHz), uncertainties Unc. (kHz), and residuals O–C (kHz) between frequencies measured in the laboratory and those calculated from the final spectroscopic parameters. Unresolved asymmetry splitting (two transitions having the same K_a and the same transition frequency) has been treated as intensity-weighted average of the two lines.

J', K'_a, K'_c	–	J'', K''_a, K''_c	Frequency	Unc.	O–C
2, 0, 2	–	1, 0, 1	11912.654	10	–18
2, 1, 2	–	1, 1, 1	11384.045	10	–0
2, 1, 1	–	1, 1, 0	12508.374	10	–10
3, 0, 3	–	2, 0, 2	17785.949	10	6
3, 1, 3	–	2, 1, 2	17055.610	5	1
2, 1, 2	–	1, 0, 1	18176.781	5	1
4, 1, 3	–	4, 0, 4	10286.601	5	0
5, 1, 4	–	5, 0, 5	12167.868	5	–3
6, 1, 5	–	6, 0, 6	14609.404	5	1
7, 1, 6	–	7, 0, 7	17634.822	5	1
2, 2, 1	–	2, 1, 2	22064.261	5	0
24, 3, 21	–	25, 2, 24	5073.952	5	0
10, 3, 7	–	9, 4, 6	12670.827	5	–2
11, 3, 9	–	10, 4, 6	16546.819	5	–3
28, 3, 26	–	27, 4, 23	19891.929	5	1
36, 4, 32	–	37, 3, 35	19547.899	5	1
13, 4, 10	–	12, 5, 7	15362.409	5	0
38, 4, 35	–	37, 5, 32	9991.617	5	0
39, 4, 36	–	38, 5, 33	5311.217	5	1
15, 5, 10	–	14, 6, 9	13597.769	5	1
12, 7, 6	–	13, 6, 7	13549.701	5	–1
12, 7, 5	–	13, 6, 8	13551.095	5	5
13, 7, 7	–	14, 6, 8	7398.401	5	–2
13, 7, 6	–	14, 6, 9	7401.855	5	4
15, 8, 8	–	16, 7, 9	9498.238	5	–4
15, 8, 7	–	16, 7, 10	9498.794	5	–5
19, 7, 12	–	18, 8, 11	9123.186	5	–1
19, 7, 13	–	18, 8, 10	9116.781	5	–1
20, 7, 14	–	19, 8, 11	15398.422	5	0
22, 8, 14	–	21, 9, 13	13221.090	5	–0
22, 8, 15	–	21, 9, 12	13218.792	5	–2
23, 8, 15	–	22, 9, 14	19511.211	5	2
23, 8, 16	–	22, 9, 13	19506.528	5	0
19, 10, 10	–	20, 9, 11	13681.725	5	–1
19, 10, 9	–	20, 9, 12	13681.725	5	–1
25, 9, 17	–	24, 10, 14	17310.401	5	–6
25, 9, 16	–	24, 10, 15	17311.214	5	2
26, 9, 18	–	25, 10, 15	23599.302	5	2
26, 9, 17	–	25, 10, 16	23600.945	5	11
28, 10, 19	–	27, 11, 16	21388.390	5	–9
28, 10, 18	–	27, 11, 17	21388.670	5	–6
26, 13, 14	–	27, 12, 15	13813.369	5	–3
26, 13, 13	–	27, 12, 16	13813.369	5	–3
22, 4, 18	–	22, 4, 19	25543.715	5	–1
25, 5, 20	–	25, 5, 21	16254.957	5	2
26, 5, 21	–	26, 5, 22	21090.090	5	–1
30, 6, 24	–	30, 6, 25	16246.388	5	1
31, 6, 25	–	31, 6, 26	21145.902	5	1
34, 7, 27	–	34, 7, 28	11727.780	5	–2
36, 7, 29	–	36, 7, 30	20572.880	5	–2
37, 7, 30	–	37, 7, 31	26237.933	5	4
39, 8, 31	–	39, 8, 32	11013.037	5	–2
25, 5, 21	–	24, 4, 20	182990.23	50	19
26, 6, 21	–	25, 6, 20	157628.25	50	16
26, 7, 19	–	25, 7, 18	157477.90	50	8
26, 10, 17	–	25, 10, 16	156296.53	50	–59
26, 10, 16	–	25, 10, 15	156296.53	50	–59
26, 11, 16	–	25, 11, 15	156141.79	50	65
26, 11, 15	–	25, 11, 14	156141.79	50	65

Table 7. continued.

J', K'_a, K'_c	–	J'', K''_a, K''_c	Frequency	Unc.	O–C
26, 12, 15	–	25, 12, 14	156032.20	50	–22
26, 12, 14	–	25, 12, 13	156032.20	50	–22
26, 13, 14	–	25, 13, 13	155954.49	50	–56
26, 13, 13	–	25, 13, 12	155954.49	50	–56
26, 14, 13	–	25, 14, 12	155900.13	50	–0
26, 14, 12	–	25, 14, 11	155900.13	50	–0
26, 15, 12	–	25, 15, 11	155863.29	50	–10
26, 15, 11	–	25, 15, 10	155863.29	50	–10
26, 17, 10	–	25, 17, 9	155827.91	50	–33
26, 17, 9	–	25, 17, 8	155827.91	50	–33
26, 18, 9	–	25, 18, 8	155824.64	50	–20
26, 18, 8	–	25, 18, 7	155824.64	50	–20
26, 19, 8	–	25, 19, 7	155828.81	50	–17
26, 19, 7	–	25, 19, 6	155828.81	50	–17
28, 1, 27	–	27, 1, 26	157495.25	50	–33
28, 2, 27	–	27, 1, 26	157503.23	50	–51
28, 1, 27	–	27, 2, 26	157482.64	50	46
28, 2, 27	–	27, 2, 26	157490.60	50	8
29, 5, 25	–	28, 4, 24	189805.28	50	48
30, 4, 27	–	29, 3, 26	178167.69	50	31
30, 4, 26	–	29, 4, 25	182703.13	50	–23
30, 5, 26	–	29, 4, 25	192210.43	50	32
30, 7, 23	–	29, 7, 22	182961.27	50	–29
31, 2, 29	–	30, 2, 28	177803.90	50	–13
31, 3, 29	–	30, 2, 28	177857.94	50	–1
31, 2, 29	–	30, 3, 28	177721.22	50	6
31, 3, 29	–	30, 3, 28	177775.23	50	–12
31, 3, 28	–	30, 3, 27	182248.22	50	–22
31, 4, 28	–	30, 3, 27	183077.55	50	26
31, 3, 28	–	30, 4, 27	181050.65	50	36
31, 4, 27	–	30, 5, 26	178318.43	50	156
31, 5, 26	–	30, 5, 25	192803.61	50	6
31, 7, 25	–	30, 7, 24	188156.51	50	–20
31, 7, 24	–	30, 7, 23	189515.12	50	–74
31, 8, 23	–	30, 8, 22	187858.13	50	9
32, 2, 30	–	31, 2, 29	183183.36	50	18
32, 3, 30	–	31, 2, 29	183218.50	50	28
32, 2, 30	–	31, 3, 29	183129.35	50	37
32, 3, 30	–	31, 3, 29	183164.45	50	6
32, 4, 29	–	31, 3, 28	188119.54	50	–5
32, 4, 28	–	31, 4, 27	192927.96	50	–13
32, 4, 28	–	31, 5, 27	185714.09	50	6
32, 10, 23	–	31, 10, 22	192852.63	50	–4
32, 10, 22	–	31, 10, 21	192854.42	50	–4
32, 12, 21	–	31, 12, 20	192320.23	50	5
32, 12, 20	–	31, 12, 19	192320.23	50	5
32, 13, 20	–	31, 13, 19	192158.76	50	–19
32, 13, 19	–	31, 13, 18	192158.76	50	–19
32, 14, 19	–	31, 14, 18	192040.62	50	14
32, 14, 18	–	31, 14, 17	192040.62	50	14
33, 2, 31	–	32, 2, 30	188564.34	50	–33
33, 3, 31	–	32, 2, 30	188587.13	50	13
33, 2, 31	–	32, 3, 30	188529.24	50	–2
33, 3, 31	–	32, 3, 30	188551.94	50	–47
33, 3, 30	–	32, 3, 29	192871.17	50	–3
33, 4, 30	–	32, 3, 29	193259.00	50	18
33, 3, 30	–	32, 4, 29	192301.88	50	–16
33, 4, 30	–	32, 4, 29	192689.70	50	–5
33, 4, 29	–	32, 5, 28	192663.51	50	12
34, 2, 32	–	33, 2, 31	193946.21	50	–59
34, 3, 32	–	33, 2, 31	193960.95	50	14

Table 7. continued.

J', K'_a, K'_c	–	J'', K''_a, K''_c	Frequency	Unc.	O–C
34, 2, 32	–	33, 3, 31	193923.55	50	26
34, 3, 32	–	33, 3, 31	193938.16	50	–32
34, 6, 28	–	33, 6, 27	212120.06	50	3
35, 6, 29	–	34, 6, 28	218287.17	50	–26
35, 7, 29	–	34, 7, 28	212483.75	50	16
35, 8, 28	–	34, 8, 27	212458.29	50	–13
35, 9, 27	–	34, 9, 26	211828.06	50	142
35, 9, 26	–	34, 9, 25	211938.01	50	7
36, 4, 32	–	35, 5, 31	211527.01	50	14
36, 10, 27	–	35, 10, 26	217402.38	50	–15
36, 10, 26	–	35, 10, 25	217418.12	50	–2
36, 11, 26	–	35, 11, 25	216940.59	50	–30
36, 11, 25	–	35, 11, 24	216941.74	50	33
36, 12, 25	–	35, 12, 24	216609.17	50	–33
36, 12, 24	–	35, 12, 23	216609.17	50	–33
36, 13, 24	–	35, 13, 23	216367.23	50	–1
36, 13, 23	–	35, 13, 22	216367.23	50	–1
36, 14, 23	–	35, 14, 22	216188.17	50	23
36, 14, 22	–	35, 14, 21	216188.17	50	23
36, 16, 21	–	35, 16, 20	215956.57	50	–26
36, 16, 20	–	35, 16, 19	215956.57	50	–26
36, 17, 20	–	35, 17, 19	215885.18	50	–12
36, 17, 19	–	35, 17, 18	215885.18	50	–12
36, 18, 19	–	35, 18, 18	215835.30	50	9
36, 18, 18	–	35, 18, 17	215835.30	50	9
36, 20, 17	–	35, 20, 16	215784.95	50	23
36, 20, 16	–	35, 20, 15	215784.95	50	23
36, 21, 16	–	35, 21, 15	215779.22	50	45
36, 21, 15	–	35, 21, 14	215779.22	50	45
36, 22, 15	–	35, 22, 14	215783.85	50	5
36, 22, 14	–	35, 22, 13	215783.85	50	5
36, 23, 14	–	35, 23, 13	215797.53	50	–19
36, 23, 13	–	35, 23, 12	215797.53	50	–19
36, 24, 13	–	35, 24, 12	215819.22	50	36
36, 24, 12	–	35, 24, 11	215819.22	50	36
36, 25, 12	–	35, 25, 11	215847.81	50	–52
36, 25, 11	–	35, 25, 10	215847.81	50	–52
36, 26, 11	–	35, 26, 10	215882.85	50	–12
36, 26, 10	–	35, 26, 9	215882.85	50	–12
36, 27, 10	–	35, 27, 9	215923.60	50	10
36, 27, 9	–	35, 27, 8	215923.60	50	10
36, 28, 9	–	35, 28, 8	215969.54	50	–15
36, 28, 8	–	35, 28, 7	215969.54	50	–15
36, 32, 5	–	35, 32, 4	216198.45	50	4
36, 32, 4	–	35, 32, 3	216198.45	50	4
37, 3, 34	–	36, 3, 33	214265.30	50	–8
37, 3, 34	–	36, 4, 33	214147.29	50	–26
37, 4, 34	–	36, 4, 33	214225.81	50	–13
38, 1, 37	–	37, 2, 36	211401.39	50	59
38, 3, 36	–	37, 2, 35	215476.23	50	36
38, 2, 36	–	37, 3, 35	215469.85	50	–35
38, 3, 35	–	37, 3, 34	219628.21	50	19
38, 3, 35	–	37, 4, 34	219549.67	50	–13
38, 4, 35	–	37, 4, 34	219601.64	50	–40
39, 0, 39	–	38, 1, 38	212743.02	50	6
39, 2, 37	–	38, 2, 36	220854.26	50	–8
39, 3, 37	–	38, 2, 36	220855.81	50	–18
39, 2, 37	–	38, 3, 36	220851.79	50	–24
39, 3, 37	–	38, 3, 36	220853.34	50	–33
40, 0, 40	–	39, 1, 39	218129.30	50	18
47, 14, 34	–	46, 14, 33	282874.18	50	42

Table 7. continued.

J', K'_a, K'_c	–	J'', K''_a, K''_c	Frequency	Unc.	O–C
47, 17, 31	–	46, 17, 30	282070.21	50	4
47, 17, 30	–	46, 17, 29	282070.21	50	4
47, 19, 29	–	46, 19, 28	281801.94	50	20
47, 19, 28	–	46, 19, 27	281801.94	50	20
47, 20, 28	–	46, 20, 27	281716.83	50	33
47, 20, 27	–	46, 20, 26	281716.83	50	33
47, 21, 27	–	46, 21, 26	281656.67	50	10
47, 21, 26	–	46, 21, 25	281656.67	50	10
47, 22, 26	–	46, 22, 25	281617.41	50	–44
47, 22, 25	–	46, 22, 24	281617.41	50	–44
47, 23, 25	–	46, 23, 24	281596.02	50	–16
47, 23, 24	–	46, 23, 23	281596.02	50	–16
47, 24, 24	–	46, 24, 23	281589.94	50	8
47, 24, 23	–	46, 24, 22	281589.94	50	8
47, 25, 23	–	46, 25, 22	281597.15	50	–18
47, 25, 22	–	46, 25, 21	281597.15	50	–18
47, 26, 22	–	46, 26, 21	281616.14	50	–10
47, 26, 21	–	46, 26, 20	281616.14	50	–10
47, 27, 21	–	46, 27, 20	281645.57	50	–9
47, 27, 20	–	46, 27, 19	281645.57	50	–9
47, 28, 20	–	46, 28, 19	281684.43	50	48
47, 28, 19	–	46, 28, 18	281684.43	50	48
47, 29, 19	–	46, 29, 18	281731.64	50	–30
47, 29, 18	–	46, 29, 17	281731.64	50	–30
47, 30, 18	–	46, 30, 17	281786.66	50	–36
47, 30, 17	–	46, 30, 16	281786.66	50	–36
47, 31, 17	–	46, 31, 16	281848.86	50	31
47, 31, 16	–	46, 31, 15	281848.86	50	31
47, 33, 15	–	46, 33, 14	281992.38	50	34
47, 33, 14	–	46, 33, 13	281992.38	50	34
47, 34, 14	–	46, 34, 13	282072.85	50	–22
47, 34, 13	–	46, 34, 12	282072.85	50	–22
48, 5, 43	–	47, 5, 42	281724.06	50	0
48, 6, 43	–	47, 6, 42	281635.78	50	–33